# Correlating Genetic Change with Changes in Cell Behaviour in Squamous Cell Carcinoma of the Head and Neck

## Focus on Inactivating NOTCH1 Mutations

Pritchard, Ashley Jane

*Awarding institution:*
King's College London

# Correlating Genetic Change with Changes in Cell Behaviour in Squamous Cell Carcinoma of the Head and Neck (SCCHN); Focus on Inactivating NOTCH1 Mutations

This dissertation is submitted for the degree of

*Doctor of Philosophy*

May 2018

**Ashley Pritchard (née Ames-Draycott)** BSC, MRes

Centre for Stem Cells and Regenerative Medicine

King's College London

**Supervisor: Professor Fiona M. Watt**

**Second Supervisor: Dr John Maher**


*Dedicated to family and friends…*

# Abstract

Squamous Cell Carcinoma of the Head and Neck (SCCHN) is a heterogeneous cancer at the genetic and cellular levels. Whole exome-sequencing studies have identified inactivating mutations in NOTCH1 in 11-15% of SCCHN. It was the aim of this research to correlate genetic changes in NOTCH1 expression with changes in cell behaviour.

A human oral SCC line harbouring two truncating NOTCH1 mutations was rescued via lentiviral transduction of the NOTCH intracellular domain (NICD). *In vitro* assays provided evidence to suggest that expression of NICD was able to inhibit proliferation, clonogenicity and cell migration into a scratch wound. At high expression levels, NICD also promoted differentiation. Microarray data supported the *in vitro* findings and further associated NOTCH1 expression with increased cell death and decreased angiogenesis. SERPINE 1 was highlighted as a potential regulator of NICD-mediated changes in cell behaviour. A high number of histone related genes were also found to be down-regulated in response to increased NICD expression. These findings were not explored further in this thesis but are of interest for future work.

Microarray analysis also identified SPANXA1/2 as the most up-regulated gene in response to NICD expression. The fold change increase of SPANXA1/2 was 3x that of any other gene. In order to investigate the functional consequence of SPANXA1/2 expression, a shRNA system was used to knockdown SPANXA1/2 in the NICD-rescued cell line. Primary findings provide evidence to associate the expression of SPANXA1/2 with a potential increase in cell proliferation, increased cell migration into a scratch wound and a change in cell morphology. Current literature suggests that changes in cell morphology may be associated with the inhibition of epithelial to mesenchymal transition (EMT) and the induction of mesenchymal to epithelial transition (MET). However, data is preliminary and further studies are required to confirm this association.

A murine xenograft model was established to assess tumour formation *in vivo.* The expression of NICD resulted in significantly larger tumours. However, no difference

in proliferation was recorded over the two hour period prior to sacrifice. Histological observations also suggest that the expression of NICD may be associated with reduced keratin pearl formation and increased areas of what pathologically presents as comedo-type necrosis. Finally, the expression of NICD was not found to give rise to any significant difference in angiogenesis. Together, these findings suggest a tumour suppressor role for NOTCH1 in SCCHN.

# Abbreviations

| | |
|---|---|
| ANK | Ankyrin |
| BGI | Beijing Genome Institute |
| BSA | Bovine Serum Albumin |
| CD4 | Cluster of Differentiation 4 |
| CSC | Cancer Stem Cell |
| CSL | CBF-1, Suppressor of Hairless, Lag-2 |
| CTA | Cancer Testis Antigen |
| CTH | Cystathionine Gamma-Lyase |
| CXCR | C-X-C Chemokine Receptor Type 4 |
| DLL | Delta Like Ligand |
| DMEM | Dulbecco's Modified Eagle Medium |
| DMSO | Dimethyl Sulfoxide |
| DSL | Delta / Serrate / LAG-2 |
| ECM | Extracellular Matrix |
| EDTA | Ethylenediaminetetraacetic acid |
| EGF | Epidermal Growth Factor |
| EGFR | Epidermal Growth Factor Receptor |
| EMT | Epithelial to Mesenchymal Transition |
| EPU | Epidermal Proliferative Unit |
| FACS | Fluorescence Activated Cell Sorting |
| FBS | Fetal Bovine Serum |
| FBXW7 | F-Box And WD Repeat Domain Containing 7 |
| GFP | Green Fluorescent Protein |
| GO | Gene Ontology |
| GSEA | Gene Set Enrichment Analysis |
| HAT | Histone Acetyltransferases |
| HDAC | Histone Deacetylases |
| HEY1 | Hairy/Enhancer-Of-Split Related With YRPW Motif 1 |
| HPV | Human Papilloma Virus |
| HUVEC | Human Umbilical Vein Endothelial Cells |

| | |
|---|---|
| IPA | Ingenuity Pathway Analyser |
| IRES | Internal Ribosome Entry Site |
| ITGB6 | Integrin Subunit Beta 6 |
| ITBGL1 | Integrin Subunit Beta Like 1 |
| JAG | Jagged |
| LFNG | Lunatic Fringe |
| LNR | Lin12-NOTCH repeats |
| MAML | Mastermind Like |
| MAP | Molecule Activity Predictor |
| MET | Mesenchymal to Epithelial Transition |
| MFNG | Manic Fringe |
| MMP | Matrix Metalloproteinase |
| NCOR | Nuclear Receptor Co-Repressor |
| NCST | Nicastrin |
| NECD | NOTCH Extracellular Domain |
| NEXT | NOTCH Extracellular Truncation |
| NFAT | Nuclear Factor of Activated T cells |
| NF-κB | Nuclear Factor – κB |
| NICD | NOTCH Intracellular Domain |
| NLS | Nuclear Localisation Sequence |
| NRR | Negative Regulator Region |
| NTMIC | NOTCH Transmembrane and Intracellular (Domain) |
| PBS | Phosphate Buffered Saline |
| PEST | Proline, Glutamic Acid, Serine, Rhreonine-Rich |
| PFA | Paraformaldehyde |
| PSEN | Presenilin |
| PSENEN | Presenilin Enhancer |
| RAM | RBPJ Associated Module |
| Rb | Retinoblastoma Protein |
| RBPJ | Recombining Binding Protein for Immunoglobulin Kappa J Region |
| RFNG | Radical Fringe |
| RT-qPCR | Real Time Quantitative Polymerase Chain Reaction |

| | |
|---|---|
| SCC | Squamous Cell Carcinoma |
| SCCHN | Squamous Cell Carcinoma of the Head and Neck |
| SJG | Stephen J Goldie |
| SNAI2 | Snail Family Transcriptional Repressor 2 |
| TAD | Transcriptional Activator Domain |
| T-ALL | T-cell Acute Lymphoblastic Leukaemia |
| TBS | Tris Buffered Saline |
| TCGA | The Cancer Genome Atlas |
| TMEM27 | Transmembrane Protein 27 |
| TNFα | Tumour Necrosis Factor Alpha |
| TP53 | Tumour Protein 53 |
| VEGF | Vascular Endothelial Growth Factor |
| VIM | Vimentin |

# Acknowledgements

This research was supported by the King's Bioscience Institute and the Guy's and St Thomas' Charity Prize PhD Program in Biomedical and Translational Science.

Firstly, I would like to thank my supervisor Professor Fiona Watt for providing the opportunity to work within her lab, for allowing me the freedom to grow as a scientist and for providing support and guidance whenever required. Her enthusiasm for science is both infectious and motivating.

This thesis was made possible by work previously performed by Stephen Goldie, Kazunori Sunadome and Tyler Hayes. I owe them my thanks for providing the building blocks for this research.

Throughout this project, I have been surrounded by people I consider outstanding scientists as well as friends. I will be eternally grateful to Angela Oliveira Pisco for taking me under her wing. I couldn't have asked for a better mentor. Special thanks must also be made to Inês Sequeira for her help, guidance and patience in the xenograft experiments. I could not have completed the project without her training.

I would also like to thank Simon Broad, Helen Cunliffe, Natalia Palasz, Eamonn Morrison, Caroline Dapré and Claire Mooney for keeping the lab running so smoothly.

Although too many to name, I owe my thanks to all other members of the CSCRM. Their support scientifically and personally has made the PhD experience a very enjoyable one.

I must also acknowledge the invaluable technical assistance provided by the staff of the King's Flow Cytometry Core, Genomics Centre and BSU.

Outside of the lab, I am fortunate enough to have the most supportive group of friends. I will be forever thankful to Victoria Tickle, Rebecca Cox, Jenna Duffy, Natasha Jones and Lauren Evans. No matter where they are in the world, I know they are all only a phone call away. Their friendship has been invaluable throughout the trials of a PhD.

I owe the deepest gratitude to my parents for their support, encouragement and unwavering belief. Although there were tears when I left Liverpool, they have always

made sure I know how proud they are of all I have done in Durham and London. I could not have done this without their love.

I would also like to thank my siblings, Ben and Maddie, and my Nan and Grandad. It's always a pleasure to come back up North and I am truly blessed to have such an extensive and loving support network.

Finally, I would like to thank my husband Adam. As the person I have come home to every day of the PhD, my sanity will be eternally grateful for the ease at which he is able to pull me out of the science bubble. He has made my time in London incredibly enjoyable and I'm looking forward to our next chapter in Oxford.

# Table of Contents

# List of Figures

# List of Tables

# Chapter 1

# Introduction

The aim of this thesis is to explore the functional consequence of changes in NOTCH1 expression in Squamous Cell Carcinoma of the Head and Neck (SCCHN). This chapter provides a general overview of SCCHN, NOTCH signalling and what is currently understood about the role of NOTCH1 in SCCHN.

## 1.1 Squamous Cell Carcinoma of the Head and Neck

### 1.1.1 Epidemiology

Each year, there are over 550,000 new cases of head and neck cancer and 380,000 deaths attributed to the disease worldwide. The disease most commonly presents in the $5^{th}$-$7^{th}$ decade of life and males are significantly more affected than females, with the ratio ranging from 2:1 to 4:1 (Fitzmaurice, et al., 2017).

Squamous cell carcinomas (SCCs) are the most common malignant tumours of the head and neck region, accounting for more than 90% of all head and neck cancers. Squamous Cell Carcinoma of the Head and Neck (SCCHN) is currently recognised as the sixth most common cancer by incidence worldwide and, despite preventative measures, rates are projected to continue to increase (Jemal, et al., 2007; Union for International Cancer Control, 2014).

### 1.1.2 Risk Factors

SCCHN can be categorised into clinically distinct human papillomavirus (HPV) positive and negative cases. Approximately 25% of all SCCHN and 90% of oropharyngeal cancers are as a result of infection with the HPV virus, in particular HPV-16 (Gillison, et al., 2000). Tobacco use and moderate alcohol consumption are the most prevalent risk factors and act synergistically as causative agents in the

development of non-viral SCCHN. It is predicted that abstinence from these substances could reduce incidence by up to 90% (Rousseau & Badoual, 2012).

To a lesser extent, diet, occupational exposure to substances such as formaldehyde or asbestos, infection with the oral microflora candida, allergies, a weakened immune system, infection with the Epstein-Barr virus and poor oral health have also been demonstrated to increase risk. Prolonged U.V. exposure has also been associated with cancers of the lip (Khalesi, 2016). In addition, a number of inherited genetic conditions, such as Fanconi Anemia and Bloom's Syndrome, are known to predispose individuals to SCCHN (Kutler, et al., 2003).

### 1.1.3 Classification

Several histological variants of SCCHN are recognised, some of which are associated with unique risk factors and have different prognoses. For example, verrucous carcinomas are well-differentiated, locally destructive SCCs that rarely metastasise, whereas basaloid SCCs are a highly aggressive variant. Conventional SCC is the most commonly diagnosed neoplasm (Pereira, et al., 2007)

Non-viral tumours are the most frequent SCCHN, making up 85% of cases. At a molecular level, non-viral tumours have a significantly increased mutational landscape compared to those associated with the HPV or Epstein-Barr virus. HPV-related tumours are more often associated with tumours at the back of the oral cavity, oropharynx, hypopharynx and larynx rather than tumours of the tongue or lip (Gillison, et al., 2000; Shah, et al., 2014).

SCCHN encompasses a number of pathologically distinct diseases that can be characterised by the sub-location of the primary tumour: (1) oral cavity and tongue, (2) nasal cavity and paranasal sinuses, (3) nasopharynx, oropharynx and hypopharynx, and (4) larynx (Figure 1.1) (National Cancer Institute, 2013). Non-viral conventional SCCs of the oral cavity will be the main focus of this thesis.

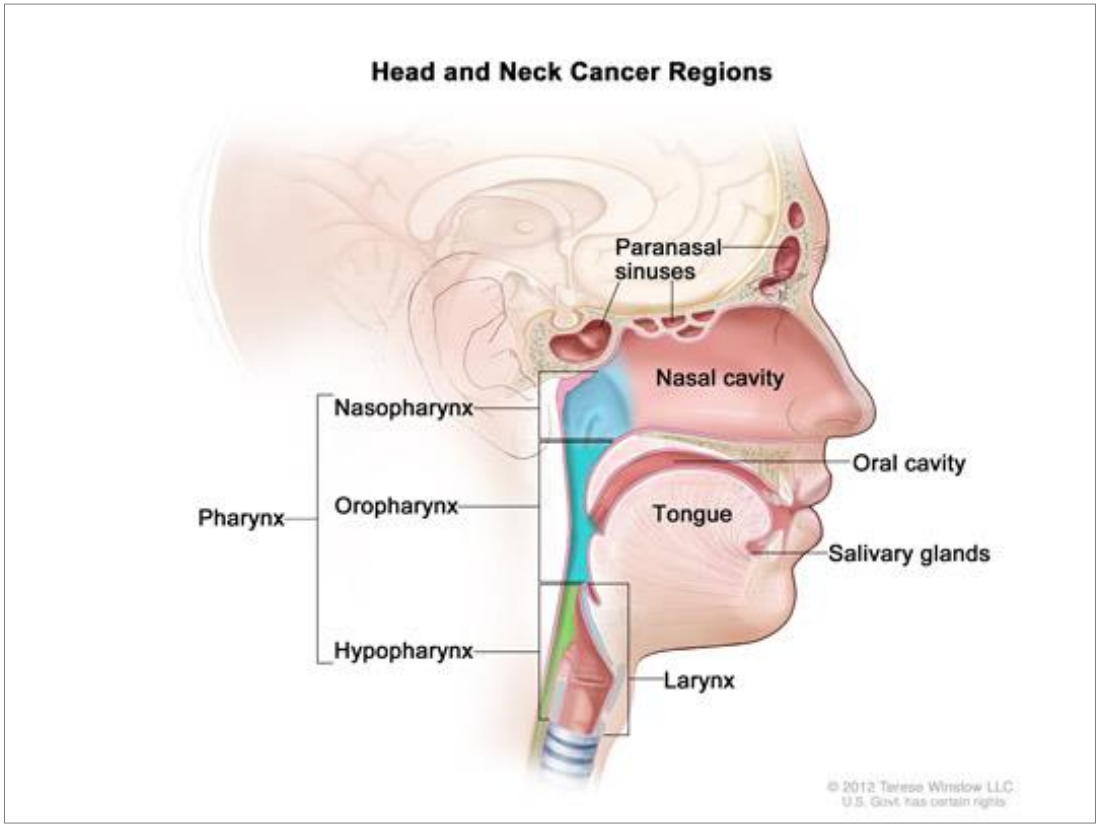


*Figure 1 1: Common primary tumour sites of squamous cell carcinomas of the head and neck. Figure adapted from the National Cancer Institute, 2013 (National Cancer Institute, 2013).*

### 1.1.4 Squamous Epithelium

SCCHN begins with the malignant transformation of the squamous cells that make up the epithelial lining of the mucosal surfaces of the upper aero-digestive tract. The epithelial linings of the body protect underlying tissues from damage by forming an effective barrier against environmental stresses. The moist linings of the body, such as those lining the oral cavity, nasal passage and pharynx, are mucous membranes. In the oral cavity, this lining is called the oral mucosa. The skin is the dry covering of the body exterior and is continuous with the oral mucosa. The skin and oral mucosa share structural similarities and much of what is understood about the structure and function of the oral mucosa has been learnt from skin and vice versa (Squier & Brogden, 2010).

This squamous epithelium can be sub-divided into three types of sub-mucosa: (1) the masticatory mucosa, which is a stratified squamous keratinized epithelium (e.g. gingiva), (2) the lining mucosa, a non-keratinized epithelium (e.g. inner lining of the cheeks and oesophagus), and (3) the specialised mucosa, a non-keratinized epithelium

that contains nerve endings for taste perception (e.g. dorsal and lateral surfaces of the tongue) (Nanci, 2013). Keratinized epithelium resembles the epidermis of the skin and lines areas that are subject to mechanical force. Conversely, non-keratinized epithelium lines regions that require more flexibility (e.g. for chewing or swallowing) (Squier & Brogden, 2010; Papagerakis, et al., 2014). Figure 1.2 details the anatomic location of these three types of sub-mucosa in the oral cavity.

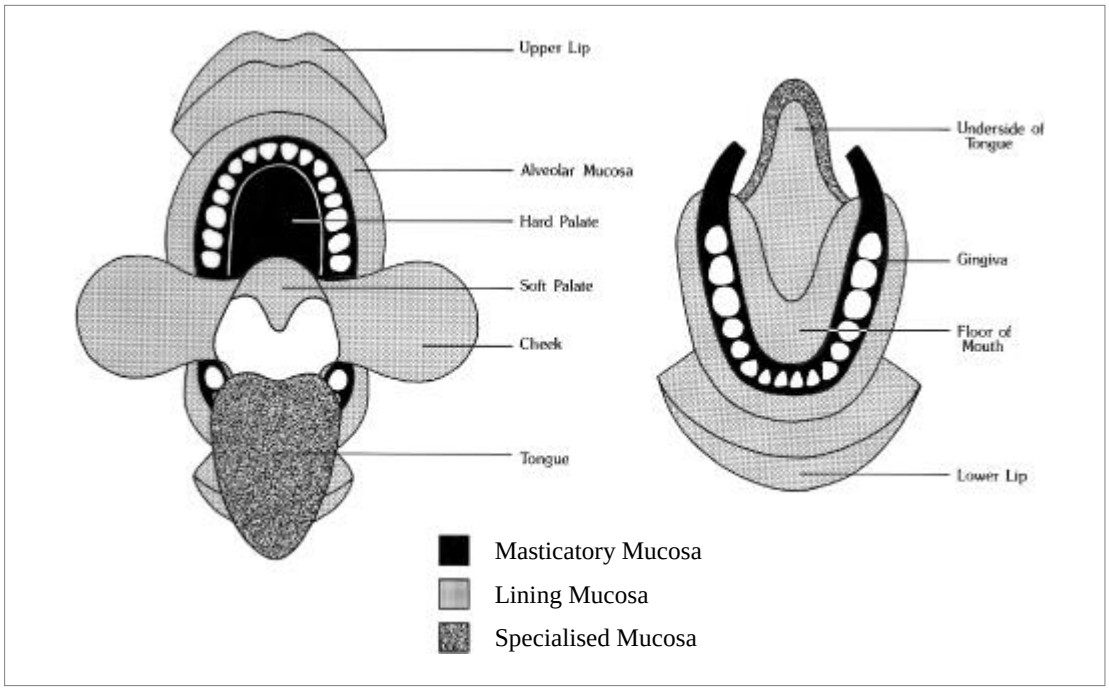


*Figure 1 2: The anatomic location of the three types of sub-mucosa in the oral cavity. Black = masticatory mucosa. Grey shading = lining mucosa. Stippled = specialised mucosa. Figure adapted from Roed-Petersen and Renstrup, 1969 (Roed-Petersen & Renstrup, 1969).*

The human epithelium is made up of stratified layers. During normal homeostasis, the epithelium is maintained by stem cells in the basal layer. As the cells progress towards terminal differentiation, they migrate upwards through the suprabasal layers until they are eventually sloughed off at the epithelial surface. Normally, the rates of cell proliferation and cell loss are balanced and form a 'steady state' (Mackenzie & Fusenig, 1983; Calenic, et al., 2015). The human skin is made up of interfollicular epidermis as well as structures such as sebaceous glands and hair follicles. Evidence suggests the existence of multiple stem cell pools that, although able to differentiate into all epidermal lineages, are lineage-restricted as a result of

local environmental cues (Oshima, et al., 2001; Ito, et al., 2005; Silva-Vargas, et al., 2005; Clayton, et al., 2007; Levy, et al., 2007).

Early epidermal studies identified a proliferative heterogeneity in cell cycle time. This gave rise to the hypothesis that stem cells the basal layer divide asymmetrically to form both a replacement stem cell and a transit amplifying cell, an intermediate cell which retains self-renewal potential for a small number of divisions before becoming a post-mitotic cell. Post-mitotic cells are no longer able to divide and undergo terminal differentiation as they progress through the suprabasal cell layers. As such, a single stem cell surrounded by transit amplifying cells was predicted to reside at the base of a column (or epidermal proliferative unit (EPU)) made up of their differentiated progeny (Potten, 1988).

Lineage tracing studies have been performed to track the fate of tail epidermal stem cells in the basal layer of a murine model. Findings confirmed that terminally differentiated cells of the suprabasal layers were the progeny of undifferentiated cells beneath them. However, linage tracing did not support the EPU model. Studies revealed that the average number of basal cells per clone increased over time. The clones remained cohesive and formed distributions consistent with a single progenitor cell capable of undergoing unlimited divisions (Clayton, et al., 2007).

A second model proposes that homeostasis in the epithelium is maintained by a balance in cell division in a subset of basal cells. When a cell divides, the daughter cells can retain the ability to undergo self-renewal or be fated to undergo terminal differentiation. A cell division can be symmetric, whereby both daughter cells share the same destiny or asymmetric, whereby one follows each fate (Clayton, et al., 2007; Jones, et al., 2007; Watt & Jensen, 2009; Ghadially, 2012).

When primary cultures of epidermal cells are derived three types of colonies are formed, namely holoclones, meroclones and paraclones. Holoclones have a long replicative lifespan and are considered representative of stem cells. Paraclones have a short replicative potential and are thought to behave as transit amplifying cells. Meroclones act as an intermediate. Culture of holocone populations give rise to paraclones and meroclones (Barrandon, 1987). In a recent study, the De Luca group described the use of autologous transgenic keratinocytes to regenerate an entire functioning epidermis for a 7 year old junctional epidermolysis bullosa patient. The group demonstrated that the original post graft cultures where made up of many holoclones, meroclones and paraclones with thousands of genetic integrations. After 8

months, the number of integrations had dropped to a few hundred and those found in paraclones and meroclone were the same as those found in the holoclone population. It was therefore predicted that the meroclons and paraclones were lost over time and the skin graft was maintained by a limited number of holoclones or long-lived stem cells (Hirsch, et al., 2017).

In keratinized epithelium of the oral cavity, the basal layer is made up of cuboidal cells which are attached to the underlying basement membrane. These cells begin to acquire mechanical strength through the formation of a cytoskeletal network of keratin filaments. On initiation of terminal differentiation, cells lose adherence to the basement membrane and migrate upwards to form the spinous layer, which comprises several layers of prickle cells. Cells then advance to form the granular layer of cells filled with keratohyaline granules. At this stage, the keratin filaments form bundles and cells lose organelles, become flattened and secrete phospholipids stored in lamella bodies. Finally, terminally differentiated cells at the epithelial surface make up the cornified layer. By this stage, cells are flat, free of nuclei and full of keratin (Figure 1.3a). As cells migrate apically from the basal layer of non-keratinized epithelium, they also differentiate and flatten. However, they do not accumulate keratin or lose their nuclei. As such, the granular and cornified layers are replaced with intermediate and superficial layers (Figure 1.3b) (Janes & Watt, 2006; Nanci, 2013; Calenic, et al., 2015).

### 1.1.5 Clinical Presentation

Patients with SCCHN present with a variety of symptoms depending on the location of the primary tumour. The most common signs of oral cancer are a sore in the mouth that doesn't heal and / or a discomfort in the mouth that doesn't go away (Macmillan, 2017).

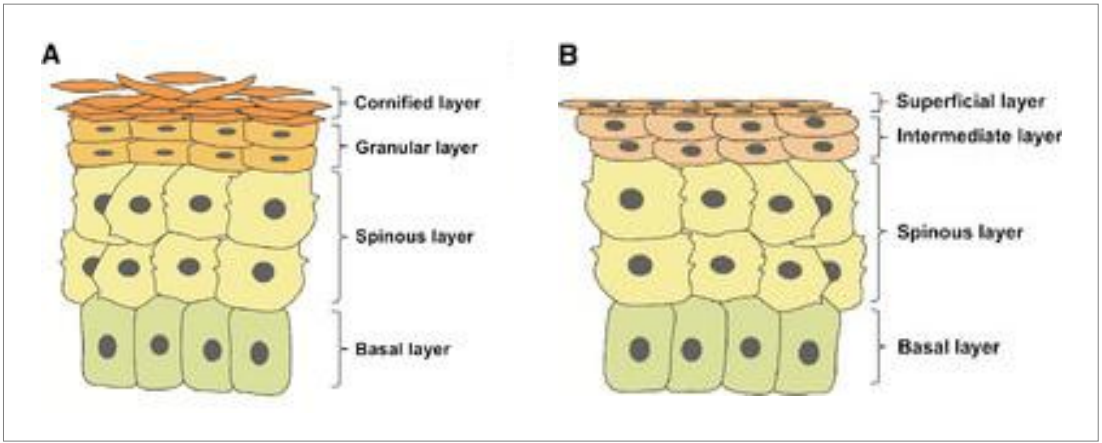


*Figure 1 3: The organisation of the human stratified oral epithelium. (a) The keratinized epithelium is maintained by progenitor cells in the basal layer. On initiation of differentiation, cells flatten, acquire keratin and lose their nuceli as they progress through the spinous, granular and cornified layers. Terminally differentiated cells are eventually sloughed off from the epithelial surface. (b) As cells migrate apically through the non-keratinized epithelium, they also differentiate and flatten. However, they do not acquire keratin or lose their nuclei. Therefore the granular and cornified layers are replaced with the intermediate and superficial layers. Figure adapted from Calenic et al. (Calenic, et al., 2015).*

### 1.1.6 Treatment

The cancer stage, tumour location and patient health are considered in tailoring a treatment plan. Conventionally, in early stage cancers, surgery and radiotherapy are the usual treatments. At later stages, a combination of surgery, post-surgery radiotherapy and chemotherapy is often used (Macmillan, 2017).

The anatomical sites of SCCHN are important for speech, swallowing, taste and smell. As such, the effect of both the cancer and treatment often has a considerable impingement on quality of life. Frequently, a significant quantity of tissue is required to be removed during surgery. As such, organ preservation has been a major consideration over the past three decades and reconstructive work is often performed (Poole, et al., 2001).

Despite improvements in treatment, survival rates have remained largely unchanged. Neoadjuvant chemotherapy is sometimes used in combination with radiotherapy in order to shrink tumours prior to surgery. However, this therapy has only been seen to improve outcome in a select subset of patients with locally advanced and unresectable SCCHN (Vishak, et al., 2015).

Existing chemotherapeutic agents are toxic and non-selective. By better understanding the molecular mechanisms underpinning SCCHN, properties specific to the tumours can be exploited to target drugs to cancer cells whilst having a minimal effect on other cells of the body. Dysregulation of the epidermal growth factor receptor (EGFR) pathway is detectable in most SCCHN patients, with a high expression of EGFR being associated with poor survival. Arguably, the most significant advancement in SCCHN treatment in the past decade has been the approval of cetuximab, an EGFR inhibitor. Although effects are modest, research has shown that the use of cetuximab with cisplatin-based chemotherapy or radiotherapy has improved patient survival (Wen & Grandis, 2015; Argiris, et al., 2017).

### 1.1.7 Prognosis

SCCHN prognosis varies according to the stage at diagnosis, which is determined by histopathology of the primary tumour post-surgery and the extent of lymph node and distant metastasis (Rousseau & Badoual, 2012). Patients diagnosed at early clinical stages (I and II) have similar survival rates of 70-90%; however prognosis of patients with advanced stage disease is strongly associated with tumour location and histopathology (Denis, et al., 2004). Notably, two-thirds of patients present with advanced stage disease. (Duray, et al., 2011; Leemans, et al., 2011; Rothenberg & Ellisen, 2012).

Unlike most solid tumours, where metastatic spread is the main cause of death, the dominant clinical problem in SCCHN is local recurrence or locally progressive disease. Despite surgical removal presenting tumour-free margins, 10-30% of patients develop a locally recurrent tumour. This persistence post-treatment is a major clinical challenge and responsible for a substantial proportion of SCCHN mortalities (Tabor, et al., 2004; Duray, et al., 2011; Rousseau & Badoual, 2012). This high level of recurrence is partially explained by the field cancerisation model, which is discussed further in section 1.1.8.

In the U.K., as of 2016, the overall five year survival for cancers of the oral cavity was approximately 55%. Hypopharyngeal cancers had the lowest five year survival of all SCCHN subtypes at approximately 28%. Conversely, cancers of the salivary gland had the highest five year survival at approximately 67% (Cancer Research UK, 2016).

### 1.1.8 Field Cancerisation

As aforementioned, post treatment, SCCHN patients have a high level of recurrence at the primary tumour site as well as a high incidence of independent tumour formation elsewhere in the head and neck region. In 1953, Slaughter et al. studied the presence of histologically abnormal tissue surrounding oral SCCs. The group subsequently proposed the 'field cancerisation' model, in which primary tumours develop from a field of dysplastic pre-cancerous tissue (Slaughter, et al., 1953). In 1996, Califano's group confirmed the molecular basis of this theory, associating loss of heterozygosity at specific loci with dysplasia (Califano, et al., 1996).

This progression model is comprised of the following stages: (1) a cell capable of self-renewal acquires a genetic alteration, (2) this cell and its similarly mutated daughters make up a clonal unit termed a patch, (3) cumulative genetic alterations advances this patch into a field made up of various sub-clones, (4) this field expands and displaces areas of normal epithelium, (5) a carcinoma develops through clonal selection of cells within the field (Braakhuis, et al., 2003).

The clonal units are often detectable through mutations in Tumour Protein-53 (TP53), widely recognised as one of the first oncogenic changes in the squamous epithelium (Nees, et al., 1993; Rothenberg & Ellisen, 2012). Molecular analysis of SCCHN has identified a number of chromosomal aberrations that precede histological changes in the field (Welkoborsky, et al., 2000; Tabor, et al., 2001). Using these markers, Tabor et al. confirmed that at least 35% of oral and oropharyngeal tumours are surrounded by this genetically-altered epithelium (Tabor, et al., 2001).

Clinically, the field cancerisation model provides an explanation for the frequent recurrence of tumours at the same anatomical location from which a tumour has been surgically excised. These fields are often found at the margins of surgical excisions and hence remain in the patient post-surgery (Leemans, et al., 2011). Studies have shown that these fields play a major role in local tumour recurrence and are a source of second primary tumours (Tabor, et al., 2004; Roesch-Ely, et al., 2007; Schaaij-Visser, et al., 2009).

By investigating squamous epithelia adjacent to and at a variety of sites significantly separated from the primary tumour, different mutations in TP53 have also

been recorded in distant epithelia in the same patient. This data provides a potential molecular basis for the development of multiple tumours (Nees, et al., 1993).

The detection of biomarkers for areas of field cancerisation has tremendous potential in early detection and clinical outcome (Jaiswal, et al., 2013).

### 1.1.9 Heterogeneity

SCCHN is strikingly heterogeneous and differs significantly in aggressiveness and response to treatment (Ramshankar & Krishnamurthy, 2013). In part, this is due to differences at the site of the primary tumour. However, RNA and DNA expression profiling has highlighted molecular heterogeneity and complex karyotype changes independent of tumour-location (Hermsen, et al., 2001; Jin, et al., 2006). Subclasses of SCCHN have been classified by their genetic profiles and shown to harbour distinct clinical behaviours and ultimately different prognoses (Chung, et al., 2004; De Cecco, et al., 2015). Comparative genome hybridisation has also identified sub-groups based on levels of chromosome aberration and confirmed a negative correlation between groups with higher aberrations and survival (Smeets, et al., 2009).

Biologically, limited understanding of this heterogeneity makes it particularly challenging to identify causative cancer genes. Clinically, it is hindering accurate prognostics, treatment planning, and translation of new therapies.

In 2011, Agrawal and Stransky simultaneously published next generation sequencing data for 32 and 74 SCCHN tumours respectively. These studies highlighted the power of whole exome sequencing as a tool for exploring cancer genomics and began to elucidate the genetic heterogeneity of SCCHN (Agrawal, et al., 2011; Stransky, et al., 2011).

### 1.1.10 Analysis of SCCHN epidemiology using The Cancer Genome Atlas (TCGA)

The results shown in this section are based upon data generated by the TCGA Research Network: http://cancergenome.nih.gov/. TCGA is a publically accessible database of cancer sequencing data from international research groups. The cBioPortal for Cancer Genomics tool was used to mine the most recent large-scale SCCHN

genomic data set from TCGA to explore the mutational landscape (Cerami, et al., 2012; Gao, et al., 2013).

Tumour biopsies were sequenced for a total of 504 patients. Consistent with epidemiology data, a high proportion (73%) of patients were male and the most common age of diagnosis was 50-70 years. The overall mutation frequency per primary tumour varied from less than 30 to more than 300. Mutation count followed a normal distribution around the median of 90-120. The frequency of mutations is not specified over the count of 300; however, approximately 8% of samples harboured more than 300 mutations (Figure 1.4). For reference, the average frequency of mutations in solid tumours ranges from 33-66. Leukaemia's have the lowest frequency of mutations at 9.6 per tumour whereas the highest are found in lung cancers and melanomas, which have an average of approximately 200. The higher than average mutation frequency may be associated with the relatively high exposure of the head and neck region to environmental and carcinogenic influences. This is especially true of tobacco-associated cancers (Chen & Wong, 2014).

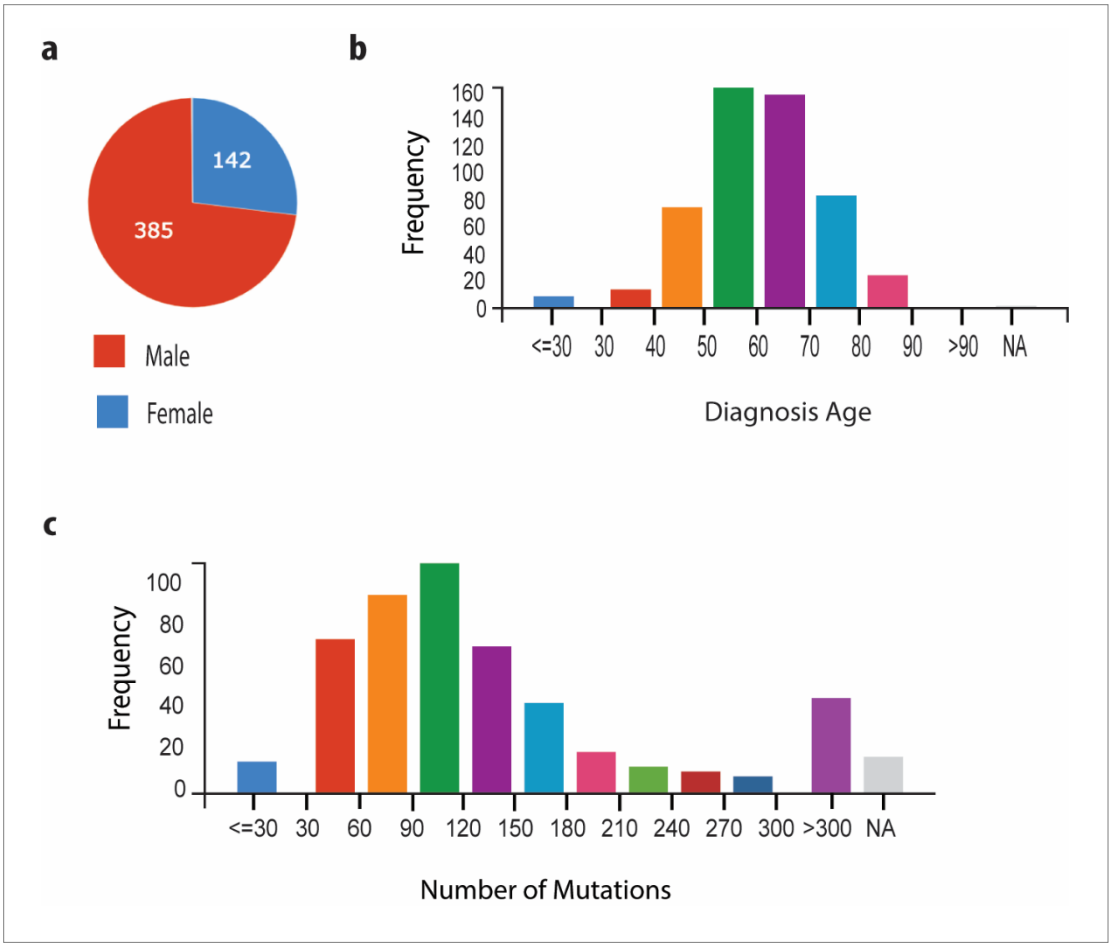


*Figure 1 4: Investigation into sequencing data for SCCHN patients stored by TCGA. a) Patient gender. b) Patient age at diagnosis. c) Frequency of mutations per tumour. Figure adapted from cBioPortal (Cerami, et al., 2012; Gao, et al., 2013).*

## 1.2 The NOTCH Signalling Pathway

### 1.2.1 Functionality

The NOTCH pathway is a highly conserved signalling system that was first described in Drosophila (Poulson, 1939). It is a key player in cell-to-cell communication and functions via the processes of lateral inhibition and boundary induction (Cabrera, 1990). NOTCH signalling plays a vital role in development and is involved in a wide array of key cellular processes such as the government of cell fate, the maintenance of stem cells, cell survival, proliferation and apoptosis (Go, et al., 1998; Miele & Osborne, 1999; Ehebauer, et al., 2006; Bray, 2006; Kopan & IIagan, 2009). In order to regulate these processes, NOTCH signalling interacts with a range

of different pathways and mediates both cell autonomous and non-autonomous changes (Watt, et al., 2008). The core NOTCH signalling pathway signals through 'CBF-1, Suppressor of Hairless, Lag-2' (CSL; named after its mammalian, Drosophila and Caenorhabditis Elegans orthologues) (Kopan & IIagan, 2009). However, signalling can occur through CSL dependent and independent mechanisms (Brennan & Gardner, 2002; Arias, et al., 2002; Bray, 2006).

### 1.2.2 NOTCH Receptors

NOTCH proteins are heterodimeric single-pass Type 1 transmembrane receptors that reside at the cell surface. They are made up of the NOTCH extracellular domain (NECD) and the NOTCH transmembrane and intracellular domain (NTMIC). These two subunits are held together by non-covalent interactions which cause auto-inhibition of the protein. In humans there are four known NOTCH isotypes (NOTCH 1-4) which share this same basic structure (Kopan & IIagan, 2009).

The NECD is located at the N-terminus and is primarily involved in ligand binding. Depending on isotype, it comprises 29-36 tandem epidermal growth factor (EGF)-like repeats with embedded ligand binding sites (Wharton, et al., 1985). They are each approximately 40 amino acids in length and undergo extensive post-transcriptional N- and O- glycosylation that is thought to regulate ligand specificity.

The EGF-like repeats are flanked by a Negative Regulator Region (NRR), which is made up of three Lin12-NOTCH repeats (LNR) and a heterodimerization domain. The NRR prevents ligand-independent activation of NOTCH (Gordon, et al., 2007).

The NOTCH intracellular domain (NICD) is comprised of four distinct domains. (1) The RBPJ associated module (RAM) domain is responsible for initiating transcriptional activation by binding to transcription factor CSL in the nucleus (Johnson & Barrick, 2012). (2) Seven ankyrin repeats make up the ANK domain and mediate protein interactions involved in the activation of chromatin remodelling proteins (Kadam & Emerson, 2003). (3) NOTCH 1 and 2 contain a transcriptional activator domain (TAD) that is absent in NOTCH 3 and 4. (4) Finally, a proline, glutamic acid, serine, threonine-rich (PEST) domain resides at the C-terminus. The PEST domain contains degradation signals that regulate the stability and ubiquitination of the NICD (Öberg, et al., 2001). The NICD also harbours two nuclear

localisation signals (NLS), situated before and after the ANK domain (Fryer, et al., 2004; Kopan & IIagan, 2009; Yavropoulou & Yovos, 2014). The common structural motif of the NOTCH receptors is depicted in Figure 1.5.

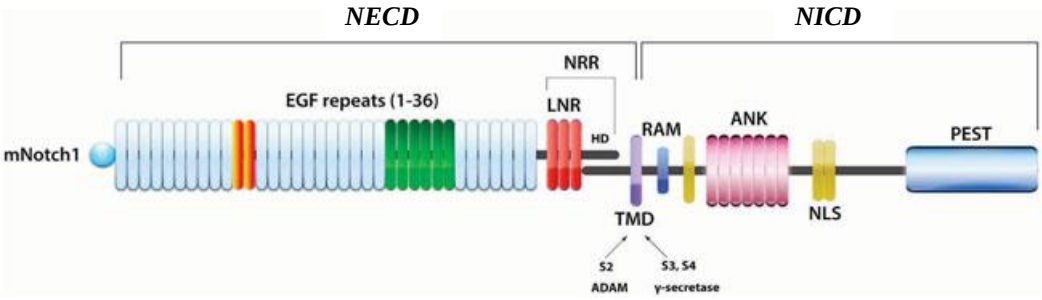


*Figure 1 5: Basic structure of NOTCH receptors. The NOTCH extracellular domain (NECD) is made up of epidermal growth factor (EGF)-like repeats and a negative regulator region (NRR). The NRR comprises Lin12-NOTCH repeats (LNR) and a heterodimerization domain (HD). The transmembrane domain (TMD) spans the cell membrane. The NICD comprises four distinct domains: (1) the RBPj associated module (RAM), (2) ankyrin (ANK), (3) a transcriptional activator domain (TAD) that is absent in NOTCH 3 and 4, and (4) a c-terminal proline, glutamic acid, serine, threonine-rich (PEST) domain. The NICD also harbours two nuclear localisation sequences (NLS). Figure adapted from Yavropoulou and Yovos (Yavropoulou & Yovos, 2014).*

### 1.2.3 The Canonical NOTCH Signalling Pathway

Despite the wide-scale influence of NOTCH signalling, the pathway is relatively simple. Following proteolytic cleavage, the NICD translocates directly to the nucleus to act as a transcriptional regulator; there is no amplification of signal via secondary messenger cascades. The number of NOTCH ligands and receptors at the cell membrane is regulated by endocytosis and membrane trafficking (Bray, 2006; Kopan & IIagan, 2009; Kandachar & Roegiers, 2012).

On translation, the receptor is glycosylated by enzymes O-fut and Rumi. Most NOTCH receptors then undergo a site-1 cleavage event by furin-like convertases within a loop protruding from the heterodimerization domain. This cleavage event converts the NOTCH polypeptide to the NOTCH extracellular domain – NOTCH transmembrane and intracellular domain heterodimer (NECD-NTMIC). In cells expressing Fringe, carbohydrate chains can be added to the extracellular domain by

enzymatic Fringe activity, resulting in altered ability of NOTCH receptor activation by specific ligands (Kopan & IIagan, 2009; Kakuda & Haltiwanger, 2017).

NOTCH ligands belong to the Delta / Serrate / LAG-2 (DSL) protein family and are also single-pass transmembrane proteins. In mammals, there are two classes of recognised ligands known as Delta-like (DLL) and Jagged (JAG), which differ by the absence of a cysteine rich domain in the DLL ligands. Signalling occurs via juxtacrine signalling, with receptors and ligands interacting over short distances between neighbouring cells (Gray, et al., 1999).

As aforementioned, ligands bind to the EGF-like repeats of the NECD. It is now understood that the repeats are able to mediate ligand specificity. Repeats 11-12 are responsible for productive interactions with ligands expressed on neighbouring cells (*trans* interactions), whereas repeats 24-29 are responsible for the inhibitory interaction of NOTCH receptors with ligands co-expressed on the same cell (*cis* interactions). Many of the EGF-like repeats are also able to bind calcium, which contributes to the structure and affinity of NOTCH to its ligands (Raya, et al., 2004; Cordle, et al., 2008; Kopan & IIagan, 2009)

Ligand binding to the EGF-like domain induces the proteolytic cleavage of the NECD by an ADAM-family metalloproteinase at site-2, twelve amino acids from the TMD within the NRR (Brou, et al., 2000). It is hypothesised that mechanical force generated by the initiation of ligand endocytosis leads to conformational changes that exposes the S2 site from the NRR. On release, the ligand-receptor complex is endocytosed into the ligand-expressing cell (Ploscariu, et al., 2014).

The remaining membrane-tethered intermediate NOTCH extracellular truncation (NEXT) is a substrate for progressive site-3 cleavage within the TMD by an enzyme called γ-secretase (De Strooper, et al., 1999). The resultant cleaved protein, the NICD, is then able to translocate into the nucleus where it can modify gene expression through interaction with the transcription factor CSL via the RAM domain. In the absence of NICD, CSL associates with ubiquitous co-repressor proteins and represses gene-transcription; on binding NICD, allosteric changes induce the displacement of transcriptional repressors (Johnson & Barrick, 2012). The ANK domain of the NICD then also associates with CSL in order to recruit the co-activator Mastermind / Lag-3. This tri-complex is then able to recruit the MED8 mediator complex and activate transcription at target promoters. The most recognised downstream targets of the NOTCH pathway are the HES and HEY gene families

(Kitagawa, et al., 2001). Upon activation of NOTCH targets, the PEST domain of the NICD is targeted for ubiquitin-mediated degradation via phosphorylation (Jarriault, 1995; Öberg, et al., 2001; Kopan & IIagan, 2009). An overview of the NOTCH signalling pathway is depicted in Figure 1.6.

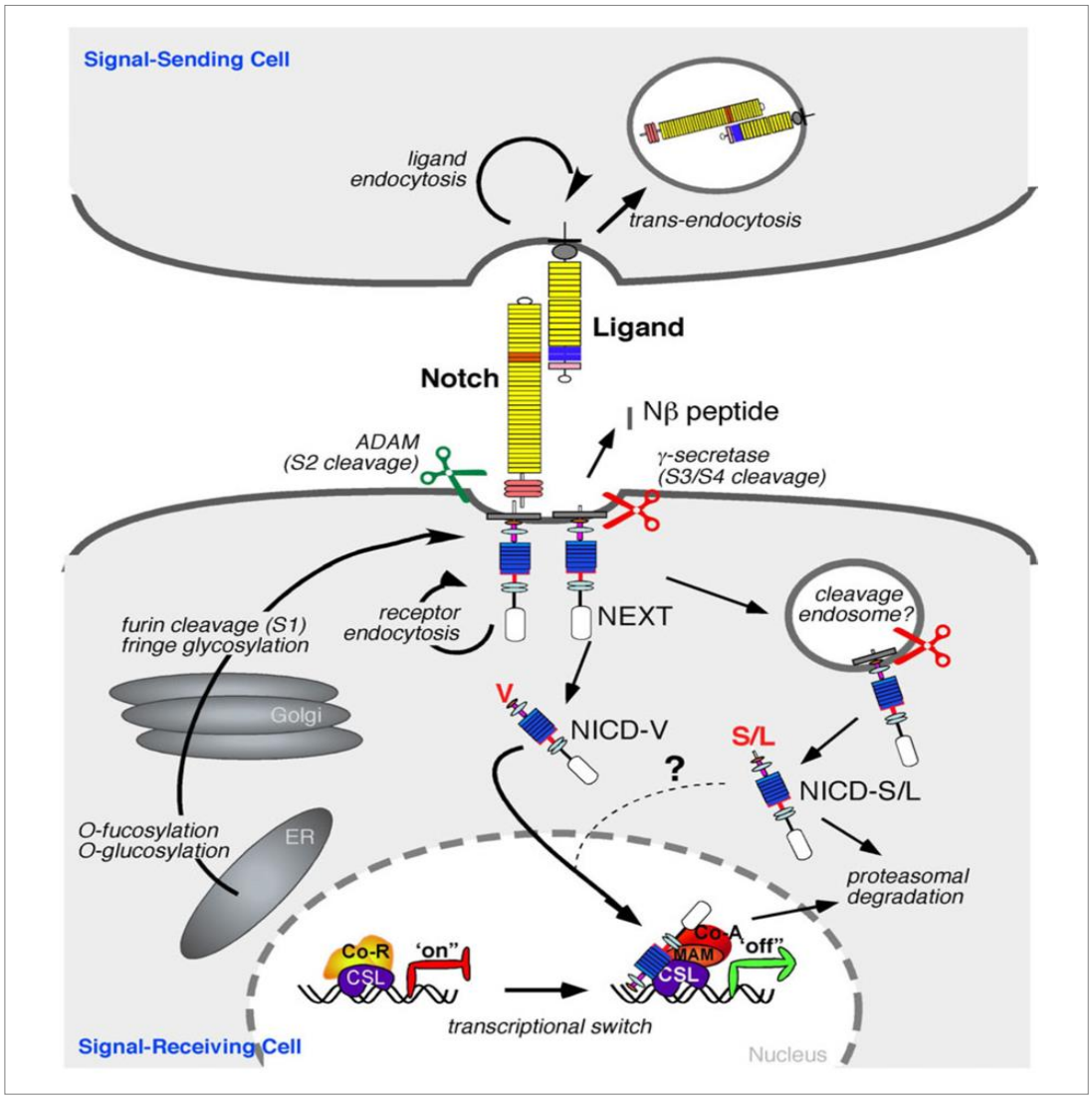


*Figure 1 6: NOTCH Signalling Pathway. Transcribed NOTCH is glycosylated by O-fut and Romi and cleaved by a furin-like covertase to give rise to the NECD-NTMIC heterodimer. Signalling occurs through association with a NOTCH ligand. On binding, the NECD is cleaved by an ADAM-family metalloproteinase and endocytosed. The remaining NEXT can then be cleaved by γ-secretase. The resultant NICD is able to translocate into the nucleus where it can modify gene expression through interactions with the transcription factor CSL. In the absence of NICD, CSL associates with ubiquitous co-repressor proteins; on binding NICD, allosteric changes induce their displacement. NICD-CSL then associates with Mastermind; this tricomplex is able to recruit co-activators and activate transcription at target promoters, often the HES and HEY gene families. The complex is then targeted for proteasomal degradation. Figure reproduced from Kopan and IIagan (Kopan & IIagan, 2009).*

### 1.2.4 NOTCH Signalling in Squamous Epithelium

In the skin, NOTCH expression has been associated with growth arrest and entry into differentiation. The expression of NOTCH 1-3 in the epidermis has been well documented to coincide with cells that are committed to, or undergoing, terminal differentiation and is hence upregulated in the suprabasal layers. Active NOTCH signalling has also been confirmed in these cells by staining for NICD. (Lowell, et al., 2000; Thélu, et al., 2002; Blanpain, et al., 2006; Vooijs, et al., 2007).
specific ablation of NOTCH1 gives rise to hyperplasia and deregulated expression of differentiation markers (Rangarajan, et al., 2001). Interestingly, although cells undergoing terminal differentiation must first exit the cell cycle, the processes of growth arrest and terminal differentiation are under separate control.

Activation of NOTCH1 has been shown to induce growth arrest via p21 induction. Induction is achieved through both direct CSL-dependent transcription and HES1 dependent up-regulation of transcription factor Nuclear Factor of Activated T-cells (NFAT) (Rangarajan, et al., 2001; Mammucari, et al., 2005).

NOTCH-induced differentiation is complex and incompletely understood. Loss and gain of function studies have associated canonical NOTCH signalling with commitment to terminal differentiation in epidermal cells. CSL has been shown to be required for both the induction of spinous layer genes and the repression of genes in the basal layer. HES1, which is expressed in the spinous layer, has been shown to be required for the induction of spinous layer genes. However, basal gene repression is mediated via HES1 independent mechanisms (Blanpain, et al., 2006).

In normal epithelium, NOTCH and EGFR are negative regulators of each other and work together to regulate differentiation. EGFR expression is associated with increased proliferative potential, whereas NOTCH signalling promotes differentiation (Fuchs, 2008). In addition, ΔNp63 expression is highest in the basal cells where it encourages self-renewal and down-regulates NOTCH expression. Contrariwise, it becomes down-regulated during the process of terminal differentiation, coincident with NOTCH up-regulation (Dotto, 2009; Rothenberg & Ellisen, 2012).

Moreover, NOTCH plays a role in cell adhesion and therefore cell location. The location of a cell in the epithelium is important as it dictates the microenvironment signals it receives. The NOTCH receptors, effectors and ligands themselves are expressed in a dynamic pattern throughout the epidermis (Figure 1.7). This patterning

also plays a major role in cell fate, i.e. directing self-renewal or differentiation (Watt, et al., 2008).

JAG1 is primarily expressed in the suprabasal layers and in some cells of the basal layers. Deletion of JAG1 has been shown to cause a thickening of the epidermis (Estrach, et al., 2006). JAG2 and DLL1 are solely expressed in the basal cells and DLL1 expression has been associated with stem cell clusters (Watt, et al., 2008). DLL1-deficient epidermis presents with increased proliferation and disturbed differentiation marker expression (Estrach, et al., 2008; Watt, et al., 2008). Further, DLL1 inhibits NOTCH expression, protecting stem cells from NOTCH-mediated differentiation. Studies using transgenic reporter lines confirm an absence of NOTCH activity in the stem cell compartments. DLL1 has also been shown to actively promote differentiation in neighbouring cells (Lowell, et al., 2000).

Consistent with findings of the skin, Casey et al. associated the activation of NOTCH1 with oral epithelial differentiation during development. Via the use of a JAG2 deficient mouse, the group showed that JAG2 is required for NOTCH1 activation during differentiation (Casey, et al., 2006). There are fewer studies investigating the role of NOTCH in adult oral epithelium. However, staining for NOTCH1 reveals scanty and weak expression localised to the basal and parabasal layers (Sakamoto, et al., 2012; Yoshida, et al., 2013; Barakat & Siar, 2015).

Whilst studies in skin can help to guide the understanding of molecular mechanisms in the oral mucosa, it is important to note that there are intrinsic differences between the tissues at both the structural and genetic levels. As a result, there are also functional differences between the two epithelia. For example, wounds in the oral mucosa heal faster and with less inflammation than equivalent wounds in skin. There are a number of potential evolutionary reasons for the differences between the two sites. Environmentally, the tissues have different base temperatures, microflora and exposure to air / salivary flow. Moreover, the microenvironment of the cells is affected by different anatomical structures such as the presence of hair follicles and sweat glands in skin but not in oral mucosa and the absence of salivary glands in skin (Slominski, 2014).

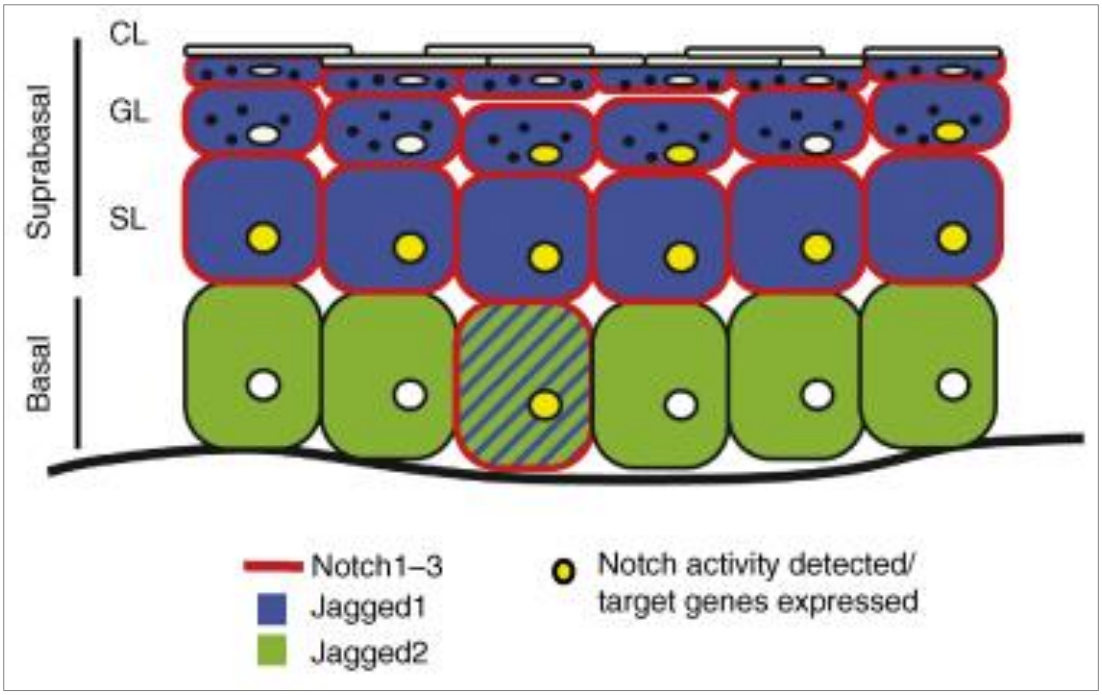


*Figure 1 7: Expression of NOTCH ligands and receptors in the epidermis. CL: cornified layer; GL: granular layer; SL: spinous layer. This figure is reproduced from Watt et al. (Watt, et al., 2008).*

## 1.3 Genetic Alterations in the NOTCH Signalling Pathway in SCCHN

### 1.3.1 Overview of the Role of NOTCH Signalling in SCCHN; Tumorigenic or Tumour Suppressive?

NOTCH signalling is one of the most commonly deregulated signalling pathways in cancer and has been shown to exert both oncogenic and tumour-suppressive effects. Activating translocations in NOTCH1 are present in a large percentage of T-cell acute lymphoblastic leukaemia (T-ALL), chronic lymphocytic leukaemia, and diffuse large B-cell lymphoma tumours. As such, NOTCH is considered an oncogene in these cancers (Weng, et al., 2004; Lee, et al., 2009; Puente, et al., 2011). Conversely, inactivating mutations in lung, myelomonocytic leukaemia and cutaneous cancers have indicated a tumour suppressor role for NOTCH (Wang, et al., 2011; Klinakis, et al., 2011; Sun, et al., 2014).

Figure 1.4c details the frequency of NOTCH1 mutations in SCCHN but does not provide information on the nature of these mutations or how they affect the expression of NOTCH1 and NOTCH signalling pathway members. A number of

genetic studies have been performed to investigate the role of NOTCH signalling in SCCHN.

Initially, NOTCH signalling was believed to play an oncogenic role in the development of SCCHN, largely as a result of the increased gene expression of pathway members. Approximately 30% of tumours are recorded to display an up-regulation of downstream targets HES1/HEY1 as a result of mutations and copy number alterations in several components of the signalling pathway (Hijioka, et al., 2010; Yoshida, et al., 2013; Gokulan & Halagowder, 2014; Sun, et al., 2014).

In the past decade, evidence to suggest a tumour suppressor role for NOTCH1 in SCCHN has come to light (Dotto, 2008; Agrawal, et al., 2011; Stransky, et al., 2011). Mandasari et al. confirmed that the conditional knockout of NOTCH1 in the epidermis gave rise to increased susceptibility to oesophageal tumorigenesis in a mouse model. The protocol used a combined construct that induced the expression of single guide RNA targeting NOTCH1 and Cas9 via the KRT14 promotor (Mandasari, et al., 2016).

Interestingly, in the skin, reduced NOTCH1 expression has been identified in pre-cancerous lesions and NOTCH1 mutations have been recorded in dysplastic regions prior to the development of cutaneous SCC, suggesting potential gate-keeper properties (South, et al., 2014).

Subsequent comprehensive genome analysis of cell lines cultured from oral SCCs further supported a tumour suppressor role for NOTCH1 (Pickering, et al., 2013). Members of the canonical NOTCH signalling pathway were found to be mutated in 66% of oral SCC patients. Copy number gains were recorded in ligands, JAG 1 and 2, and negative regulator NUMB. Consistent with mouse studies performed by Proweller et al., a loss of co-activator mastermind-like protein 1 (MAML1) was also recorded (Proweller, et al., 2006). As well as being able to activate the NOTCH pathway, JAG 1 and 2 are also able to inhibit signalling through cis-inhibition. As all other alterations pointed to a tumour suppressor function of NOTCH1, Pickering et al. suggested the amplifications were also likely to inhibit the signalling pathway (Pickering, et al., 2013).

A further comprehensive genome analysis was carried out on a further 44 SCCHN samples by Sun et al. in 2014. Consistent with previous studies, inactivating NOTCH1 mutations were recorded in 11% of tumours. Expression of downstream signalling targets HES1 and HEY1 was also documented as significantly reduced in

these samples (Sun, et al., 2014). Like Pickering et al., Sun et al. also revealed an upregulation of a number of NOTCH pathway components, including JAG 1 and 2. Interestingly, an upregulation of HES1/HEY1 was recorded in 32% of tumours, all of which were wild type for NOTCH1. The group put forth the notion of a mutually exclusive dual role of NOTCH signalling in SCCHN (Sun, et al., 2014).

Inconsistent with previous studies, in 2016, Upadhyay et al. performed whole transcriptome sequencing on 68 early stage tongue SCC primary tumour samples and found only 4% harboured inactivating NOTCH1 mutations. Furthermore, the group observed a somatic amplification and upregulation in NOTCH1 expression in approximately 31% and 37% of tumours respectively. Cell lines with an upregulation of NOTCH1 were shown to express more stem cell markers and form spheroids. Spheroid forming ability was shown to be inhibited by the both the inhibition of NOTCH1 via a gamma secretase inhibitor and the shRNA mediated knockdown of NOTCH1 (Upadhyay, et al., 2016).

Frequent mutations have also been recorded in ΔNp63 and F-Box and WD Repeat Domain Containing 7 (FBXW7), both of which are negative regulators of NOTCH. (Agrawal, et al., 2011; Stransky, et al., 2011). As previously described, ΔNp63 expression is highest in the basal cells where it encourages the renewal of keratinocytes and down-regulates NOTCH1 expression. Contrariwise, it becomes down-regulated during the process of terminal differentiation, coincident with Notch1 up-regulation (Dotto, 2009; Rothenberg & Ellisen, 2012). FBXW7 is known to target NOTCH1 for degradation. Interestingly, a significant proportion of FBXW7 mutations identified in the whole exome sequencing studies were located in a region known to block this targeting mechanism (Baldus, et al., 2009; Agrawal, et al., 2011). Decreased expression of FBXW7 has been associated with poor prognosis in patients with oesophageal SCC (Naganawa, et al., 2010). Collectively, this data highlights the complexity of NOTCH1 signalling in SCCHN. It is possible that the NOTCH signalling pathway is able to confer both tumour suppressive and tumorigenic actions in SCCHN depending on the genetic landscape of the individual tumour.

### 1.3.2 Analysis of the TCGA Suggests Mutations in NOTCH1 may act as Drivers of SCCHN

It is now understood that genetic variation exists not only between patients, but between cells of the same tumour. Tumours are made up of distinct subpopulations of cells known as 'clones'. A recent paper has coined a 'big bang' model of tumour growth by which a cancer develops as a single uniform expansion of a large number of intermixed clones (Sottoriva, et al., 2015).

Sequencing studies of human cancers have found the genomic landscape to be made up of two distinct classes of mutations, namely passengers and drivers. Passenger mutations make up the main body of mutations in a tumour but confer no selective growth advantage. Conversely, a typical tumour will carry 2-8 driver mutations in genes able to alter core cellular processes to promote tumorigenesis (Vogelstein, et al., 2013).

Although simple to define, it can be difficult to identify which somatic mutations are drivers. Standard statistical methods often consider a high proportion of mutations in a particular gene indicative of driver function in that cancer. The predicted mutational effect is also considered (Vogelstein, et al., 2013). As aforementioned, NOTCH1 was identified as the second most frequently mutated gene in SCCHN after TP53, providing evidence for the role of NOTCH1 as a driver gene in SCCHN (Agrawal, et al., 2011; Stransky, et al., 2011). The alterations were further classified as follows: (1) 8.5% amplifications, (2) 10.5% deep deletions, (3) 35% truncating mutations, (4) 1% in-frame mutations, and (5) 45% missense mutations (Figure 1.8a).

However, it is important to note that there is a difference between a driver gene and a driver mutation. A driver gene will harbour driver mutations able to promote tumour progression; however, they can also contain non-functional passenger mutations (Vogelstein, et al., 2013).

Without extensive functional studies, it is difficult to assess the functional significance of a mutation in the initiation and progression of a given cancer. Similar to the assessment of driver genes, standard statistical methods consider the frequent recurrence of a mutation an indication of functional significance. More recently, the recurrence of mutations in '3D hotspots', i.e. spatially close residues in protein structures that harbour clusters of mutations, have been considered an indication of potential driver function. In SCCHN, a 3D hotspot has been identified in NOTCH1

between amino acids 455-468. TCGA data shows 8% of all NOTCH1 mutations occur within this 3D hotspot, despite it making up less than 1% of the exonic NOTCH1 coding sequence (Gao, et al., 2017). Several of these mutations were also found to recur in multiple patients (Figure 1.8b).

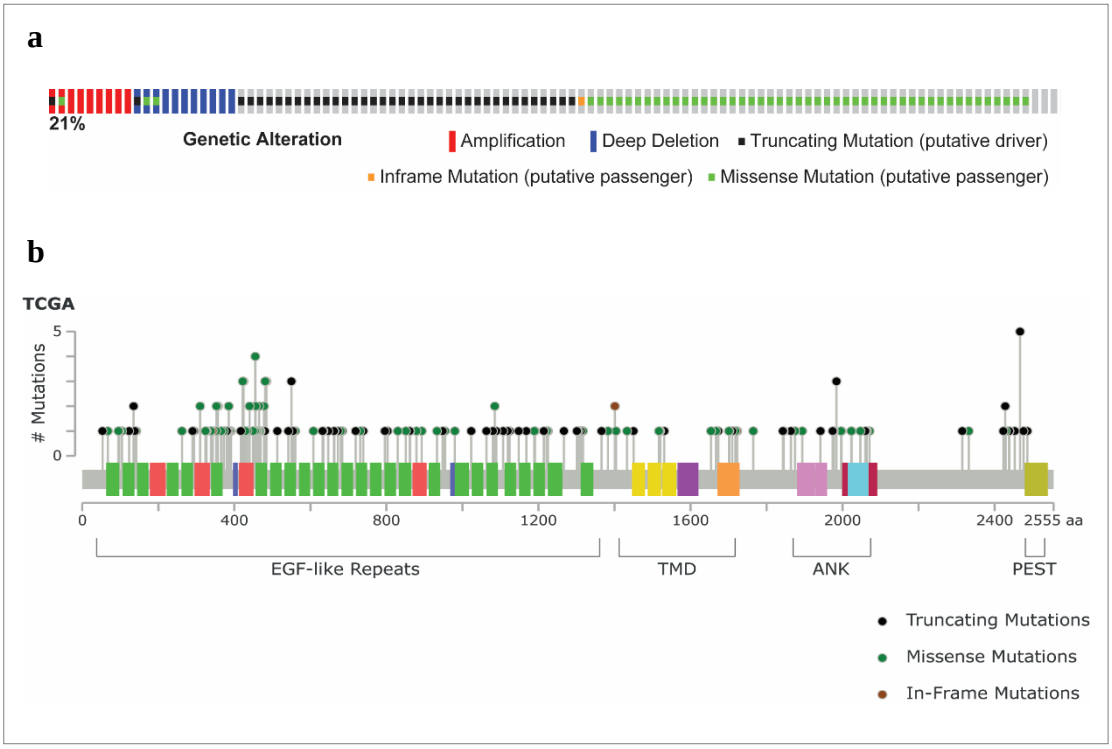


*Figure 1 8: Investigation into sequencing data for 504 SCCHN patients stored by TCGA for NOTCH1 mutations. a) Visual representation of the proportions of genetic alterations in NOTCH1. b) Location of NOTCH1 mutations. EGF-like Repeats = Epidermal Growth Factor-like Repeats. TMD = transmembrane domain. ANK = ankyrin domain. PEST = proline, glutamic acid, serine, threonine-rich domain. Figure adapted from cBioPortal (Cerami, et al., 2012; Gao, et al., 2013).*

The EGF-like repeats surrounding the 3D hotspot present with a higher mutation frequency than the remaining receptor, potentially indicating a wider region of functional importance. Specifically, 66% of NOTCH1 mutations occur between amino acids 295-481, which makes up just 13% of the total exonic coding sequence. Further, 89% of mutations occur in the EGF-like ligand binding domain. This finding aligns with the observations of Agrawal et al., who also noted a high frequency of NOTCH1 mutations in the EGF-like ligand binding domain in sequenced primary tumours (Agrawal, et al., 2011). Of tumours sequenced by Agarwal et al. 40% of

NOTCH1 mutations were found to be truncations and 60% were found to be missense. Most commonly, missense mutations that occur within the NOTCH1 extracellular domain are also found to be inactivating as they prevent effective ligand binding (Islaslab.org, 2014).

Further investigation into the TCGA data set showed that the median survival for patients with a NOTCH1 mutation was 37 months, 19 months less than those with unaltered NOTCH1 who had a median survival of 56 months (Figure 1.9). As the majority of mutations are predicted to be either null or inactivating, this data suggests a tumour suppressor role for NOTCH1 in SCCHN.

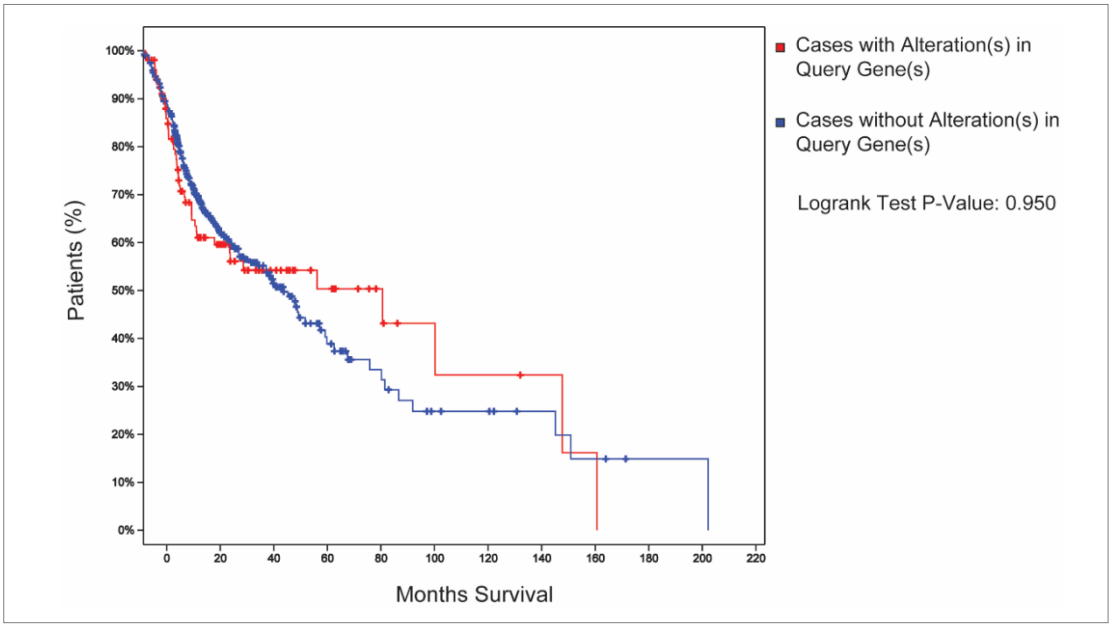


*Figure 1 9: Kaplan Meier estimate curves of the overall survival of a cohort of 504 SCCHN patients recorded in the TCGA. In this figure, the query gene was NOTCH1. Figure reproduced from cBioPortal (Cerami, et al., 2012; Gao, et al., 2013) .*

## 1.4 The Functional Consequence of NOTCH Signalling in SCCHN; Focus on NOTCH1

As well as genetic studies, a number of functional studies have investigated the biological significance of NOTCH signalling in SCCHN. Current understanding of the role of NOTCH signalling on field cancerisation, tumour growth, differentiation, cell death, invasion, cancer stem cells, angiogenesis and inflammation in SCCHN is reviewed in this section.

### 1.4.1 Field Cancerisation

In 2012, Hu et al. associated the loss of mesenchymal CSL, an important NOTCH effector, with field cancerisation in the skin (Hu, et al., 2012). In 2014, Alcolea et al. used a mouse model with a conditional dominant negative mutation in MAML1 (DNM) to inhibit NICD-induced transcription in murine oesophageal epidermis. A drug-inducible form of Cre recombinase was used to inhibit NOTCH in small number of scattered single oesophageal basal cells. The DNM cells were tagged with GFP for visualisation. The group showed that the inhibition of NOTCH1 in these cells prevented cell divisions that produced two differentiated daughter cells. As such, the mutant clones were no longer lost by differentiation and underwent clonal expansion. In addition, similar to the NOTCH negative / DLL positive stem clusters in skin epithelium, these NOTCH-inhibited clones were shown to promote NOTCH signalling and subsequent differentiation in adjacent wild type cells. Said cells were consequentially lost from the population (Lowell, et al., 2000). Within one year, the DNM cell population had replaced the entire epithelium and formed a new homeostasis i.e. the balance of proliferation and differentiation was restored.

Stabilising p53 mutations in the DNM epithelium were found to generate large areas of double-mutant epithelium. In addition, the DNM epithelium was found to give rise an increased number and size of tumours in response to carcinogen treatment. As such, the authors hypothesised that field cancerisation occurs as a result of an imbalance in progenitor cell differentiation as a result of genetic mutation (Alcolea, et al., 2014).

Interestingly, in 2015, Martincorena et al. published deep-sequencing data showing that known cancer drivers were found in 18-32% of normal skin cells which

still maintained the normal function of the epidermis. NOTCH1 was the most frequently mutated genes with relatively high bi-allelic loss in normal skin. (Martincorena, et al., 2015). However, no studies were performed to assess whether this population was at heightened risk for SCC.

Collectively, these two studies provide evidence to suggest that endogenous NOTCH expression is not essential for epidermal integrity but may contribute to the formation of field cancerisation. Further research is required to investigate the combination of mutation events sufficient for tumour formation.

### 1.4.2 Tumour Growth

Inhibition of the NOTCH signalling pathway by treating cells with a γ-secretase inhibitor (preventing the final cleavage event), has been shown to reduce cell proliferation in human tongue and oral carcinoma cell lines (Yao, et al., 2007; Yoshida, et al., 2013; Sun, et al., 2014). The knockdown of NOTCH1 and HEY1 was also found to correlate with the inhibition of cell proliferation (Yoshida, et al., 2013; Sun, et al., 2014).

Conversely, Duan et al. showed that the overexpression of NICD in tongue carcinoma cell lines resulted in reduced cell growth and cell cycle arrest at G0-G1 (Duan, et al., 2006). Similarly, Pickering at al. demonstrated that the rescue of oral carcinoma cells lines harbouring NOTCH1 mutations with NICD led to reduced cell proliferation and cell cycle arrest in the G1 phase (Pickering, et al., 2013). A downregulation of free β-catenin and Wnt / β-catenin mediated signalling has been recorded in human tongue carcinoma cells overexpressing NICD, the active portion of the NOTCH protein, and has been suggested to act as a mechanism in NICD-mediated cell cycle arrest (Duan, et al., 2006).

Crosstalk between the NOTCH and Wnt / β-catenin signalling pathways is well documented. Several NOTCH pathway genes are upregulated in response to β-catenin activation in the skin (Ambler & Watt, 2007). Further, JAG1 is a direct target of the canonical Wnt signalling pathway (Estrach, et al., 2006) and β-catenin has been shown to drive NOTCH signalling via the activation of JAG1 in colorectal cancer (Rodilla, et al., 2009).

However, there is also evidence for antagonism between the two pathways. Work by Nicolas et al. demonstrated that NOTCH1 inactivation in mouse skin inhibits

β-catenin signalling in cells that would normally undergo differentiation. The group then demonstrated that increased β-catenin signalling could be reversed via the introduction of NICD. This led to a reduction in the pool of free β-catenin able to initiate signalling. Collectively, these findings suggest NOTCH is able to inhibit β-catenin mediated signalling (Nicolas, et al., 2003).

NOTCH also plays a non-canonical role in the negative regulation of Wnt / β-catenin signalling in progenitor cells. Of note, NOTCH does alter transcriptional levels of β-catenin, but instead regulates the active protein. Studies have demonstrated that membrane-bound NOTCH is able to form a complex with β-catenin and facilitate destruction-complex-independent endolysosomal degradation of both NOTCH and β-catenin (Hayward, et al., 2005; Kwon, et al., 2011). The complexity of the crosstalk between the NOTCH and Wnt signalling pathways may contribute to cell heterogeneity in SCCHN tumours.

The conflicting observations as to the effect of NOTCH signalling on tumour growth in SCCHN provides evidence to suggest that the functional consequence of NOTCH1 expression may be dependent on molecular landscape. Research performed by Kagawa et al. confirmed the role of NICD in the induction of cell cycle arrest in oesophageal cell lines and showed the senescent phenotype to be associated with both CSL signalling and the p16 pathway. Cellular senescence was corroborated by a flat and enlarged cell morphology, β-galactosidase activity Retinoblastoma protein (Rb) dephosphorylation and induction of G0/G1 cell cycle arrest. However, the group went on to show that the loss of p16 not only prevented NICD-induced senescence, but also permitted NICD to increase xenograft tumour growth and proliferation and reduce squamous cell differentiation. As such, the authors suggest that cellular senescence check points determine the role of NOTCH1, either as an oncogene or as a tumour suppressor (Kagawa, et al., 2015).

### 1.4.3 Differentiation

As previously described, NOTCH signalling is known to promote differentiation in normal skin epithelium (Lowell, et al., 2000; Rangarajan, et al., 2001; Nickoloff, et al., 2002). Fewer studies have been performed in the oral epithelium; however, consistent with findings in the skin, Casey et al. associated the activation of NOTCH1 with the differentiation of oral epithelium during development. In addition,

the inhibition of NOTCH signalling (via the direct deletion of NOTCH1 or overexpression of dominant negative inhibitor of MAML1) has been shown to inhibit terminal differentiation and result in the formation of immature epithelium and tumour development in mouse skin (Nicolas, et al., 2003; Proweller, et al., 2006; Sakamoto, et al., 2012). Likewise, a decreased expression of NOTCH1 is observed in poorly and moderately differentiated oral SCC tumours (Ravindran & Devaraj, 2012).

However, Kagawa et al. were able to demonstrate that, in certain contexts, NICD was able to reduce squamous cell differentiation in cell lines derived from oesophageal SCC. Specifically, the group associated this switch with the loss of p16 expression (Kagawa, et al., 2015).

As well as cell autonomous effects, studies in the skin have shown that NOTCH is able to inhibit differentiation in neighbouring cells (Bray, 2006). Conversely, DLL is expressed in stem cell clusters and promotes differentiation in neighbouring cells (Lowell, et al., 2000).

### 1.4.4 Cell Death

The expression of NOTCH1 has been positively associated with apoptosis in laryngeal and oesophageal SCC cell lines (Lu, et al., 2008; Jiao & Li, 2012). Conversely, the knockdown of NOTCH1 in laryngeal SCC has also been shown to induce apoptosis (Dai, et al., 2015).

Treatment of SCCHN lines with curcumin has been shown to inhibit growth and induce apoptosis, as reviewed by Gao et al. (Gao, et al., 2012). In 2011, Liao et al. provided evidence to suggest that this mechanism works via the down-regulation of NOTCH1 in an oral SCC line (Liao, et al., 2011). In 2012, Subramaniam et al. confirmed that curcumin induced cell death by targeting the NOTCH1 activating γ-secretase proteins in oesophageal cell lines (Subramaniam, et al., 2012).

### 1.4.5 Invasion

Metastasis is the spread of cancer to secondary sites in the body. Cancer cells metastasise by invading the blood and lymphatic systems to travel to distant secondary sites. Epithelial to mesenchymal transition (EMT) is a developmental process in which

epithelial cells lose cell-cell adhesions and polarity and acquire migratory mesenchymal phenotypes. This process is often re-activated in cancer and is associated with cell invasion. Mesenchymal to epithelial transition (MET) is the reverse process and allows metastatic cancer cells to seed at distant sites (Birchmeier, et al., 1996).

In tongue and laryngeal SCC, NOTCH1 protein expression has been positively correlated with both lymph node metastasis and the depth of tumour invasion (Joo, et al., 2009; Zhang, et al., 2011; Dai, et al., 2015). Moreover, strong NICD expression has been recorded in cells located at the invasive tumour front of oral SCCs (Yoshida, et al., 2013). These findings have been further explored experimentally, and several studies have confirmed a reduction of invasive and metastatic phenotypes in response to NOTCH1 downregulation in SCCHN (Yu, et al., 2012; Yoshida, et al., 2013; Dai, et al., 2015; Li, et al., 2015; Jing, et al., 2016). Further, recent research has shown that miR-140-5p is able to supress tumour migration by inhibiting the expression of ADAM10 and thus decreasing NOTCH signalling in hypo-pharyngeal SCC (Jing, et al., 2016).

Studies by Yoshida et al. suggest that the expression of NOTCH1 contributes to the maintenance of Tumour Necrosis Factor-α (TNF-α)-mediated invasion in oral SCC, which functions via the transcriptional regulation of SNAI2 and TWIST (Casas, et al., 2011). During EMT, TWIST is known to induce SNAI2, which supresses the epithelial phenotype; TWIST and SNAI2 then work together to promote EMT and metastasis. Notably, Ambler et al. also showed an increased TNF-α and SNAI2 expression in response to NICD expression in the epidermis (Ambler & Watt, 2010). In addition, the increased epidermal NOTCH expression was shown to give rise to an accumulation of cells in the dermis. As SNAI2 has been associated with EMT, the group postulated whether these dermal cells could be epidermis-derived (Leong, et al., 2007). A Green Fluorescent Protein (GFP) reporter was used to investigate this theory but SNAI2-mediated EMT was not found to occur (Ambler & Watt, 2010).

Targeting NOTCH-mediated metastasis as a potential therapy for SCCHN has been explored. Treatment of oral SCCs with the γ-secretase inhibitor, GSI, has been shown to successfully inhibit this TNF-α-mediated invasiveness (Yoshida, et al., 2013).

Finally, in order to undergo metastasis, cells must first detach from the primary tumour and degrade the basement membrane and surrounding extracellular matrix

(ECM). Matrix metalloproteinases (MMPs) are a family of enzymes involved in the degradation of ECM. They are commonly up-regulated in cancers and aid in tumour invasion. There is evidence to suggest that NOTCH1 is able to mediate metastasis via the regulation of MMP2 and MMP9 in lingual SCC (Yu, et al., 2012). Collectively, this data suggests a key role for NOTCH1 in metastasis and tumour invasion in SCCHN.

### 1.4.6 Cancer Stem Cells

The Cancer Stem Cell (CSC) hypothesis states that not all cells of the tumour population are equally able to initiate tumour growth, metastasis and recurrence. Instead, it is theorised that there is a small population of CSCs which is able to undergo self-renewal and differentiate into the entire heterogeneous tumour (Mackenzie, 2008; Routray & Mohanty, 2014). CSCs have been shown to be able to undergo EMT and MET. The plasticity to switch between an epithelial and post-EMT population has been associated with enhanced therapeutic resistance (Biddle, et al., 2016).

In other cancers, NOTCH expression has also been associated with EMT and chemo-resistance (Capaccione & Pine, 2013). In lung adenocarcinoma cell lines, NOTCH pathway activity has been associated with cells with CSC-like properties. Treatment of these cells with γ-secretase inhibitors has been shown to inhibit tumour formation in serial re-implantation studies, suggesting that NOTCH inhibition may be appropriate for targeting lung adenocarcinoma CSCs (Hassan, et al., 2013). Further, the inhibition of NOTCH signalling in murine glioblastoma xenografts resulted in significantly reduced tumour growth and stem cell marker expression (Chu, et al., 2013).

Increased NOTCH1 expression has also been associated with CSCs in SCCHN (Upadhyay, et al., 2015; Wilson, et al., 2016). In 2016, Zhao et al. confirmed elevated NOTCH1 / HES1 expression in SCCHN lymph node metastases and post-chemotherapy tissue; both of which are associated with CSCs. The group went on to show that the expression of NOTCH1 and HES1 positively correlated with CSC markers CD44, SOX2 and ALDH1. The introduction of DAPT, a NOTCH1 inhibitor, was shown to reduce the proportion of cells expressing CSC markers and tumour self-renewal both *in vitro* and in a mouse xenograft model (Zhao, et al., 2016).

Further, the prolonged exposure of oral SCC lines to the pro-inflammatory cytokine TNF-α has been shown to enhance the CSC phenotype. In this study stemness was associated with increased tumour sphere forming ability, tumorgenicity, chemo-resistance and increased expression of CSC associated genes. Consistent with findings from Zhao et al, enhanced NOTCH signalling was confirmed in cells exposed to TNF-α. Further, the inhibition of either NOTCH1 or HES1 was shown to reverse the CSC phenotype. As such, the group concluded that exposure to TNF-α is able to enhance the CSC phenotype of oral SCC via NOTCH / HES1 signalling (Lee, et al., 2012). Likewise, the overexpression of NOTCH1 has been associated with the maintenance of a stem-like phenotype in tongue SCC lines. Similarly, this group utilised tumour-sphere formation assays and the expression of CSC markers as a measure of stemness (Upadhyay, et al., 2016).

### 1.4.7 Angiogenesis

Angiogenesis is the formation of new blood vessels. The process involves the migration, growth and differentiation of endothelial cells to form the vessel walls. This neovascularisation is essential to the progression of cancers as the sustained proliferation and growth of solid tumours requires an oxygen supply and the removal of waste products. Moreover, it facilitates metastatic spread (Nishida, et al., 2006). The presence of EMT markers has been associated with pro-angiogenic protein expression. Both EMT and angiogenesis are key promoters of carcinogenesis and there is evidence to suggest that the same factors that promote EMT may also drive endothelial cells towards an angiogenic phenotype (Holderfield & Hughes, 2008; Ribatti, 2017).

The expression of NOTCH1 has been positively associated with micro-vessel density in oral SCC (Joo, et al., 2009). In addition, NOTCH1 expression has been correlated with the expression of vasculature endothelial growth factor (VEGF), a direct stimulant of angiogenesis. However, the same study did not find any correlation between NOTCH1 and EGFR (a NOTCH antagonist in the epidermis), a distal but well recognised promoter of angiogenesis in SCCHN. The authors therefore suggest that NOTCH1 is able to induce angiogenesis independently of EGFR signalling in SCCHN (Troy, et al., 2013).

Conversely, Sun et al. reported a reverse correlation between NOTCH1 and VEGF expression in oesophageal SCC (Su, et al., 2009). Further, treatment of SCCHN with cetuximab, an EGFR inhibitor, has been shown to downregulate NOTCH1 and reduce angiogenesis, indicating a potential link between EGFR and NOTCH1 in the regulation of angiogenesis (Wang, et al., 2015).

### 1.4.8 Inflammation

Inflammation is a consequence of the host response to the detection of cancer cells. It is well recognised that a chronic inflammatory compartment is critical to solid tumour progression (Grivennikov, et al., 2010). Deregulation of NOTCH in the epidermis has been associated with a JAG1-mediated Cluster of Differentiation 4 (CD4) -positive T cell infiltrate as a result of barrier dysfunction. It has been shown that NOTCH activation induces TNF-α which in turn activates JAG1 expression via NF-κB. AS JAG1 also activates NF-κB, it is predicted that a positive auto-regulatory loop is formed (Ambler & Watt, 2010).

Further, several studies have associated NOTCH signalling with inflammatory mediators in cancer (Fazio & Ricciardiello, 2016). Specifically, in tongue SCC, pro-inflammatory cytokine IL-β1 has been shown to increase the expression of CXC Chemokine Receptor 4 (CXCR) via NOTCH1. CXCR4 is a known regulator of cancer growth and metastasis (Sun, et al., 2015).

## 1.5 Summary

A number of high throughput genomic sequencing studies have identified loss-of-function NOTCH1 mutations in approximately 11% of SCCHN tumours, suggesting a tumour suppressor role for NOTCH1 (Agrawal, et al., 2011; Stransky, et al., 2011; Sun, et al., 2014). However, approximately one third of SCCHN tumours have also been shown to exhibit activated NOTCH signalling, as indicated by the upregulation of downstream targets HES1/HEY1. Importantly, inactivating NOTCH1 mutations and the overexpression of HES1/HEY1 have been found to be mutually exclusive (Sun, et al., 2014).

Section 1.4 provides an overview of the current understanding of the functional significance of NOTCH1 in SCCHN. SCCHN is highly heterogeneous. Whether NOTCH1 acts as a tumour suppressor or oncogene is likely to depend on the mutational landscape of the individual tumour as well as interactions with the microenvironment. For example, for NOTCH1 to act as a tumour suppressor, other factors must override the NOTCH-mediated promotion of metastasis.

A better understanding of the complexities of the functional consequence of NOTCH signalling in SCCHN is essential before the pathway could be targeted therapeutically. *In vitro* and *in vivo* functional studies are required to elucidate the mechanisms by which different genetic alterations in NOTCH1 result in changes in cell behaviour in SCCHN. Moreover, the interplay of NOTCH1 with other SCCHN mutations must be considered as well as the effect of the tumour microenvironment.

## 1.6 Aims of this Thesis

This chapter has discussed the clinical significance of SCCHN worldwide and highlighted the need for further research to improve the 5 year survival, which currently stands at approximately 50%. By better understanding the molecular mechanisms underpinning SCCHN, properties specific to the tumours can be exploited therapeutically.

This research will build upon work performed by Hayes et al. (Hayes, et al., 2016). Whole exome sequencing studies have identified NOTCH1 mutations in 11-15% of original tumours suggesting a potential tumour suppressor role in SCCHN. Subsequent functional studies suggest a complex and context dependent role of NOTCH signalling in SCCHN. It is the aim of this thesis to further understanding of NOTCH signalling in SCCHN by investigating the effect of NOTCH1 inactivating mutations on cell behaviour. It is hoped that better understanding of the functional consequence of changes in NOTCH1 expression will ultimately aid in the development of more targeted treatment plans.

It is the aim of this thesis to investigate the effect of NOTCH1 expression on the following cellular functions in SCCHN: (1) tumour growth, (2) differentiation, (3) migration and invasion and (4) angiogenesis.

# Chapter 2

## Materials and Methods

This chapter details the materials and experimental methods used within this research project.

## 2.1 Cell Line Derivation

### 2.1.1 Cell culture medium and supplements

*Culture medium for J2-3T3 feeder cells*

Dulbecco's Modified Eagle's Medium (DMEM) (Sigma-Aldrich) supplemented with 10% bovine serum (Life Technologies), 100 U/ml penicillin (Life Technologies) and 100 µg/ml streptomycin (Life Technologies). Medium was stored at 4$^{o}$C for up to two weeks.

*Culture medium for oral SCCs*

Based on the Rheinwald and Green method (Rheinwald & Green, 1975): FAD medium, made from one part Ham's F12 medium and three parts DMEM supplemented with 1.8x10$^{-4}$ M adenine (Life Technologies), was further supplemented with 10% fetal bovine serum (FBS) (Life Technologies), 100 U/ml penicillin (Life Technologies), 100 µg/ml streptomycin (Life Technologies), 5 µg/ml insulin (Sigma-Aldrich), 450 µg/ml glutamine (Life Technologies), 1.8 µm calcium chloride (Sigma-Aldrich) and a cocktail (HCE) of 0.5 µg/ml hydrocortisone (ThermoFisher Scientific), 10$^{-10}$ M cholera toxin (Enzo Life Science) and 10 ng/ml EGF. Medium was stored at 4$^{o}$C for up to two weeks.

*Culture medium for oral SCCs during experimental assays*

Keratinocyte-SFM (KSFM; Life Technologies) was supplemented with 25 mg bovine pituitary extract and 2.5 µg human recombinant EGF, as supplied by the manufacturer. Medium was stored at 4$^{o}$C. Cells were moved into serum free medium for experimental assays as serum composition is variable between batches. As such, results from serum-free conditions have increased reproducibility and are more comparable. KSFM has been optimised to meet the nutritional needs for the growth and maintenance of epithelial cells without the need for a feeder layer (Thermo Fisher Scientific, 2003). It is worth noting that changing cells to KSFM medium from FAD medium can have an effect on cell morphology. However, all comparative observations in this study are between cells cultured in identical conditions.

*Culture medium for HEK293 cells*

DMEM (Sigma-Aldrich) supplemented with 10% FBS (Life Technologies), 100 U/ml penicillin (Life Technologies), 100 µg/ml streptomycin (Life Technologies) and 900 µg/ml glutamine (Life Technologies). Medium was stored at 4$^{o}$C for up to two weeks.

### 2.1.2 Isolation of human oral SCCs

This work was carried out in compliance with the UK Human Tissue Act (2004) and with appropriate ethical approval from the National Research Ethics Service (08/H0306/30) by Mr Simon Broad (Centre for Stem Cells and Regenerative Medicine, King's College London). Samples were donated to research, with informed consent, from patients diagnosed with oral SCC in Addenbrooke's Hospital, Cambridge. Reports derived by the consultant pathologist were used to define the depth of invasion and grade of differentiation of tumour samples, as detailed in Table 2.1. Cell lines were derived as previously described (Rheinwald & Beckett, 1981).

Table 2 1: Patient and Primary Tumour Background for Derived Cell Lines

| *Line* | *Gender* | *Age* | *Smoker* | *Alcohol Consumption* | *Depth of Invasion* | *Differentiation* | *Max Diameter* | *Lymph Nodes* | *Pathological Grade* |
|---|---|---|---|---|---|---|---|---|---|
| *3* | Male | 61 | Ex | Minimal | 13 | Well | 20 | N0 | T4a |
| *4* | Female | 49 | Yes | Moderate | 4.1 | Poor | 20 | N1 | T2 |
| *6* | Female | 63 | No | Minimal | 12 | Poor | 46 | Nx | T4a |
| *8* | Male | 68 | Ex | Heavy | 2 | Well | 18 | N0 | T1 |
| *13* | Female | 54 | No | Minimal | 12 | Well | 35 | Nx | T4a |
| *15* | Female | 51 | No | None | 9 | Well | 22 | N1 | T2 |
| *16* | Male | 28 | Ex-Cannabis | Minimal | 4 | Moderate | 7 | N0 | T1 |
| *17* | Female | 48 | Yes | Moderate | 6 | Well | 8 | Nx | T1 |
| *18* | Female | 79 | Yes | Moderate | 12.1 | Moderate | 14.6 | N0 | T1 |
| *21* | Male | 76 | Ex | None | 14 | Poor | 26 | N0 | T2 |
| *24* | Female | 55 | Ex | Minimal | 16.2 | Moderate | 40 | N2c | T3 |
| *25* | Male | 59 | Yes | Heavy | 1.5 | Well | 24 | N0 | T2 |
| *26* | Male | 74 | Ex | Minimal | 14.2 | Moderate | 22 | N1 | T4a |
| *27* | Male | 30 | No | None | 10.5 | Moderate | 35 | N2b | T2 |
| *28* | Female | 37 | Ex | Minimal | 7 | Well | 18.5 | N0 | T1 |
| *31* | Female | 65 | Ex | Moderate | 6.5 | Moderate | 16 | Nx | T4a |
| *32* | Female | 79 | Ex | Minimal | 9 | Moderate | 20 | N0 | T1 |
| *33* | Male | 78 | Ex | Minimal | 8.5 | Well | 13 | N0 | T1 |
| *37* | Male | 29 | No | Minimal | 0.7 | Moderate | 1.7 | N0 | T1 |
| *41* | Female | 55 | Ex | Minimal | 8.5 | Poor | 25 | N1 | T2 |
| *42* | Female | 56 | Ex | None | 2.6 | Well | 29 | N0 | T2 |

### 2.1.3 Culture of J2-3T3 cells as feeder layers

The culture of oral SCC lines is supported by co-cultivation with inactivated J2-3T3 cells, a.k.a. feeder cells (Rheinwald & Green, 1975). On thawing, J2-3T3 were quickly re-suspended in supplemented DMEM medium, seeded onto the surface of a T75 flask and maintained in a humidified incubator at 37ºC and 5% $CO_2$. The medium was changed three times per week and the cells split and re-seeded at a density of $1x10^5$ when they reached confluence. Cells were lifted using a solution of Trypsin-Ethylenediaminetetraacetic acid (Trypsin-EDTA; 0.25%) (Sigma Aldrich) further diluted in Versene (Life Technologies) at a ratio of 1:4 for approximately 2 minutes at 37ºC.

To prepare J2-3T3 cells as a feeder layer for oral SCC co-culture, they were grown to a density of approximately $1.8x10^6$ – $2.0x10^6$ and mitotically inhibited by incubation with 4 µg/ml Mitomycin-C (Sigma Aldrich) for 2hrs at 37ºC. Following treatment, the cell layers were washed three times with PBS and oral SCCs were introduced at a density of $1x10^5$ per T75 in complete FAD medium.

### 2.1.4 Culture of human oral SCC lines

On thawing, oral SCC lines were quickly re-suspended in complete FAD medium, seeded in co-culture with a mitotically inactivated J2-3T3 feeder layer and maintained in a humidified incubator at 37ºC and 5% $CO_2$. The medium was changed three times per week and the cells were split and re-seeded at a density of $1x10^5$ per T75 flask when they reached confluence. When splitting cells, the feeder layer was first removed by incubating with Versene (Life Technologies) for 5 minutes at 37ºC. The oral SCC lines were then lifted using a solution of Trypsin-EDTA (0.25%) (Sigma Aldrich) further diluted in Versene (Life technologies) at a ratio of 1:4 for approximately 10 minutes at 37ºC.

### 2.1.5 Culture of HEK 293 cells

On thawing, HEK 293 cells were quickly re-suspended in supplemented DMEM medium, seeded onto the surface of a T175 flask and maintained in a humidified incubator at 37ºC and 5% $CO_2$. The medium was changed three times per

week and the cells split and re-seeded at a density of $2x10^6$ when they reached confluence. Cells were lifted via pipetting in Versene (Life Technologies).

### 2.1.6 Freezing Cell Stocks

Cells were frozen at a concentration of $5x10^5$ – $1x10^6$ in a solution of 10% Dimethyl Sulfoxide (DMSO) in FBS. A Nalgene container was used to slowly cool the cell suspensions to -80$^o$C before transferring to liquid nitrogen for long-term storage.

## 2.2 Plate Coating

### 2.2.1 Collagen coating

Plates were coated with Collagen Type 1, Rat Tail, (Corning®) at a dilution of 10 µg/cm$^2$ of growth surface in sterile PBS (Sigma Aldrich) at room temperature. After 2hrs, the solution was removed and plates washed 3x in PBS.

### 2.2.2 Fibronectin coating

Plates were coated with Human Fibronectin (Corning®) at a dilution of 1, 5 or 25 µg/ml in sterile PBS (Sigma Aldrich) at room temperature. After 2hrs, the solution was removed and plates washed 3x in PBS.

## 2.3 Genomic Analysis

### 2.3.1 Analysis of the TCGA

TCGA has collected sequencing data from over 500 head and neck cancer patients (http://cancergenome.nih.gov/). This publically accessible database was mined using cBioPortal for information on the frequency, type and location of

NOTCH1 mutations in SCCHN as well as survival statistics (Gao, et al., 2013; Cerami, et al., 2012).

### 2.3.2 Whole exome sequencing

Genomic DNA from passaged oral SCC lines and patient-matched blood was extracted by Dr Nathan Beniach using a Blood & Tissue Kit (Qiagen) with RNase treatment according to the manufacturer's instructions. Samples were eluted in Buffer AE (Qiagen). Whole exome sequencing was performed by Beijing Genomics Institute (BGI, Hong Kong) and raw image files were processed as previously described (Hayes, et al., 2016). The sequencing data for each cell line was mined for mutation frequency as well as the presence, type and location of NOTCH1 mutations.

### 2.3.3 Sanger sequencing

Genomic DNA from passaged oral SCC lines and patient-matched blood was extracted using a Blood & Tissue Kit (Qiagen). PrimeSTAR GXL DNA Polymerase (TaKaRa) was used to perform PCR amplification of Notch receptor genes 1-3 according to the manufacturer's instructions. The PCR products were run on a 1.5% Ultrapure Agarose gel (Life Technologies) and gel extraction was performed using a Gel Extraction Kit (Qiagen) according to the manufacturer's instructions. This work was performed by Dr Kazunori Sunadome. Sanger sequencing was performed by Source Bioscience (UK) and analysed using Lasergene 11 (DNASTAR) and CodonCode Aligner software.

## 2.4 Lentiviral Transduction

### 2.4.1 Plasmid derivation

In order to achieve constitutive expression of NICD, 3xFlagNICD (Ong, et al., 2006) was cloned into the multiple cloning site, and under the SFFV promoter, of the LeGO-iC2 plasmid (Weber, et al., 2008) using gateway cloning. In order to make the LeGO-IC2 vector into a Gateway compatible destination vector, The Gateway Vector Conversion System (ThermoFisher Scientific) was used. An internal ribosome entry

site (IRES) was used to express the mCherry selectable marker. The 3xFlagNICD was a gift from Raphael Kopan (Adgene plasmid #20183), and the LeGO-iC2 plasmid was a gift from Boris Fehse (Adgene plasmid #27345). This work was performed by Dr Kazunori Sunadome and Dr Samuel Woodhouse. SnapGene software was used to visualise the resultant plasmid (Figure 2.1).

In order to perform a knock-down of SPANXA1/2, a SMARTvector Human Doxycycline Inducible shRNA targeting the 3'UTR from Dharmacon was used (V3SH11252-226413760 GTTGAGAGATGTAGCTTC). The mCMV promoter system was utilised and Turbo GFP expression acted as a selectable marker.

Second generation packaging plasmid, psPAX2, and VSV-G envelope expressing plasmid, pMD2.G, were used as packaging vectors. Both were gifts from Didier Trono (Adgene plasmid #12260 and #12259 respectively).

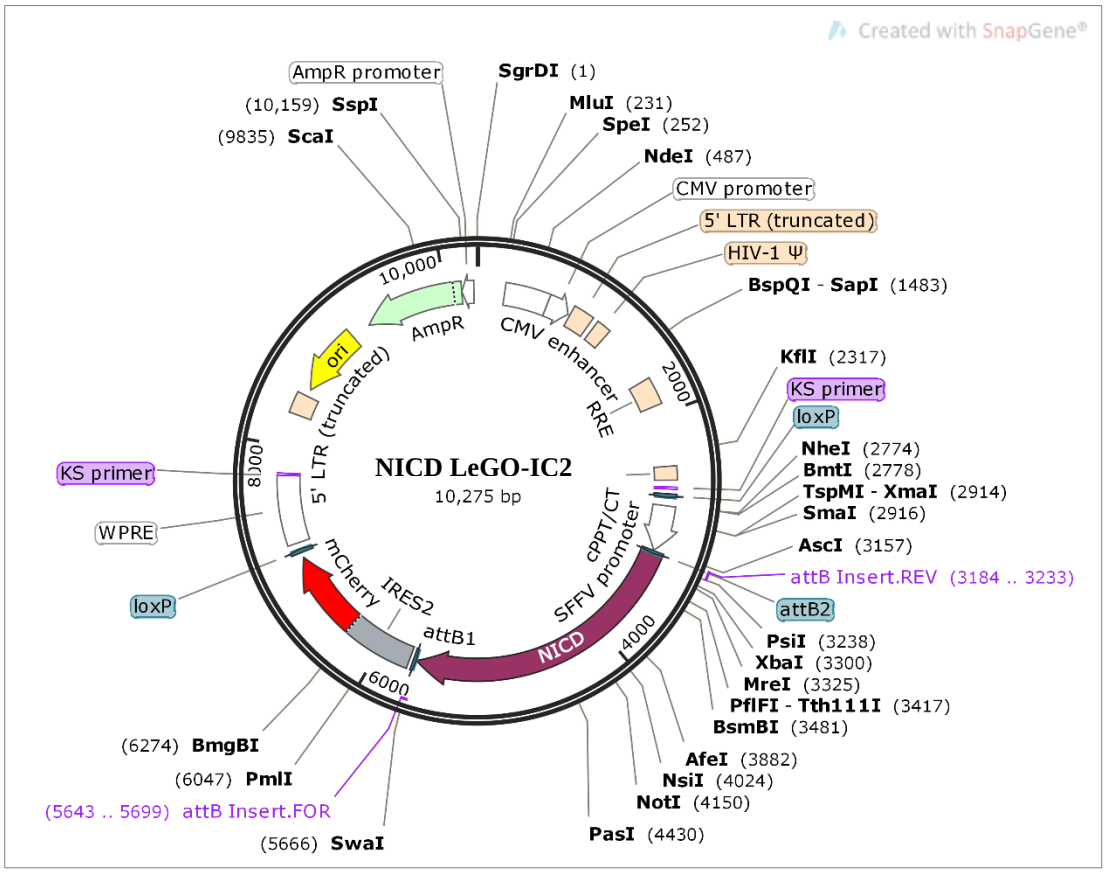


*Figure 2 1: NICD - LeGO-IC2 plasmid map.*

### 2.4.2 Viral component cloning and maxi prep

E. coli competent cells were used as the host system to clone and expand DNA fragments of interest. 1 µl of DNA was gently mixed with 50 µl One Shot Top10 Chemically Competent E. Coli (ThermoFisher Scientific) and incubated on ice for 30 minutes. To allow the DNA to enter the host cell, the solution was then heat shocked for 45 seconds at 42ºC before returning to ice for a further 2 minutes. Samples were then incubated at 37ºC in 500 µl LB Broth (Sigma Aldrich), a growth medium used for the cultivation of E.coli, for 1hr.

As the number of colonies formed can vary significantly, the reaction mixture was seeded at a 10% and 90% density on ampicillin-agar plates to ensure a good density was acquired. Ampicillin resistance was used as a selectable marker (10 µg/ml). The plates were then inverted and incubated overnight at 37ºC.

A small number of colonies were selected using an inoculation loop and incubated at 37ºC in 5 ml LB Broth and 50 µl ampicillin. After 8hrs, 100 µl was transferred into a solution of 1L LB Broth and 1 ml ampicillin for overnight incubation. Maxi prep was performed using an EndoFree Plasmid Maxi Kit (Qiagen) according to the manufacturer's instructions.

### 2.4.3 Lentiviral packaging

HEK293 cells, seeded at a concentration of $1x10^7$ per T175 flask in supplemented DMEM medium, were used as the host system. At 24hrs, 15 µg of lentiviral vector, 11.25 µg psPax2 and 2.75 µg pMD2.G were introduced. JetPRIME® (Polyplus Transfection) was used as a transfection reagent according to the manufacturer's guidelines for lentiviral production.

At 48hrs, cell medium was changed. At 72 and 96hrs, medium was collected and filtered through a Corning® 0.45 µm Bottle Top Vacuum Filter System (Sigma Aldrich). Lenti-X Concentrator (Clontech) was added at a dilution of 1:4 to the resultant filtrate and the solution was incubated at 4ºC. After 24hrs, the lentivirus particles were pelleted by centrifuging at 15,000 RPM for 45 minutes.

### 2.4.4 Lentiviral transduction

The SJG6 oral SCC cell line was seeded at a density of $1x10^6$ per well of a collagen coated 6 well plate. Derived lentivirus and 5 µg/ml polybrene (Sigma Aldrich) was diluted in serum and antibiotic free FAD medium and incubated with cells at 37ºC. At 72hrs, the medium was replaced with complete FAD. At 96hrs, cells were collected and sorted for the expression of markers of interest. To select for constitutively expressing NICD cells, Fluorescence-Activated Cell Sorting (FACS) for mCherry expression was performed using a BD Aria II by the BRC Core Facility, King's College London. In order to select for cells which had incorporated the SPANXA1/2 shRNA, puromycin selection was performed at a concentration of 1 µg/ml. Both sets of cell lines were expanded in culture and stocks were frozen in liquid nitrogen for future use.

### 2.4.5 Induction of SPANXA1/2 shRNA

In order to induce the SPANXA1/2 shRNA, doxycycline was introduced to the cell medium at a concentration of 1.5 µg/ml. The co-expression of turbo-GFP acted as a marker for successful transcription of the shRNA. At 48hrs post-induction, cells were seeded for *in vitro* assays and RNA and protein samples were collected.

## 2.5 Molecular Biology

### 2.5.1 RNA isolation

Total RNA was collected from cell cultures. Cells were first lifted using a solution of Trypsin-EDTA (0.25%) (Sigma Aldrich) further diluted in Versene (Life technologies) at a ratio of 1:4 for approximately 10 minutes at 37ºC, then centrifuged at 1,200rpm for 3 minutes. The supernatant was removed and the cell pellet was re-suspended in 350 µl RLT Lysis Buffer with 1% β-Mercaptoethanol.

Total RNA was also collected from xenograft tumour samples which had been embedded in OCT and frozen at -80ºC. A cryostat was used to cut 50 µm sections, which were collected in 350 µl RLT Lysis Buffer with 1% β-Mercaptoethanol. A gentleMACS dissociator (Miltenyi Biotec) was used to homogenise samples.

For both sample types, the RNeasy Mini Kit (Qiagen) was used according to the manufacturer's instructions. RNA quantity was calculated using a NanoDrop spectrophotometer by measuring sample absorbance at 260nm. The ratio of absorbance at 230/260nm and 260/280nm was used to ensure samples were acceptably pure (based on a score of approximately 2.0-2.2 and 2.0 respectively). Total RNA was stored at -80$^{o}$C.

### 2.5.2 Reverse transcription

The SuperScript III Reverse Transcriptase kit (Life Technologies) was used, according to the manufacturer's instructions, to synthesise cDNA from 500 ng total RNA. Derived cDNA was diluted 1:10 in RNase free water and stored at -80$^{o}$C.

### 2.5.3 Quantitative Real Time Polymerase Chain Reaction (RT-qPCR)

RT-qPCR reactions were set up using TaqMan ® probes (Invitrogen) as detailed in Table 2.2. Samples were run in triplicates on a 384 well plate and analysed using a CFX 384 Touch RT-qPCR machine (Bio-Rad). The RT-qPCR reaction mix was prepared as described in Table 2.3. The reactions took place under conditions described in Table 2.4. Gene expression was normalised to housekeeping probes, GAPDH and 18S, and expression levels were calculated using the ΔΔCT method. Statistical analysis was performed using GraphPad Prism 7. Based on a normal distribution of sample means, a student's t-test was used to test the null hypothesis that the mean values of two groups are equal. A t-test value less than 0.05 was considered a statistically significant difference.

### 2.5.4 Human NOTCH1 Signalling Pathway RT$^{2}$ Profiler Array

The Human NOTCH Signalling Pathway RT$^{2}$ Profiler Array (Qiagen) was used according to manufacturer's guidelines. Each well of a 96 well plate contained a single probe for a panel of 35 NOTCH related genes, 5 housekeeping genes and patented controls to monitor PCR quality and efficiency. The array allows for the simultaneous RT-qPCR expression analysis of the 35 NOTCH-related genes in two cDNA samples. Similar to other RT-qPCR reactions, a solution of Taqman ® Fast

Universal PCR Master Mix, cDNA and nuclease free water was added to the probes in the equivalent proportions to those detailed in Table 2.3. The reactions took place under conditions described in Table 2.4. Gene expression was normalised to housekeeping probes, GAPDH and 18S, and expression levels were calculated using the ΔΔCT method. Statistical analysis was performed using GraphPad Prism 7. Based on a normal distribution of sample means, a student's t-test was used to test the null hypothesis that the mean values of two groups are equal. A t-test value less than 0.05 was considered a statistically significant difference.

Table 2 2: TaqMan ® probes

| ***Probe*** | ***ID*** | ***Supplier*** |
|---|---|---|
| *NOTCH1* | Hs01062014_m1 | Invitrogen |
| *Custom mCherry* | **Forward Primer Sequence:** GACCACCTACAAGGCCAAGAAG **Reverse Primer Sequence:** AGGTGATGTCCAACTTGATGTTGA **Probe Sequence:** CAGCTGCCCGGCGCCTACA | Invitrogen |
| *SPANXA1+A2* | Hs03007483_gH | Invitrogen |
| *SPANXB1* | Hs02387419_gH | Invitrogen |
| *SPANXC+D* | Hs04191733_gH | Invitrogen |
| *TMEM27* | Hs00252907_m1 | Invitrogen |
| *HEY1* | Hs01114113_m1 | Invitrogen |
| *CTH* | Hs00542282_m1 | Invitrogen |
| *ITGBL1* | Hs01557019_m1 | Invitrogen |
| *ITGB6* | Hs00168458_m1 | Invitrogen |
| *GAPDH* | Hs02786624_g1 | Invitrogen |
| *18S* | Hs01375212_g1 | Invitrogen |

Table 2 3: Taqman® RT-qPCR reaction mix

| ***Component*** | ***Volume for one reaction (µl)*** |
|---|---|
| *Taqman ® Fast Universal PCR Master Mix (2x)* | 5 |
| *TaqMan ® Probe* | 0.5 |
| *Nuclease Free Water* | 3.5 |
| *cDNA* | 1 |
| ***Total Volume*** | **10** |

Table 2 4: TaqMan ® FAST RT-qPCR method

| ***Cycles*** | ***Step*** | ***Time (seconds)*** | ***Temperature (°C)*** |
|---|---|---|---|
| *1* | Activate | 20 | 95 |
| *40* | Denature | 1 | 95 |
| | Anneal / Extend | 20 | 60 |

### 2.5.5 Preparation of protein lysates

Protein lysates were collected from cells cultured on collagen-coated six well plates. Plates were kept on ice, the cell medium was removed and wells were washed twice with ice cold PBS. 100 µl RIPA buffer was added to each well and cells were collected into a pre-cooled Eppendorf using a cell scraper. RIPA buffer composition is described in Table 2.5; stocks were aliquoted and frozen at -20°C for future use.

Samples were left to lyse on ice, with frequent agitation, for 30 minutes before centrifuging at 15,000 rpm for 20 minutes at 4°C. The supernatant, which contained the protein lysate, was then transferred to a fresh pre-cooled Eppendorf. Protein concentration was calculated using a Pierce BCA Protein Assay Kit (ThermoFisher Scientific) according to the manufacturer's instructions and samples were stored at -80°C for future use.

Table 2 5: RIPA buffer composition

***10x RIPA Buffer (New England BioLabs)***

| ***Component*** | ***Quantity*** |
|---|---|
| *Tris HCl (pH 7.5)* | 20 mM |
| *NaCl* | 150 mM |
| *$Na_2EDTA$* *EGTA* | 1 mM |
| *NP-40* | 1 % |
| *Sodium deoxycholate* | 1 % |
| *Sodium pyrophosphate* | 2.5 mM |
| *β-glycerophosphate* | 1 mM |
| *$Na_3VO_4$* | 1 mM |
| *Leupeptin* | 1 µg/ml |

***1x Complete RIPA Buffer***

| ***Component*** | ***Quantity*** |
|---|---|
| 10x RIPA | 1 ml |
| $ddH_2O$ | 9 ml |
| PhosSTOP Inhibitor Cocktail tablet (Roche) | 1 tablet |
| Complete Mini EDTA-free Protease Inhibitor Cocktail tablet (Roche) | 1 tablet |

### 2.5.6 Western blot

10 µg protein lysate was diluted with RIPA buffer to a volume of 7.5 µl and added to 2.5 µl 4x Laemmli sample buffer containing 10% β-mercaptoethanol (Bio-Rad). Samples were reduced and denatured by heating to 95ºC for 5 minutes.

The 10 µl lysates were loaded into pre-cast 4-15% Mini-PROTEAN® TGX™ Gels (Bio-Rad) alongside Precision Plus Protein™ Dual Colour Standard (Bio-Rad) and run at 300V in Tris/Glycine/SDS Running Buffer (Bio-Rad). The run was stopped when the lysates reached the indicator line at the bottom of the gel.

Protein was transferred from gels to membranes using a Trans-Blot® Turbo™ Mini PVDF Transfer Pack. As cleaved NOTCH1 was the protein of interest (approximately 100 kDa), the high molecular weight setting on the Trans-Blot Turbo System (Bio-Rad) was used.

Resultant membranes were washed in TBST (a mixture of Tris Buffered Saline and Tween 20), the components of which are described in Table 2.6.

Table 2 6: TBST components

***10x TBS***

| ***Component*** | **Quantity** |
|---|---|
| *NaCl* | 150 mM |
| *KCl* | 2 mM |
| *Tris* | 25 mM |
| *$ddH_2O$* | |
| ***Adjust pH to 7.4 with HCl*** | |

***1x TBST***

| **Component** | **Quantity** |
|---|---|
| 10x TBS | 100 ml |
| $ddH_2O$ | 900 ml |
| Tween20 | 1 ml |

Membranes were blocked for one hour at room temperature in 5% skimmed milk powder diluted in TBST. As the predicted molecular weights of cleaved NOTCH1 and the loading control (Cyclophilin B) was approximately 100kDa and 20kDa respectively, membranes were cut at the 37kDa ladder mark and staining was performed simultaneously. Primary antibodies were used at 1:1,000 in the blocking buffer. Staining was performed overnight at 4$^{o}$C and membranes were washed for 3 x 10 minutes in TBST prior to introduction of the species-specific secondary antibody. Secondary antibodies were used at 1:10,000 in 5% Bovine Serum Albumin (BSA; Sigma Aldrich) diluted in TBST. After staining for 2hrs at room temperature, a further 3 x 10 minutes washes in TBST were performed. Table 2.7 details the antibodies used.

Clarity™ ECL Western Blotting Substrate (Bio-Rad) was used according to the manufacturer's guidelines to image the membranes. Imaging was performed using a ChemiDoc Touch (Bio-Rad).

Table 2 7: Western blot antibodies

| ***Antibody (Primary)*** | ***ID*** | ***Supplier*** |
|---|---|---|
| *Cleaved NOTCH1 (Rabbit)* | Val1744 | Cell Signalling Technologies |
| *Cyclophilin B (Mouse)* | MAB5410 | R&D Systems |

| ***Antibody (Secondary)*** | ***ID*** | ***Supplier*** |
|---|---|---|
| *Peroxidase AffiniPure Donkey Anti-Rabbit IgG (H+L)* | 711-035-152-JIR | Stratech |
| *Peroxidase AffiniPure Donkey Anti-Mouse IgG (H+L)* | 715-035-150-JIR | Stratech |

### 2.5.7 Immunocytochemistry

Cells were seeded at a density of $2x10^3$ / well in a collagen-coated flat bottomed 96 well plate in supplemented KSFM medium. Prior to staining, cells were fixed for 10 minutes in 4% paraformaldehyde (PFA; diluted in 1x PBS) and permeabilised for a further 10 minutes in 0.05% Triton-X (Sigma Aldrich; diluted in deionised water). Non-specific antibody binding was inhibited by blocking for 1hr at room temperature. The blocking buffer composition is detailed in Table 2.8.

Primary antibodies were diluted in blocking buffer and samples incubated overnight at 4ºC. The primary antibodies and the concentrations used are detailed in Table 2.9.

Table 2 8: Blocking buffer composition

| ***Component*** | ***Quantity*** |
|---|---|
| *1x TBS (Table 6; diluted in deionised water)* | 0.01 M |
| *Donkey Serum (Sigma Aldrich)* | 10 % |
| *BSA (Sigma Aldrich)* | 0.3 % |
| *Triton (Sigma Aldrich)* | 0.05 % |
| *Tween20 (Sigma Aldrich)* | 0.05 % |
| *Gelatin from Fish Skin (Sigma Aldrich)* | 0.25 % |

Table 2 9: Primary antibodies for immunocytochemistry and immunohistochemistry

| ***Antibody*** | ***Species*** | ***Reference*** | ***Supplier*** | ***Dilution*** |
|---|---|---|---|---|
| *NOTCH1* | Rabbit | ab27526 | Abcam | 1:200 |
| *SPANXA1 / A2* | Rabbit | ab115632 | Abcam | 1:200 |
| *Transglutaminase* | Mouse | (Ruhrberg, et al., 1996) | In house | 1:500 |
| *RFP* | Rabbit | 600-401-379 | Rockland Inc. | 1:100 |
| *CD31* | Rat | 553370 | BD Pharming | 1:200 |

Following 3 x 10 minute washes in TBS, samples were stained with appropriate species-specific Alexa Fluor conjugated secondary antibodies (1:1,000), DAPI (Life Tech; 1 µg/ml) and Cell Mask Deep Red Plasma Membrane Stain (ThermoFisher Scientific; 1:500) in blocking buffer for 1hr at room temperature. Samples were then washed 3 x 10 minutes in TBS before imaging with the Perkin Elmer Operetta High Content Imaging System. Analysis pipelines were derived using Harmony Software, as depicted in Figure 2.2.

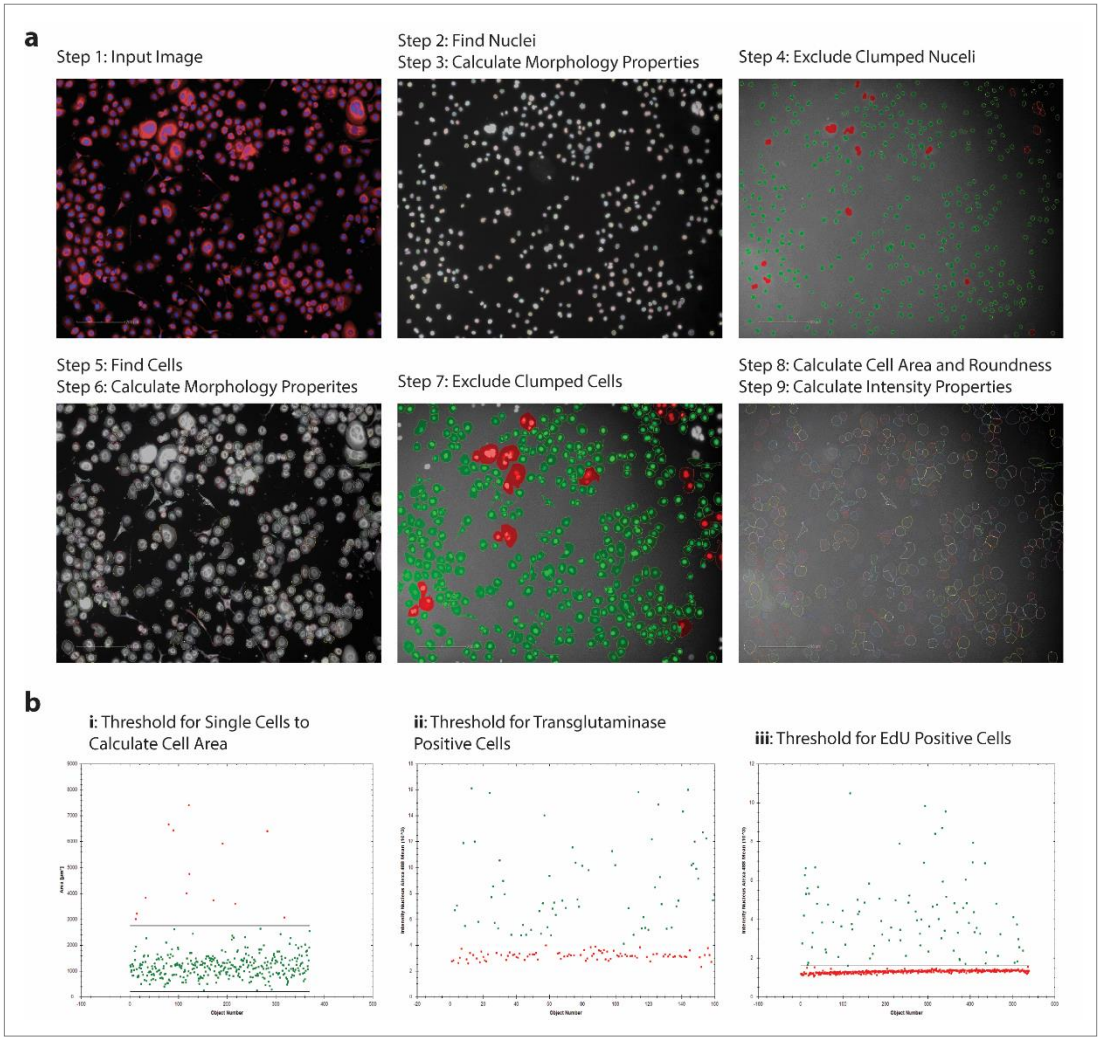


*Figure 2 2: a) Pipeline for analysis of cells using Harmony Software on the Perkin Elmer High Content Imaging System: Images were acquired and DAPI staining was used to find nuclei. Nuclei morphology was calculated and those measuring over 500 µm$^2$ were considered unlikely to be single nuclei and excluded from further analysis. Based on selected nuclei, Cell Mask Deep Red Plasma Membrane Stain was used to find cell boarders. Cell morphology was calculated and selections considered unlikely to be single cells were excluded (detailed further in bi). Respective staining intensities were then calculated for each cell and the mean value for cells per well was exported. b) Downstream pipelines. bi) In order to accurately investigate differences in cell area, thresholds were applied to ensure only single cells were included in downstream analysis: cells measuring under 400 µm$^2$ were considered debris and cells measuring over 3000 µm$^2$ were considered unlikely to be single cells. bii and biii) Cells could be considered either Transglutaminase 1 or EdU positive or negative. As such, a staining intensity threshold was applied in order to count the number of positive cells as a percentage of the total cell population. A threshold of 4 x 10$^3$ and 1.8 x 10$^3$ (a.u.) was applied for transglutaminase and EdU respectively.*

### 2.5.8 Microarray

Total RNA was extracted from passaged oral SCC line SJG6 (Table 2.1) transformed with a lentiviral vector either expressing NICD or an empty control (Figure 2.2). Three biological replicas were used for each line.

The microarray was performed by King's Genomics Centre (King's College London, London) using the Affymetrix GCS3000 system. Briefly, DNA probes able to capture the whole human transcriptome were deposited via photolithography onto silicon chips (Affymetrix GeneChip® Human Exon 1.0 ST array). The total RNA samples underwent reverse transcription to cDNA followed by *in vitro* transcription to cRNA. Note that only polyadenylated RNA undergoes reverse transcription; therefore, the microarray identifies mRNA expression but not that of microRNA or other non-polyadenylated sequences. Samples were then biotin-labelled, fragmented and hybridised to complementary sequences on the chips. Wash steps removed any unbound fragments prior to staining and optical detection.

Statistical analysis of the raw microarray data was performed using Genespring 14.5. The raw optical image of the hybridised chip was processed alongside an annotation file that describes the layout of the chip (HuGene 2_0). Differential significance between the two experimental groups was assessed using a 2-way analysis of variance (ANOVA) and quality control was assessed via Principal Component Analysis. Data was then filtered by expression; transcripts that did not express above the $20^{th}$ percentile in any of the six samples were removed from further analysis to reduce background. Differences in fold change between the two experimental groups were assessed and a cut-off of 1.2 fold difference in expression was applied. A Go-Term and Gene Set Enrichment Analysis (GSEA) was run prior to exporting the resultant gene list and fold change values to Ingenuity Pathway Analysis (IPA) Software.

Top canonical pathways and molecular and cellular functions with an Activation Z-Score greater than 2 or less than -2 (considered significant by software guidelines) were identified by the IPA core analysis platform for further analysis. Gene members that were predicted by the IPA database or published literature to be directly or indirectly linked to NOTCH signalling were identified and possible pathways were explored. The Molecule Activity Predictor (MAP) tool was used to simulate

directional consequence of known changes in gene expression on other pathway members.

## 2.6 *In Vitro* Assays

### 2.6.1 Colony formation assay

Cells were seeded at a density of 500 cells per well onto a J2-3T3 feeder layer in a 6 well plate. Supplemented FAD medium was replaced every 2-3 days. On day 14, the remaining feeder cells were removed by pipetting in PBS and SCC colonies were stained for 2hrs with 1% Rhodanile Blue. Plates were imaged using a Molecular Imager Gel Doc XR+ (BioRAD), and analysed using the Colony Area plug-in for FIJI. Statistical analysis was performed using GraphPad Prism 7. Based on a normal distribution of sample means, a student's t-test was used to test the null hypothesis that the mean values of two groups are equal. A t-test value less than 0.05 was considered a statistically significant difference.

### 2.6.2 EdU and cell morphology assay

Cells were seeded onto fibronectin-coated 96 well plates at a density of $2x10^3$ cells / well in KSFM. Cells were removed from the J2 feeder layer to ensure no feeder contamination during analysis. KSFM was used to promote single cell attachment for high content analysis. At 22hrs, pre-warmed EdU (Life Technologies) was added to the cell medium at a concentration of 10 µM. At 24hrs, cells were fixed for 10 minutes in 4% PFA (Sigma Aldrich). Following 3 x washes in PBS, the Click-iT Alexa Fluor 488 Imaging Kit (Life Technologies) was used according to the manufacturer's instructions to measure proliferation over the 2hr period. Nuclei were stained with DAPI (ThermoFisher Scientific) at a concentration of 1 µg/ml and cytoplasm was stained with Cell Mask Deep Red Plasma Stain at a concentration of 1:500 for 1hr at room temperature. The percentage of EdU positive cells, cell area and cell roundness was calculated using Harmony Software on the Operetta High Content Imaging System (PerkinElmer). The derived pipelines are detailed in Figure 2.2. Statistical analysis was performed using GraphPad Prism 7. Based on a normal distribution of

sample means, a student's t-test was used to test the null hypothesis that the mean values of two groups are equal. A t-test value less than 0.05 was considered a statistically significant difference.

### 2.6.3 Differentiation assay

Cells were seeded onto fibronectin-coated 96 well plates at a density of $2x10^3$ cells / well in KSFM medium. At 24hrs post-seeding, cells were fixed and stained for Transglutaminase 1 via the immunocytochemistry method previously detailed. The percentage of differentiated cells was calculated using Harmony Software on the Operetta High Content Imaging System (PerkinElmer). The derived pipeline is detailed in Figure 2.2. Statistical analysis was performed using GraphPad Prism 7. Based on a normal distribution of sample means, a student's t-test was used to test the null hypothesis that the mean values of two groups are equal. A t-test value less than 0.05 was considered a statistically significant difference.

### 2.6.4 Cell migration assay

Cells were seeded onto collagen-coated 96 well image-lock plates (Essen BioScience) at a density of $5x10^4$ cells / well in KSFM medium and mitotically inhibited by incubation with 4 µg/ml Mitomycin-C (Sigma Aldrich) for 2hrs at 37ºC. A wound was created using the Essen 96-Well Wound Maker (Essen BioScience) according to the manufacturer's instructions. The plates were secured in the IncuCyte Zoom (Essen BioScience) and imaged once per hour at 10x magnification. The IncuCyte Zoom software was used to calculate the confluence of cells in the wound area over a period of 20hrs. The analysis process is detailed in Figure 2.3. Statistical analysis was performed using GraphPad Prism 7. Based on a normal distribution of sample means, a student's t-test was used to test the null hypothesis that the mean values of two groups are equal. A t-test value less than 0.05 at each time point was considered a statistically significant difference.

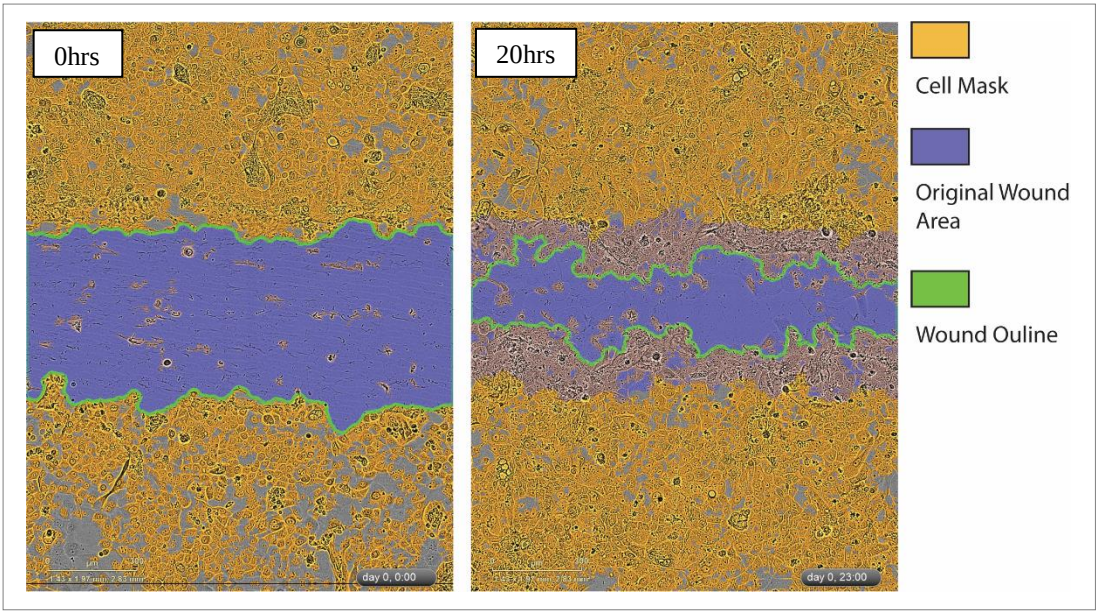


*Figure 2 3: Analysis of cell migration assays using the IncuCyte Zoom Software. A number of phase focus images from different wells and time points were used as a representative cohort; cells were characterised and a cell mask applied (orange). The software calculates the original wound area and creates a new wound outline for each time lapse image (green). Each hour, the percentage of original wound area overlaid with the cell mask was measured and data exported for analysis.*

## 2.7 Xenografts

### 2.7.1 Establishing the xenograft

All animal experiments were subject to local ethical approval and performed under the terms of the UK Government Home Office Licence. The technical staff of the animal facility in King's College London maintained the mice according to University guidelines. Mice were housed in a pathogen-free environment and exposed to a 12hr light / dark cycle. Caging, food, water and bedding were autoclaved prior to use. This experiment was performed in collaboration with Dr Inês Sequeira.

The role of NICD *in vivo* was explored using a tongue xenograft assay that recapitulates aspects of SCCHN (Goldie, et al., 2012; Benaich, et al., 2014). The methodology was derived from previously published literature, which has been well reviewed by Sano and Myers (Sano & Myers, 2009). Female NSG (Jax Strain) mice, 4-6 weeks old, were sourced from Charles River and acclimatised for two weeks. Mice were anesthetised via intraperitoneal injection of ketamine and xylazine, as previously

described by Sequeira et al. (Sequeira, et al., 2014). For a 2 ml solution, 0.5 ml Imalgene 1000 (Ketamine, 100 mg/ml, Merial) was mixed with 0.25 ml Rompun Injection Solution 2% (xylazine hydrochloride, Bayer) and 1.25 ml PBS. A dose of 0.1 ml / 25 g body weight was administered using a 0.3 ml U-100 insulin syringe with needle (VWR). The anaesthetised mice were maintained on a heated block for the duration of the procedure.

The SJG6 oral SCC cell lines (Table 2.1), transduced with either NICD or a blank vector control, were re-suspended in pre-warmed PBS. Forceps were used to secure the mouse tongues and a 30-gauge hypodermic needle with a 0.3 ml insulin syringe was used to perform a submucosal injection of either $10^5$ or $10^4$ cells, in a volume of 30 µl, into the lateral tongue. An analgesic of 1.5 µl Carprieve, diluted in 30 µl sterile water, was administered by subcutaneous injection using a 0.3 ml U-100 insulin syringe with needle.

Mice were observed until they had recovered from anaesthesia and were housed with paper bedding, paper lining and gel food. Mice were weighed twice per week and culled on ethical grounds if they lost more than 20% of their body weight.

### 2.7.2 Harvesting the tumours

Mice were sacrificed on day 30 or 60 via cervical dislocation. The tongues were removed and washed in PBS. 2hrs prior to harvesting, mice were injected intraperitoneally with EdU (ThermoFisher Scientific) at a concentration of 50 µg / gram of body weight using a 0.3 ml U-100 insulin syringe with needle.

### 2.7.3 Macroscopic imaging

The dorsal and ventral surfaces of the tongue were imaged using the Nikon SMZ18 Stereo Zoom Microscope and DS-R12 camera. FIJI software was used to measure the volume of visible tumours.

### 2.7.4 Embedding

Following macroscopic imaging, the tongues were embedded in OCT (VWR) in 22 $mm^2$ square Peel-A-Way embedding moulds (Sigma Aldrich) and frozen at -80$^oC$ for future use.

### 2.7.5 Sectioning

Frozen OCT samples were sectioned using a CryoStar NX70 (ThermoFisher Scientific). For H&E and immunohistochemistry staining, 8 and 10 µm samples respectively were mounted onto slides and stored at -80$^oC$ for future use. For PCR, 50 µm sections, collected from several tumour depths, were collected into lysis buffer and processed as previously described (section 2.5.1-2.5.3).

### 2.7.6 H&E staining

H&E staining was performed according to standard protocols. OCT sections of 8 µm were fixed in 4% PFA (diluted in 1x PBS) for 10 minutes at room temperature. Slides were then washed in 1x PBS followed by Millipore water prior to staining with Hematoxylin solution for 1 minute. Slides were again washed 3 x in distilled water and 1x in Millipore water before counter-staining for 1 minute in Eosin. Slides were dehydrated through 10 second incubations in 75%, 90% and 2 x 100% ethanol, and cleared via 2 x 5 minute incubations in xylene. Finally, samples were mounted in DPX mounting medium (Sigma Aldrich) and imaged using the NanoZoomer 2.RS (Hamamatsu).

### 2.7.7 Immunohistochemistry

OCT sections of 10 µm were thawed for 5 minutes at room temperature. A Dako Pen (Sigma Aldrich) was used to form a hydrophobic seal around the sections for staining. The sections were washed twice in PBS, fixed for 2 minutes in 2% PFA and washed a further 2x prior to permeabilising with 0.5% Trition X-100 for 10 minutes. The blocking buffer detailed in Table 2.8 was used to block samples for 1hr at room temperature.

Primary antibodies were diluted in blocking buffer and samples were incubated overnight at 4$^{o}$C. The primary antibodies used are detailed in Table 2.9. Following 3 x 10 minute washes in TBS, samples were stained with appropriate species-specific Alexa Fluor conjugated secondary antibodies, diluted 1:200, and DAPI (Life Tech), diluted 1 µg / ml, in blocking buffer for 1hr at room temperature. Samples were again washed 3 x 10 minutes in TBS before mounting with Prolong Gold Anti-fade Reagent (Invitrogen) according to the manufacturer's guidelines. Imaging was performed using an A1 Nikon Upright Confocal Microscope (located at the Nikon Imaging Centre, King's College London) and NIS Elements Software.

FIJI software was used to measure the area of positive Transglutaminase 1 staining (488 channel) as a percentage of total tumour area. Statistical analysis was performed using GraphPad Prism 7. Based on a normal distribution of sample means, a student's t-test was used to test the null hypothesis that the mean values of two groups are equal. A t-test value less than 0.05 was considered a statistically significant difference.

### 2.7.8 EdU

Mice were injected intraperitoneally with EdU at a concentration of 10 mg / kg body weight 2hrs prior to harvesting. The Click IT EdU kit was used to fluorescently label 10 µm OCT sections according to manufacturer's instructions. Cell nuclei were stained with DAPI, diluted 1 µg/ml, and FIJI was used to calculate proliferating cells as a percentage of total tumour cells. The tumour area was selected, an image threshold was applied for both DAPI and EdU (Alexa Flour 488) and cell number was calculated using the measurement tool. Statistical analysis was performed using GraphPad Prism 7. Based on a normal distribution of sample means, a student's t-test was used to test the null hypothesis that the mean values of two groups are equal. A t-test value less than 0.05 was considered a statistically significant difference.

# Chapter 3

## Validation and Rescue of a Truncating NOTCH1 Mutation in Oral SCC Line SJG6

---

This chapter provides the building blocks for this research project. SCCHN patient derived cell lines have been characterised and the truncating NOTCH1 mutation identified in SJG6 was validated. The rescue of SJG6 via lentiviral transduction of NICD was used to create a tool for studying the role of NOTCH1 in SCCHN.

---

### 3.1 Analysis of NOTCH1 Mutations in SCCHN Patient Derived Cell Lines

Cell lines have been derived from 21 anonymised SCCHN patient biopsies and named SJG after the initials of the scientist principally responsible for their derivation, Stephen J Goldie. The biopsies were obtained from surplus material taken for investigative histological examination. Females made up 57% of the sample group and the median age was 55. All samples were HPV negative.

Of the 21 SJG lines, patient matched blood was available for 17 and 16 passed DNA quality control measures for whole exome sequencing. Whole exome sequencing confirmed the lines were representative of the mutational spectrum of primary oral SCC lines in The Cancer Genome Atlas (Hayes, et al., 2016). Patient and primary tumour data is detailed in Table 2.1.

The number of nonsynonymous somatic mutations in the lines varied from 32 to 639 (Figure 3.1). Of the 16 sequenced lines, 3 (18.75%) were found to harbour mutations in NOTCH1, namely SJG6, SJG17 and SJG41. Further, 2 of 4 mutations (50%) were found to be truncating, both of which were identified in the SJG6 line (Table 3.1). Sanger sequencing performed by Dr Kazunori Sunadome confirmed the presence of the two heterozygous truncating mutations. There was no correlation

between NOTCH1 mutation status and the mutation count per line. The two nonsynonymous SNV mutations and one of the truncating mutations were located in the EGF-like ligand binding domain of the NOTCH1 receptor. The second truncating mutation was recorded in the TMD (Figure 3.2)

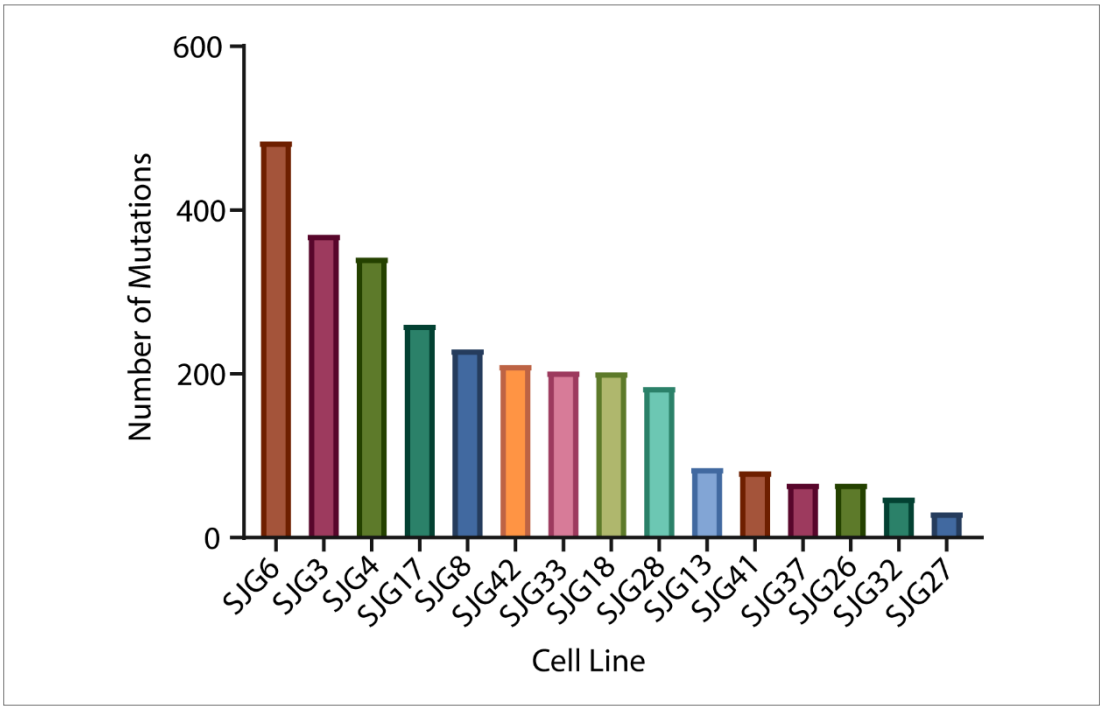


*Figure 3 1: Frequency of somatic mutations identified by whole genome sequencing in SJG lines.*

Table 3_1: NOTCH1 mutations in established SJG lines

| ***Line*** | ***CDS Mutation*** | ***AA Mutation*** | ***Genome Mutation*** | ***Mutation Effect*** | ***Mutation Type*** |
|---|---|---|---|---|---|
| *SJG6* | C936A | C312X | G → T | Stopgain SNV | Heterozygous |
| *SJG6* | G5529A | W1843X | C → T | Stopgain SNV | Heterozygous |
| *SJG17* | C2903T | T968M | G → A | Nonsynonymous SNV | Heterozygous |
| *SJG41* | G3836A | R1279H | C → T | Nonsynonymous SNV | Heterozygous |

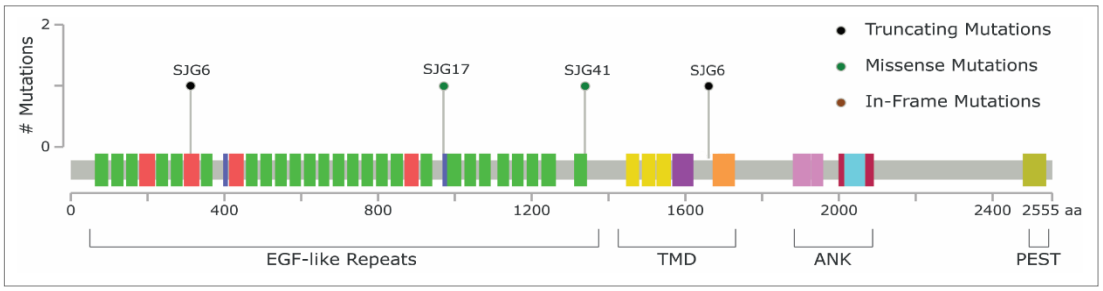


*Figure 3 2: Location of NOTCH1 mutations in patient derived SJG lines. EGF-like Repeats = epidermal growth factor-like repeats. TMD = transmembrane domain. ANK = ankyrin domain. PEST = proline, glutamic acid, serine, threonine-rich domain. Figure created using cBioPortal (Cerami, et al., 2012; Gao, et al., 2013).*

## 3.2 Validation of Inactivating NOTCH1 Mutations in SJG6

As the aim of this study is to investigate the effect of changes in NOTCH1 expression on changes in cell behaviour in SCCHN, the truncating mutations in SJG6 made it the most promising line for further investigation. I sought to further characterise and validate these potentially inactivating mutations.

### 3.2.1 Relative Expression of NOTCH1 in SJG6: mRNA Level

In order to investigate the relative expression of NOTCH1 in the SJG6 line, a comparative RT-qPCR was performed alongside two SJG lines that did not harbour any NOTCH pathway mutations: SJG13 (Figure 3.3a) and SJG32 (Figure 3.3.b). NOTCH1 expression was found to be significantly reduced in SJG6 compared to said lines: approximately 12% and 18% of SJG13 and SJG32 respectively. There was no significant difference between the expression levels of NOTCH1 in SJG13 and SJG32.

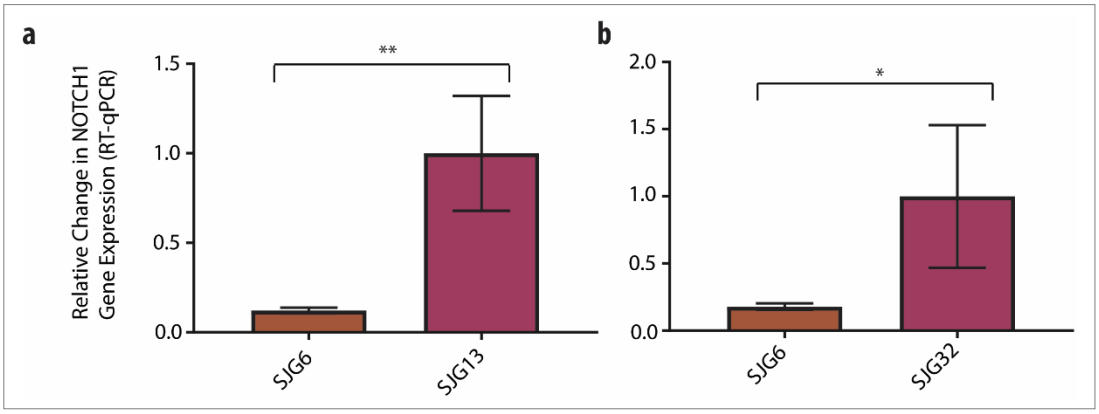


*Figure 3 3: RT-qPCR analysis of NOTCH1 expression in SJG6 compared to two SJG lines that do not harbour any NOTCH pathway mutations; SJG13 (a) and SJG32 (b). Expression was normalised to s18 and GAPDH housekeeping genes. n=3. * = student's t-test value <0.05. ** = student's t-test value <0.01. RT*

### 3.2.2 Relative Expression of NOTCH1 in SJG6: Protein Level

In order to investigate the expression of NOTCH1 at the protein level, western blots were performed (Figure 3.4). SJG6 lysate was run with SJG32 for comparison. A cleaved NOTCH1 antibody that recognises an epitope downstream of both truncating mutations was used. To validate the cleaved NOTCH1 antibody, a siRNA-mediated knockdown of NOTCH1 in SJG32 was undertaken. DharmaFECT NOTCH1 siRNA and control transfection reagents were used according to manufacturer's guidelines. Following a 72hr incubation, protein lysates were derived from respective cell cultures. A clear reduction in the level of cleaved NOTCH1 expression can be seen in the SJG32 knockdown compared to the original line, GAPDH control and scrambled control line, hence confirming the specificity of the antibody. There was no cleaved NOTCH1 band in either of the SJG6 biological replicates, suggesting a lack of protein expression.

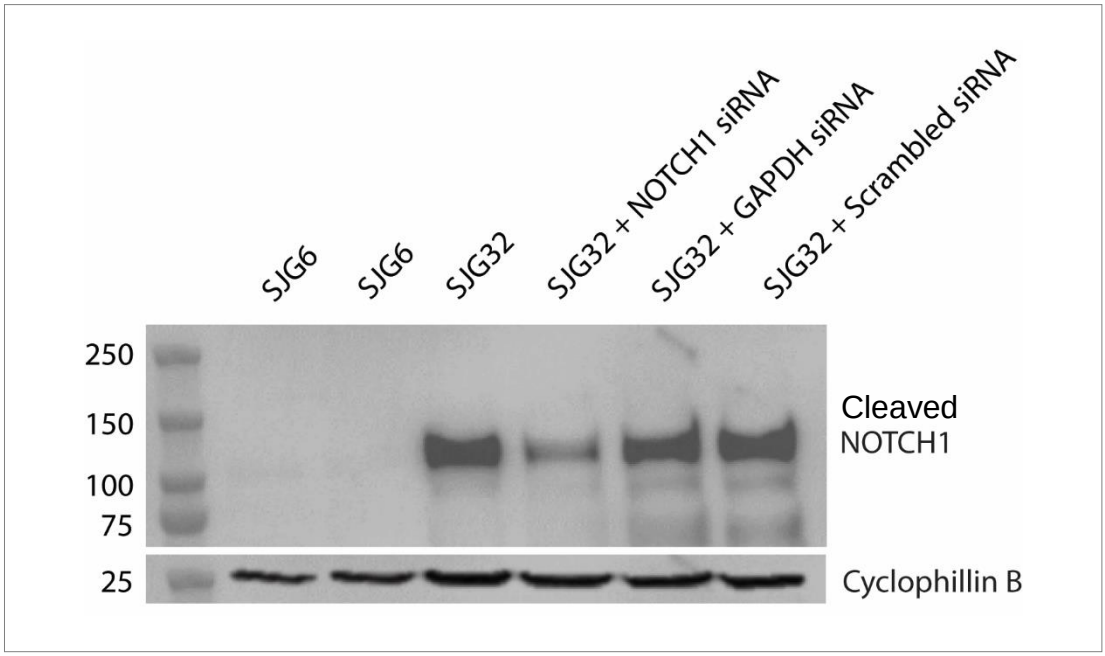


*Figure 3 4: Western blot showing the protein expression of cleaved NOTCH1 in SJG6, SJG32, SJG32 + NOTCH1 siRNA, SJG32 + GAPDH siRNA control and SJG32 + scrambled siRNA control.*

## 3.3 NOTCH Signalling Pathway in SJG6

### 3.3.1 Mutational Landscape of the NOTCH Signalling Pathway in SJG Lines

Although NOTCH1 is the focus of this study, the four NOTCH receptors are highly conserved, meaning there is potential for compensation. Whole exome sequencing did not identify any somatic mutations in the NOTCH 2-4 receptors in SJG6, SJG13 or SJG32. However, deeper-depth Sanger sequencing at the NOTCH target region identified a small number of further mutations. Of these mutations, only one in SJG6 was found to be both in a coding region and non-synonymous: namely, a homozygous SNV in the PEST domain of NOTCH3 (A2223). Sanger sequencing was performed by Dr Kazunori Sunadome.

Whole exome sequencing data was also mined for other key components of the NOTCH signalling pathway for SJG6, SJG13 and SJG32. SJG13 and SJG32 were not found to harbour any nonsynonymous mutations in other pathway members. On the contrary, SJG6 was found to have mutations in a number of other pathway members, as detailed in Table 3.2. The mutational status of the following genes or gene families were sought: (1) ADAM, (2) JAG, (3) DLL, (4) CTNNB1, (5) FBXW7, (6) HAT1, (7)

HDAC, (8) FNG, (9) MAML, (10) NCOR2, (11) NOTCH, (12) PSEN, (13) CSL, (14) HES, (15) HEY and (16) SNW1.

Table 3_2: Somatic mutations in members of the NOTCH signalling pathway in SJG6

| ***Gene*** | ***CDS Mutation*** | ***AA Mutation*** | ***Genome Mutation*** | ***Mutation Effect*** |
|---|---|---|---|---|
| *ADAM15* | G884A | R295Q | G → A | Nonsynonymous SNV |
| *ADAM29* | G1650C | Q550H | G → C | Nonsynonymous SNV |
| *JAG1* | C1124T | S375L | G → A | Nonsynonymous SNV |
| *DLL4* | C1707A | N569K | C → A | Nonsynonymous SNV |
| *HDAC1* | G1186A | E396K | G → A | Nonsynonymous SNV |
| *HDAC7* | C106G | Q36E | G → C | Nonsynonymous SNV |
| *RFNG* | G378C | K126N | C → G | Nonsynonymous SNV |

### 3.3.2. Relative Expression of NOTCH Signalling Pathway Members in SJG6

In order to investigate the wider effect of the truncating NOTCH1 mutations in SJG6, a $RT^2$ Profiler PCR Array (Qiagen) for the human NOTCH signalling pathway was performed for SJG6 and SJG32. The array is in a 96 well format. Each well contains a single probe for a panel of 35 NOTCH related genes, 5 housekeeping genes and patented controls to monitor PCR quality and efficiency. The array allows for the simultaneous RT-qPCR expression analysis of the 35 NOTCH-related genes in two cDNA samples. Findings indicated a down-regulation of a high proportion of NOTCH pathway associated genes in SJG6 compared to SJG32 (Figure 3.5a).

Ingenuity Pathway Analyser was used to visualise expression differences in key members of the canonical NOTCH signalling pathway (Figure 3.5b). As well as reduced NOTCH1 expression, SJG6 was found to have a lower expression of ligands JAG1, JAG2 and DLL1; co-activators MAML1-3 and CSL; and post-transcriptional regulators LFNG and MFNG. Conversely, cleavage enzymes ADAM17 (TACE) and γ-secretase (represented in the array heatmap by subunits APH1A and APH1B) were found to be upregulated in SJG6 compared to SJG32.

Of the 35 genes analysed using the PCR array, none were significantly upregulated in SJG6 relative to SJG32, but 6 were found to be significantly downregulated: (1) JAG1 (21%), (2) HDAC8 (61%), (3) MAML2 (27%), (4) MAML3 (16%), (5) MFNG (5%), and (6) NOTCH2 (13%) (Figure 3.5c). As discussed in section 3.3.1, JAG1 has been shown to harbour a non-synonymous SNV mutation in SJG6. No mutations were identified in the remaining five genes by whole exome sequencing in the SJG6 line.

The NOTCH array did not assess any downstream targets of the NOTCH signalling pathway. Therefore, a further RT-qPCR was performed to calculate the relative expression of the well-documented down-stream targets HES1, HES5 and HEY1 in SJG6 relative to SJG32 (Figure 3.6). HES5 expression was found to be lower and HES1 and HEY1 expression was found to be significantly lower in SJG6 compared SJG32: approximately 47%, 69% and 14% respectively.

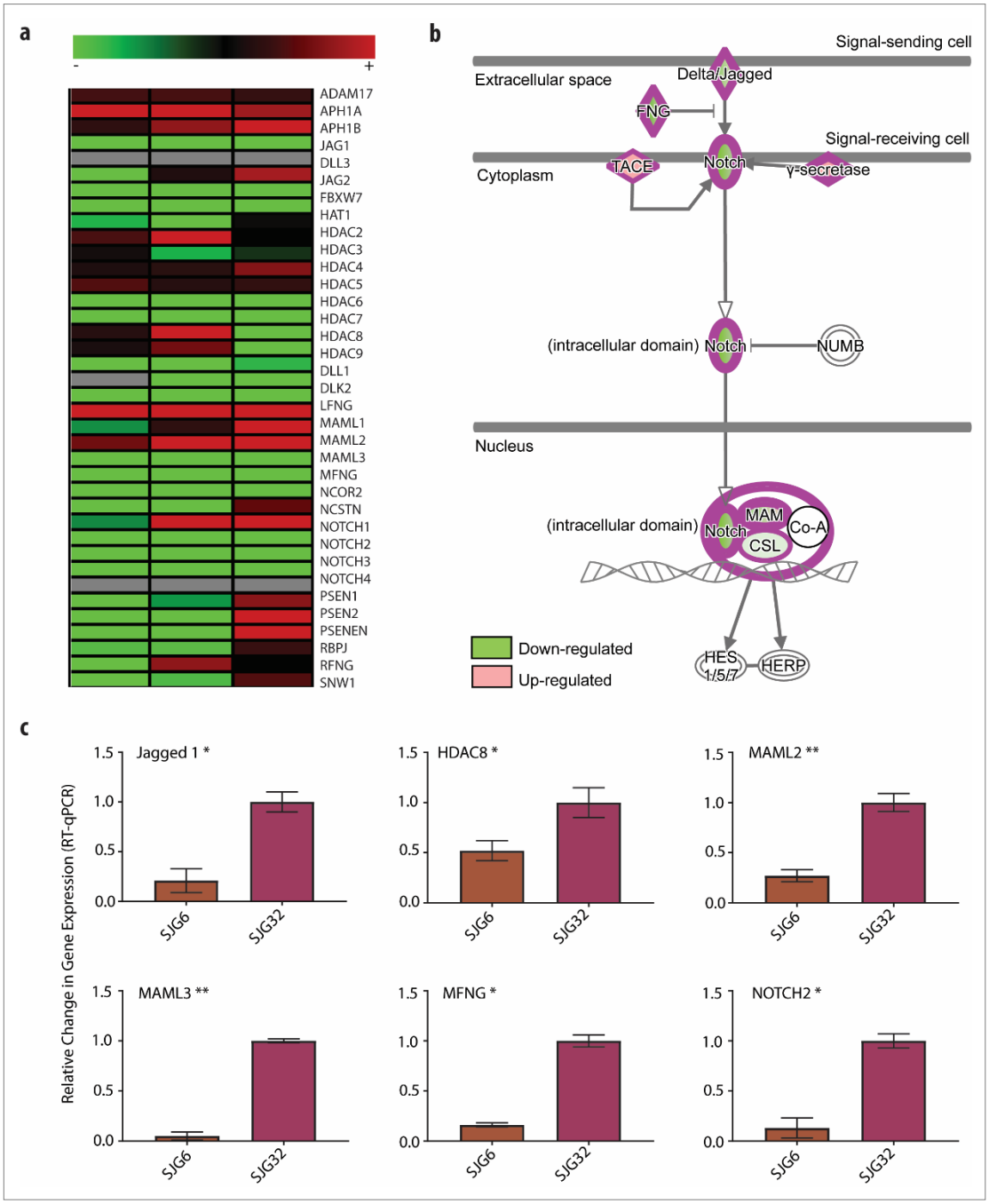


*Figure 3 5: RT² Profiler PCR Array for the human NOTCH signalling pathway. SJG6 was normalised to SJG32. a) Heat map of 3 biological replicates for each of the 35 genes. Green = downregulation. Red = upregulation. Jag = Jagged. DLL = Delta-like Canonical NOTCH Ligand. FBXW = F-Box/WD. HAT = Histone Acetyltransferase. HDAC: Histone Deacetylase. DLK = Delta-like Non-Canonical NOTCH Ligand. LFNG = Lunatic Fringe. MAML = Mastermind-like. MFNG = Manic Fringe. NCOR = Nuclear Receptor Co-Repressor. NCSTN: Nicastrin. PSEN: Presenilin. PSENEN: Presenilin Enhancer. RBPJ = Recombining Binding Protein Supressor of Hairless. RFNG = Radical Fringe. b) Canonical NOTCH signalling pathway overlay with expression data. The pathway was created using Ingenuity Pathway Analyser (Qiagen). c) Relative expression of the 6 genes which were found to have statistically significant expression differences. n=3. *= student's t-test value <0.05. **= student's t-test value <0.01.*

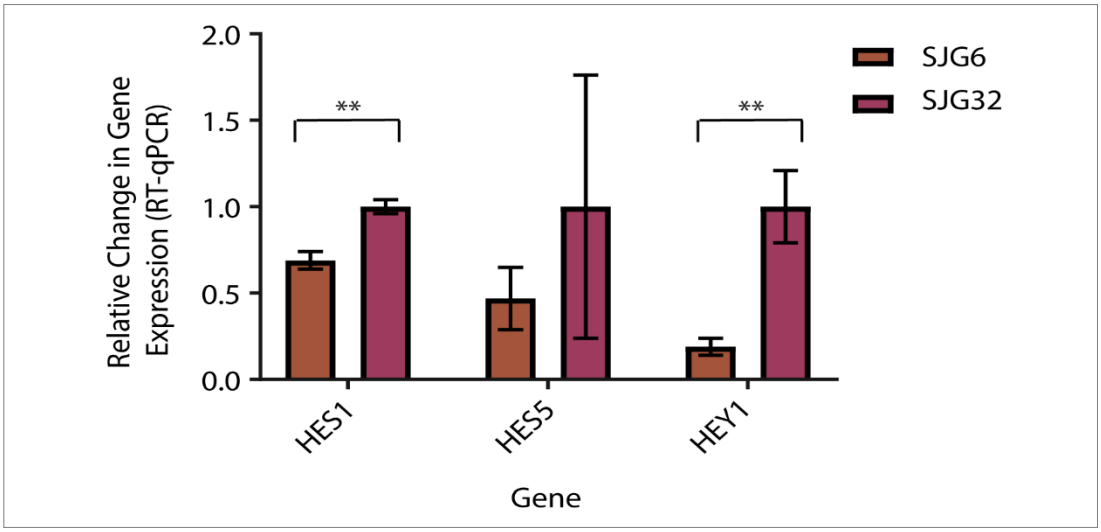


*Figure 3 6: RT-qPCR analysis of HES1, HES5 and HEY1 expression in SJG6 and SJG32. Expression was normalised to s18 and GAPDH housekeeping genes. n=4. ** Student's t-test calculated at <0.01.*

## 3.4 Validation of NOTCH1 Rescue in SJG6

A lentiviral system was used to rescue NOTCH1 signalling in SJG6 by introducing NICD, the active domain of the NOTCH1 receptor. A control line was derived by transfecting SJG6 with the empty vector (here-on referred to as SJG6 Blank). In both cases, expression of mCherry was used as a marker of successful transfection and mCherry positive cells were selected by FACS. Figure 3.7a shows both stably expressing cell lines growing on J2 feeder layers.

In order to confirm the expression of NICD at the protein level, a western blot was performed (Figure 3.7b). A strong band can be seen immediately post-sorting and a fainter band can be seen in the stably expressing cell line (here-on referred to as SJG6 + NICD. No band is detected for SJG6 Blank. This western blot was performed by Dr Kazunori Sunadome.

RT-qPCR was performed to quantify the mRNA expression levels of NICD. NICD expression in SJG6 + NICD was found to be approximately 3x higher than in the empty vector control (Figure 3.7c).

It is proposed that the stably expressing cell line has lower NICD protein expression than the cell line immediately post sorting as the cells with the highest levels of NICD differentiate and are lost from the population. Therefore, the resulting stably expressing cell line is made up of cells expressing lower levels of NICD, which is more representative of wild type expression. In order to investigate this, a colony

formation assay was performed on cells which had been FACS sorted for high and low mCherry expression. Consistent with the differentiation hypothesis, cells expressing higher levels of mCherry formed fewer colonies than those with low expression levels (Figure 3.7d).

Finally, immunocytochemistry staining for activated NOTCH1 was performed on the SJG6 Blank and SJG6 + NICD line. Activated NOTCH1 staining intensity was greater in the SJG6 + NICD cell line (Figure 3.7e).

## 3.5 Discussion

### 3.5.1 The SJG Lines are Representative of SCCHN

Previously published work has characterised the SJG lines and whole exome sequencing confirmed the mutational spectrum of the lines to be representative of primary oral SCCs in TCGA (Hayes, et al., 2016). Consistent with the larger TCGA database, whole exome sequencing identified NOTCH1 mutations in 18.75% of SJG lines. Moreover, 50% of these mutations were truncating and 75% were found to occur in the EGF-like ligand binding domain. In SCCHN patient samples, a 3D hotspot for mutations has been identified in NOTCH1. One of the truncating mutations recorded in SJG6 was located 143 amino acids towards the N-terminus of this 3D hotspot and within the wider region of increased mutation clustering (Cerami, et al., 2012; Gao, et al., 2013; Gao, et al., 2017).

It is worth noting that 57% of the SJG lines were derived from females, compared to 27% of the TCGA lines. The epidemiology of SCCHN currently records these tumours to occur more frequently in males, by a ratio of 2:1 to 4:1. However, the number of cases in females is steadily increasing (although a proportion of this increase is due to an increase in HPV positive cancers) and there is no published evidence to suggest mutational differences in the genetic landscape of SCCHN between the sexes. The median age at which the biopsies were collected is consistent in both data sets and representative of the wider patient population (Fitzmaurice, et al., 2017).

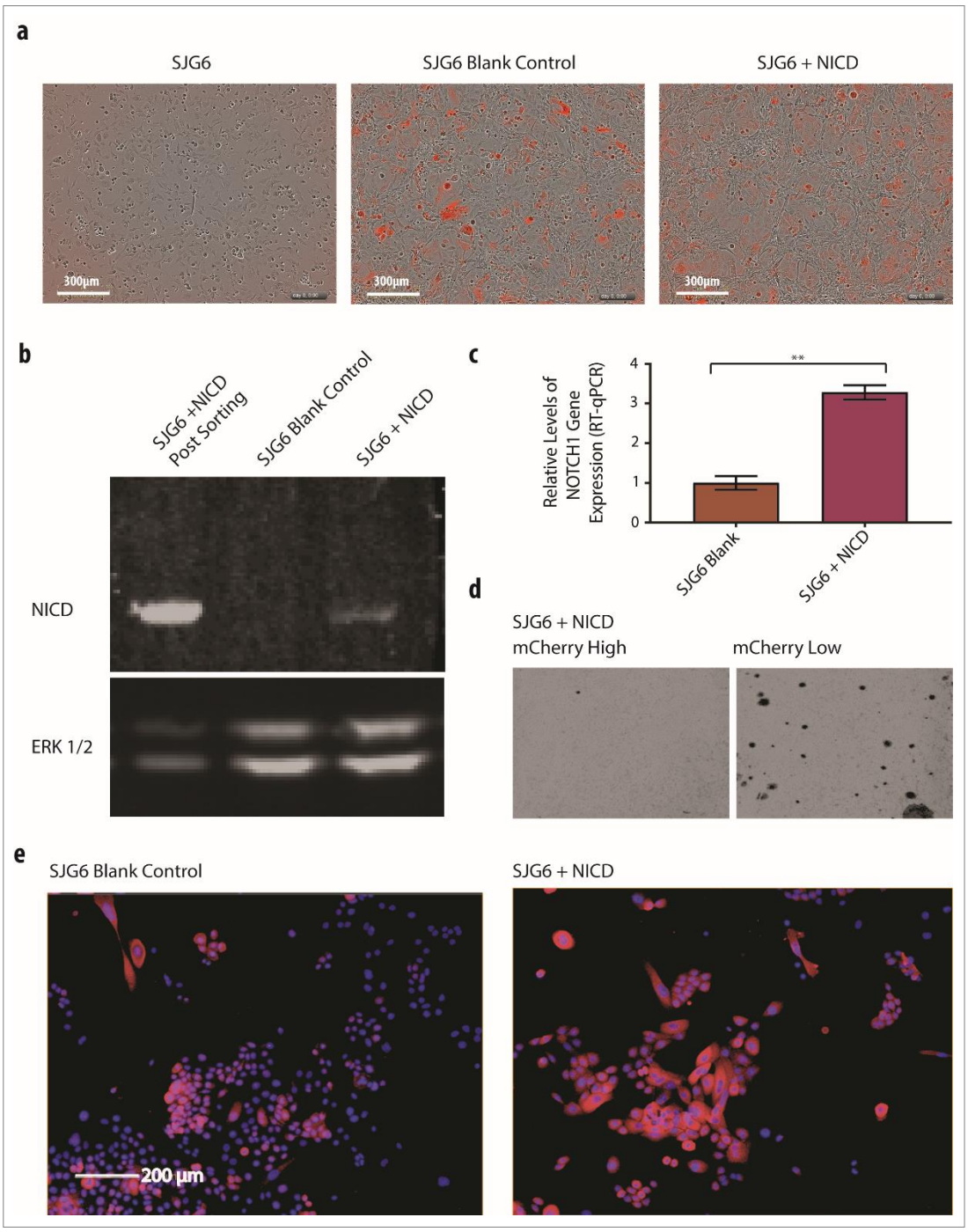


*Figure 3 7: Validation of successful transfection of SJG6 with NICD. a) Phase focus image showing mCherry expression in the non-transfected SJG6 line, SJG6 cells transfected with a blank vector control and SJG6 transfected with an NICD-expressing lentiviral plasmid. b) Western blot showing the protein expression of NICD in the SJG6 + NICD cell line immediately post FACS for mCherry expression, the SJG6 Blank vector control line and the stable SJG6 +NICD line. c) RT-qPCR showing the relative expression of NOTCH1 (Taqman probe targeted to the NICD domain) in SJG6 Blank and SJG6 + NICD. Expression was normalised to housekeeping genes s18 and GAPDH. n=3. ** = student's t-test value <0.01. (d) Colony formation assay comparing SJG6 + NICD cells FACS sorted for high and low mCherry expression. (e) Activated NOTCH1 immunocytochemistry staining (red) for SJG6 Blank and SJG6 + NICD. Nuclei were stained with DAPI (blue).*

### 3.5.2 Characterisation of NOTCH1 Mutations in SJG6

The aim of this study is to assess the role of NOTCH1 in SCCHN, as such, the truncating mutations in SJG6 makes it the most appropriate line for in depth analysis.

SJG6 was found to harbour the highest number of genetic alterations of all the SJG lines. High mutation counts are often associated with cancers caused by mutagen exposures. However, the patient was categorised as a non-smoker and was not found to consume alcohol excessively (Table 2.1).

The SJG6 primary tumour was graded at stage 4a, suggesting rapid growth and spread. In addition, the tumour was found to be the largest by diameter, have deep invasion and be poorly differentiated. As such, it is possible that the tumour had acquired higher levels of genetic alterations as it was biopsied at a later stage and had undergone excessive cell cycling. Alternatively, the reverse may be true. Higher chromosomal abnormality has been positively associated with more aggressive tumours and reduced survival. As such, the advanced tumour stage may be as a direct result of the high mutation rate rather than the other way round (Smeets, et al., 2009).

The mRNA levels of NOTCH1 in SJG6 were confirmed to be approximately 15% of that measured for SJG lines that do not harbour any NOTCH pathway mutations. Notably, the Taqman probe targeted downstream of both truncating mutations but the Ct value of NOTCH1 mRNA in SJG6 still exceeded the water control threshold. No NOTCH1 was detected at the protein level via western blot. However, the western blot image is at an exposure time immediately prior to pixel saturation for the SJG32 NOTCH1 protein band. It is therefore possible that a longer exposure time would have identified a low level of NOTCH1 expression in the SJG6 lysates.

There are two potential NOTCH1 statuses in the SJG6 line. (1) The two heterozygous truncating mutations occur on the same allele and do not confer compound heterozygosity. (2) The two heterozygous truncating mutations occur on different alleles giving rise to compound heterozygosity. As the NOTCH1 mRNA expression is substantially lower than 50%, it is likely that the mutations occur on two separate alleles. There is high conservation between the four NOTCH receptors, it is therefore possible that the low levels detected by RT-qPCR could be a result of unspecific amplification. As the cells were grown from resected tumours on a feeder layer to reduce selective pressures, another possibility is that the two heterozygous

mutations occur on the separate alleles but there is a heterogeneous cell population in which some cells harbour the truncating mutations and some do not. This would be consistent with the big bang theory of clonal evolution in cancer and the most representative of a tumour cell population (Sottoriva, et al., 2015). This theory is further supported by NOTCH1 staining performed on the SJG6 Blank cell population in Figure 3.7e which appears to show positive staining in a proportion of the cell population. Single cell sequencing analysis will be required to confirm the mutation status.

Of note, the majority of published NOTCH1 mutations are heterozygous and NOTCH proteins commonly demonstrate haploinsufficiency in tissue patterning. As such, the loss of function of a single copy of NOTCH1 or mosaic inactivation in a cell population is predicted to be sufficient to impede signalling and contribute to tumorigenesis (Wang, et al., 2011). Therefore, the rescued SJG6 cell line provides an adequate tool for studying the role of NOTCH1 in SCCHN.

### 3.5.3 Characterisation of the NOTCH1 signalling pathway in SJG6

Further investigation into the genomic landscape of SJG6 identifies mutations in several other members of the NOTCH signalling pathway. Ligands, DLL4 and JAG1 were both found to harbour non-synonymous SNVs and JAG1 was found to be significantly reduced at the mRNA level in SJG6 compared to a line that does not harbour any NOTCH pathway mutations. As discussed in section 1.2.4, there are few studies investigating the role of JAG1 as a ligand of NOTCH1 in the oral epithelium. However, low ligand expression is predicted to decrease overall NOTCH signalling due to reduced pathway activation. Further, studies in a murine model have shown JAG2 to be essential for NOTCH activated differentiation in the oral epithelium during platelet development (Casey, et al., 2006). As a result, this down-regulation of JAG1 must be considered when analysing the role of NOTCH1 in SJG6. Cell rescue via the introduction of the NICD domain will bypass ligand-mediated activation of the NOTCH signalling pathway in order to investigate the effect of downstream pathway activation in the SJG6 cell line. The consequence of mutations in NOTCH pathway members will be discussed further in Chapter 8.

During the induction of NOTCH mediated transcription, CSL switches from a transcriptional repressor to activator. The HDAC family of proteins interact with CSL

as part of a co-repressor complex and it has been shown that the inhibition of HDAC1 can lead to increased activation of downstream targets. Conversely, the mastermind like protein family (MAML) make-up part of the co-activator complex and their down-regulation has been shown to inhibit downstream NOTCH signalling (Moellering, et al., 2009).

SJG6 was found to harbour mutations in histone deacetylases (HDAC) 1 and 7. mRNA expression of HDAC1 was not calculated as part of the NOTCH array, however, HDAC7 was confirmed to be reduced and HDAC8 was found to be significantly reduced. SJG6 was not found to harbour mutations in any of the MAML genes, however, MAML 2 and 3 were found to be significantly down regulated compared to SJG32, a line that does not harbour any NOTCH pathway mutations. In order to assess the status of downstream targets of the NOTCH pathway, a RT-qPCR was performed to compare the mRNA levels of HES1, HES5 and HEY1 compared to the SJG32 control line. All targets were found to be expressed at reduced levels when compared to the control line, providing further evidence for reduced NOTCH signalling in SJG6.

SJG6 was also found to harbour mutations in ADAM 15 and 29. ADAM 17 was assessed as part of the NOTCH array but not found to be significantly altered. The ADAM family of proteins are responsible for the first NOTCH cleavage event. As such, mutations in these genes may contribute to the deregulation of NOTCH signalling by preventing the successful dissociation of the NOTCH heterodimer.

Finally, the NOTCH receptors are a highly conserved protein family. Therefore, the possibility of compensation must be considered. In the SJG6 line, NOTCH2 was found to harbour no somatic mutations but Sanger sequencing identified a single non-synonymous SNV in NOTCH3. As calculated by RT-qPCR, mRNA expression of NOTCH 2 and 3 was found to be significantly and non-significantly reduced when compared to a line that does not harbour any NOTCH1 mutations. As such, this data provides evidence against NOTCH family compensation in SJG6.

### 3.5.4 NOTCH1 expression was successfully rescued in SJG6

In order to investigate the consequence of truncating NOTCH1 mutations in SCCHN, SJG6 was rescued via the lentiviral re-introduction of NICD; the active portion of the NOTCH1 gene.

Immediately after FACS for the selectable marker, mCherry, the protein levels of NICD were substantially higher than that of the stably expressing cell lines. NICD is known to promote terminal differentiation in epithelial cells. As such, it is predicted that cells expressing the highest levels of NICD undergo terminal differentiation during the first passages and those that remain may be a closer representation of wild type levels. Colony formation assays assess the ability of single cells to undergo numerous rounds of self-renewal in order to form a colony (Franken, et al., 2006). As such, a colony formation assay comparing SJG6 + NICD cells with high mCherry expression (and therefore high NICD expression) to those with low mCherry expression was performed. Consistent with the differentiation hypothesis, the cells with higher NICD expression formed much fewer colonies.

The expression of NICD mRNA in SJG6 was found to be 12% and 18% of SJG13 and SJG32 respectively (Figure 3.3). Therefore the three-fold increase in NICD expression in the SJG6 + NICD cell line is still less than SCC lines that do not harbour any NOTCH pathway mutations. However, the Taqman probe used to identify NICD expression recognises both NICD and membrane bound NOTCH1 in the SJG13 and SJG32 cell lines. Therefore, a direct comparison cannot be made.

As detailed in section 1.4.1, Alcolea et al. investigated the conditional knock-out of NOTCH1 in a small percentage of oesophageal progenitor cells in a mouse model. The group demonstrated that within one year, the NOTCH1 knock-out cells had replaced the normal epithelium and entered a new state of homeostasis (Alcolea, et al., 2014). It is possible that the SJG6 cell line has acquired a steady state between proliferation and differentiation in the absence of NOTCH1. Therefore, lower NICD expression would be sufficient to induce differentiation.

RT-qPCR of the stably expressing cell line confirmed a 3 fold higher mRNA expression of NICD in the rescued vs the blank control line and immunocytochemistry showed a higher intensity and more extensive staining for activated NOTCH1. Staining was present in the cytoplasm as well as the nuclear compartment. As the NICD domain has a NLS, stronger staining is expected in the nucleus. Therefore, the specificity of this antibody requires further testing. However, NICD is known to interact with a number of proteins in both the cytoplasm and the nucleus. Therefore competitive protein binding could influence the staining location. For example, under certain conditions, NICD is known to interact with sonic hedgehog in the cytoplasm (Fortini & Artavanis-Tsakonas, 1994).

### 3.5.5 SJG6 as a tool for investigating the role of NOTCH1 in SCCHN

SJG6 was successfully rescued for NICD. A control line was also derived using a blank plasmid. However, it is important to consider the disadvantages as well as the advantages of SJG6 as a system for studying the role of NOTCH1 in SCCHN.

The use of SJG6 is advantageous as it is an oral SCC line which harbours NOTCH1 mutations representative of those commonly seen in wider SCCHN studies, i.e. two truncating mutations. Further, one of these truncating mutations occurs in the frequently-mutated EGF-like ligand binding domain.

A disadvantage of the SJG6 line for use is the high mutation rate in the line. In particular, mutations presence in other members of the NOTCH pathway which may complicate analysis. However, SCCHN is a highly heterogeneous cancer and it is important to further understanding of the interaction of mutations. As such, this study could be strengthened in future by repeating on other NOTCH-mutant SCCHN lines with a known mutational landscape. It would also be of interest to knock-down NOTCH1 expression in a cell line without mutations in NOTCH pathway members.

A further disadvantage of a lentiviral based system is the potential for activation of viral response genes. In particular, viral transfer has been shown to induce an immune response (Follenzi, et al., 2007). However, the use of a blank vector line will minimises the influence of viral response genes on results.

### 3.5.6 Conclusion

In summary, whole exome sequencing of derived SJG lines found their mutational landscape to be representative of SCCHN as a whole. SJG6 was found to harbour two truncating NOTCH1 mutations and was therefore considered a good tool for the study of the functional consequence of these mutations. The NOTCH signalling pathway was further characterised in the SJG6 line and downstream targets were confirmed to be reduced compared to a line that does not harbour any NOTCH pathway mutations.

In order to investigate the consequence of inactivating NOTCH1 mutations in SCCHN, SJG6 was successfully rescued for NICD. A control line was also derived using a blank plasmid. This provides a useful tool to study the effect of NOTCH1 in an otherwise genetically identical system and forms the foundation of this study.

# Chapter 4

## Investigating the Role of NOTCH1 in SCCHN *in vitro*

---

This chapter begins to explore the role of NOTCH1 in SCCHN. A range of *in vitro* assays have been derived to provide a direct comparison of the original and rescued SJG6 cell lines characterised in Chapter 3.

---

This chapter aims to provide an overview of the effect of NICD on cellular properties associated with cancer in SCCHN. The most basic definition of cancer is a collection of cells with uncontrolled proliferation. As such, the rate of proliferation over a short time period will be assessed using an EdU assay. A colony formation assay will investigate the ability of cells to undergo long-term self-renewal. Coupled to uncontrolled proliferation, another characteristic of most cancer cells is failure to undergo normal differentiation. Staining for Transglutaminase 1, a maker of epithelial differentiation, will be used to compare differentiation in the two SJG6 cell lines. Cell morphology can also provide information on cell behaviour. As such, staining with Deep Red Plasma Cell Mask and analysis of cell phenotype will be performed using the Operetta High Content Imaging System. Finally, locally progressive tumours are a dominant clinical problem in SCCHN. Therefore, the rate of cell migration in the two lines will be compared by investigating the closure of a scratch wound.

### 4.1 Clonogenicity

A colony formation assay was used to assess the ability of single cells to undergo numerous rounds of self-renewal in order to form a colony (Figure 4.1a) (Franken, et al., 2006). SJG6 Blank and SJG6 + NICD were seeded onto inactivated J2 feeder layers at single cell density. Total colony area was calculated as a percentage

of the well area. After two weeks, SJG6 Blank presented with a significantly higher average colony area percentage (12%) than SJG6 + NICD (9%) (Figure 4.1bi).

The FIJI colony intensity percentage tool uses image pixel intensity as a measure of relative cell density between two colonies of the same size. The colonies formed by SJG6 Blank were found to have a significantly higher colony intensity percentage (7%), and therefore cell density, than those of SJG6 + NICD (5.7%) (Figure 4.1bii).

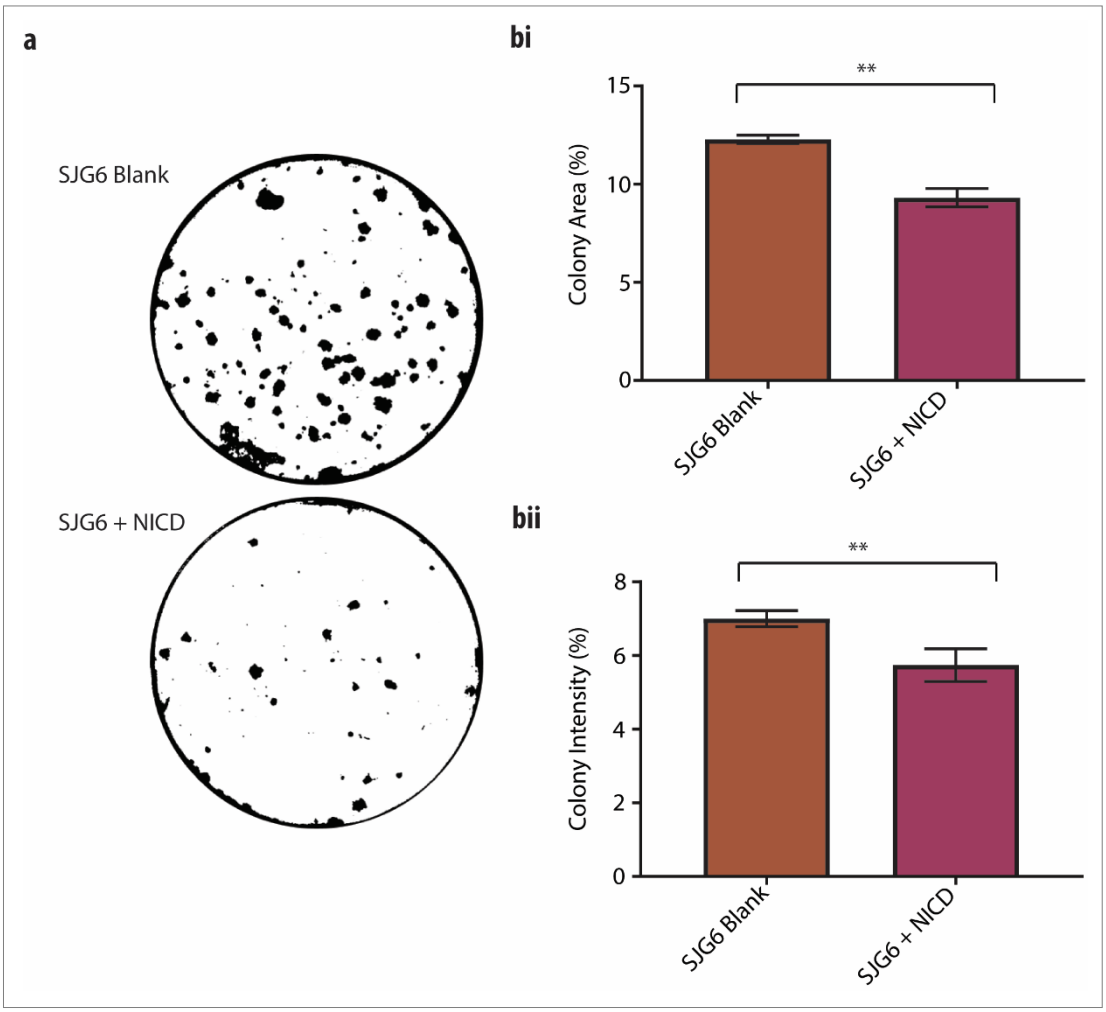


*Figure 4. 1: Colony formation assay to compare the clonogenicity of SJG6 Blank and SJG6 + NICD. (a) Representative colony images of the two cell lines. (b) Colony area percentage. (c) Colony intensity percentage. n=3. ** Student's t-test value <0.01.*

## 4.2 Proliferation

An EdU assay was performed to compare the proliferative potential of SJG6 Blank and SJG6 + NICD (Figure 4.2a). The cells lines were seeded at a concentration of 2,000 cells per well in KSFM medium onto collagen-coated 96 well plates and fixed at 24hrs. At 22hrs, EdU was introduced. The EdU incorporates with the newly synthesised DNA of proliferating cells and can be detected by fluorescent labelling. Over the two hour period, a significantly higher percentage of proliferating cells were recorded in SJG6 Blank (33.9%) than in SJG6 + NICD (26.7%) (Figure 4.2b).

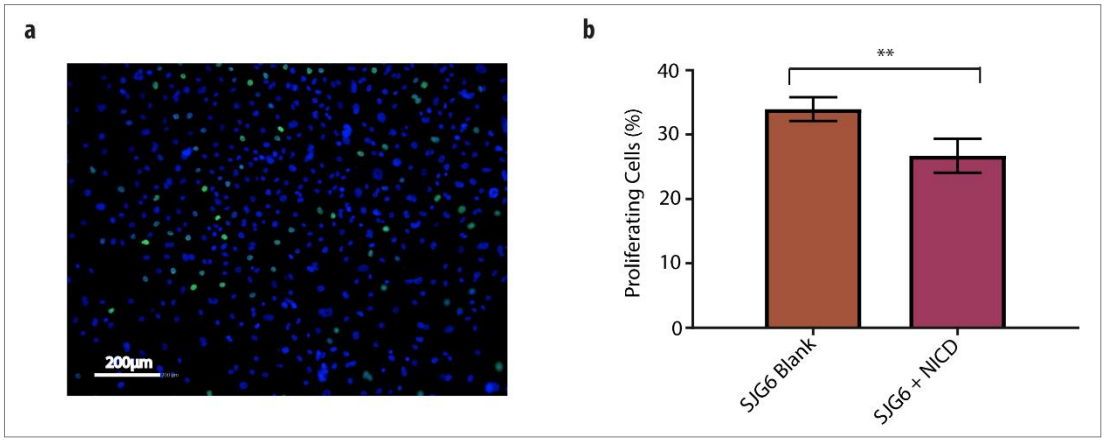


*Figure 4. 2: EdU assay comparing the proliferative potential of SJG6 Blank and SJG6 + NICD. (a) Representative image of nuclei (DAPI; blue) staining positive for EdU (Alexa 488; green). (b) Percentage of proliferating cells. n=8. ** Student's t-test value <0.01.*

## 4.3 Differentiation

In order to compare the level of differentiation in SJG6 Blank and SJG6 + NICD, cells were stained with Transglutaminase 1; a marker of epithelial differentiation (Figure 4.3a). Both cell lines were seeded at a concentration of 2,000 cells per well in KSFM medium onto collagen coated 96 well plates. At 24hrs, the cells were fixed and stained with Transglutaminase 1. Nuclei were stained with DAPI. The Operetta High Content Imaging system was used to identify the percentage of Transglutaminase 1 positive cells in both populations (Figure 2.2). A significantly

higher proportion of differentiated cells were recorded in the SJG6 Blank (8.5%) than in the SJG6 + NICD (3.6%) cell line (Figure 4.3b).

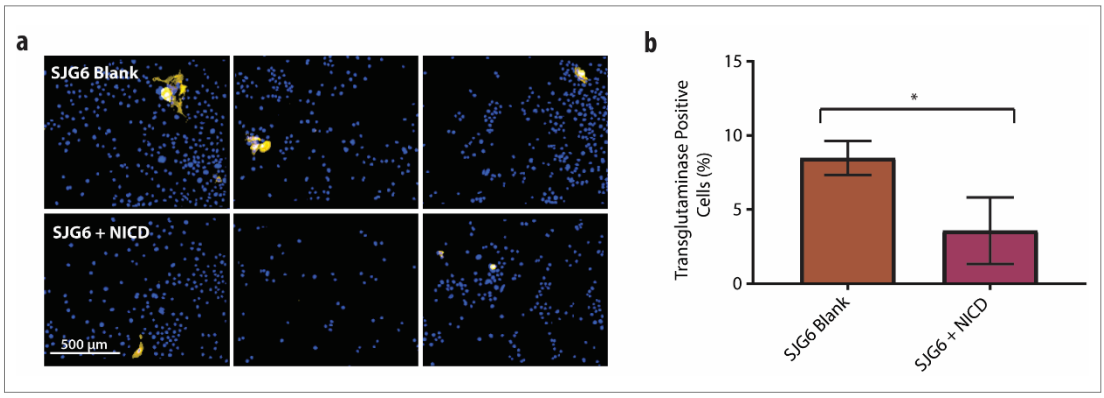


*Figure 4. 3: Transglutaminase 1 staining to compare the percentage of differentiated cells in the SJG6 Blank and SJG6 + NICD cell lines. (a) Representative image of Transglutaminase 1 staining (yellow) in SJG6 Blank (top) and SJG6 + NICD (bottom). Nuclei were stained with DAPI (blue). (b) Percentage of differentiated cells. n=3. * Student's t-test >0.05.*

## 4.4 Cell Morphology

Cytoplasmic Cell Mask staining was performed to investigate morphological differences between SJG6 + NICD and SJG6 Blank. The cell lines were seeded at a concentration of 2,000 cells per well in KSFM medium onto four concentrations of fibronectin (0 µg/ml, 1 µg/ml, 5 µg/ml and 25 µg/ml) in 96 well plates. Fibronectin was used in line with a previously established protocol (Leha, et al., 2016). At 24hrs, cells were fixed, stained with Cell Mask and DAPI and analysed using the Operetta High Content Imaging System. The analysis pipeline is detailed in Figured 2.2a.

Morphological differences were observed between the two cell lines (Figure 4.4a). In both lines, cells were found to have a larger cell area when seeded onto higher fibronectin concentrations (Figure 4.4b). SJG6 Blank was found to be significantly larger than SJG6 + NICD on fibronectin concentrations greater than 1 µg/ml. At each fibronectin concentration, SJG6 + NICD was found to be more rounded than SJG6 Blank (Figure 4.4c). This finding was statistically significant at fibronectin concentrations of 1 µg/ml and 5 µg/ml.

In both cell populations, a small number of elongated cells were observed (Figure 4.4di). Cells were identified using Cell Mask Deep Red Plasma Stain by the High Content Operetta Imaging System as detailed in Figured 2.2a. The percentage of elongated cells in each line was then calculated by thresholding for cells with a roundness ratio of less than 0.6. SJG6 Blank was found to have a higher percentage of elongated cells than SJG6 + NICD at all fibronectin concentrations and a significantly higher percentage at fibronectin concentrations greater than 5 µg/ml. In both cell lines, the percentage of elongated cells increased with increasing fibronectin concentrations (Figure 4.4dii). Duan et al. previously associated an elongated cell morphology in tongue carcinoma cells with cellular senescence (Duan, et al., 2006). This will be discussed further in section 4.6.

## 4.5 Cell Migration

A scratch wound assay was performed to compare the rate of cell migration between SJG6 Blank and SJG6 + NICD (Figure 4.5). Both cell lines were first treated with mitomycin-C to remove bias from potential differences in the rates of proliferation between the lines. Both cell lines were seeded at a concentration of 50,000 cells per well in KSFM medium onto collagen coated 96 well plates. A scratch wound was then created using the Essen BioScience 96-Well Wound Maker and the confluence of cells in the wound area was calculated over a 20hr period. SJG6 Blank was found to migrate into the wound area at a significantly faster rate than SJG6 + NICD.

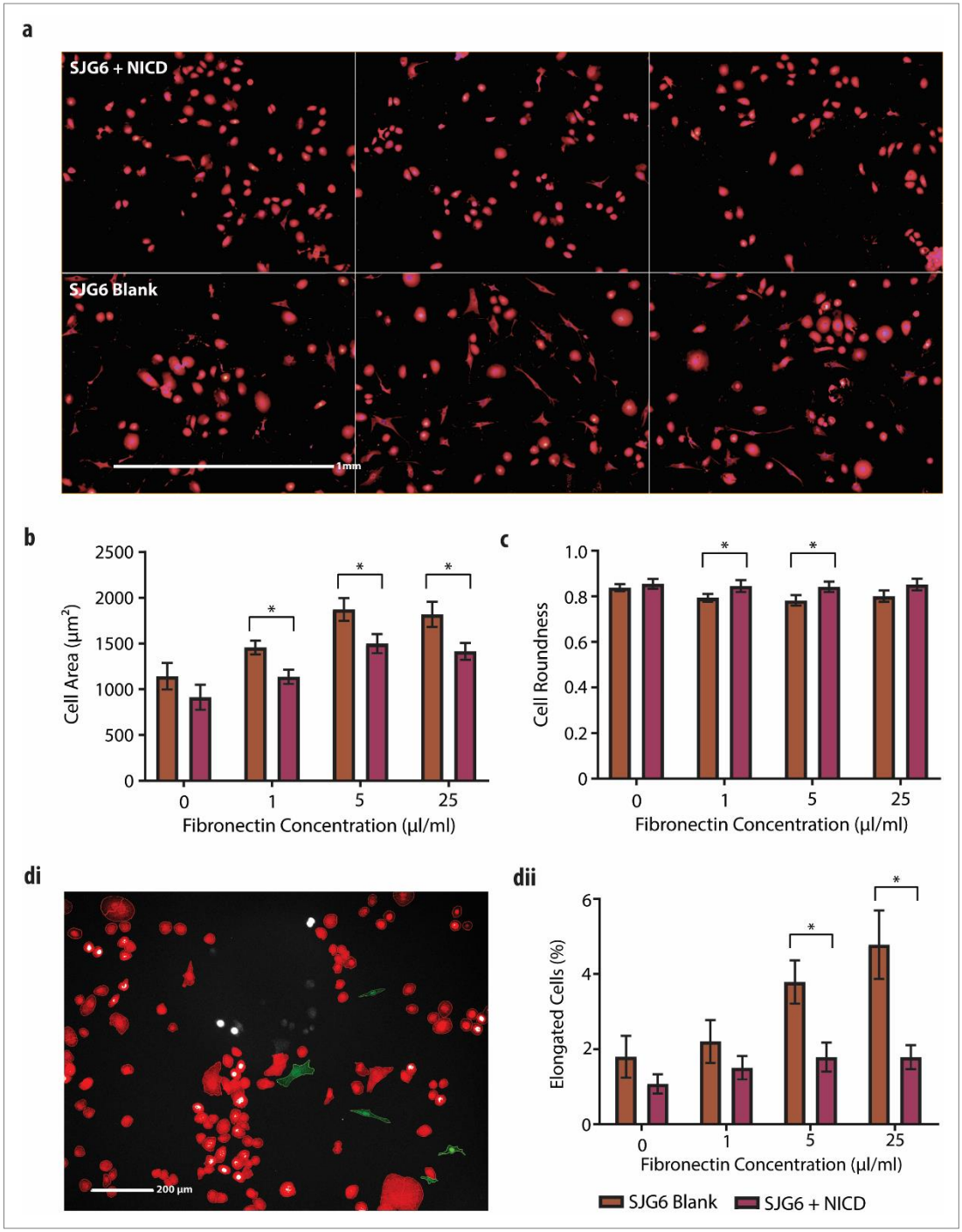


*Figure 4. 4: Operetta analysis comparing the morphology of SJG6 Blank and SJG6 + NICD on four concentrations of fibronectin (0 µg/ml, 1 µg/ml, 5 µg/ml and 25 µg/ml). (a) Representative images of SJG6 + NICD (top) and SJG6 Blank (bottom) on 5 µg/ml fibronectin. Nuclei were stained with DAPI (blue) and cytoplasm was stained with cell mask (red). (b) Measure of cell area. (c) Measure of cell roundness ratio. (d) By thresholding and excluding cells with a roundness ratio of less than 0.6 (red), elongated cells in the population were identified (green). (Note: the red and green colours are an overlay mask from the analysis pipeline and not representative of staining. White dots are EdU positive nuclei which was stained for in the same assay) (i) and calculated as a percentage of total cell number (ii). n=3. * Student's t-test value <0.05.*

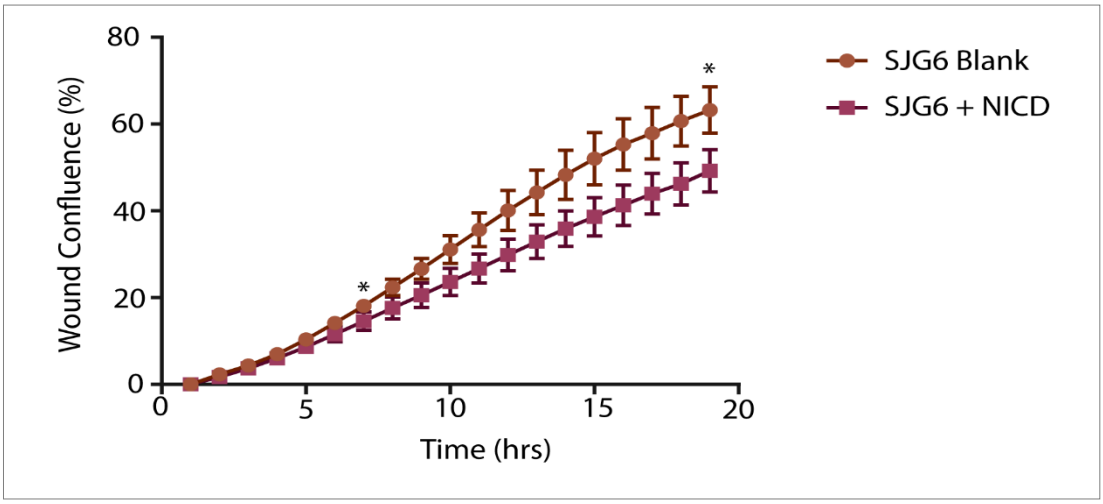


*Figure 4. 5: Scratch wound assay to compare the rate at which SJG6 Blank and SJG6 + NICD migrate to recolonise the initial wound area. n=5. *Student's t-test value <0.05 between 7 and 20hrs.*

## 4.6 Discussion

### 4.6.1 NICD expressing cells exhibit reduced clonogenicity

Colony formation assays test the ability of individual cells in a population to undergo numerous rounds of self-renewal. As discussed in the introduction, when primary cultures of epidermal cells are derived, three types of colonies are formed; namely holoclones, meroclones and paraclones. Holoclones form large colonies, have a long replicative lifespan and are considered representative of stem cells. Paraclones form small colonies, have a short replicative potential and are thought to behave as transit amplifying cells. Meroclones act as an intermediate and form both growing and abortive colonies. Culture of holocone populations give rise to paraclones and meroclones (Barrandon, 1987).

This approach has been extended to cancer cell lines. Data from colony formation assays suggest that the expression of NICD gives rise to cells with reduced clonogenicity i.e. reduced colony area and density (Figure 4.1). Not all cells within a tumour are equally able to initiate growth, metastasis and recurrence. This behaviour has been associated with a small population of CSCs. As such, this data provides evidence to suggest that NICD may act as a tumour suppressor by reducing the proportion of CSCs in the population. This data is not consistent with studies that have associated increased NOTCH1 expression with CSCs in SCCHN (Upadhyay, et al.,

2015; Wilson, et al., 2016). Further experiments would be required to confirm this finding. It would be of interest to serially passage the colonies to further assess the potential for self-renewal. Staining for CSC markers (CD44, SOX2 and ALDH1) would also be required (Harper, et al., 2007).

### 4.6.2 NICD expressing cells exhibit reduced proliferation

Findings suggest that the expression of NICD gives rise to cells with a reduced ability to proliferate (Figure 4.2). This data is consistent with previous studies that have associated NICD expression with cell cycle arrest in oral and tongue SCC lines (Duan, et al., 2006; Pickering, et al., 2013). As such, data suggests a tumour suppressor role for NOTCH1 in SCCHN.

However, there have been several studies showing the opposite effect, associating the loss of NOTCH1 expression with reduced proliferation (Yao, et al., 2007; Yoshida, et al., 2013; Sun, et al., 2014). The effect of NOTCH1 signalling is likely to be influenced by the mutational landscape of individual tumours. Duan et al. provided evidence to suggest that the downregulation of Wnt / β-catenin signalling may act as a mechanism for cell cycle arrest in cell lines showing an anti-proliferative effect in response to NOTCH1 expression in SCCHN (Duan, et al., 2006). This idea will be further explored in Chapter 5.

Interestingly, in this study as well as those also showing reduced proliferation in response to NOTCH1 expression, NICD was constitutively introduced. Conversely, NOTCH1 had been targeted for knockdown in studies showing the opposite effect. In a number of cancers, the effect of NOTCH signalling has been shown to be highly context dependent and contingent on signal strength and timing, which may go some way to explain inconstancies between studies (Radtke & Raj, 2003; Weng & Aster, 2004).

### 4.6.3 NICD expressing cells exhibit deregulated differentiation

As discussed in Chapter 3, it is predicted that cells expressing the highest levels of NICD underwent terminal differentiation prior to the formation of a stable cell line. This data is consistent with the known role of NOTCH1 in the commitment to terminal differentiation in normal keratinocytes and studies that have previously associated

NOTCH1 expression with differentiation in SCC (Lowell, et al., 2000; Rangarajan, et al., 2001; Nickoloff, et al., 2002; Nicolas, et al., 2003; Sakamoto, et al., 2012; Ravindran & Devaraj, 2012).

Surprisingly, a lower percentage of cells in the stably expressing SJG6 + NICD line were found to express differentiation marker, Transglutaminase 1, when compared to the empty vector control (Figure 4.3). As described in the previous section, the effect of NOTCH signalling has been shown to differ, even within the same tumour type, as a result of signal strength and timing. It is therefore possible that whilst high levels of NICD expression results in terminal differentiation, those cells with lower NICD expression could give rise to the opposite effect. Kagawa et al. showed that under certain conditions, NICD expression could switch from being a driver of cellular senescence to actively decreasing levels of differentiation. Kagawa et al. linked this senescence checkpoint to the loss of p16 expression (Kagawa, et al., 2015). This theory shall be explored further in Chapter 5.

Alternatively, Alcolea et al. investigated the conditional knock-out of NOTCH1 in a small percentage of oesophageal progenitor cells in a mouse model. The group demonstrated that within one year, the NOTCH1 knock-out cells had replaced the normal epithelium and entered a new state of homeostasis (Alcolea, et al., 2014). It is therefore possible that both SJG cell lines have acquired independent steady states between proliferation and differentiation irrespective of their NOTCH1 status.

It is also important to note that Transglutaminase 1 is an intermediate differentiation expression marker. In normal epithelium it is expressed in the granular and spinous layers. In future experiments it would therefore be of interest to stain for earlier (such as Keratin 1 and 10) and later (such as filaggrin) markers of differentiation in order to get a more thorough picture of the whole differentiation process in both cell lines.

### 4.6.4 NICD expression alters cell morphology

Both cell lines showed an increased cell area when seeded onto higher fibronectin concentrations. It is predicted that the higher concentrations of fibronectin provide a preferable environment for cells to seed and spread (Adams & Watt, 1993).

The expression of NICD gave rise to a smaller, more rounded morphology with fewer elongated cells in the population. The presentation of a more rounded

morphology in lines constitutively expressing NICD is consistent with the observations of Pickering et al. Complementary to proliferation data, Pickering et al. also confirmed the induction of β-galactosidase in these rounded cells, suggesting they had become senescent (Pickering, et al., 2013).

Conversely, Duan et al. noted that the expression of NICD gave rise to a more elongated cell population. The group suggested that this may be reflective of senescence, cell cycle arrest or apoptosis, but no validating experiments were performed (Duan, et al., 2006).

Another potential explanation for changes seen in cell morphology is EMT. When epithelial cells undergo EMT, they lose their cobblestone-like epithelial phenotype and acquire an elongated invasive mesenchymal phenotype (Krisanaprakornkit & Iamaroon, 2012). Therefore, the increased percentage of elongated cells identified in the SJG6 Blank cell line may associate NICD expression with reduced EMT, supporting a tumour suppressor role for NOTCH1. This idea is consistent with the increase in elongated cells at higher fibronectin concentrations as ECM substrates have been confirmed to enhance EMT (Kumar, et al., 2014). Staining for epithelial (such as E-cadherin and desmoplankin) and mesenchymal (such as N-cadherin and vimentin) cell markers would be required to confirm this hypothesis.

### 4.6.5 NICD expression is associated with reduced cell migration

Findings suggest that the expression of NICD results in reduced cell migration. This data is inconsistent with that of currently published literature (Joo, et al., 2009; Zhang, et al., 2011; Yu, et al., 2012; Yoshida, et al., 2013; Dai, et al., 2015; Li, et al., 2015; Jing, et al., 2016).

However, it is important to note that wound closure is not a direct measure of invasive potential. Other factors must be considered, such as the ability to invade through the ECM. Nonetheless, this data demonstrates that the expression of NICD is able to successfully alter cell motility. This is of particular interest in SCCHN as locally progressive tumours are a dominant clinical problem.

This work provides an observation of cell motility in SJG6 + NICD and SJG6 Blank. Potential mechanisms will be explored in Chapter 5 and the role of NICD in tumour invasion will be investigated further in Chapter 6.

### 4.6.6 Conclusion

Broadly, *in vitro* findings suggest that the expression of NICD is able to reduce clonogenicity and proliferation, promote differentiation and inhibit cell migration, thereby providing potential mechanisms for a tumour suppressor function of NOTCH1 in SCCHN. However, within the framework of previously published literature, these findings add to existing evidence to suggest that the effect of NOTCH1 is highly context dependent and highlights the need for further study to better understand this complexity of NOTCH1 signalling in SCCHN.

# Chapter 5

## Investigating the Role of NOTCH1 in SCCHN: Microarray

This chapter begins to explore the effect of NOTCH1 expression within the wider genetic landscape of SCCHN. A microarray was used to investigate how the rescue of NOTCH1 in SJG6 altered gene expression in the whole transcriptome. Microarray was chosen for the study as it is a robust, economical and well established method of gene expression analysis. In addition, validated analysis pipelines are available and several lab members had previous experience of processing microarray data in-house.

### 5.1 Microarray Analysis Confirms that the Expression of NICD Alters the Genetic Landscape of SJG6

In order to investigate how the expression of NICD alters the genetic landscape in SCCHN, microarray analysis of SJG6 Blank and SJG6 + NICD was undertaken. The three biological replicates naturally clustered into the two respective groups, suggesting that the expression of NICD changes the wider genetic landscape of the cell line (Figure 5.1a). The top 10 up- and down- regulated genes are highlighted in Figure 5.1b. Notably, fold changes identified in the SPANX family (co-increased with NICD) were 3x greater than that of any other gene. SPANX expression will be considered further in Chapter 6.

Before further analysis was performed, the validity of the microarray was assessed. RT-qPCR was used to confirm the relative expression of 5 genes (TMEM27, HEY1, CTH, ITGBL1 and ITGB6) that microarray showed to be significantly different between the SJG6 Blank and SJG6 + NICD lines (Figure 5.1c).

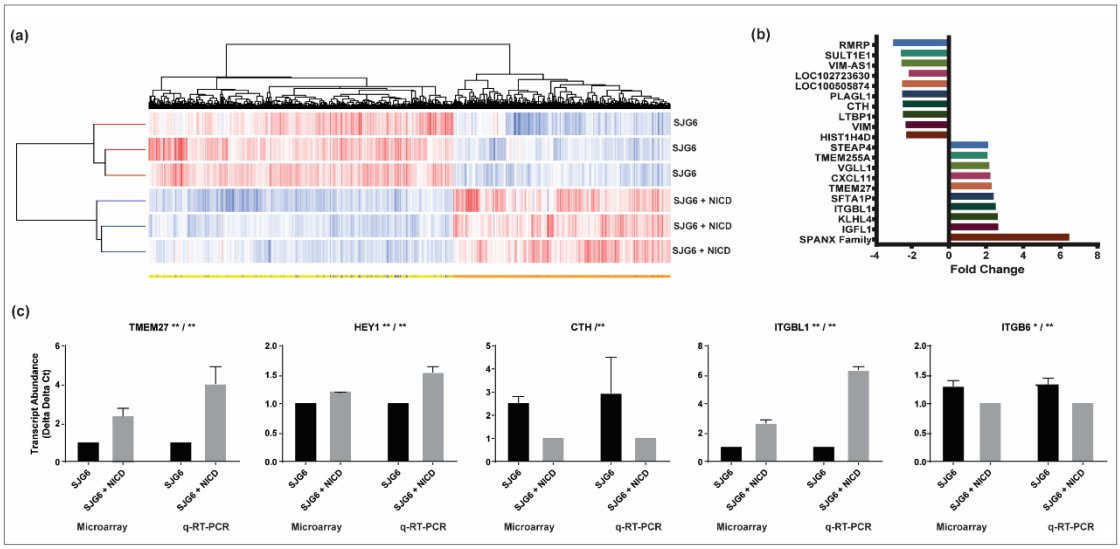


*Figure 5. 1: Microarray analysis comparing gene expression in SJG6 Blank and SJG6 + NICD. (a) Heatmap showing that the three biological replicas of SJG6 Blank and SJG6 + NICD cluster with clear areas of up- (red) and down- (blue) regulation. (b) Top ten genes up- and down- regulated. (c) RT-qPCR validation of 5 (TMEM27, HEY1, CTH, ITGBL1, ITGB6) genes found to differ between SJG6 Blank and SJG6 + NICD via microarray. n=3. x / x = microarray / RT-qPCR. n=3. * = Student t-test value <0.05. ** = Student's t-test value <0.01.*

## 5.2 The Differentially Expressed Gene Set between SJG6 Blank and SJG6 + NICD can be linked to Functional Characteristics

The Gene Ontology (GO) project was established to form a common language for describing a gene product's cellular component, molecular function and biological process. This consistency of vocabulary allows gene sets to be interpreted for shared functional characteristics. This analysis technique is a GO term enrichment analysis. Genes are assigned to 'bins' based on their functional characteristics. One gene can be assigned to numerous bins. By assessing the bins which have been allocated to the full gene set, statistical tests can assess whether a bin is enriched for the input genes. As such, underlying cellular components, molecular functions and biological processes can be identified. (Ashburner, et al., 2000).

The top 20 GO terms for the differentially expressed gene set between SJG6 Blank and SJG6 + NICD are shown in Figure 5.2a. Seven of the top eight terms are linked to cell location and include the nucleosome, intracellular region and extracellular region. A high proportion of derived GO terms are also linked to DNA organisation: (1) nucleosome, (2) DNA packaging complex, (3) histone H4-K20

demethylation, (4) histone demethylase activity (H4-K20 specific), (5) protein-DNA complex assembly and (6) nucleosome assembly. Two terms describe protein targeting to the membrane and endoplasmic reticulum respectively, and two terms are associated with viruses. Metabolic processes, differentiation of megakaryocytes and cell cycle progression are also included in the list.

Due to the high number of GO terms related to DNA organisation and histone modification, microarray data was mined for changes in the expression of histone related genes. Of the 3150 genes found to have greater than a 1.2 fold change difference, 68 were found to be histones or histone regulators (2.2%). Further, 62 of the 68 genes were found to be downregulated (91%). These genes are detailed in Table 5.1.

A gene set enrichment analysis (GSEA) is a computational method to determine whether sets of genes show significant differences between two biological states or phenotypes (Subramanian, et al., 2005). The top 18 hits for microarray data comparing SJG6 Blank and SJG6 + NICD are shown in Figure 5.2b. Of note, 7 of these hits are associated with cancers and 2 are directly linked to oesophageal cancers. Further, and in corroboration with *in vitro* data in Chapter 4, proliferation and invasiveness are also some of the top GSEA hits.

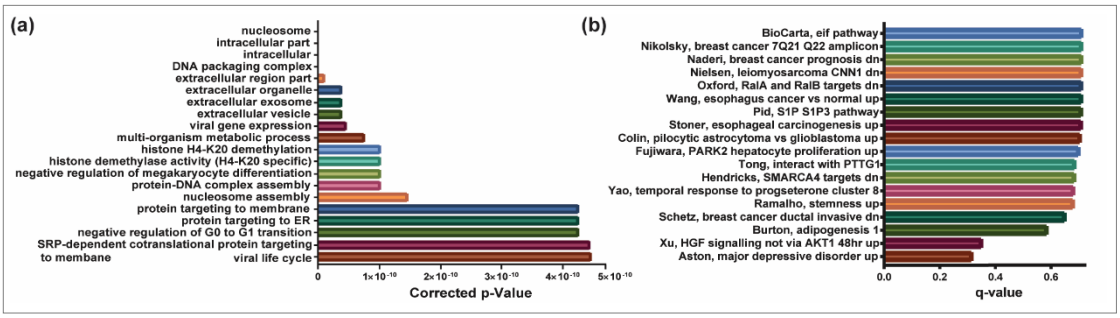


*Figure 5. 2: Analysis of the differentially expressed gene set between SJG6 Blank and SJG6 + NICD. (a) GO term analysis which interprets the gene set in relation to the Gene Ontology classification system. Genes are assigned to 'bins' based on their functional characteristics. One gene can be assigned numerous bins. By assessing the bins which have been allocated to the full gene set, statistical tests can assess whether a bin is enriched for the input genes. As such, underlying cellular components, molecular functions and biological processes can be identified. Findings are plotted by corrected p-value. (b) Gene Set Enrichment Analysis (GSEA) which determines whether the pre-defined set of genes shows a statistical difference between two biological states or phenotypes. Top findings are plotted by q-value. n=3.*

Table 5 1: Expression fold change in histone related genes in SJG6 + NICD compared to SJG6 Blank

| *Gene* | *Expression Fold Change* | | *Gene (Cont.)* | *Expression Fold Change (Cont.)* | |
|---|---|---|---|---|---|
| *ALKBH1* | -1.217889 | ↓ | *HIST1H4A* | -1.525091 | ↓ |
| *ASF1A* | -1.212881 | ↓ | *HIST1H4B* | -1.525091 | ↓ |
| *ASH1L* | -1.393696 | ↓ | *HIST1H4C* | -1.525091 | ↓ |
| *CDK1* | 1.2140411 | ↑ | *HIST1H4D* | -2.294169 | ↓ |
| *DUSP1* | -1.266398 | ↓ | *HIST1H4E* | -1.525091 | ↓ |
| *DUSP12* | -1.217831 | ↓ | *HIST1H4F* | -1.525091 | ↓ |
| *DUSP22* | -1.257568 | ↓ | *HIST1H4H* | -1.525091 | ↓ |
| *H1F0* | -1.238573 | ↓ | *HIST1H4I* | -1.525091 | ↓ |
| *H1FX* | -1.577241 | ↓ | *HIST1H4J* | -1.525091 | ↓ |
| *H2AFY2* | -1.569221 | ↓ | *HIST1H4K* | -1.525091 | ↓ |
| *HIST1H1A* | -1.310469 | ↓ | *HIST1H4L* | -1.525091 | ↓ |
| *HIST1H1B* | -1.503214 | ↓ | *HIST2H2AA3/4* | -1.637142 | ↓ |
| *HIST1H1C* | -1.559918 | ↓ | *HIST2H2AB* | -1.804308 | ↓ |
| *HIST1H1D* | -1.522174 | ↓ | *HIST2H2BA* | -1.556849 | ↓ |
| *HIST1H1E* | -1.607831 | ↓ | *HIST2H2BE* | -1.305367 | ↓ |
| *HIST1H2AB* | -1.251657 | ↓ | *HIST2H3D* | -1.536129 | ↓ |
| *HIST1H2AC* | -1.356173 | ↓ | *HIST2H4A* | -1.525091 | ↓ |
| *HIST1H2AD* | -1.315778 | ↓ | *HIST2H4B* | -1.525091 | ↓ |
| *HIST1H2AG* | -1.290961 | ↓ | *HIST4H4* | -1.525091 | ↓ |
| *HIST1H2AH* | -1.290961 | ↓ | *PTP4A1* | -1.269656 | ↓ |
| *HIST1H2AI* | -1.290961 | ↓ | *PTPN13* | -1.354828 | ↓ |
| *HIST1H2AK* | -1.290961 | ↓ | *PTPN7* | 1.2007923 | ↑ |
| *HIST1H2AL* | -1.290961 | ↓ | *PTPRH* | -1.251692 | ↓ |
| *HIST1H2AM* | -1.664963 | ↓ | *PTPRJ* | 1.5388035 | ↑ |
| *HIST1H2BG* | -1.23888 | ↓ | *PTPRM* | -1.799454 | ↓ |
| *HIST1H2BI* | -1.301587 | ↓ | *PTPRR* | 1.3578755 | ↑ |
| *HIST1H2BJ* | -1.23888 | ↓ | *PTPRS* | -1.376989 | ↓ |
| *HIST1H2BK* | -1.228102 | ↓ | *PTPRZ1* | -1.830176 | ↓ |
| *HIST1H2BN* | -1.283633 | ↓ | *RBBP5* | -1.252708 | ↓ |
| *HIST1H2BO* | -1.446285 | ↓ | *RBBP7* | 1.3903811 | ↑ |
| *HIST1H3E* | -1.463825 | ↓ | *SETD7* | -1.428182 | ↓ |
| *HIST1H3F* | -1.34566 | ↓ | *SIN3A* | -1.36823 | ↓ |
| *HIST1H3G* | -1.384561 | ↓ | *SMYD2* | -1.230749 | ↓ |
| *HIST1H3I* | -1.613932 | ↓ | *UBASH3B* | 1.2828555 | ↑ |

## 5.3 The Expression of NICD Alters Cellular and Molecular Functions in SJG6

Ingenuity pathway analyser (IPA) is an omics tool able to identify the most relevant signalling and metabolic pathways, networks and functions for a list of genes based on current literature (Krämer, et al., 2013).

Figure 5.3a shows the 52 cellular and molecular functions with an activation Z score of more than 2 for the genes found to differ between SJG6 Blank and SJG6 + NICD. In collaboration with differences presented in cell behaviours in Chapter 4, the majority of these functions could be related to decreased cell migration (35%; green) and proliferation (10%; blue). Further, a significant proportion could be associated with reduced angiogenesis (17%; red), which will be explored further in Chapter 7, and increased cell death (13%, brown). In order to assess potential mechanisms for the difference in each of these cell behaviours, the network with the most gene members for each function was selected as a representative for further analysis. This included: (1) proliferation of cells, (2) migration of tumour cell lines, (3) cell death and (4) angiogenesis.

In order to identify the potential key players in each network, the relationship between each gene member and NOTCH1 was assessed. In order to create the most direct potential mechanism for each phenotype, genes found to directly interact with NOTCH1 and have an expression change consistent with their known role in the respective cell behaviours were selected. The interactions between the selected genes were then also assessed (Figure 5.3b).

### 5.3.1 Proliferation

NOTCH1 has been shown to inhibit the expression of ITGB1, ITGB4 and SERPINE1, each of which have been positively correlated with cell proliferation. Notably, ITGB1 is also known to increase the expression of ITGB4 and SERPINE. Further, HEY1 has been shown to inhibit cell proliferation and is increased as a downstream target of NOTCH signalling (Figure 5.3bi).

### 5.3.2 Migration of tumour cell lines

Similarly to proliferation, NOTCH1 is known to inhibit the expression of ITGB1 and SERPINE1, each of which have been positively correlated to the migration of tumour cells lines. Equally, GATA3 has been shown to inhibit the migration of tumour cell lines and is increased in response to increased NOTCH1 expression (Figure 5.3bii).

### 5.3.3 Cell Death

ITGB4 and SERPINE1 have been negatively correlated with cell death. In addition, NOTCH1 is able to promote the expression of HEY1, IL7R and NRG1, each of which have been shown to increase cell death (Figure 5.3biii).

### 5.3.4 Angiogenesis

Once again, NOTCH1 has been shown to inhibit the expression of ITGB1 and SERPINE1, each of which have been positively correlated to angiogenesis. Conversely, AHR, FOXC1, CD44 and HEY1 have been shown to inhibit angiogenesis and are increased in response to increased NOTCH1 expression (Figure 5.3biv).

### 5.3.5 SERPINE1 as a common regulator

Analysis of each cell behaviour identified SERPINE1 as a common key regulator. NOTCH1 is known to actively inhibit the expression of SERPINE1, which in turn has been associated with increased angiogenesis, cell migration, proliferation, and reduced cell death (Figure 5.3c).

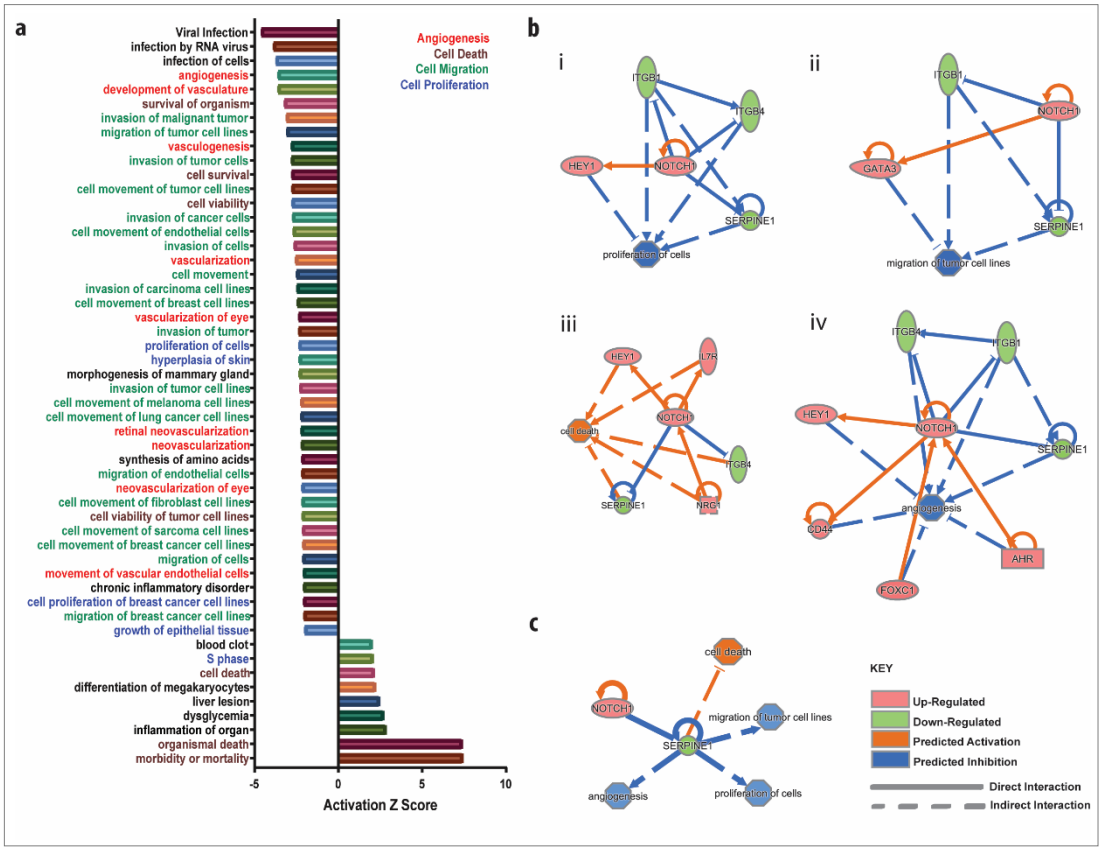


*Figure 5. 3: (a) Cellular and molecular functions with an activation Z score of more than 2 for genes found to differ between SJG6 Blank and SJG6 + NICD using microarray analysis. Many functions could be associated with angiogenesis (red), cell death (brown), cell migration (green) and cell proliferation (blue). (b) The most direct potential mechanism for the effect of NOTCH1 in the proliferation of cells (i), migration of cell lines (ii), cell death (iii) and angiogenesis (iv). (c) SERPINE1 is a common key regulator of each cell behaviour. n=3.*

## 5.4 The Expression of NICD Alters Key Genes in SCCHN

Previously published literature has associated the effect of NOTCH1 expression on cell behaviour with a number of key genes, as described in Chapter 1. Microarray analysis was used to assess relative expression fold change of the following genes in SJG6 + NICD compared to SJG6 Blank: (1) WNT, (2) CTNNB1, (3) CSL, (4) p16, (5) MMP2, (6) MMP9, (7) TNF-α, (8) SNAI2, (9) TWIST, (10) miR-140-5P, (11) ADAM10, (12) VEGF, (13) EGFR and (14) NF-κB. An up- or down- regulation of more than 20% was recorded in WNT (up; 23%), MMP9 (down; -32%), SNAI2 (down; -31%), and VEGF (down, -37%). Findings are detailed in Table 5.2.

Table 5 2: Key genes with a relative expression fold change of more than 1.2 in SJG6 + NICD compared to SJG6 Blank

| ***Gene*** | ***Cellular Function*** | ***% Expression Change*** |
|---|---|---|
| *WNT (family member 10A)* | Tumour Growth Differentiation | +23% |
| *MMP9* | Invasion | -32% |
| *SNAI2* | Invasion | -31% |
| *VEGF (family member A)* | Angiogenesis | -37% |

## 5.5 The Expression of NICD Alters Key Pathways in SCCHN

As well as individual genes, previously published literature has associated the effect of NOTCH1 expression with Wnt / β-catenin and p16 signalling pathways. IPA analysis of microarray data was used to assess how NICD-mediated changes in gene expression altered said pathways as well as the wider NOTCH signalling pathway.

### 5.5.1 NOTCH signalling pathway

As expected, there was an overall increase in NOTCH signalling in the SJG6 + NICD line, with 6 out of 11 (55%) pathway members showing altered expression. The constitutive lentiviral expression of NICD was reflected by a recorded increase in NOTCH and downstream targets, HES1/5/7 and HERP. Coactivator, CSL, and ligands, DLL / JAG, were also upregulated. There was a downregulation in γ-secretase. This would usually result in inhibition of NOTCH signalling by reducing the cleavage of full length NOTCH, however, it is unable to decrease ectopic levels of NICD (Figure 5.4).

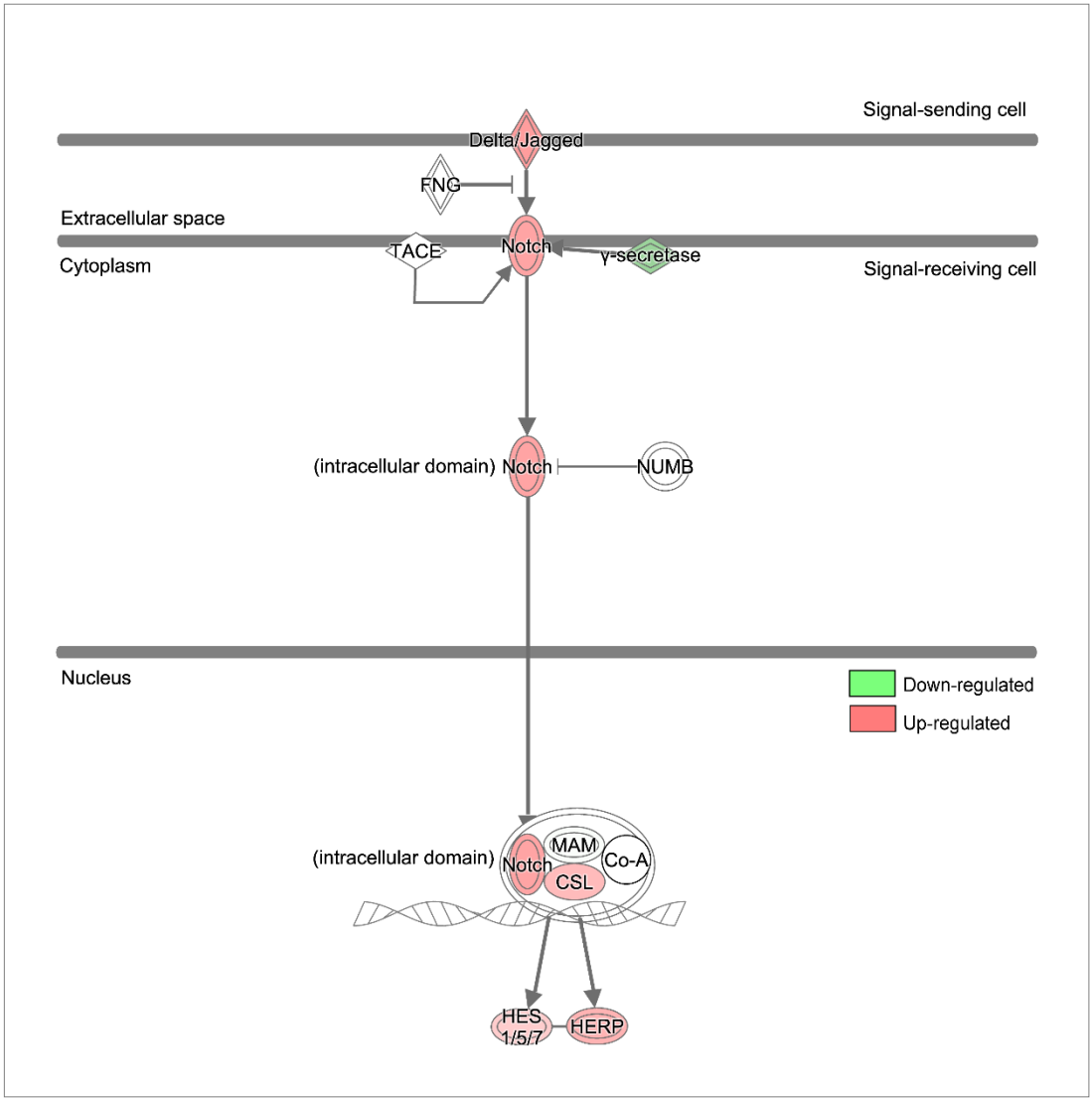


*Figure 5. 4: NICD-mediated gene expression changes in SJG6 + NICD compared to the SJG6 Blank in the NOTCH signalling pathway. The pathway was created using IPA (Qiagen).*

### 5.5.2 Wnt / β-catenin signalling pathway

In the Wnt / β-catenin signalling pathway, 18 out of 65 (28%) gene members were found to be altered as a result of NICD expression in SJG6. Despite an upregulation in WNT, the majority of pathway members were found to be downregulated (Figure 5.5).

In order to further elucidate the consequence of expression changes within the pathway, the IPA Molecule Activity Predictor (MAP) tool was used and findings overlaid. The MAP tool uses known expression states to predict the activity of neighbouring molecules. Although microarray analysis assesses the whole transcriptome, the stringent filter removes expression changes in genes that were not

consistent across the three biological replicas or less than 1.2 fold. Further, the microarray analysis only provides a snapshot of expression data. Whilst repeating the experiment minimises this limitation, the cells were still treated identically prior to analysis, i.e. lifted, centrifuged and FACS sorted. As such, valuable information can still be gained from MAP. The MAP analysis predicted an overall decrease in Wnt / β-catenin signalling targets and a resultant reduction in proliferation as a result of NICD expression.

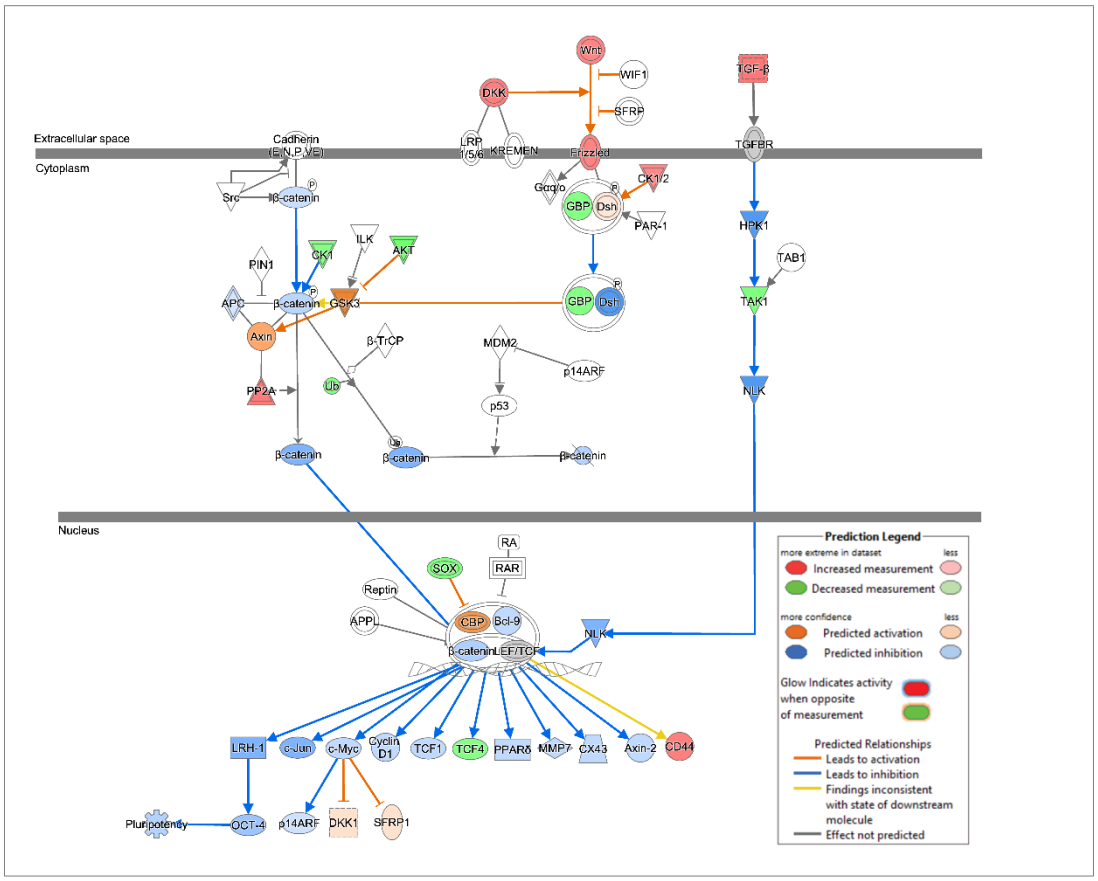


*Figure 5. 5: NICD-mediated gene expression changes in SJG6 + NICD compared to SJG6 Blank in the Wnt / β-catenin signalling pathway. The pathway was created using IPA (Qiagen).*

### 5.5.3 p16 signalling pathway

The expression of p16 was not found to significantly differ between SJG6 + NICD and SJG6 Blank. Further, only 6 out of the 45 (13%) pathway members were found to be altered (Figure 5.6).

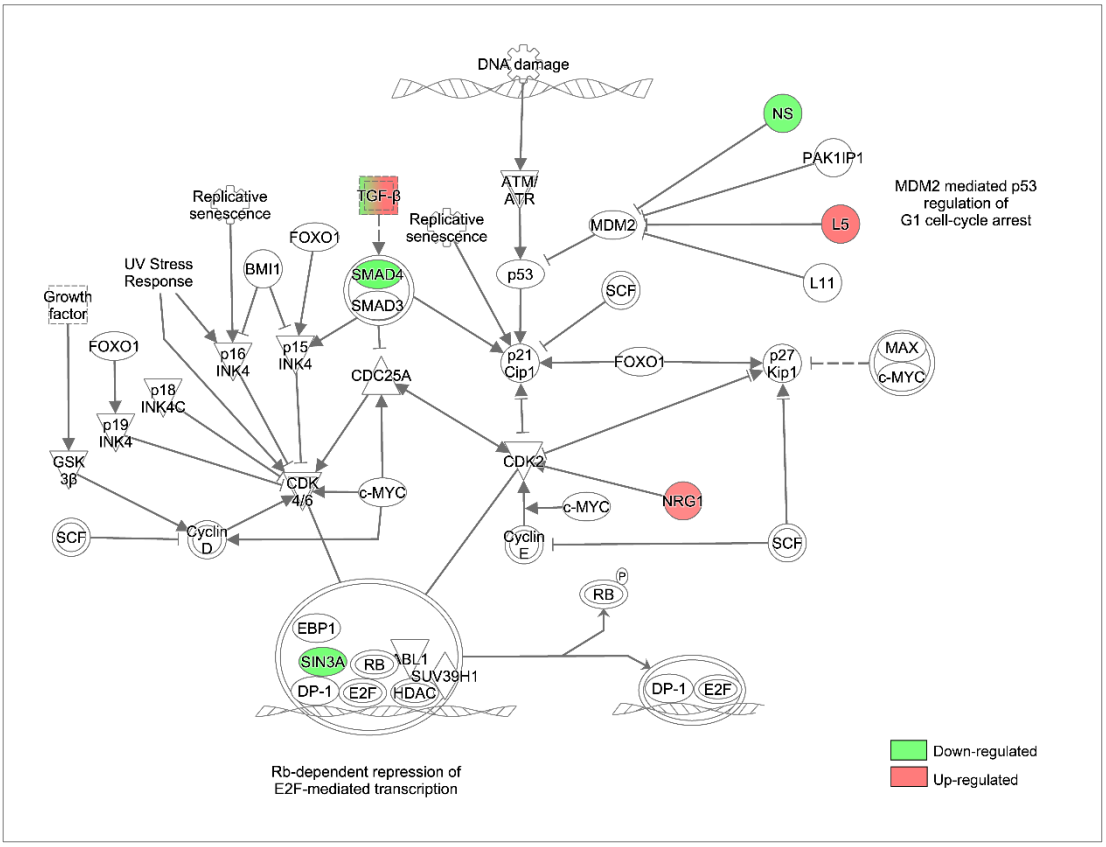


*Figure 5. 6: NICD-mediated gene expression changes in SJG6 + NICD compared to SJG6 Blank in the p16 signalling pathway. The pathway was created using IPA (Qiagen).*

## 5.6 Discussion

### 5.6.1 The expression of NICD alters the genetic landscape of SJG6

Microarray analysis shows a distinct difference in the genetic expression profile of SJG6 as a result of NICD expression. Further, GSEA analysis showed the difference in the biological state aligned with the genetics of several cancers, including oesophageal SCC. This data provides further evidence for the importance of NOTCH1 in SCCHN.

Of the top ten genes found to be up- or down- regulated in response to NICD expression, only STEAP4 has been previously recognised as a target of NOTCH1 (Wang, et al., 2017). Of the down-regulated genes, the expression of PLAG1, CTH and Vimentin (VIM) has been positively correlated with SCCHN (Marques Filho, et al., 2006; Giefing, et al., 2008; Bayo, et al., 2015). Further, increased expression of RMRP, SULT1 and LTBP1 has been recorded in other cancers (Xu, et al., 2012; Cao,

et al., 2015; Meng, et al., 2016). Therefore, the downregulation of this gene set in response to NICD expression provides evidence to suggest a tumour suppressor role for NOTCH1 in SCCHN.

Synonymously, the expression of VGLL4, a recognised tumour suppressor of oesophageal SCC, was found to decrease in response to NICD in SJG6 (Jiang, et al., 2015). In addition, TMEM27 and SFTA1P have been shown to act as tumour suppressors in other cancer and were also shown to be downregulated in response to NICD in SJG6 (Javorhazy, et al., 2016; Zhang, et al., 2017).

Conversely, CXCL11 and SPANX have been shown to be upregulated in SCCHN and are co-increased with NICD in SJG6 (Xia, et al., 2011; Zamunér, et al., 2015). STEAP4 and ITGB1 are also recognised oncogenes in other cancers and are found to be upregulated in response to NICD (Wu, et al., 2015; Kurozumi, et al., 2016).

Collectively, findings show that NICD is able to alter the expression of a number of key oncogenes and tumour suppressors in SJG6. Of the top 20 genes, the expression change in 9 would suggest a tumour suppressor role for NOTCH1 in SCCHN, whereas the expression change of 4 would indicate an oncogene function. Further research would be required to see how these genes work together in SCCHN to alter phenotype. One possibility is that the expression changes in individual genes compete with each other and the 'winning' genes govern the resultant changes in cell behaviour. Inversely, a single change in cell behaviour, such as EMT, could be responsible for expression changes in all genes. As aforementioned, NOTCH1 has been shown to have opposing role in SCCHN. This data highlights how the wider mutational landscape may influence this (Yap, et al., 2005).

Notably, fold changes identified in the SPANX family (co-increased with NICD) were 3x greater than that of any other gene. This will be explored further in Chapter 6.

### 5.6.2 NICD alters the expression of histones and their regulators

More than a quarter of GO terms for NICD-mediated expression differences in SJG6 were related to DNA organisation and 10% were specifically histone-related. As such, microarray data was mined for changes in the expression of histone related genes. Of the 3150 genes found to have greater than a 1.2 fold change difference, 68

were found to be histones or histone regulators (2.2%). Further, 62 of the 68 genes were found to be downregulated (91%).

Histones are the chief proteins involved in shaping chromatin structure and, consequently, gene expression. Recently, a role for histone variants in cancer progression has been suggested (Vardabasso, et al., 2014). More specifically, histone modifications have been associated with CSC plasticity in SCCHN and several histone regulator genes have been found to be frequently altered in oesophageal SCC (Le, et al., 2014; Song, et al., 2014). Interestingly, one of these genes, ASHL1, was found to be downregulated in the rescued SJG6 + NICD line (Song, et al., 2014).

Histone gene expression is cell cycle regulated. Histone protein synthesis is restricted to the S-phase of the cell cycle, coupled to DNA replication. During DNA replication, histones are essential for packaging DNA into chromosomes (Pogo, et al., 1966; Meshi, et al., 2000). As such, a decrease in histone related genes is consistent with *in vitro* and microarray data that have provided evidence to suggest that NICD expression gives rise to reduced cell proliferation.

To my knowledge, there are no studies linking NOTCH1 expression with that of histones or histone regulators. Further experiments would be required to confirm the association and underpin potential mechanisms. It is possible that NICD expression could lead to a downregulation in histone-related genes which subsequently gives rise to a decrease in cell proliferation. Alternatively, the decrease in histone related genes could be as a result of decreased cell proliferation.

### 5.6.3 Microarray analysis supports *in vitro* data and highlights SERPINE1 as a potential master regulator of NOTCH1 in SCCHN

In collaboration with *in vitro* data detailed in Chapter 4, proliferation and invasiveness were some of the top hits for GSEA analysis. The differentially expressed gene set between SJG6 + NICD and SJG6 Blank was assessed using IPA for molecular and cellular functions with an activation score of more than 2. Of the 52 functions, 18 suggested NICD expression could be associated with a decrease in cell migration and 5 predicted a decrease in proliferation. This data supports the *in vitro* findings. Further, 9 functions were related to decreased angiogenesis and 7 to increased cell survival, both of which shall be further considered in Chapter 7. It is important to note that IPA

is only able to provide information on known pathways. Therefore the 52 significant functions is unlikely to be exhaustive of all NICD-mediated changes.

Microarray data was mined for genes which could link NOTCH1 to the respective phenotypes. Interestingly, a downregulation of SERPINE1 was found to be common to all pathways, providing evidence to suggest a potential key role in instigating the effect of NOTCH1 in SCCHN. NICD expression has previously been linked to the inhibition of SERPINE1 in thyroid cancer (Yu, et al., 2016). Little is known about the role of SERPINE1 in SCCHN but, consistent with *in vitro* and microarray data, high expression has been correlated with increased cell migration (Pavón, et al., 2015). Moreover, the expression of SERPINE1 in the tumour microenvironment has been shown to promote amoeboid cell behaviour associated with cell migration in the metastatic process. Studies by Cartier-Michaud et al. showed a heterogeneous distribution of SERPINE1 at the tumour periphery and confirmed it is required for cells of a colorectal cancer cell line to undergo mesenchymal-amoeboid transition (Cartier-Michaud, et al., 2012).

### 5.6.4 Exploring the role of NOTCH1 in SCCHN in association with changes in key genes and pathways

*Cell Cycle Arrest*

Both *in vitro* and microarray data have provided evidence to suggest that the expression of NICD gives rise to cells with a reduced proliferative potential. A downregulation of free β-catenin and Wnt / β-catenin mediated signalling has been recorded in cells overexpressing NICD and has been suggested to act as a mechanism in NICD mediated cell cycle arrest (Nicolas, et al., 2003; Duan, et al., 2006). Although microarray data shows Wnt to be upregulated in response to NICD, overall Wnt / β catenin signalling is predicted to be decreased. Of note, in normal mouse epidermis, the deletion of β-catenin was not found to alter proliferation or differentiation of keratinocytes (Posthaus, et al., 2002).

In addition, in the skin, NOTCH1 expression induces growth arrest via p21 induction. In corroboration, microarray data confirmed a 1.21 expression fold increase in CDK1 (aka p21) in in response to NICD rescue (Table 5.1)

Finally, Kagawa et al. showed cell cycle arrest to be associated with both canonical CSL and p16 signalling. Microarray data confirmed the upregulation of CSL

and downstream target in SJG6 in response to NICD expression. However, expression of p16 was not found to change and fewer than 15% of pathway members were altered (Kagawa, et al., 2015).

*Invasion*

Of the 52 cellular and molecular functions identified within the differentially expressed gene set between SJG6 Blank and SJG6 + NICD, 19 were associated with a decrease in cell migration (13) and invasion (6) as a result of NICD expression.

Both *in vitro* and microarray data suggest that the expression of NICD reduces cell migration in SCCHN. This is inconsistent with research performed by Jing et al., who demonstrated a reduction in cell migration as a result of ADAM10 mediated downregulation of NOTCH1 in hypopharyngeal carcinoma (Jing, et al., 2016). Further, NOTCH1 expression has been shown to localise to the invasive tumour front in oral SCC and the expression of NOTCH1 has been positively associated with the depth of tumour invasion in tongue SCC (Joo, et al., 2009; Yoshida, et al., 2013).

Microarray data also suggests that expression of NICD reduces cell invasion in SCCHN. This is inconsistent with research by Yu et al. that provided evidence to suggest that NOTCH1 is able to mediate metastasis via the regulation of MMP2 and MMP9 in SCCHN (Yu, et al., 2012). Further, studies by Yoshia et al. suggest that the expression of NOTCH1 contributes to the maintenance of Tumour Necrosis Factor-α (TNF-α)-mediated invasion via the transcriptional regulation of SNAI2 and TWIST. During EMT, TWIST is known to induce SNAI2 which supresses the epithelial phenotype; TWIST and SNAI2 then work together to promote EMT and metastasis (Yoshida, et al., 2013). On the contrary, microarray data identified a decrease in MMP9 and SNAI2 in response to NICD. These findings add to the growing body of evidence showing that the effect of NOTCH signalling is highly context dependent and contingent on signal strength and timing (Radtke & Raj, 2003; Weng & Aster, 2004), which may go some way to explain its apparent opposing effects (Sun, et al., 2014).

*Angiogenesis*

Microarray data provides evidence to suggest that the expression of NICD reduces angiogenesis and downregulates the expression of VEGF. Likewise, Sun et al. reported a reverse correlation between NOTCH1 and VEGF expression in oesophageal SCC (Su, et al., 2009). Conversely, Troy et al. showed a positive correlation between NOTCH1 and VEGF expression. NOTCH1 has also been associated with increased micro-vessel density in oral SCC (Joo, et al., 2009; Troy, et al., 2013). Once again, this data provides further evidence for a context dependent role of NOTCH1 in SCCHN (Radtke & Raj, 2003; Weng & Aster, 2004).

### 5.6.5 Conclusion

In conclusion, microarray data has confirmed the expression of NICD in SJG6 is able to alter the genetic landscape, supporting the importance of NOTCH1 expression in SCCHN. Many of the top up- and down- regulated genes were found to be recognised oncogenes and tumour suppressors as well as histones and histone regulators. The genome wide effect of histone alterations opens up avenues for further understanding the role of NOTCH1 in SCCHN.

Overall, microarray data has provided evidence to suggest NICD expression gives rise to decreased proliferation, decreased cell migration, reduced angiogenesis and increased cell death. As such, and consistent with *in vtiro* data, findings suggest a tumour suppressor role for NOTCH1 in SCCHN. Inhibition of SERPINE1 was also highlighted as a potential mediator of NICD-induced changes in cell behaviour. Taken with current literature, findings further highlight the complexity of NOTCH signalling in SCCHN.

Notably, fold changes identified in the SPANX family were 3x greater than that of any other gene. This will be explored further in Chapter 6.

# Chapter 6

## Investigating the Relationship between NOTCH1 and SPANX in SCCHN

---

This chapter begins to explore the relationship between NOTCH1 and SPANX in SCCHN. Microarray analysis identified a large increase in SPANX family gene expression in the SJG6 cell line rescued for NICD (SJG6 + NICD) compared to the empty vector control (SJG6 Blank). In order to investigate the functional consequence of SPANX expression, a shRNA system was used to knockdown SPANX in SJG6 + NICD. *In vitro* assays developed in Chapter 3 were then performed to compare cell behaviour in SGJ6 + NICD and the SJG6 + NICD – SPANX Knockdown (hereby referred to as 'SPANX Knockdown').

---

### 6.1 Introduction to SPANX

A number of genes that are normally expressed in the testis are found to be induced in tumour cells and are collectively referred to as Cancer Testis Antigens (CTAs) (Old, 1982). The human SPerm Associated with the Nucleus on the X chromosome (SPANX) genes make up a family of 5 recognised members (SPANX-A1, -A2, -B, -C and –D), all of which are CTAs. The gene family encodes small unfolded proteins able to make complexes with other proteins (Westbrook, et al., 2000). In transformed mammalian cells, the SPANX family proteins have been affiliated with the nuclear envelope (Westbrook, et al., 2004).

The SPANX genes map to a region of the X chromosome (Xq27) shown to be associated with cancers. The most well studied association is with familial prostate cancer (Peters, et al., 2001; Stephan, et al., 2002; Kouprina, et al., 2005; Yaspan, et al., 2008). However, The Atlas of Genetics and Cytogenetics in Oncology and Haematology details chromosomal abnormalities in Xq27 in the following tumour types: pharynx, skin, breast, bone, brain, brain stem, pancreas, ovary, liver, large

intestine, haematopoietic and lymphoid tissue, endometrial and kidney (Huret, et al., 2012 ).

Staining for SPANX family members in both cancerous and normal prostate tissue has confirmed a significant upregulation of SPANX in the cancerous tissue. SPANX expression was found to be both cytoplasmic and nuclear in the cancerous tissue, compared to normal tissue which presented with localised nuclear expression (Salemi, et al., 2010).

In a similar study by the same group, SPANX staining was found to be recorded in 80% of melanomas. Approximately 44-54% of cells within each tumour stained positive for SPANX and staining was found to be largely nuclear. In comparison, no SPANX expression was recorded in normal skin tissue (Salemi, et al., 2009). SPANX B and C have both been recorded in melanomas, however, SPANXA has been showed to be the most frequently expressed variant (Zendman, et al., 2003; Salemi, et al., 2008). Increased SPANX staining has also been associated with more aggressive melanomas, in particular distant, non-lymphatic metastases (Westbrook, et al., 2004).

The expression of SPANX has been positively correlated with invasion and metastasis in several tumour types, including skin, liver, breast, colorectal and lung (Westbrook, et al., 2004; Chen, et al., 2010; Yilmaz-Ozcan, et al., 2014; Maine, et al., 2016; Hsiao, et al., 2016). In breast cancer studies, SPANX A/C/D has been shown to localise to the nuclear membrane where it associates with laminin A/C and is essential for the formation of actin-rich cell projections which are able to reorganise the extracellular matrix. SPANXA/C/D has been shown to be required for metastasis of primary breast tumours into the lung (Maine, et al., 2016).

SPANX expression has also been associated with EMT/MET. Yilmaz-Ozcan et al. correlated increased SPANX B expression with the spontaneous differentiation of a colorectal cell line and demonstrated that differentiation of these cells led to MET. MET was confirmed by the increased expression of mesenchymal markers (CDX2, claudin-4 and E-cadherin) and the downregulation of epithelial markers (vimentin, fibronectin and transgelin). The group showed that the reversal of differentiation gave rise to a downregulation of SPANX and the induction of EMT markers (Yilmaz-Ozcan, et al., 2014). Further, Hsiao et al. showed that the expression of SPANXA was able to supress epithelial to mesenchymal transition (EMT) in lung adenocarcinoma by inhibiting c-JUN / SNAI2 signalling (Hsiao, et al., 2016).

In 2009, a study performed by Almanzar et al. confirmed an increased expression of SPANX B in 146 tumours from skin, lung, ovary, colon and breast. Interestingly, PCR, western blot and immunostaining confirmed an immunogenic response by CD4+ and CD8+ T-cells. The largely tumour specific expression of SPANX and immunogenic properties indicate promise for targeting SPANX expression in immunotherapies (Almanzar, et al., 2009).

Finally, increased SPANX expression has been associated with CSCs in triple negative breast cancer. Knockdown of SPANX was shown to give rise to a decrease in the percentage of CSC markers in the cell population (Shahin, et al., 2017).

Overall, the SPANX gene family has been found to be overexpressed in a number of cancers and has been associated with enhanced metastasis and maintenance of CSCs. The expression of SPANX genes in tumour cells has also been positively correlated with poor prognosis (Yang, et al., 2015).

Very little is known about the role of SPANX in SCCHN, but SPANXC/D has been shown to be expressed in 71.9% of tumours (Zamunér, et al., 2015). This chapter aims to further elucidate the functional consequence of SPANX expression in SCCHN and the relationship between SPANX and NOTCH1.

## 6.2 The Expression of SPANXA1/2 Increases in Response to NICD

Microarray analysis identified a 6-fold increase in SPANX family gene expression in SJG6 + NICD compared to SJG6 Blank. RT-qPCR was used to validate this expression change and investigate the individual gene family members (Figure 6.1). RT-qPCR confirmed a large fold expression increase of SPANXA1/2 (5.73 x) in the rescued SJG6 line. However, SPANXB1 and SPANXC/D were not found to be expressed in SJG6 Blank or SJG6 + NICD.

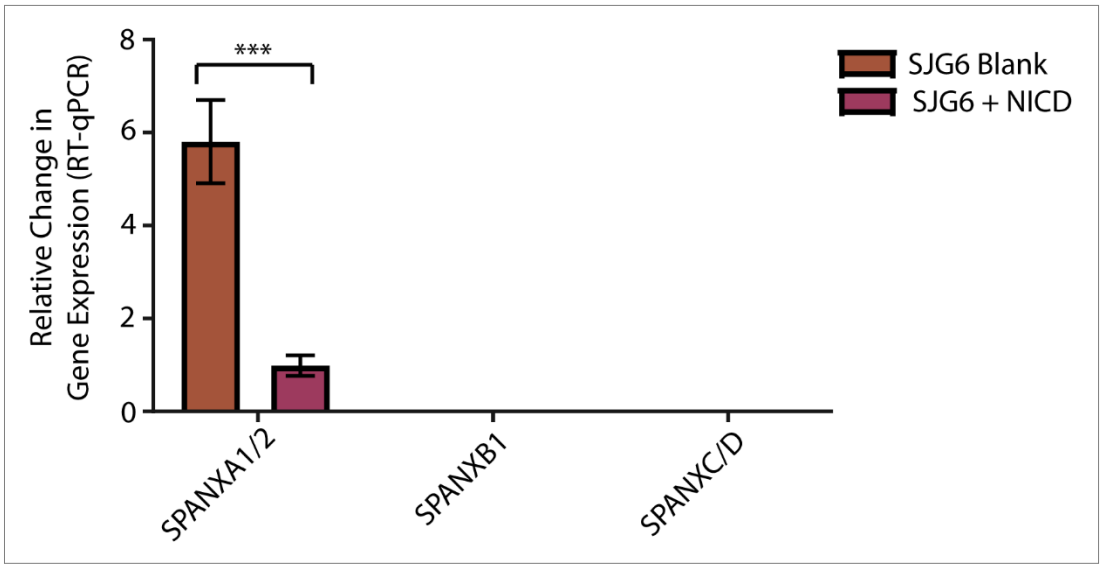


*Figure 6 1: RT-qPCR expression analysis of SPANXA1/2, SPANXB1 and SPANXC/D in SJG6 Blank and SJG6 + NICD. Gene expression was normalised to the s18 and GAPDH housekeeping genes. *** Student's t-test value <0.005. n=3.*

## 6.3 SPANXA1/2 was Successfully Knocked Down in SJG6 + NICD

In order to investigate the functional consequence of this increase in SPANXA1/2 expression, a doxycycline inducible puromycin-resistant shRNA system was used to knockdown SPANXA1/2 in SJG6 + NICD (Dharmacon). SJG6 + NICD was incubated with the SPANXA1/2-targeted shRNA for 72hrs. Cells were then split and allowed to recover for 48hrs before selecting the successfully transduced cells in 1 µg/ml puromycin. The resultant 'SPANX Knockdown' population was expanded in culture and stocks frozen. Due to time constraints, all experiments from the SPANXA1/2 Knockdown were only run twice. Although statistical tests can be run on n=2, the power is significantly reduced. As such, no statistics were performed. Instead, measurements from both experiments have been displayed to show the level of consistency.

In order to validate the knockdown, SPANXA1/2 expression was assessed at the protein level by immunohistochemistry staining (Figure 6.2a). The SJG6 + NICD, SPANX Knockdown and SJG6 Blank cell lines were plated on collagen coated 96 well plates at a density of 2 x $10^3$ / well. The knockdown of SPANXA1/2 was induced by introducing 1.5 µg/ml doxycycline to the culture media. The same concentration of doxycycline was introduced to the SJG6 + NICD and SJG6 Blank cell lines as a

control. At 48hrs, cells were fixed in 4% PFA and stained for SPANXA1/2 (red). Nuclei were stained with DAPI (blue). A clear reduction in the expression of SPANXA1/2 was observed in the SPANX Knockdown compared to SJG6 + NICD. SPANX expression in the knockdown returned to similar levels to that seen in SJG6 Blank.

The mRNA expression of SPANXA1/2 was assessed via RT-qPCR (Figure 6.2b). In both experiments, the mRNA expression of SPANXA1/2 in the SPANX Knockdown was found to decrease to 39.1% and 41.1% of SJG6 + NICD.

The mRNA expression of NOTCH1 and several genes that were found to be altered by NICD expression via microarray were also assessed. NOTCH1 expression showed a similar decrease in both SPANX Knockdown experiments to 86.5% and 84.6% of SJG6 + NICD levels. Conversely, expression changes in TMEM27, HEY1, CTH, ITGBL1 and ITGB6 were more variable between the two experiments.

As a control, SJG6 + NICD was also transduced with a doxycycline inducible non-targeting control shRNA. SPANXA1/2 expression was not found to decrease in this line, further confirming the validity of the SPANX Knockdown (Figure 6.2c).

## 6.4 Expression of SPANXA1/2 Potentially Increases Cell Proliferation

An EdU assay was performed to compare the proliferative potential of SJG6 + NICD and the SPANXA1/2 Knockdown (Figure 6.3). The cell lines were seeded onto collagen-coated 96 well plates at a density of 2 x $10^3$ and doxycycline was introduced at a concentration of 1.5 µg/ml to induce the SPANX Knockdown. At 46hrs, EdU was introduced. At 48hrs, cells were fixed in 4% PFA. Over the two hour period, a higher percentage of proliferating cells were recorded in SJG6 + NICD (37.5% and 37.0%) than in the SPANX Knockdown (34.3% and 34.0%). Although the difference between the percentages of proliferating cells was small, it was highly consistent between the two experiments. Many factors can effect proliferation and further experiments would be required. However, this finding provides preliminary evidence for a potential relationship between SPANX expression and proliferation.

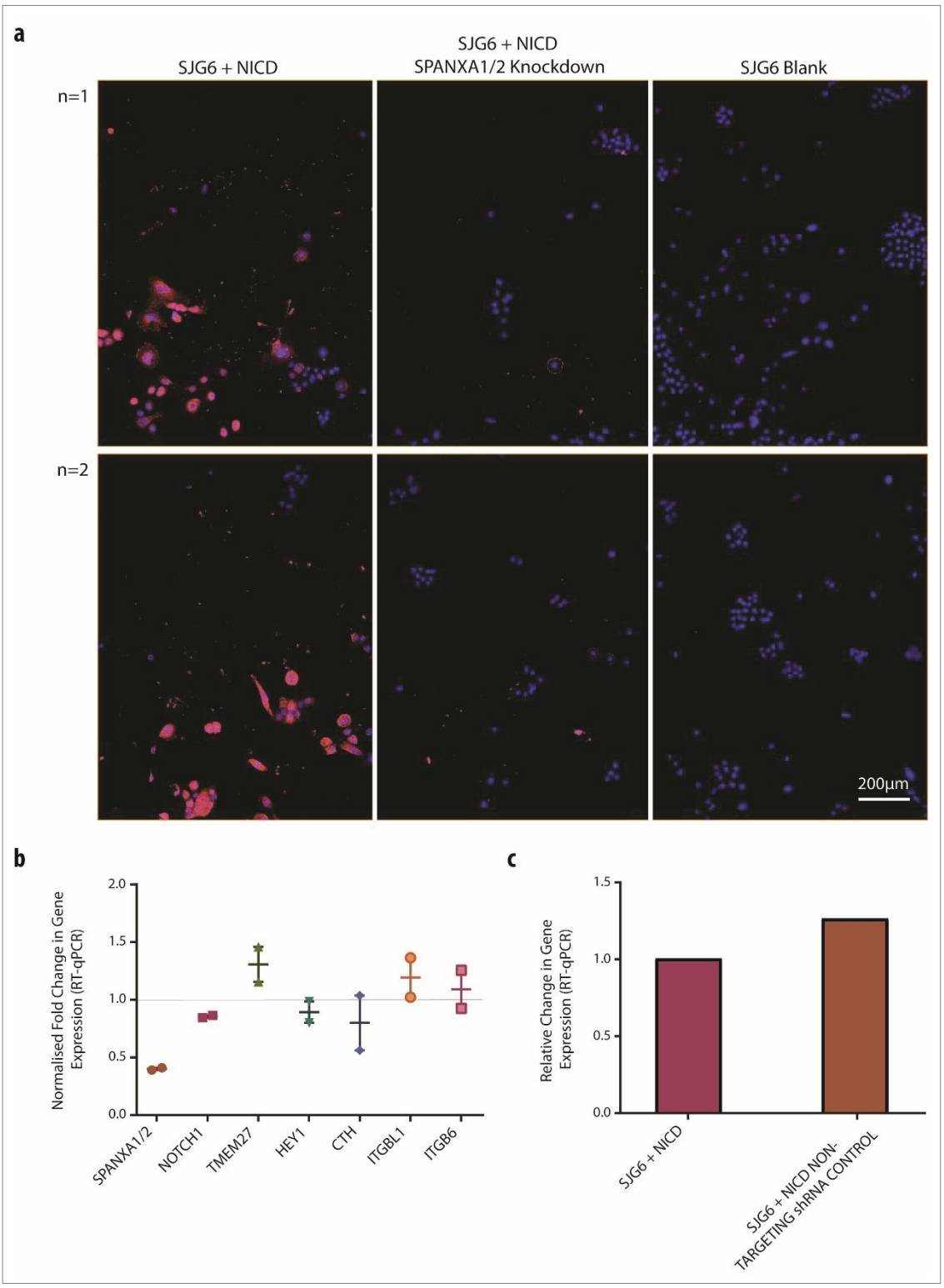


*Figure 6 2: (a) Immunohistochemistry staining of SJG6 + NICD, SPANX Knockdown and SJG Blank. Red = SPANXA1/2. Blue = DAPI. (b) RT-qPCR analysis showing changes in the expression of SPANXA1/2, NOTCH1, TMEM27, HEY1, CTH, ITGBL1 and ITGB6 in SPANX Knockdown compared to SJG6 + NICD. The expression of SJG6 + NICD is normalised to 1 and shown by the grey line. (c) RT-qPCR analysis of SPANXA1/2 expression in SJG6 + NICD compared to SJG6 + NICD transduced with a non-targeting shRNA control. Gene expression was normalised to s18 and GAPDH housekeeping genes. n=2.*

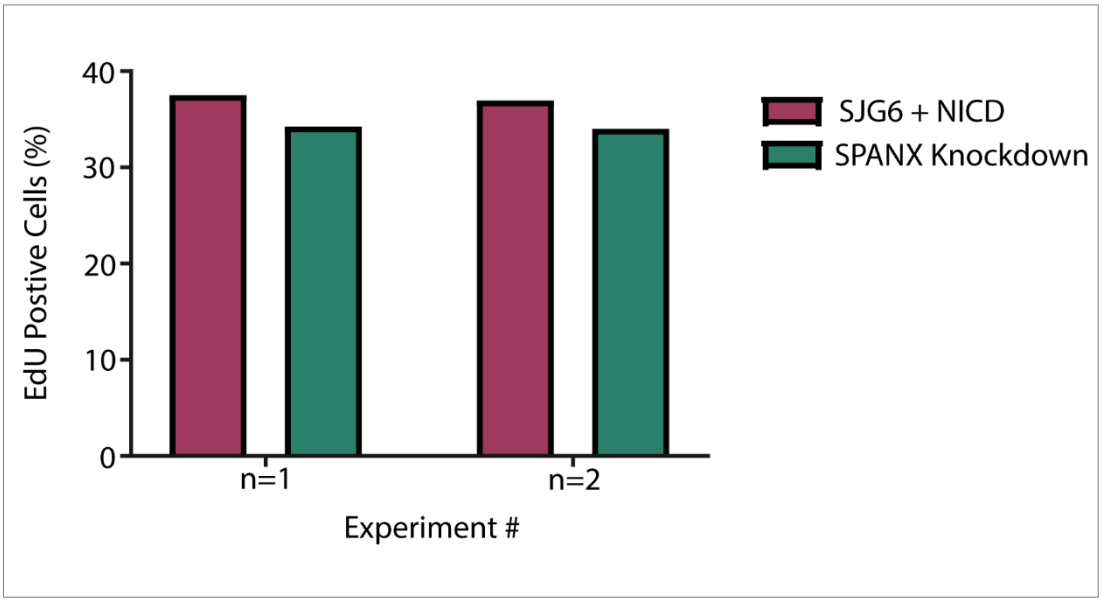


*Figure 6 3: EdU assay comparing the percentage of proliferating cells in SJG6 + NICD and the SPANX Knockdown. n=2.*

## 6.5 Expression of SPANXA1/2 does not Alter Commitment to Differentiation

In order to compare the level of differentiation in SJG6 + NICD and the SPANX Knockdown, cells were stained with antibodies to Transglutaminase 1, a marker of epithelial differentiation (Figure 6.4). Both cell lines were seeded onto collagen coated 96 well plates and doxycycline was introduced at a concentration of 1.5 µg/ml to induce the SPANXA1/2 Knockdown. At 48hrs, the cells were fixed and stained with Transglutaminase 1. Nuclei were stained with DAPI. The Operetta High Content Imaging system was used to identify the percentage of Transglutaminase 1 positive cells in both populations (pipeline detailed in Figure 2.2). No consistent difference was recorded.

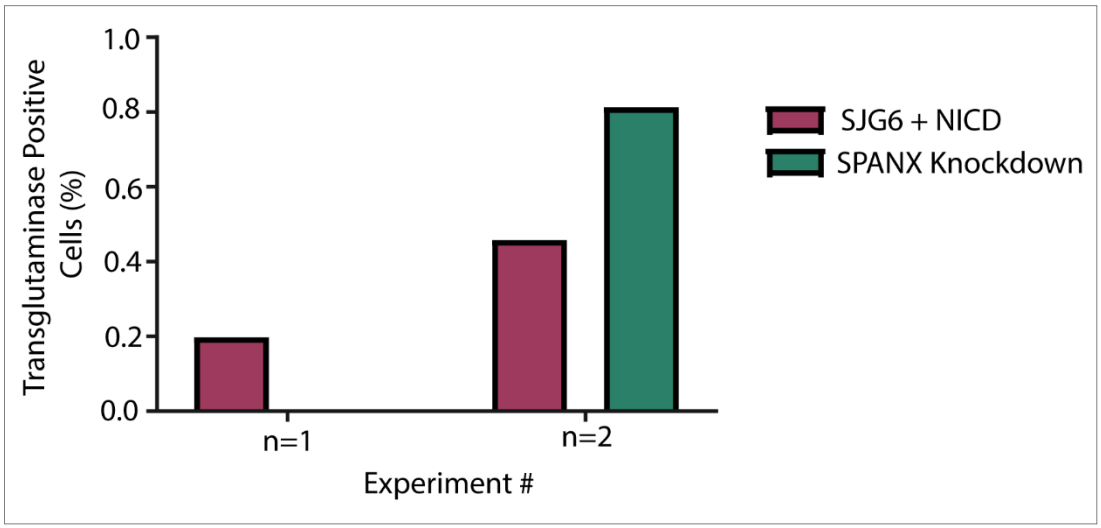


*Figure 6 4: Transglutaminase 1 staining to compare the percentage of differentiated cells in the SJG6 + NICD and SPANX Knockdown lines. n=2.*

## 6.6 Expression of SPANXA1/2 Alters Cell Morphology

Cytoplasmic Cell Mask staining was performed to investigate morphological differences between SJG6 + NICD and the SPANX Knockdown. Both cell lines were seeded onto 5 µg/ml of fibronectin in 96 well plates and doxycycline was introduced at a concentration of 1.5 µg/ml to induce the SPANXA1/2 Knockdown. At 48hrs, cells were fixed, stained with Cell Mask and DAPI, and analysed using the Operetta High Content Imaging System (pipeline detailed in Figure 2.2).

Morphological differences were observed between the two cell lines (Figure 6.5). In both experiments, SJG6 + NICD was substantially and consistently smaller and more round than the SPANX Knockdown. There was also fewer elongated cells (roundness <0.6) in the SJG6 + NICD population. Potential implications will be discussed further in the discussion of this chapter.

## 6.7 Expression of SPANXA1/2 Potentially Increases Cell Migration

A scratch wound assay was performed to compare the rate of cell migration between SJG6 + NICD and the SPANX Knockdown (Figure 6.6). Both cell lines were first treated with mitomycin-C to remove proliferation bias. A scratch wound was then created and the confluence of cells in the wound area was calculated over a 25hr

period. In both experiments, SJG6 + NICD cells were found to migrate into the wound area at a substantially faster rate than the SPANX Knockdown cells.

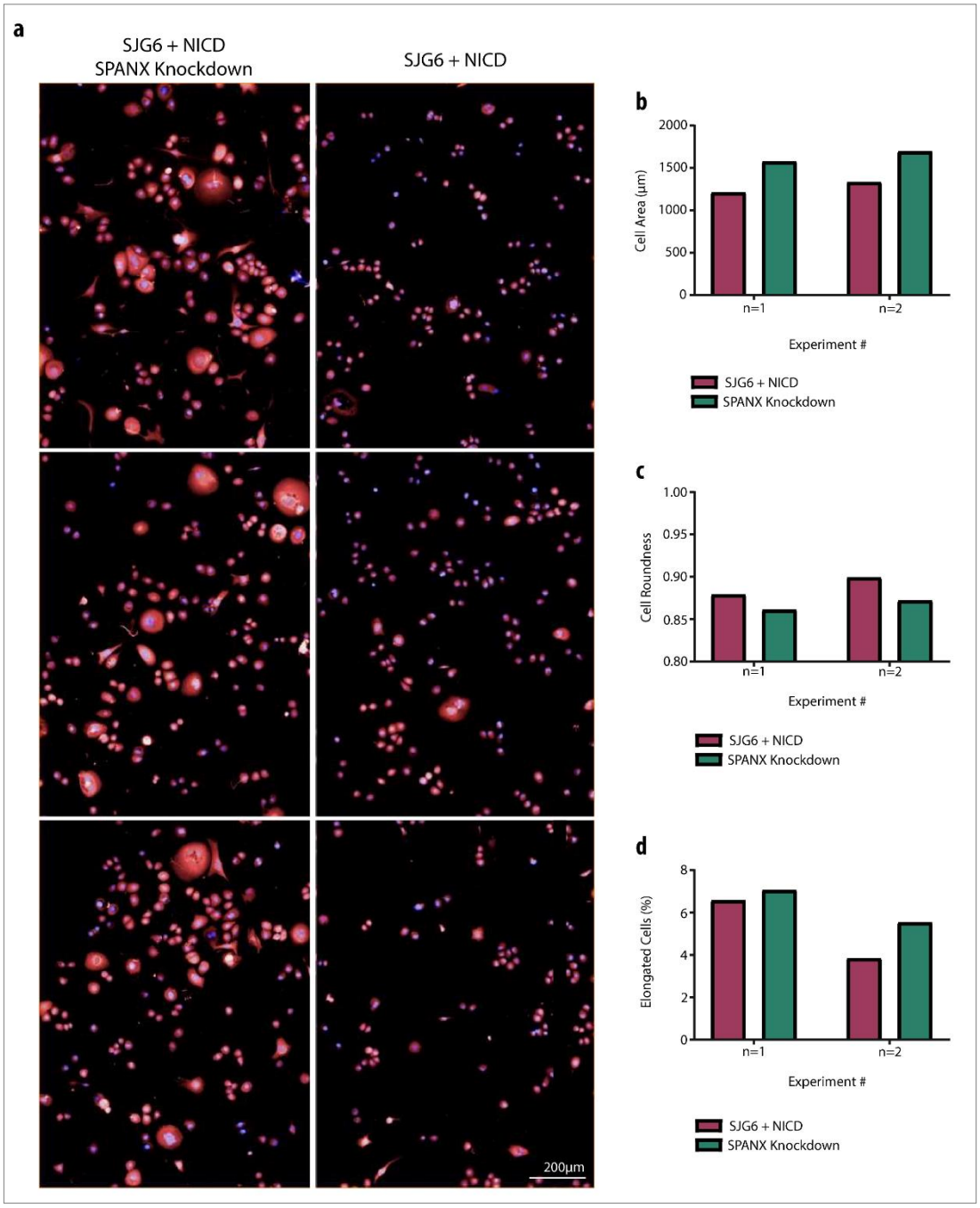


*Figure 6 5: Operetta analysis comparing the morphology of the SJG6 + NICD and the SPANX Knockdown lines. (a) Representative images of SPANX Knockdown (left) and SJG6 + NICD (right). Nuclei were stained with DAPI (blue) and cytoplasm was stained with Cell Mask (red). (b) Measure of cell area. (c) Measure of cell roundness ratio. (d) By thresholding for cells with a roundness ratio of less than 0.6, elongated cells in the population were identified and calculated as a percentage of total cell number. n=2.*

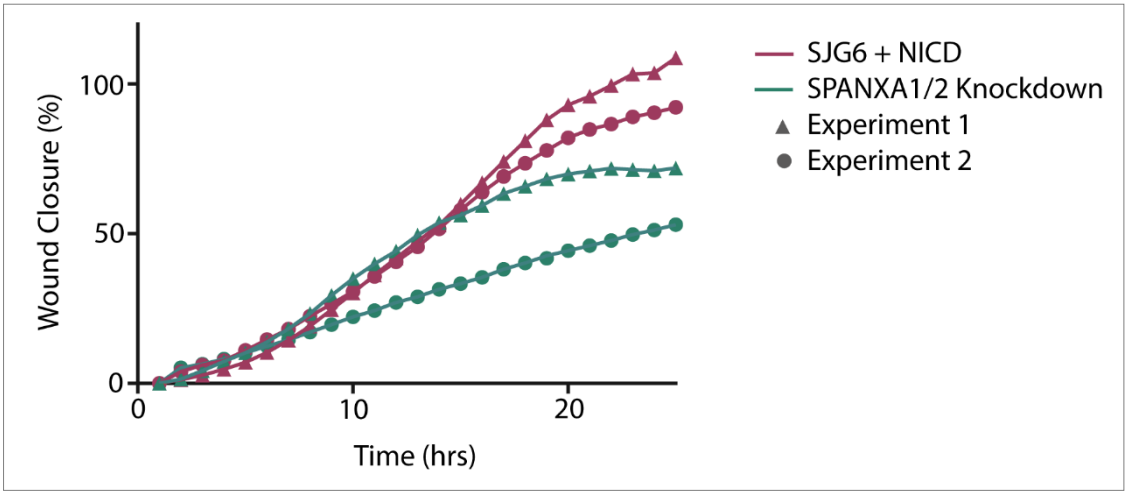


*Figure 6 6: Scratch wound assay to compare the rate at which the SJG6 + NICD and the SPANX Knockdown cell lines migrate to recolonise the initial wound area. n=2.*

## 6.8 Discussion

### 6.8.1 Evidence suggests a correlation between NOTCH1 and SPANXA1/2 Expression in SCCHN

RT-qPCR data confirmed a large increase in SPANXA1/2 expression in response to NICD. Conversely, family members SPANXB1 and SPANXC/D were not found to be expressed in the SJG6 cell line. Equally, the knockdown of SPANXA1/2 in SJG6 + NICD resulted in a reduction of NOTCH1 expression, suggesting a feedback loop may exist between the two genes. Interestingly, an approximate 3x fold change increase in NICD resulted in a 6x fold change increase in SPANXA1/2 expression. Likewise, a decrease in SPANXA1/2 expression to approximately 40% of that of SJG6 + NICD led to a decrease in NOTCH1 expression to 85%. In both cases, the change in SPANXA1/2 expression is approximately double that of NICD, providing further evidence for a relationship between the two genes. Notably, this exaggerated expression change could be an interesting target to utilise SPANXA1/2 as a NOTCH1 biomarker.

The expression of SPANXC/D has been previously recorded in 71.9% of head and neck cancers, but no evidence exists on the expression pattern of SPANXA1/2 (Zamunér, et al., 2015). Moreover, evidence to suggest a relationship between SPANXA1/2 and NOTCH is novel.

### 6.8.2 SPANXA1/2 does not mediate NICD-induced differentiation or cell cycle arrest

No association between SPANXA1/2 and terminal differentiation was recorded. However, EdU data showed a potential decrease in proliferation in the SPANX Knockdown compared to the SJG6 + NICD cell line. As such, it is unlikely that SPANX mediates the NICD-induced cell cycle arrest detailed in Chapter 4. Very little is known about the role of SPANXA1/2 on tumour cell proliferation. However, CTA expression has been associated with poor prognosis in a number of cancers, which would be consistent with a positive correlation of SPANXA1/2 with cell proliferation (Yang, et al., 2015). However, as aforementioned, many factors can effect proliferation and further experiments would be required to investigate a potential relationship between proliferation and SPANX expression.

### 6.8.3 The knockdown of SPANXA1/2 reverses NICD-mediated changes in cell morphology

The knockdown of SPANXA1/2 was found to increase cell area, reduce cell roundness and increase the percentage of elongated cells in the population. In 2016, Hsiao et al. showed that the expression of SPANXA was able to supress epithelial to mesenchymal transition (EMT) in lung adenocarcinoma by inhibiting c-JUN / SNAI2 signalling. Consistent with data in this study, the group found that the increased expression of SPANXA was able to markedly change cell morphology from mesenchymal- to epithelial- like, i.e. less elongated and more rounded. Furthermore, as detailed in Chapter 5, SNAI2 was found to be decreased as a result of increased NICD expression. Overall, this data provides preliminary evidence to suggest that SPANXA may also be able to supress EMT by inhibition of c-JUN/SNAI2 signalling in SCCHN. Further, NOTCH1 may act as an upstream regulator of this signalling (Hsiao, et al., 2016). Further experiments would be required. These findings are inconsistent with the role of NOTCH1 as a positive regulator of SNAI2 (Niessen, et al., 2008; Ambler & Watt, 2010).

In addition, the expression of SPANX B in colorectal tumours has been associated with the induction of MET as measured by the induction of epithelial markers and downregulation of mesenchymal markers. In corroboration, microarray

data found vimentin to be one of the top downregulated genes in response NICD expression (Yilmaz-Ozcan, et al., 2014). As such, it would be of interest to investigate potential relationships between NOTCH and SPANX expression with EMT/MET in future experiments.

### 6.8.4 SPANXA1/2 expression is associated with increased cell migration

Scratch wound data suggests that the expression of SPANXA1/2 is associated with increased cell migration. This finding is inconsistent with the role of SPANXA as a suppressor of EMT (Hsiao, et al., 2016). However, it is important to note that wound closure is not a direct measure of metastatic potential. Although cells may be more motile *in vitro*, they may not have the ability to invade through the extracellular matrix or enter a mesenchymal state. Conversely, SPANXC/D have been associated with malignant progression (Yang, et al., 2015; Maine, et al., 2016).

### 6.8.5 Conclusion

This study provides evidence to suggest a positive correlation between NOTCH1 and SPANXA1/2 expression, whereby a fold change in NOTCH1 is reflected by a 2x fold change in SPANXA1/2.

SPANXA1/2 was found to potentially increase cell proliferation, consistent with its proposed role tumorigenesis (Yang, et al., 2015). This is inconsistent with the role of NICD in cell cycle arrest. Therefore, if findings prove to be correct, other NICD-mediated changes in gene expression must able to out-compete the inducing action of SPANXA1/2 to dictate the final cell proliferation phenotype in SJG6.

NICD-mediated changes in cell morphology observed in SJG6 were reversed by SPANXA1/2 knockdown. Further, SNAI2 expression was increased. Collectively, findings suggest NICD expression may be able to suppress EMT in SCCHN via SPANX-mediated inhibition of c-JUN/SNAI2 expression (Maine, et al., 2016). Moreover, a decrease in vimentin provides further basis for investigating the potential role of SPANXA1/2 expression on EMT/MET in future experiments. SPANXA1/2 expression was also found to increase cell migration, consistent with the role of SPANXC/D in metastatic progression (Yang, et al., 2015; Maine, et al., 2016).

This study begins to investigate the relationship between NOTCH1 and SPANXA1/2 in SCCHN. More extensive studies are required. However, preliminary

data provides evidence to warrant further investigation into the potential role of NOTCH mediated SPANX signalling in SCCHN cell behaviour and in particular in EMT/MET. This will be discussed further in Chapter 8.

# Chapter 7

## Investigating the Role of NOTCH1 in SCCHN *in vivo*

---

*Although in vitro studies can provide valuable information on cancer cell behaviour, they are limited as they do not recapitulate the tumour microenvironment. Cancer cell genomics and cell behaviour are influenced by both the mechanics of the 3D tumour architecture and the interaction of cancer cells with the stroma. This chapter begins to investigate the effect of NOTCH1 expression on tumour development in vivo using a xenograft model.*

---

A suspension of 100,000 SJG6 Blank or SJG6 + NICD cells were injected into the dorsal tongue of immunocompromised mice and tumours were allowed to develop over 60 days (Goldie, et al., 2012). A cohort of 7 mice (pooled from two experiments) was used for SJG6 Blank and SJG6 + NICD. Unfortunately, one SJG6 + NICD mouse did not recover from surgery, so analysis was performed on the remaining 6. In addition, one SJG6 Blank mouse did not form a tumour. A smaller cohort of 2 mice was injected with PBS as a control for the process of injecting a liquid volume into the tongue.

Notably, a further experiment was performed in which 50,000 cells were injected and mice were harvested after 30 days; however, no tumours formed. Although immunocompromised, the NSG mice still produce neutrophils and monocytes capable of clearing tumour cells (The Jackson Laboratory, 2017). It is possible that 50,000 cells is below the threshold required to overcome the murine model's innate immune system in order to successfully form a tumour. Successful xenograft formation has been recorded in more than 80% of mice injected with 10,000 SCC13 cells (an established facial SCC line) and approximately 40% of mice injected with 1,000 SCC13 cells (Benaich, et al., 2014). However, the cell threshold required for tumour formation will be specific to the cell line. For example, a cell line with a higher proportion of CSCs will have a lower threshold than a highly differentiated cell

line. It is also possible that 30 days was too short for effective tumour development. A study into xenografts established from gastric cancer biopsies taken from different patients revealed a range of latency periods, from 11-160 days (Zhu, et al., 2015).

This chapter highlights preliminary results from the two experiments that did yield tumours and provides the basis for further study into the role of NICD in SCCHN *in vivo.* Plans for continuation of the study are detailed in Chapter 8.

## 7.1 The Expression of NICD Resulted in Increased Weight Loss in Xenograft Hosts

The weight of mice was monitored for the duration of the experiments. Figure 7.1 shows the week-by-week changes for mice injected with SJG6 Blank cells, SJG6 + NICD cells and PBS. Due to the young age of the mice (6 weeks), the average weight of all three groups increased during the first 5 weeks of the experiment. Between 5 and 10 weeks, weight plateaued. Until week 10, weight changes were similar between the three groups. However, between weeks 10 and 12, the average weight of mice injected with SJG6 + NICD significantly decreased by approximately 15%. To note, due to ethical concerns, two mice of this cohort were culled at day 58, 48hrs sooner than the experimental end point of 60 days (hereby referred to as Xenografts A and D of SJG6 + NICD).

Dissection of the mouse lymph nodes showed that they were clear of secondary growths. RT-qPCR of the lymph node tissue also confirmed an absence of mCherry and human markers. Further, flow cytometry did not identify mCherry or EpCAM (an epithelial cell marker) in the blood. The primary tumours made up the sole focus of this study.

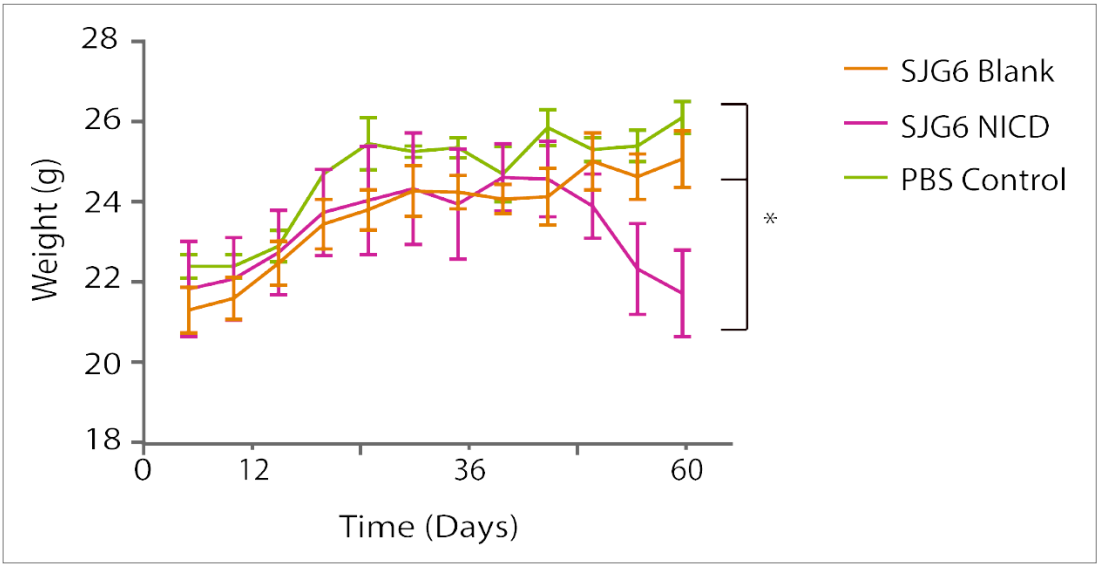


*Figure 7 1: Average weight of mice injected with either SJG6 Blank cells (orange), SJG6 + NICD cells (pink) or PBS (green) over a 60 day period. *The SJG6 + NICD cohort weighed significantly less than the SJG6 Blank cohort and PBS control at day 60. Student's t-test < 0.05. n = 7 for SJG6 + NICD. n= 6 for SJG6 + Blank. n=2 for PBS control.*

## 7.2 SJG6 + NICD Cells gave rise to Significantly Larger Tumours than SJG6 Blank Cells

On day 60, the mice were sacrificed and tongues collected. Tumours were visible by eye and macroscopic imaging in tongues that had been injected with SJG6 Blank and SJG6 + NICD cells. No tumours had formed in the PBS controls.

Of the 7 mice injected with SJG6 Blank, 6 developed tumours. The tongues were frozen in OCT and a cryostat was used to create serial sections from different points along the width of the tumours. The absence of a tumour in the 7$^{th}$ SJG6 Blank mouse was confirmed by H&E staining of 8 µm serial sections (Figure 7.2). All mice injected with SJG6 + NICD developed tumours. Tumour area was measured using FIJI. Tumours derived from SJG6 + NICD were found to be significantly larger than those derived from SJG6 Blank (Figure 7.3).

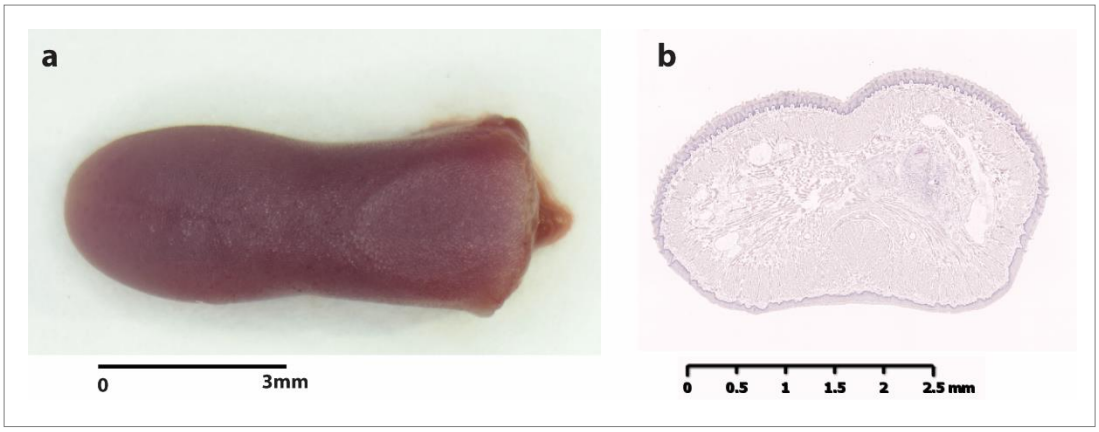


*Figure 7 2: 100,000 SJG6 Blank cells were injected into the tongues of 7 mice in a xenograft experiment. One mouse did not form a tumour. (a) Macroscopic image of said tongue (b) Representative H&E image from serial sections confirming the absence of a tumour.*

## 7.3 Enhanced NICD Expression was Diminished by Day 60 but Increased SPANXA1/2 Remained

The cells of 50 µm sections were lysed, RNA was extracted and reverse transcription was performed. The resultant cDNA was analysed by RT-qPCR for the expression of human NOTCH1 (primer specific for the NICD domain), mCherry and SPANXA1/2 (Figure 7.4).

Xenografts derived from SJG6 Blank and SJG6 + NICD showed no significant difference in NICD expression. However, 4/6 SJG6 + NICD xenografts were recorded to have a higher expression of SPANXA1/2 than the highest expressing xenograft of SJG6 Blank (25, 46, 105 and 267 fold respectively). Xenografts derived from SJG6 + NICD also presented with significantly reduced mCherry expression compared to SJG6 Blank xenografts. Potential explanations for these findings are considered in the discussion of this chapter.

Tumour sections of 10 µm were processed for immunohistochemistry. Unfortunately, NICD and SPANXA1/2 staining was unconvincing. Both NOTCH1 and SPANXA1/2 proteins are conserved in mice, which may go some way to explain the high background and unspecific staining (Kouprina, et al., 2004). In addition, there is high conservation between the four human NOTCH receptors. Further experiments will be required to investigate the protein expression levels of NOTCH1 and SPANXA1/2 *in vivo,* as detailed in Chapter 8.

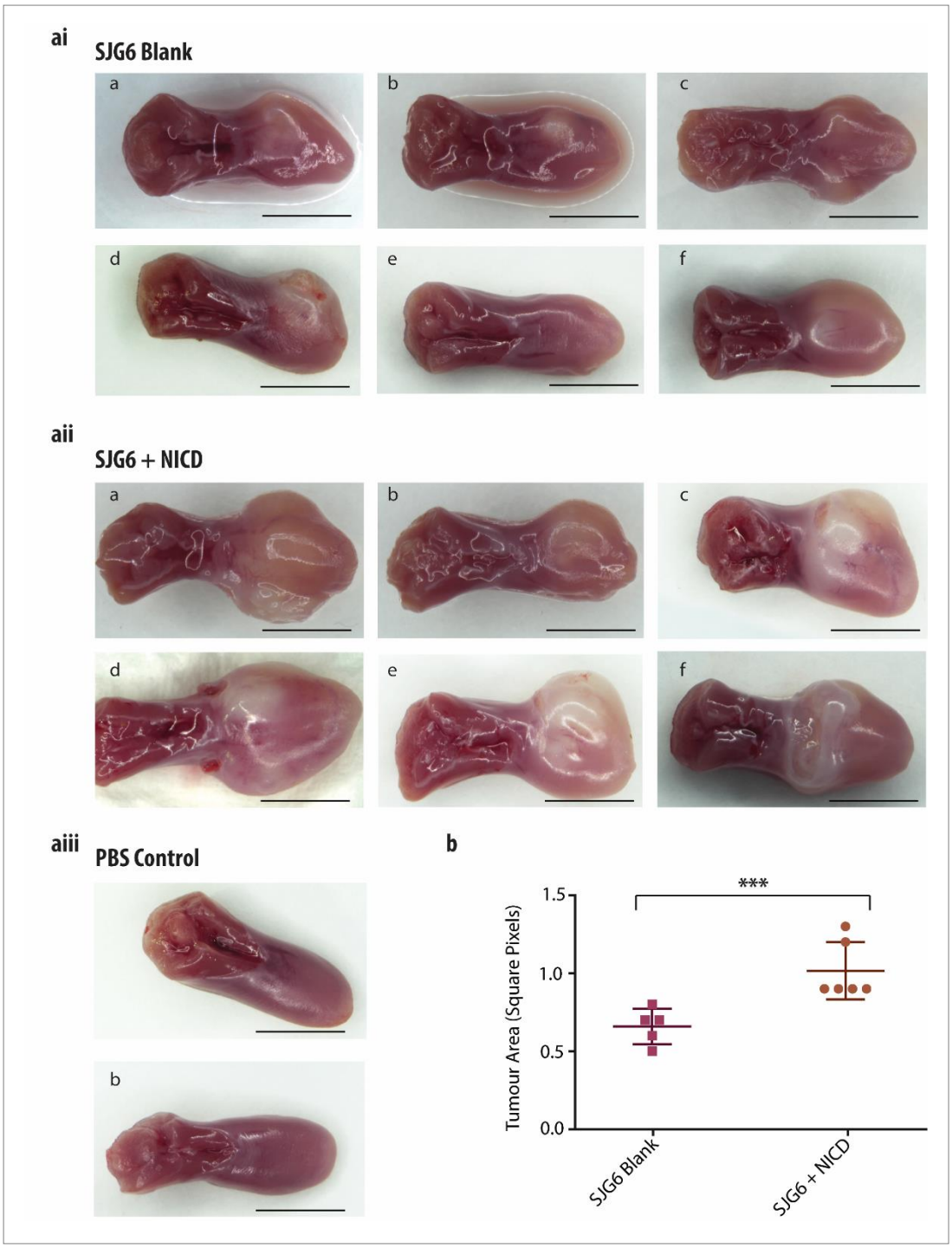


*Figure 7 3: A suspension of 100,000 SJG6 Blank cells (ai), SJG6 + NICD cells (aii) or a PBS control (aiii) was injected into the dorsal tongue of immunocompromised mice. Tumours were allowed to develop for 60 days before mice were sacrificed and tongues were collected. Scale bar = 3mm. (b) FIJI was used to measure tumour area. ***Student's t-test < 0.005.*

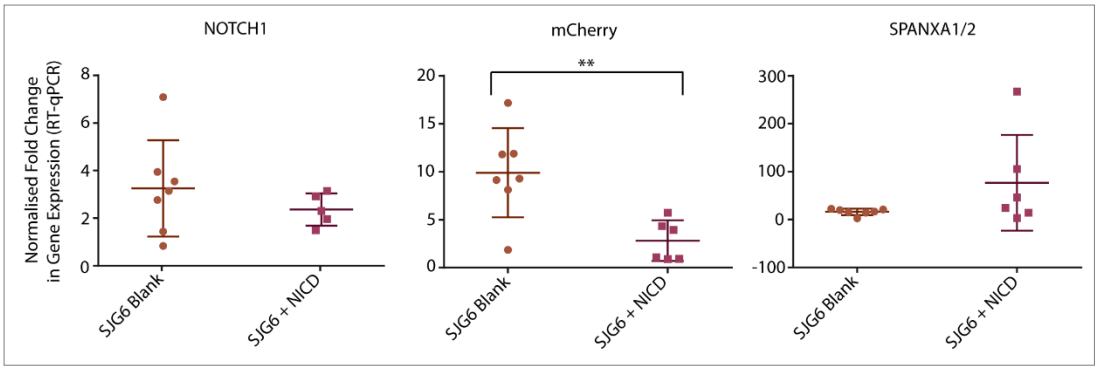


*Figure 7 4: RT-qPCR analysis of NOTCH1, mCherry and SPANXA1/2 expression in xenografts derived from SJG6 Blank and SJG6 + NICD. Results normalised to PBS controls. n=3. ** Student's t-test calculated at <0.01.*

## 7.4 Preliminary Assessment of H&E Staining Provides Evidence to suggest that Tumours Derived from SJG6 + NICD may have Increased Comedo Necrosis and Fewer Keratin Pearls than those Derived from SJG6 Blank

Xenograft sections of 8 µm were used for H&E analysis. A representative stain from the approximate middle of each tumour is displayed in Figure 7.5. A common feature of SCCHN is keratin pearls, i.e. keratin structures made up of concentric layers of SCC cells (Jaimes, et al., 2012). Apparent keratin pearl structures can be observed in the histological sections (arrows). Tumours derived from cells expressing NICD were found to have fewer keratin pearl structures than those derived from empty vector control cells. However, immunostaining for keratin markers would be required to confirm the structures are in fact keratin pearls. This observation is based on pathological descriptions and images presented by AAMC MedPics under the path Dermatological Disease; Squamous Cell Carcinoma; H&E stain as well as published literature (Das, et al., 2015; UCSD School of Medicine, 2018).

NICD-expressing xenografts were also found to have increased areas of what histologically presents as comedo-type necrosis, i.e. dead cell build up within the tumour body. This observation is based on pathological descriptions and images presented in the Atlas of Genetics and Cytogenetics in Oncology and Haematology (Rousseau & Badoual, 2011). Again, immunostaining for dead cell markers would be required to confirm this observation.

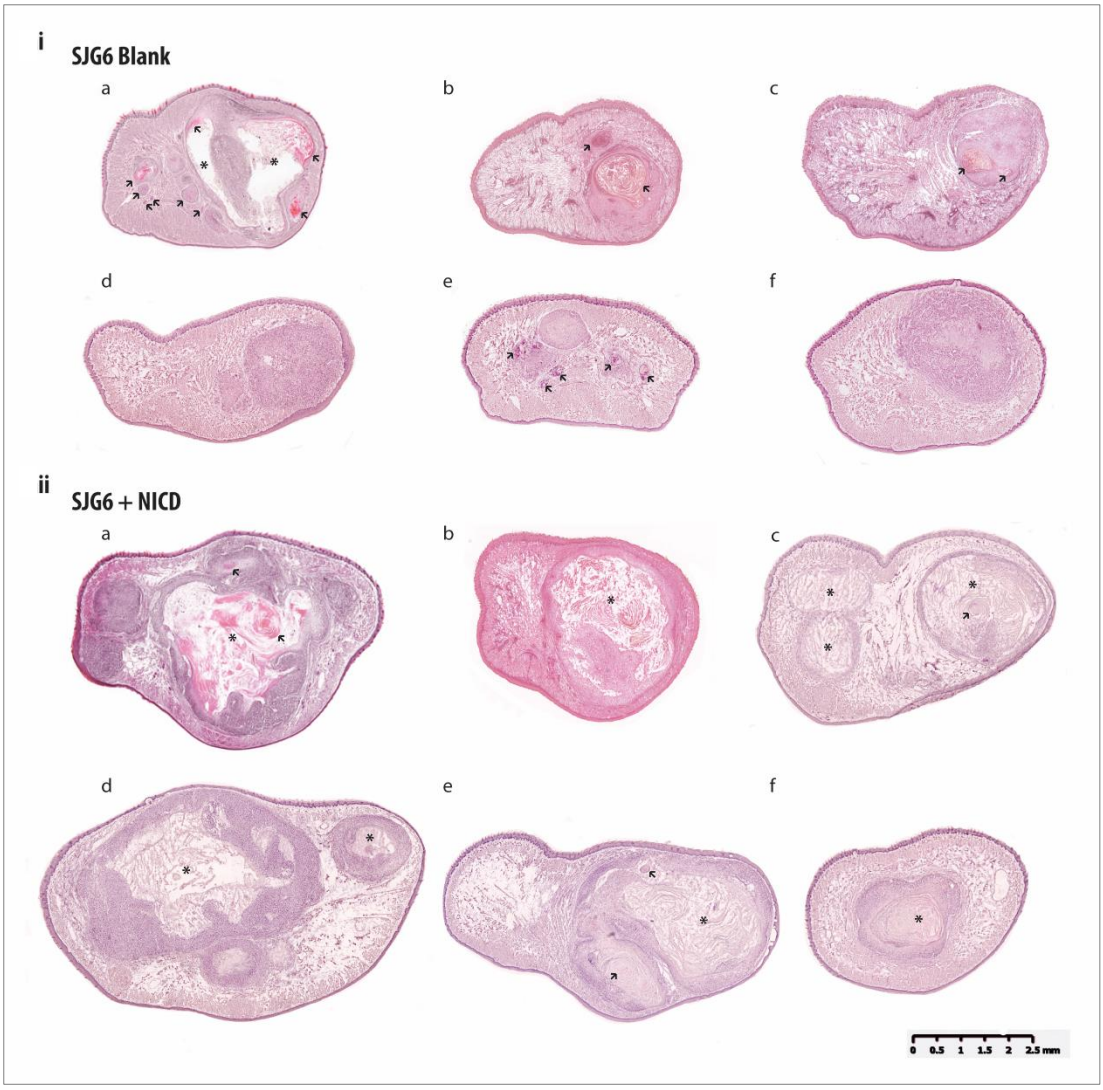


*Figure 7 5: H&E staining of xenografts derived from SJG6 Blank (i) and SJG6 + NICD (ii). Arrows = keratin pearls. * = areas of comedo necrosis.*

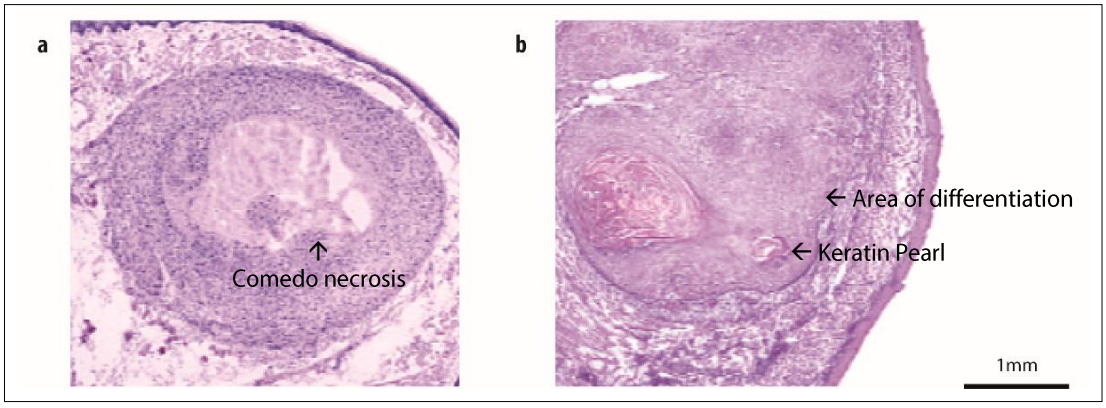


*Figure 7 6: Higher magnification H&E staining of representative pathological features considered to be comedo necrosis (a) and keratin pearls (b) in xenografts derived from the two SJG6 cell lines.*

## 7.5 No Significant Difference in Tumour Cell Proliferation was recorded between Xenografts Derived from SJG6 + NICD and SJG6 Blank

Mice were injected with EdU 2hrs prior to harvesting. The EdU incorporated into proliferating cells, which were then fluorescently labelled using the EdU Click IT kit in 10 µm sections. Cell nuclei were stained with DAPI and FIJI was used to calculate proliferating cells as a percentage of total tumour cell number in a representative image from each xenograft. No significant difference was recorded between the percentages of proliferating cells in xenografts derived from SJG6 + NICD and SJG6 Blank. In all tumours, proliferating cells were localised to the tumour front (Figure 7.7).

## 7.6 Xenografts Derived from SJG6 + NICD show Reduced Differentiation Compared to those Derived from SJG6 Blank

Immunostaining for the epithelial differentiation marker, Transglutaminase 1, was performed on a representative xenograft section of 10 µm from each xenograft (Figure 7.8). FIJI was used to measure areas of differentiation as a percentage of total tumour area. Xenografts derived from SJG6 Blank displayed significantly larger areas of differentiation than those derived from SJG6 + NICD. Both cell lines formed tumours consistent with the histology of moderate- to well- differentiated SCCs. Differentiated tissue formed towards the centre of the tumour, behind the proliferating cells of the margin. In tumours presenting with what appeared to be large areas of comedo necrosis, differentiated layers formed around the inner mass of predicted dead cells (Rousseau & Badoual, 2012).

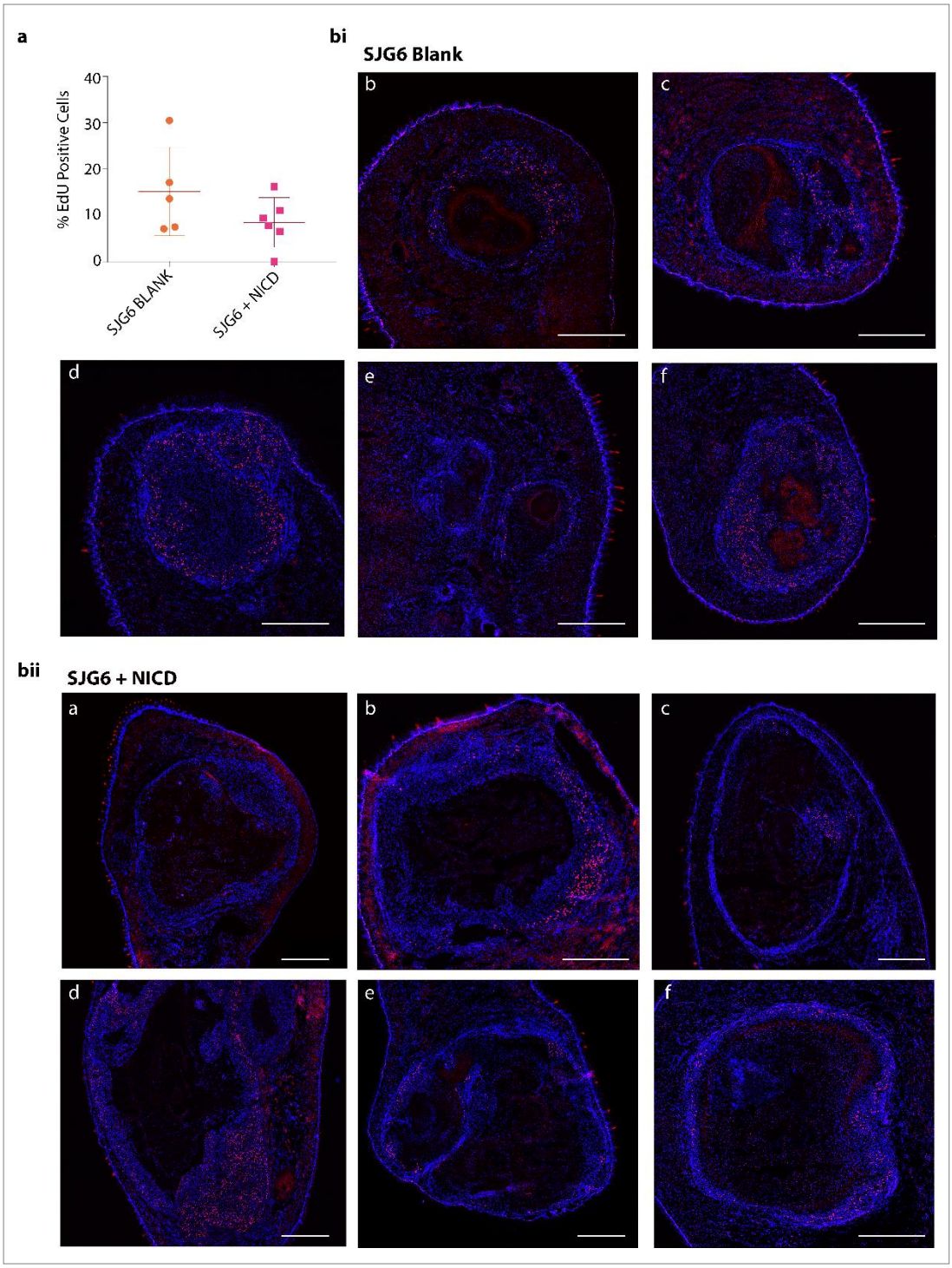


*Figure 7 7: EdU analysis of xenografts derived from SJG6 Blank and SJG6 + NICD. Mice were injected with EdU 2hrs prior to harvesting. (a) Percentage of proliferating cells. (b) Representative staining of SJG6 Blank (i) and SJG6 + NICD (ii). EdU = red. DAPI = blue. Scale bar = 1mm.*

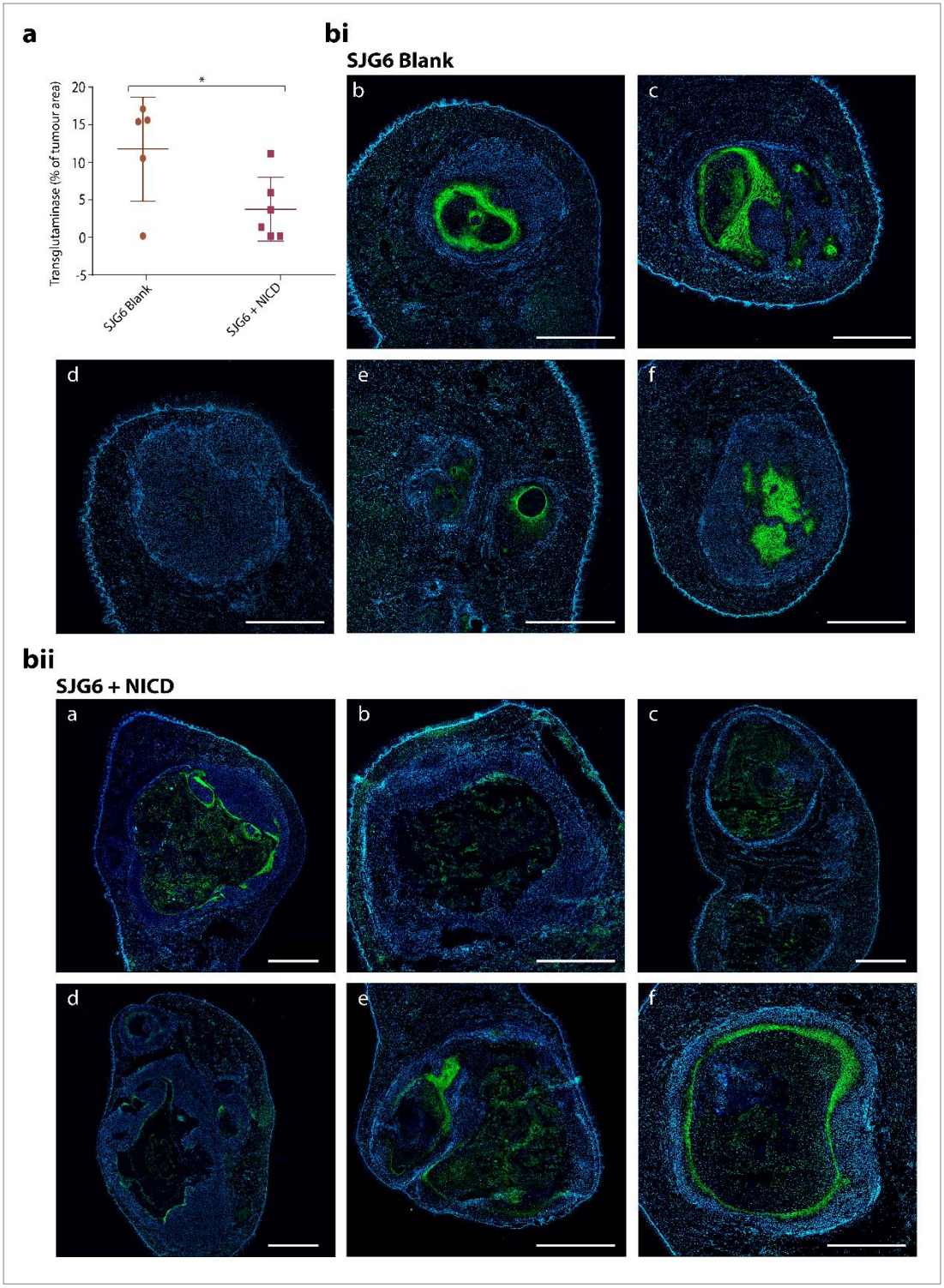


*Figure 7 8: Transglutaminase 1 analysis of xenografts derived from SJG6 Blank and SJG6 + NICD. (a) Transglutaminase 1 positive staining as a percentage of total tumour area. (b) Representative immunohistochemistry staining of xenografts derived from SJG6 Blank (i) and SJG6 + NICD (ii). Green = Transglutaminase 1. Blue = DAPI. Scale bar = 1mm.*

## 7.7 No Significant Difference in Angiogenesis was recorded between Xenografts Derived from SJG6 Blank and SJG6 + NICD

Immunostaining for the endothelial cell marker CD31 was performed on xenograft sections of 10 µm (Figure 7.9a-c). CD31 stains blood vessel walls and is a well-established marker of angiogenesis (Albelda, et al., 1991). In Figure 7.9, white arrows indicate the invasion of blood vessels into the tumour as well as potential micro-vessels within the xenograft. SJG6 Blank – Xenograft A presented with a more developed tumour vasculature than all other tumours. However, no striking difference in angiogenesis was observed between the remaining xenografts derived from SJG6 Blank compared to SJG6 + NICD. Quantification would be required for confirmation. However, staining of the two experiments was performed on different days and, consequentially, different image settings were used. The same image settings must be used for accurate quantification. This will make up part of planned future work and will be discussed further in Chapter 8.

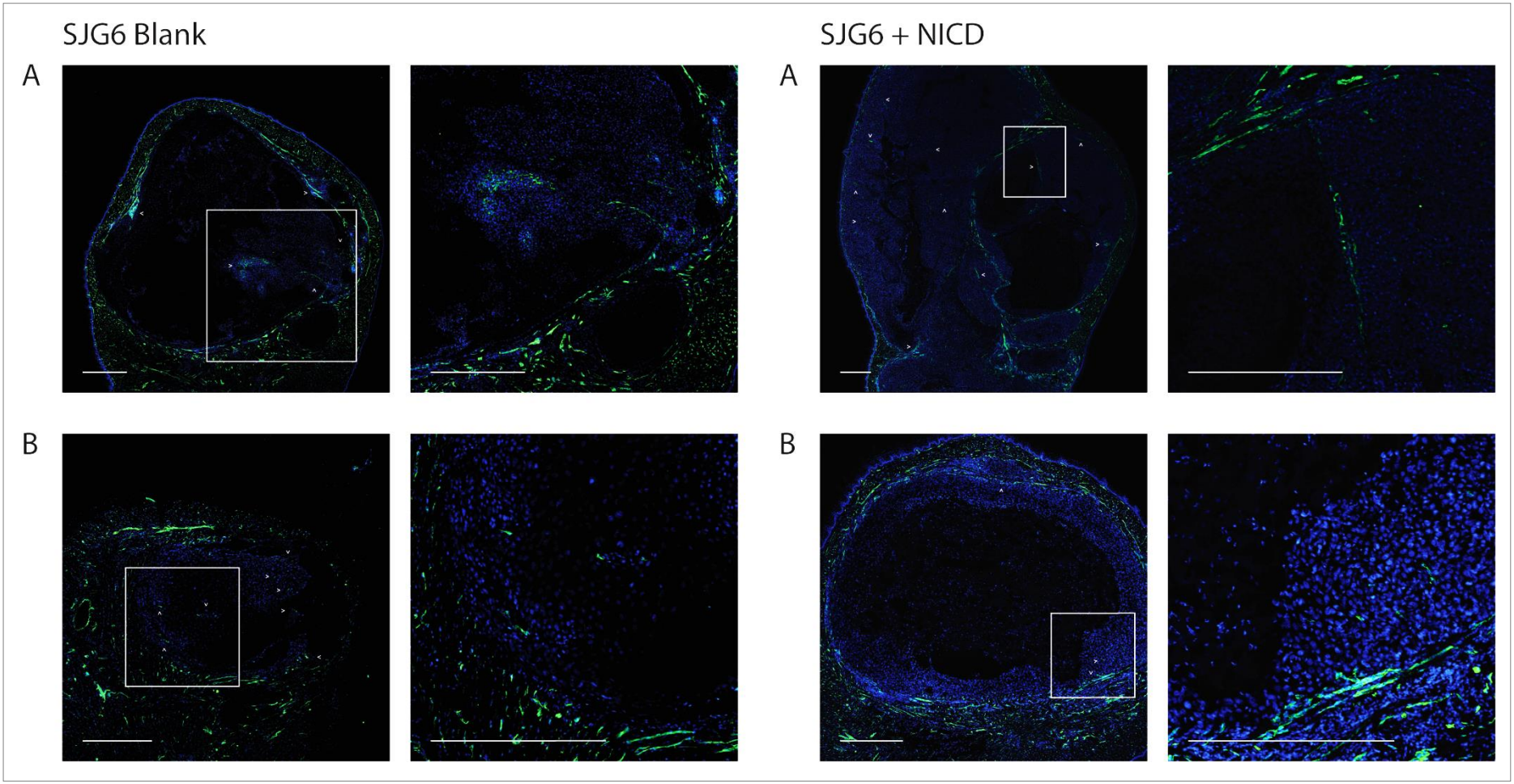


*Figure 7 9a: Analysis of angiogenesis in xenografts A-B: Immunohistochemistry staining of xenografts derived from SJG6 Blank and SJG6 + NICD. Left-hand image = 10x. White box indicates region of interest shown at 40x in right-hand image. Green = CD31. Blue = DAPI. White arrows = areas of angiogenesis. Scale bar = 0.5mm.*

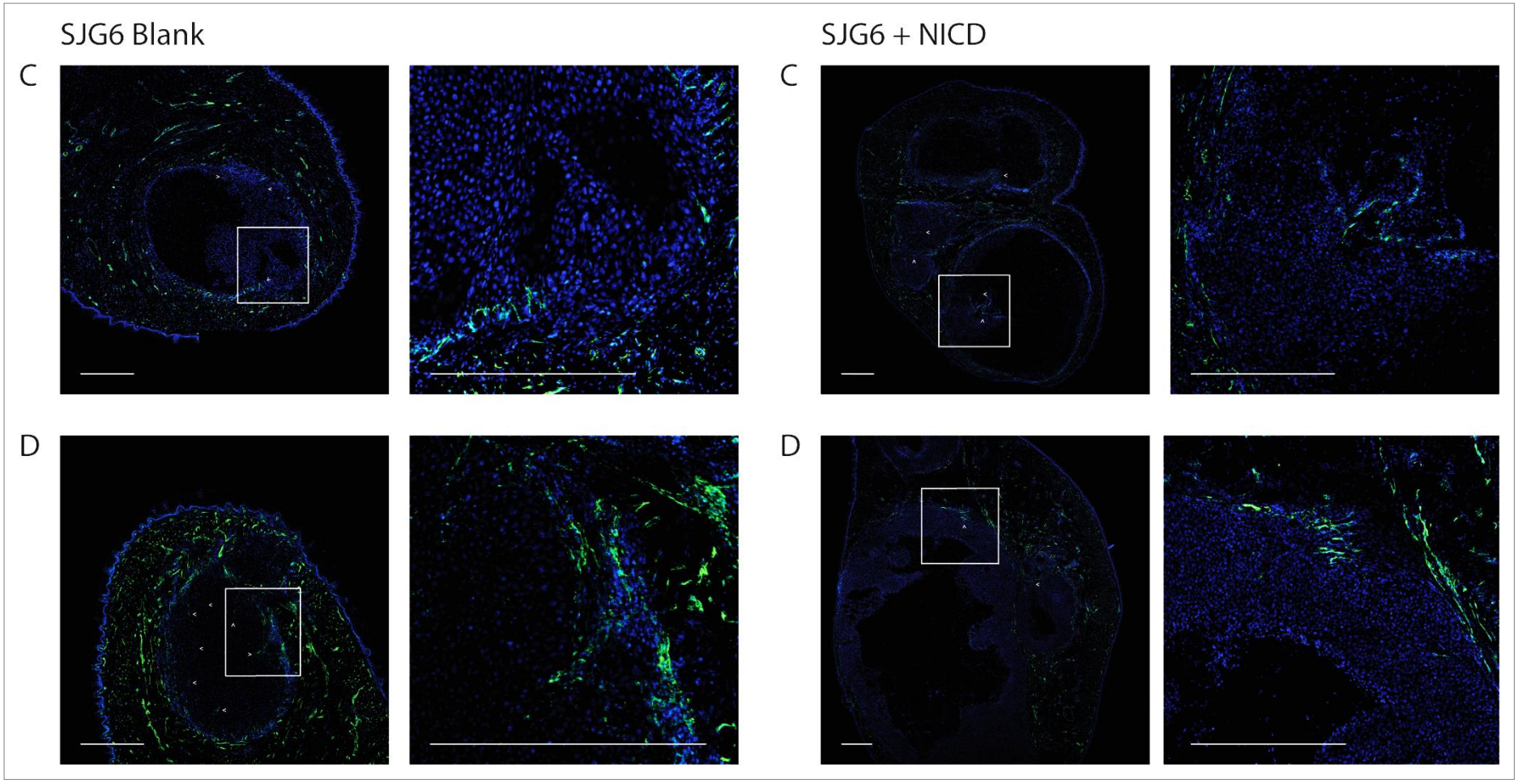


*Figure 7 9b: Analysis of angiogenesis in xenografts C-D: Immunohistochemistry staining of xenografts derived from SJG6 Blank and SJG6 + NICD. Left-hand image = 10x. White box indicates region of interest shown at 40x in right-hand image. Green = CD31. Blue = DAPI. White arrows = areas of angiogenesis. Scale bar = 0.5mm.*

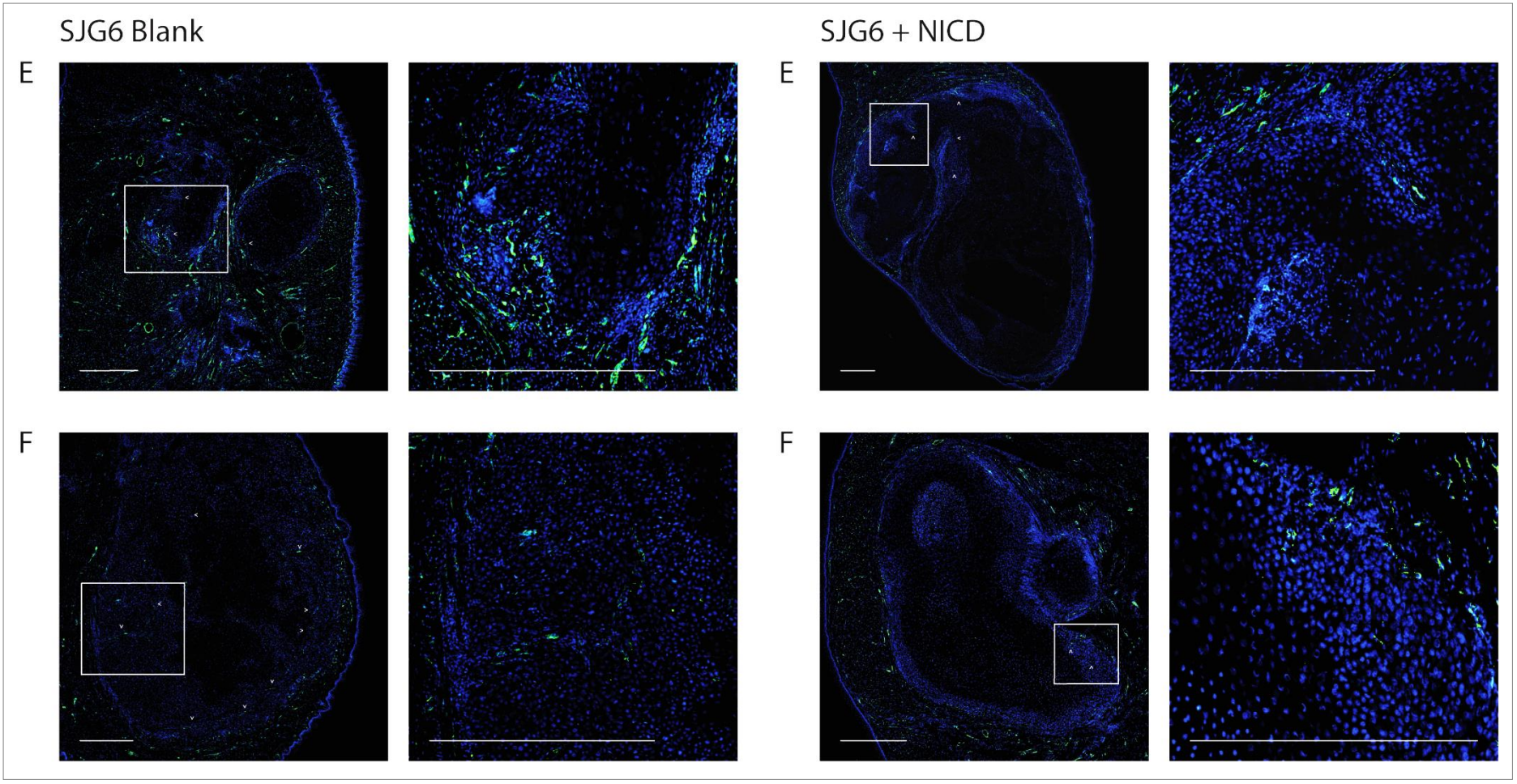


*Figure 7 9c: Analysis of angiogenesis in xenografts E-F: Immunohistochemistry staining of xenografts derived from SJG6 Blank and SJG6 + NICD. Left-hand image = 10x. White box indicates region of interest shown at 40x in right-hand image. Green = CD31. Blue = DAPI. White arrows = areas of angiogenesis. Scale bar = 0.5mm.*

## 7.8 Discussion

### 7.8.1 SPANXA1/2 remains up-regulated after loss of NICD expression

At 60 days, mRNA expression of NICD was not significantly different between xenografts derived from SJG6 Blank and SJG6 + NICD. As commonly seen in lentiviral-transduced cell populations, the SJG6 + NICD line is not made up of 100% transfected cells. This is in part due to FACS purity, as well as gene silencing and loss of cells with unstable genome integration. The high percentage of transfected cells (approximately 80%) is maintained in culture by supported growth on J2 3T3 feeders. However, the microenvironment *in vivo* introduces selective pressures. It is predicted that cells expressing NICD in the xenografts were at a selective disadvantage and therefore substantially reduced in the population over the 60 day incubation. This finding is supported by the mirrored reduction in mCherry expression recorded in SJG6 + NICD compared to SJG6 Blank. It is also consistent with *in vitro* data showing reduced proliferation of SJG6 + NICD compared to the empty vector control when removed from feeder layers and assessed over 24hrs as well as microarray data that associated NICD expression with a decrease in proliferation.

This data is consistent with previous studies that have associated NICD expression with cell cycle arrest in oral and tongue SCC lines (Duan, et al., 2006; Pickering, et al., 2013). However, it opposes several studies associating the loss of NOTCH1 expression with reduced proliferation (Yao, et al., 2007; Yoshida, et al., 2013; Sun, et al., 2014). Duan et al. provided evidence to suggest that the downregulation of Wnt / β-catenin signalling may act as a mechanism for cell cycle arrest in cell lines showing an anti-proliferative effect in response to NOTCH1 expression in SCCHN (Duan, et al., 2006). Consistent with this, microarray data provided evidence to suggest a down regulation of the Wnt / β-catenin signalling pathway in SJG6 + NICD. This data acts to further highlight the highly context dependent role of NICD in cancer.

Interestingly, despite the depletion of the NICD-expressing cell population, SPANXA1/2 expression in 4/6 xenografts derived from SJG6 + NICD was higher than that of the highest expressing SJG6 Blank xenograft. This data suggests that, once initiated, the NICD-mediated increase in SPANXA1/2 expression is maintained in the absence of NICD. As it is predicted that NICD-expressing cells are negatively selected

in the population, it is hypothesised that NICD induces SPANXA1/2 expression in neighbouring cells rather than, or as well as, cell autonomously.

Consistent with *in vitro* data, large fold increases (25, 46, 105 and 267) were recorded in SPANXA1/2 expression in SJG6 + NICD derived xenografts. The wide range of fold changes potentially suggests a delayed reduction in SPANXA1/2 expression as a result of NICD-loss. This is further supported by the absence of SPANXA1/2 in 2/6 SJG6 + NICD expressing xenografts.

Collectively, this data provides evidence to suggest that NICD is able to initiate an exaggerated and more stable increase in SPANXA1/2 expression in cells in SCCHN. As NICD expressing cells are lost from the population, it is predicted that induction of SPANXA1/2 expression must be non-cell-autonomous. However, further experiments comparing NICD and SPANXA1/2 expression over a series of time points and at the single-cell level would be required to confirm this hypothesis. This is further detailed in Chapter 8. To date, there are no studies associating NOTCH1 and SPANXA1/2.

### 7.8.2 Xenografts derived from SJG6 + NICD were significantly larger than those derived from SJG6 Blank despite no significant difference in the proportion of proliferating cells

At experimental day 60, xenografts derived from SJG6 + NICD were significantly larger than those derived from SJG6 Blank. Although gel food was provided to the mice, it is predicted that the weight loss recorded in the SJG6 + NICD mouse cohort could be related to tumour size causing difficulty eating.

Interestingly, despite the larger tumour volume, the percentage of proliferating cells was not found to be increased in SJG6 + NICD tumours. It is important to note that EdU data is a snapshot of proliferation in the 2hrs prior to harvesting the xenografts. Therefore, variation in proliferation earlier in tumour development could account for the difference in tumour size. However, both *in vitro* and microarray data suggest a reduced proliferation in SJG6 + NICD cells compared to the blank vector control. Together with the predicted reduction of SJG6 + NICD cells in the xenograft, it is unlikely that hyper-proliferation would have occurred earlier in tumour development.

### 7.8.3 The difference in tumour size recorded between xenografts derived from SJG6 Blank and SJG6 + NICD may be related to cell death and differentiation

H&E staining revealed variation in the histology of all tumour samples. This may be as a result of the difficulty in ensuring the accurate injection of 100,000 cells in the small volume of 30µl. As all SJG6 + NICD xenografts were larger than SJG Blank xenografts over two separate experiments, it is unlikely that potential inaccuracies influenced comparative findings between the two cell lines. However, it may account for the range of histology observed. Another potential reason for histological discrepancies between tumours derived from the same cell line is where in the tongue the cells were injected and whether the needle could have moved to secondary locations. All cells were injected into the dorsal tongue using the same technique. However, the total mouse tongue is approximately 1cm long and 0.5cm wide. As such, it is difficult to ensure consistency between injection locations.

Nevertheless, H&E staining revealed more of what appeared to be keratin pearls in xenografts derived from SJG6 Blank than SJG6 + NICD. This finding was further supported by Transglutaminase 1 staining, which revealed a lower differentiated tumour percentage in SJG6 + NICD xenografts. This data is consistent with *in vitro* data that recorded increased differentiation in the SJG6 Blank cell line. There is little known about the role of NOTCH1 on keratin pearl formation. However, this finding is inconsistent with the role of NOTCH1 as a promotor of differentiation in normal keratinocytes and oral SCC cells (Lowell, et al., 2000; Rangarajan, et al., 2001; Nickoloff, et al., 2002; Nicolas, et al., 2003; Sakamoto, et al., 2012; Ravindran & Devaraj, 2012).

As discussed in Chapter 3, it is predicted that SJG6 + NICD cells transformed with high levels of NICD underwent differentiation prior to forming the stable cell line. Therefore the SJG6 + NICD cell population is predicted to be made up of cells expressing lower, or wild type, levels of NICD. A colony formation assay comparing SJG6 + NICD cells with high mCherry expression (and therefore high NICD expression) to those with low mCherry expression was performed. Consistent with the differentiation hypothesis, the cells with higher NICD expression formed much fewer colonies (Figure 3.7d). RT-qPCR also confirmed that the NICD mRNA expression in the SJG6-NICD line was approximately 65% of that recorded in two SCCHN lines wild type for NOTCH pathway genes (discussed in depth in section 3.5.4). Consistent with this finding, and as discussed in Chapter 4, Kagawa et al. showed that NICD expression could switch from

being a driver of cellular senescence to an active promotor of differentiation (Kagawa, et al., 2015).

Histology observations based on pathological descriptions and images presented in the Atlas of Genetics and Cytogenetics in Ocology and Haematology, suggest that xenografts derived from SJG6 + NICD present with larger areas of comedo necrosis when compared to those derived from SJG6 Blank (Rousseau & Badoual, 2011). These findings are consistent with microarray data that associated NICD expression with increased cell death. The expression of NOTCH1 has also been positively associated with apoptosis in laryngeal and oesophageal SCC cell lines (Lu, et al., 2008; Jiao & Li, 2012). Comedo necrosis is often associated with basaloid SCCs, a highly aggressive and rapidly growing tumour type (Rousseau & Badoual, 2012). This data is consistent with the larger tumour volume recorded in SJG6 + NICD derived xenografts. As aforementioned, further experiments are required to investigate the nature of the advanced tumour growth.

The histological difference resulting from reduced differentiation and predicted increase in comedo necrosis in xenografts derived from SJG6 + NICD compared to SJG6 Blank may go some way to explaining the difference in tumour volume. Comedo necrosis forms when tumour cells undergo necrosis and die. The dead cells often attract other components, such as calcium, and form a 'plug'. Conversely, keratin pearls are made up of tightly packed concentric circles of keratinized SCC cells. Therefore, the tumour area occupied by the same number of cells would be different. Further experiments would be required to confirm the pathological differences. This is explored further in Chapter 8.

### 7.8.4 Despite significantly larger tumour areas, xenografts derived from SJG6 + NICD did not show more developed vasculature when compared to those derived from SJG6 Blank

Immunostaining showed Xenograft A of SJG6 Blank was the only tumour to present with a more developed vasculature. In combination with microarray data, that demonstrated reduced VEGF in response to NICD expression and predicted a general decrease in angiogenesis, this data is consistent with that of Sun et al. The group reported a reverse correlation between NOTCH1 and VEGF expression in oesophageal SCC (Su, et al., 2009). The remaining xenografts derived from SJG6 Blank and SJG6

+ NICD were found to have similar levels of angiogenesis. However, a key trigger of angiogenesis is a hypoxic environment, therefore, the significantly larger SJG6 + NICD xenografts would be expected to have increased angiogenesis (Liu, et al., 1995).

In the previous section, it was hypothesised that the larger tumour size in xenografts derived from SJG6 + NICD could be as a result of increased comedo necrosis. An alternative possibility is that the comedo necrosis was a consequence of tumours becoming too large without adequate angiogenesis. Further experiments would be required and are detailed further in Chapter 8.

### 7.8.5 Conclusion

It is predicted that cells expressing NICD were at a selective disadvantage when transferred to an *in vivo* environment and were therefore lost in the xenografts by day 60. Despite the loss of NICD, a large fold increase (up to 267x) of SPANXA1/2 was recorded in 4/6 SJG6 + NICD derived tumours compared to those derived from SJG6 Blank. It is therefore put forth that the expression of NICD is able to initiate an exaggerated and longer-lived increase in SPANXA1/2 in SCCHN. As NICD expressing cells are predicted to be lost from the population, it is also projected that induction of SPANXA1/2 expression must be non-cell-autonomous.

At the time of measurement, no difference in proliferation was recorded between SJG6 Blank- and SJG6 + NICD- tumours. However, SJG6 + NICD tumours were found to be significantly larger than those derived from SJG6 Blank. It is suggested that this may be due to histological variance. Observational studies provide evidence to suggest that xenografts derived from SJG6 Blank may harbour more tightly packed keratin pearls and less narcotic build-up, in the form of comedo necrosis, than those derived from SJG6 + NICD.

However, this theory assumes that tumour size is a result of cell death. A potential alterative is that cell death occurs as a direct consequence of tumour size. Despite the significantly larger tumour areas of SJG6 + NICD- compared to SJG6 Blank- xenografts, there was no recorded difference in angiogenesis; in fact, one SJG6 Blank xenograft presented with a more developed vasculature. Therefore, cell necrosis may be as a result of hypoxia in the NICD tumour centre.

Collectively, these findings indicate that NICD expression gives rise to larger local tumours with reduced cell proliferation, differentiation and survival. This chapter

provides preliminary data on the role of NICD in an oral SCC cell line *in vivo*. Due to time constraints, the role of NICD on EMT/MET was not explored in *in vivo* samples. This would be of interest in future experiments. In addition, it would be of interest to compare findings with xenografts from a SCCHN cell line wild type for NOTCH pathway members. Various avenues of investigation can be built upon these findings and suggestions for further research are detailed in Chapter 8.

# Chapter 8

## Discussion

*This chapter collates and summarise the findings of the thesis as a reflection of the initial aims. Findings are considered within the scope of current literature and future directions are discussed.*

### 8.1 Introduction

The aim of this thesis was to investigate the role of NOTCH1 in SCCHN. A panel of 16 low passage oral SCC lines was available for the study. Whole exome sequencing data were obtained in collaboration with BGI, and Sanger sequencing confirmed the presence of two truncating mutations in the SJG6 cell line. Chapter 3 validates the lentiviral rescue of SJG6 via the transduction of the NICD. Chapter 4 compares the original and rescued cell line to investigate the role of NOTCH1 expression on clonogenicity, proliferation, morphology, differentiation and cell migration *in vitro.* Chapter 5 details the findings of a microarray to investigate how the rescue of NOTCH1 in SJG6 alters gene expression in the whole transcriptome. Notably, fold changes identified in the SPANX family (co-increased with NICD) were 3 x greater than those of any other gene. Chapter 6 investigates the effect of SPANXA1/2 knock-down in the rescued SJG6 line. The cell proliferation, morphology, differentiation and migration assays developed in Chapter 4 were performed to investigate whether SPANXA1/2 played a role in mediating any NICD-induced phenotypes. Finally, Chapter 7 details xenograft experiments investigating the role of NOTCH1 in SCCHN *in vivo.*

## 8.2 Conclusions and Future Directions

This section will collate the results from each chapter of the thesis and consider how the findings have contributed to the understanding of the role of NOTCH1 in SCCHN. Specifically, the aims set out in the introduction of this thesis were to investigate the effect of NOTCH1 expression on the following cellular functions:

- Tumour Growth
- Differentiation
- Migration and invasion
- Angiogenesis

### 8.2.1 Tumour Growth

*Conclusions*

EdU assays provided evidence to suggest that the expression of NICD in SJG6 gave rise to cells with a reduced proliferative potential *in vitro*. This finding was supported by microarray data. Analysis of the differentially expressed gene set between SJG6 Blank and SJG6 + NICD identified 5 cellular and molecular functions associated with cell proliferation that were predicted to be significantly reduced as a result of NICD expression. In addition, 3 of these networks were associated with reduced proliferation in the skin, epithelium and breast cancer cell lines. Finally, NICD-expressing cells were lost from a murine xenograft by day 60, suggesting they were at a selective disadvantage.

These findings are consistent with several studies which ectopically introduced NICD into tongue, oral and oesophageal SCC cell lines (Duan, et al., 2006; Pickering, et al., 2013; Kagawa, et al., 2015). In addition, the inhibition of NOTCH1 in oesophageal epithelial progenitor cells has been shown to prevent differentiation and give rise to clonal expansion representative of field change (Alcolea, et al., 2014). Conversely, NOTCH signalling has been associated with a stem-like phenotype in oral and tongue SCC cell lines (Lee, et al., 2012; Upadhyay, et al., 2016). However, both of those studies looked at the effect of activating NOTCH signalling in lines wild type for NOTCH1, whereas this study considered the effect of rescuing NOTCH1 in lines with inactivating mutations. It is therefore predicted that the effect of NOTCH

signalling is highly dependent on timing and signal strength. Further, studies that have inhibited or knocked-down NOTCH1 in mice and tongue oral SCC lines have also shown reduced proliferation (Yao, et al., 2007; Yoshida, et al., 2013; Sun, et al., 2014). NOTCH1 is a key regulator of many cellular processes and is known to influence numerous signalling pathways. It is therefore possible that the complete knockdown of NOTCH1 and the constitutive expression of NICD could both result in reduced proliferative potential by two distinct mechanisms.

The expression of NICD has also been associated with G0-G1 cell cycle arrest and cellular senescence (Duan, et al., 2006; Pickering, et al., 2013; Kagawa, et al., 2015). Morphological observations of senescent cells in SCCHN are conflicting. In this study, the expression of NICD *in vitro* gave rise to a smaller and more rounded cell population. This morphology is consistent with a description by Pickering et al. of senescence in oral SCC lines (Pickering, et al., 2013). However, Duan et al. recorded a more elongated cell population in response to NICD expression. The group suggested that this may be reflective of senescence, cell cycle arrest or apoptosis, but no validating experiments were performed. In addition, Kagawa et al. described the senescent cell morphology as flat and enlarged in oesophageal cell lines.

There is evidence to suggest that the downregulation of Wnt / β-catenin signalling may act as a mechanism for cell cycle arrest in cell lines showing an anti-proliferative effect in response to NOTCH1 expression in SCCHN (Duan, et al., 2006; Pickering, et al., 2013). Of note, in normal mouse epidermis, the deletion of β-catenin was not found to alter proliferation or differentiation of keratinocytes (Posthaus, et al., 2002). The CSL and p16 signalling pathways have also been associated with NOTCH-mediated cellular senescence in oesophageal cell lines (Kagawa, et al., 2015).

Microarray analysis showed a down-regulation in the Wnt / β-catenin signalling pathway and an upregulation of CSL and downstream signalling molecules in response to NICD expression. The p16 pathway was unchanged. However, these results would need to be confirmed experimentally.

In the skin, NOTCH induces cell cycle arrest via the induction of p21. Consistent with findings that suggest NICD enhances senescence in SCCHN, microarray data identified a 1.21 expression fold increase in p21 in response to NICD rescue (Rangarajan, et al., 2001; Mammucari, et al., 2005).

Moreover, of the 3150 genes found to have greater than a 1.2 fold change difference in microarray analysis, 68 were found to be histones or histone regulators

(2.2%). Further, 62 of the 68 genes were found to be downregulated (91%). Histone gene expression is cell cycle regulated. Histone protein synthesis is restricted to the S-phase of the cell cycle, coupled to DNA replication. During DNA replication, histones are essential for packaging DNA into chromosomes (Pogo, et al., 1966; Meshi, et al., 2000). As such, a decrease in histone related genes is consistent with *in vitro* and microarray data correlating NICD expression with cell cycle arrest in SCCHN.

Interestingly, the knockdown of SPANXA1/2 in the SJG6 + NICD cell line reverted changes in cell morphology i.e. cells became larger and less round. It is therefore possible that SPANXA1/2 may play a role in NOTCH-mediated cell senescence.

Both SPANX and NOTCH1 have been associated with the maintenance of CSCs. Microarray and SPANXA1/2 knockdown data has confirmed a positive correlation between the expression of both genes (Upadhyay, et al., 2015; Wilson, et al., 2016; Shahin, et al., 2017). Further experiments would be required to ascertain if SPANXA1/2 and NOTCH1 are mutually exclusive regulators of CSCs or whether a common mechanism exists. However, this observation was not supported by *in vitro* data. A colony formation assay was used to assess the ability of single cells to undergo numerous rounds of self-renewal. The expression of NICD was found to give rise to reduced clonogenicity. Further, NICD expressing cells were lost from xenografts and therefore predicted to be at a selective disadvantage.

*Further Experiments*

Evidence suggests that the knockdown of NOTCH1 and the constitutive expression of NICD can both lead to reduced proliferative potential in SCCHN cell lines. To further understanding of this potential dual function of NOTCH1, it would be interesting to inhibit NOTCH1 in cell lines wild type for NOTCH pathway members and compare cell behaviour to NICD-rescued NOTCH1 null cell lines.

Further, NICD expression in SJG6 has been suggested to induce cellular senescence, in line with current literature (Duan, et al., 2006; Pickering, et al., 2013; Kagawa, et al., 2015). Moreover, the senescent-like morphology was reversed by the knockdown of SPANXA1/2. In order to confirm the senescent phenotype, comparative β-galactosidase staining should be performed on both cell lines.

If senescence is confirmed, it would be of interest to genetically target aspects of the Wnt / β-catenin signalling pathway as well as CSL and p21 to further understand the mechanism of NICD-mediated cellular senescence in SCCHN.

A number of studies have associated the expression of both NOTCH1 and SPANX family members with CSCs. A positive correlation was confirmed between the genes but colony formation assays suggested the expression of NICD gave rise to cells with reduced clonogenicity. Further analysis of the colony formation potential of the cell lines via serial passaging would be required.

Further, in order to confirm that cells expressing NICD were at a selective disadvantage in the xenografts, the loss of NICD over the 60 day incubation period would have to be confirmed. RT-qPCR and immunohistochemistry analysis of NICD expression in xenografts collectedly weekly would provide a more dynamic picture of cell behaviour.

The 'big bang' model of tumour growth describes how a cancer develops as a single uniform expansion of a large number of intermixed clones (Sottoriva, et al., 2015). Each clonal unit is made up of a mixture of dividing and differentiating cells, and will compete for dominance within the cancer (Jones, et al., 2007; Keats, et al., 2012). It would be of interest to investigate the effect of NICD expression on the clonogenicity of the SJG6 line by performing a lineage tracing experiment i.e. marking cells of interest to delineate the progeny produced (Hsu, 2015).

### 8.2.2 Differentiation

*Conclusions*

As discussed in Chapter 3, it is predicted that SJG6 + NICD cells transformed with high levels of NICD underwent differentiation prior to forming the stable cell line. A colony formation assay comparing SJG6 + NICD cells with high mCherry expression (and therefore high NICD expression) to those with low mCherry expression was performed. Consistent with the differentiation hypothesis, the cells with higher NICD expression formed much fewer colonies (Figure 3.7d). This is consistent with the known role of NOTCH1 as a promotor of terminal differentiation in normal epithelium (Lowell, et al., 2000; Rangarajan, et al., 2001; Nickoloff, et al., 2002). In addition, the downregulation of NOTCH1 was found to inhibit terminal differentiation and give rise

to an immature epithelium in mouse skin (Nicolas, et al., 2003; Sakamoto, et al., 2012). Further, in oral SCC, poorly- and moderately- differentiated tumours have also been associated with low NOTCH1 expression (Ravindran & Devaraj, 2012).

The stable SJG6 + NICD cell population is therefore predicted to be made up of cells expressing lower, or wild type, levels of NICD. RT-qPCR also confirmed that the NICD mRNA expression in the SJG6-NICD line was approximately 65% of that recorded in two SCCHN lines wild type for NOTCH pathway genes. The SJG6 + NICD cell line was found to show decreased expression of Transglutaminase 1 (an epithelial differentiation marker) *in vitro* and *in vivo* and decreased keratin pearl formation *in vivo* compared to the empty vector control. These findings are consistent with work performed by Kagawa et al., who showed that in certain contexts NICD expression could switch from being a driver of cellular senescence to an inhibitor of differentiation in oesophageal SCC lines. However, inconsistent with microarray findings in Chapter 5, this checkpoint was associated with the reduced expression of p16 (Kagawa, et al., 2015). These findings suggest other mechanisms may be actively involved in mediating the effect of NOTCH1 on differentiation in SCCHN.

Alcolea et al. investigated the conditional knock-out of NOTCH1 in a small percentage of oesophageal progenitor cells in a mouse model. The group demonstrated that within one year, the NOTCH1 knock-out cells had replaced the normal epithelium and entered a new state of homeostasis (Alcolea, et al., 2014). It is predicted that following differentiation of NICD-high expressing cells, the SJG6 + NICD line acquired a new steady state of proliferation and differentiation. Moreover, the expression of NICD has been found to inhibit differentiation in neighbouring cells (Bray, 2006). It is therefore possible that the presence of NICD-high expressing cells in the originally transduced cell population inhibited differentiation in the remaining cells and influenced the eventual steady state. However, this is highly speculative and more work is required before conclusions can be drawn.

*Further Experiments*

A colony formation assay was performed to confirm the reduced clonogenicity of cells with high NICD expression post-FACS. In order to certify that these cells underwent terminal differentiation, it would be necessary to perform live cell imaging on the cultures for the weeks immediately following mCherry selection. The IncuCyte

Zoom would allow hourly monitoring with minimal disturbance to culture conditions. Further, RT-qPCR, Western Blot and immunohistochemistry analysis of differentiation markers at the RNA and protein levels respectively could be performed every 24hrs. As it is predicted that the differentiated cells eventually detach from the adherent culture, it would also be interesting to perform RT-qPCR analysis on any cells pelleted from the culture media. In order to assess whether the NICD high expressing cells were influencing differentiation in the remaining cell population, it would be informative to split the populations based on mCherry expression immediately after transduction and seed the cells both separately and in co-culture for comparison.

It would also be of further interest to investigate potential mechanisms that may be involved in mediating the effect of NOTCH1 on differentiation in SCCHN. IPA analysis of microarray data did not highlight any known molecular or cellular functions or networks associated with differentiation. However, microarray data provides a solid base and key resource for further exploration.

Finally, Transglutaminase 1 was used to stain for differentiated cells. Transglutaminase 1 is an intermediate differentiation expression marker in normal epithelium, i.e. it is expressed in the granular and spinous layers. In future experiments it would be of interest to stain for earlier (such as Keratin 1 and 10) and later (such as filaggrin) markers of differentiation *in vitro* and *in vivo* in order to establish a more thorough picture of the whole differentiation process in both SJG6 cell lines.

### 8.2.3 Migration and invasion

*Conclusions*

In tongue and laryngeal SCC, NOTCH1 protein expression has been positively correlated with both lymph node metastasis and the depth of tumour invasion (Joo, et al., 2009; Zhang, et al., 2011; Dai, et al., 2015). Moreover, strong NICD expression has been recorded in cells located at the invasive tumour front of oral SCCs (Yoshida, et al., 2013). In corroboration, functional studies have confirmed that the downregulation of NOTCH1 in SCCHN results in reduced invasive and metastatic phenotypes (Yu, et al., 2012; Yoshida, et al., 2013; Dai, et al., 2015; Li, et al., 2015; Jing, et al., 2016). Further, a reduction in cell migration was recorded in

hypopharyngeal SCCHN as a result of ADAM10 mediated downregulation of NOTCH1 (Jing, et al., 2016).

As previously discussed, EMT is a developmental process in which epithelial cells lose cell-cell adhesions and polarity and acquire migratory mesenchymal phenotypes. This process is often re-activated in cancer and is associated with cell invasion. Mesenchymal to epithelial transition (MET) is the reverse process and allows metastatic cancer cells to seed at distant sites (Birchmeier, et al., 1996).

Studies by Yoshida et al. suggest that the expression of NOTCH1 contributes to the maintenance of TNFα-mediated invasion in oral SCC, which functions via the transcriptional regulation of SNAI2 and TWIST (Casas, et al., 2011). During EMT, TWIST is known to induce SNAI2 which supresses the epithelial phenotype; TWIST and SNAI2 then work together to promote EMT and metastasis. High NOTCH1 expression has also been recorded in CSCs. The plasticity of CSCs to be able to undergo EMT/MET has been correlated with enhanced chemo-resistance (Capaccione & Pine, 2013; Biddle, et al., 2016).

Furthermore, in order to undergo metastasis, cells must first detach from the primary tumour and degrade the basement membrane and surrounding ECM. MMPs are a family of enzymes involved in the degradation of ECM and are commonly up-regulated in cancers. There is evidence to suggest that NOTCH1 is able to mediate metastasis via the regulation of MMP2 and MMP9 in lingual SCC (Yu, et al., 2012). Collectively, this data suggests a key role for NOTCH1 in EMT, metastasis and tumour invasion in SCCHN.

Surprisingly, *in vitro* data in this study suggests that the expression of NICD reduces cell migration in SCCHN. This finding was supported by microarray analysis of the differentially expressed gene set between SJG6 Blank and SJG6 + NICD, i.e. six cellular and molecular functions associated with tumour cell invasion were predicted to be significantly reduced as a result of NICD expression. Further, in opposition to the above mentioned literature, microarray data analysis confirmed a decrease in the expression of MMP9 and SNAI2. Microarray analysis also showed a decrease in VEGF, a key gene in angiogenesis. The presence of EMT markers has been associated with pro-angiogenic protein expression. Both EMT and angiogenesis are key promoters of carcinogenesis and there is evidence to suggest that the same factors that promote EMT may also drive endothelial cells towards an angiogenic phenotype (Holderfield & Hughes, 2008; Ribatti, 2017). As such, findings provide evidence to

suggest NICD expression may give rise to reduced cell migration and EMT in the SJG6 line.

As aforementioned, the expression of SPANXA1/2 was found to significantly increase in response to NICD. Interestingly, the knockdown of SPANXA1/2 reversed morphology changes recorded in the rescued SJG6 + NICD line i.e. cells become larger, less elongated and more rounded. In section 8.2.1, this morphology was postulated to be associated with cell cycle arrest. However, this change in morphology is also consistent with findings of Hsiao et al., who showed that expression of SPANXA was able to alter the morphology of lung adenocarcinoma from mesenchymal- to epithelial- like. SPANXA has been shown to supress EMT in lung adenocarcinoma by inhibiting c-JUN / SNAI2 signalling. As aforementioned, SNAI2 was found to be decreased as a result of increased NICD expression in the SJG6 line. Together, this data provides evidence to suggest that increased NOTCH1 expression could supress EMT in SCCHN by upregulating SPANXA1/2 expression that in turn inhibits c-JUN/SNAI2 signalling (Hsiao, et al., 2016).

In corroboration, the expression of SPANX B has been associated with the spontaneous differentiation of a colorectal cell line and the progression of these cells into MET. Conversely, the reversal of differentiation was shown to give rise to a downregulation of SPANX B and the induction of EMT markers (Yilmaz-Ozcan, et al., 2014). These findings are also consistent with *in vitro* and *in vivo* data showing increased differentiation in the SJG6 + NICD cell line. Moreover, microarray data also showed a decrease in vimentin, a key mesenchymal marker, in response to NICD expression (Leader, et al., 1987).

Notably, the knockdown of SPANXA1/2 did not reverse the decreased migration recorded in the NICD-rescued line. In fact, the knockdown of SPANXA1/2 gave rise to a further decrease in cell migration, suggesting that SPANXA1/2 may enhance cell migration by mechanisms distinct from its relationship with NOTCH1. Collectively, *in vitro* and microarray data in this experiment provide evidence to suggest that the expression of NOTCH1 in SCCHN may give rise to a decrease in cell migration. This is inconsistent with current literature (Joo, et al., 2009; Zhang, et al., 2011; Yu, et al., 2012; Yoshida, et al., 2013; Dai, et al., 2015; Li, et al., 2015; Jing, et al., 2016).

The up- and down- regulation of SPANX in other cancers has been shown to promote MET and EMT respectively (Yilmaz-Ozcan, et al., 2014; Hsiao, et al., 2016).

SPANX knockdown experiments were shown to reverse NICD-mediated cell morphology changes consistent with mesenchymal phenotypes. This provides preliminary evidence to suggest that NOTCH1 may promote MET via SPANXA1/2 in SCCHN. Interestingly, literature has shown NOTCH to promote EMT via TNF-α mediated upregulation of SNAI2 (Casas, et al., 2011). Conversely, SPANX A has been shown to induce MET via the downregulation of c-Jun / SNAI2. It is therefore possible that NOTCH1 is able to promote both EMT and MET via the regulation of SNAI2 expression by two distinct mechanisms. This hypothesis would be consistent with the association of NOTCH1 with distant metastases as successful metastasis requires the ability of cells to undergo both EMT and MET. This theory is also consistent with the increased expression of NOTCH1 recorded in CSCs which show highly effective EMT/MET plasticity (Capaccione & Pine, 2013; Biddle, et al., 2016). It is important to note that this hypothesis is highly conjectural. However, it provides an interesting base for future work.

*Further Experiments*

The next step would be to investigate the role of NOTCH1 expression on tumour migration and invasion *in vivo.* Xenografts derived from SJG6 Blank and SJG6 + NICD failed to form any metastases. As such, it would be preferable to increase the incubation period to allow more time for metastasis to occur. However, following the same experimental set-up, incubation time could not be increased as tumour size at day 60 required the culling of two mice on ethical grounds. A smaller starting cell number could be injected into the mice. However, it is worth noting that 50,000 cells were too few for successful tumour formation. Alternatively, it is possible to surgically remove the majority of the primary tumour to allow increased time for secondary growths to develop (Sano & Myers, 2009). RT-qPCR of resultant circulating tumour cells and lymph node metastasis can then be assessed for key genes such as MMP2 and 9, TNF-α, SNAI2, TWIST and SPANXA1/2.

Further, immunohistochemistry staining to NOTCH1 and SPANXA1/2 in the primary xenografts needs to be optimised. The localisation of NOTCH1 and SPANXA1/2 proteins in the tumour may provide valuable information into their role in migration and invasion in SCCHN.

In order to investigate the potential role of NOTCH1 and SPANXA1/2 in EMT/MET, staining for validated epithelial (CDX2, claudin-4 and E-cadherin) and mesenchymal (vimentin, fibronectin and transgelin) markers in *in vitro* and *in vivo* experiments is required.

### 8.2.4 Angiogenesis

*Conclusions*

Microarray analysis of the differentially expressed gene set between SJG6 Blank and SJG6 + NICD identified 9 cellular and molecular functions associated with angiogenesis that were predicted to be significantly reduced as a result of NICD expression. In addition, microarray analysis associated the expression of NICD with a decrease in VEGF, a direct stimulant of angiogenesis. Further, *in vivo*, Xenograft-A of SJG6 Blank was the only tumour to present with a more developed vasculature. Notably, a key trigger of neo-vascularisation is a hypoxic environment (Liu, et al., 1995). However, even though xenografts derived from SJG6 + NICD were significantly larger than those derived from SJG6 Blank, there was no difference in the levels of angiogenesis.

This data is consistent with studies that have shown an increased micro-vessel density in response to NOTCH1 expression in oral SCC lines (Joo, et al., 2009; Troy, et al., 2013). Findings also replicate work performed by Sun et al., who confirmed a negative correlation between NOTCH1 and VEGF in oesophageal SCC (Su, et al., 2009). However, the opposite has also been shown in oral SCC (Joo, et al., 2009; Troy, et al., 2013).

*Further Experiments*

Quantification is required to confirm that there is no difference in the extent of angiogenesis in xenografts derived from SJG6 Blank and SJG6 + NICD (excluding the previously noted Xenograft-A of SJG6 Blank). CD31 staining of all xenografts under identical conditions and subsequent imaging using the same image settings will need to be carried out. FIJI software can then be used to assess CD31 positive staining as a percentage of total tumour area.

However, the extent of angiogenesis was relatively immature in all xenografts. It would therefore be of interest to extend the incubation period to allow a more developed vasculature to form. As discussed in the previous section, the incubation period cannot be extended without reducing the starting cell population. However, as a key trigger for angiogenesis is hypoxia, and the maximum tumour volume for the mouse model has been reached, a more developed vasculature may not be achieved. One option may be to implant into the cheek.

Although the mouse model is beneficial as it allows orthotopic xenografts to be performed, zebrafish models have strong advantages for the study of angiogenesis. Specifically, zebrafish are transparent in the early life stages. As such, the vasculature endothelial cells can be fluorescently labelled so tumour neovascularisation can be visualised in real time (Zhao, et al., 2015).

Alternatively, tumour formation in mice with a conditional deletion of NOTCH1 in the tongue could be assessed (Conti, et al., 2015). Current work by Dr Inês Sequeira, a post-doc in the lab, has confirmed the successful derivation of oral tumours in mice via the introduction of 4-nitroquinoline-1-oxide (4NQO) into the drinking water (Kanojia & Vaidya, 2006).

In addition, a co-culture of SJG6 Blank and SJG6 + NICD with Human Umbilical Vein Endothelial Cells (HUVEC) would provide a simple and direct functional comparison of angiogenesis in the two cell lines *in vitro*. The sprouting of HUVEC cells is a well-established method of studying neo-vascularisation (Jaffe, et al., 1973; Skovseth, et al., 2007).

### 8.2.5 Cell death

*Conclusions*

Investigating the effect of NOTCH1 on cell death in SCCHN was not part of the original aims of this thesis. However, microarray analysis of the differentially expressed gene set between SJG6 Blank and SJG6 + NICD identified 7 cellular and molecular functions associated with cell survival that were predicted to be significantly reduced as a result of NICD expression. In addition, xenografts derived from SJG6 + NICD presented with what histologically appeared to be large areas of comedo-type necrosis i.e. dead cell build up within the tumour body (Rousseau & Badoual, 2011).

These findings are consistent with research associating NOTCH1 expression with apoptosis in laryngeal and oesophageal SCC cell lines (Lu, et al., 2008; Jiao & Li, 2012). Conversely, the knockdown of NOTCH1 in laryngeal SCC has also been shown to induce apoptosis (Dai, et al., 2015). In addition, there has also been evidence to suggest that the curcumin-mediated downregulation of NOTCH1 induces cell death alongside the downregulation of Nuclear Factor- κB (NF-κB) in oral and oesophageal SCC (Liao, et al., 2011; Subramaniam, et al., 2012). Notably, NF-κB was not found to be altered in response to NICD expression in this study.

*Future Experiments*

Xenografts derived from SJG6 + NICD require staining for a dead cell marker to validate that the observed central mass is indeed dead cells. To my knowledge there are no specific markers for comedo-necrosis. However, the dead cells often attract other components, such as calcium, which can be stained for. Further, comedo-necrosis is associated with an altered basal lamina and a more disorganised collagenous network (Halls, 2017). Further analysis at 40x magnification and the opinion of a trained histologist may provide more clarity.

*In vitro* assays can also provide a quicker and more readily reproducible comparison of the effect of NICD expression on cell death in SCCHN. Hayes et al. established an assay to compare the response of cell lines to staurosporine-induced apoptosis that could be utilised (Hayes, et al., 2016).

### 8.2.6 Future Directions

Beyond the original thesis aims, this study has highlighted some potential novel research avenues. Firstly, microarray analysis provided evidence to suggest that SERPINE1 may act as a key mediator of the effect of NOTCH1 expression on cell proliferation, migration and invasion, cell death and angiogenesis in SCCHN. NICD expression has previously been linked to the inhibition of SERPINE1 in thyroid cancer (Yu, et al., 2016). SERPINE1 has also been associated with increased cell migration in SCCHN (Pavón, et al., 2015). In addition, the expression of SERPINE1 in the tumour microenvironment has been shown to promote amoeboid cell behaviour associated with cell migration in the metastatic process (Cartier-Michaud, et al., 2012).

Largely, however, very little is known about the role of SERPINE1 in SCCHN or the relationship between SERPINE1 and NOTCH1.

Microarray analysis of the differentially expressed gene set between SJG6 Blank and SJG6 + NICD also showed that of the 3150 genes found to have greater than a 1.2 fold change difference, 2.2% were found to be histones or histone regulators. Moreover, 91% of said genes were found to be downregulated. Histone variants have been identified in SCCHN and modifications have been associated with CSC plasticity (Le, et al., 2014; Song, et al., 2014; Vardabasso, et al., 2014). To my knowledge, the potential relationship between NOTCH1 and histones is novel. Given the potential genome wide effect of histone alterations, this could be a promising avenue for further understanding the role of NOTCH1 in SCCHN. However, analysis of histone regulators in further SCCHN cell lines would first be required to ensure it is not a cell line dependent association.

Finally, microarray analysis also identified a fold change increase in SPANXA1/2 expression 3x greater than any other gene in response to NICD. The expression of SPANX has been linked to poor prognosis in SCCHN (Yang, et al., 2015). However, very little is known about the functional consequence of SPANXA1/2 expression SCCHN. The relationship between NOTCH1 and SPANXA1/2 expression is also novel. SPANXA1/2 is a potentially interesting gene for targeted therapeutics as it is largely tumour-specific and naturally induces an immunogenic response (Almanzar, et al., 2009). This thesis has begun to explore the relationship between SPANXA1/2 and NOTCH1 in SCCHN. However, assessment of immune response is not possible using NSG mice as they are immune-compromised to allow for effective xenograft formation. An assessment of human tissue samples for NOTCH1, SPANXA1/2 and immune cells would be required to assess potential relationships.

SCCHN is a highly heterogeneous cancer. As such, it is essential that experiments validated using SJG6 are carried out on numerous cell lines with known genetic backgrounds. It would also be of interest to investigate whether the knock-down of NOTCH1 in SCCHN cell lines wild type for NOTCH pathway members gave rise to corroborative results. The genetic landscape of a tumour will alter the action of single genes. For example, SJG6 is known to harbour mutations in other NOTCH pathway members which could influence the effect of NICD expression. In addition, microarray analysis showed that NICD is able to alter the expression of a number of

key oncogenes and tumour suppressors in SJG6. Of the top 20 altered genes, the expression change in 9 would suggest a tumour suppressor role for NOTCH1 in SCCHN, whereas the expression change of 4 would indicate an oncogene function. Further research would be required to see how these genes work together in SCCHN to alter phenotype. One possibility is that the expression changes in individual genes compete with each other and the 'winning' genes govern the resultant changes in cell behaviour. Alternatively, a single change in cell behaviour, such as EMT, could be responsible for expression changes in all genes.

There are a number of conflicting studies assessing the role of NOTCH1 in SCCHN. A better understanding of the consequence of genomic differences, mutation combinations and disparate microenvironments on the action of NOTCH1 is required to best ascertain whether it is a viable therapeutic target in SCCHN. It is hoped that this work will provide a foundation for further exploration.

## 8.3 Concluding Statement

Collectively, the findings of this thesis have provided evidence to suggest that the expression of NOTCH1 in SCCHN gives rise to the following cell behaviours: (1) reduced clonogenicity, (2) reduced proliferation, (3) increased differentiation in response to high NICD expression, (4) reduced cell migration and invasion, (5) increased cell death and (6) reduced angiogenesis. Together, these findings suggest a tumour suppressor role for NOTCH1 in SCCHN. However, considered within the framework of current literature, it is clear that NOTCH signalling is highly complex and context dependent.

SERPINE 1 was highlighted as a potential regulator of NICD-mediated changes in cell behaviour. A high number of histone related genes were also found to be down-regulated in response to increased NICD expression.

This study identified SPANXA1/2 as the most up-regulated gene in response to NICD expression. The fold change increase of SPANXA1/2 was 3x that of any other gene. In order to investigate the functional consequence of SPANXA1/2 expression, a shRNA system was used to knockdown SPANXA1/2 in the NICD-rescued cell line. Preliminary findings provide evidence to associate the expression of SPANXA1/2 with increased cell proliferation, increase cell migration and changes in cell

morphology. Current literature suggests that changes in cell morphology may be associated with the inhibition of EMT and the induction of MET. However, data is preliminary and further studies are required.

Ultimately, it is hoped that this research has contributed to understanding of the heterogeneity of SCCHN, specifically to the complex role of NOTCH1 signalling, and that this work is able to provide a foundation for further study within the field.

# References


Adams, J. C. & Watt, F. M., 1993. Regulation of development and differentiation by the extracellular matrix. *DEVELOPMENT-CAMBRIDGE,* 117(4), pp. 1183-1183.

Agrawal, et al., 2011. Exome sequencing of head and neck squamous cell carcinoma reveals inactivating mutations in Notch1. *Science,* Volume 333, p. 1154–1157.

Albelda, S. M. et al., 1991. Molecular and cellular properties of PECAM-1 (endoCAM/CD31): a novel vascular cell-cell adhesion molecule. *The Journal of cell biology,* 114(5), pp. 1059-1068.

Alcolea, M. P. et al., 2014. Differentiation imbalance in single oesophageal progenitor cells causes clonal immortalization and field change. *Nature Cell Biology,* 16(6), p. 615.

Almanzar, G. et al., 2009. Sperm-derived SPANX-B is a clinically relevant tumor antigen that is expressed in human tumors and readily recognized by human CD4+ and CD8+ T cells. *Clinical Cancer Research,* 15(6). pp. 1954-1963.

Ambler, C. A. & Watt, F. M., 2007. Expression of Notch pathway genes in mammalian epidermis and modulation by β-Catenin. Developmental Dynamics. *Developmental Dynamics,* 236(6), pp. 1595-1601.

Ambler & Watt, 2010. Adult epidermal Notch activity induces dermal accumulation of T cells and neural crest derivatives through upregulation of jagged 1. *Development,* 137(21), pp. 3569-3579.

Argiris, A. et al., 2017. Evidence-Based Treatment Options in Recurrent and/or Metastatic Squmaous Cell Carcinoma of the Head and Neck. *Frontiers in Oncology,* 7(72).

Ashburner, M. et al., 2000. Gene Ontology: tool for the unification of biology. *Nature Genetics,* 25(1), p. 25.

Baldus, C. D. et al., 2009. Prognostic implications of NOTCH1 and FBXW7 mutations in adult acute T-lymphoblastic leukemia. *haematologica,* 94(10), pp. 1383-1390.

Barakat, S. M. M. & Siar, C. H., 2015. Differential expression of stem cell-like proteins in normal, hyperplastic and dysplastic oral epithelium. *Journal of Applied Oral Science,* 23(1), pp. 79-86.

Barrandon, Y. A. G. H., 1987. Three cloncal types of keratinocyte with different capacities for multiplication. *Proceedings of the National Acadamy of Sciecnes,* 84(8), pp. 2302-2306.

Bayo, P. et al., 2015. Loss of SOX2 expression induces cell motility via vimentin up-regulation and is an unfavorable risk factor for survival of head and neck squamous cell carcinoma. *Molecular Oncology,* 9(8), pp. 1704-1719.

Benaich, N. et al., 2014. Rewiring of an epithelial differentiation factor, miR-203, to inhibit human squamous cell carcinoma metastasis. *Cell reports,* 9(1), pp. 104-117.

Biddle, A. et al., 2016. Phenotypic plasticity determines cancer stem cell therapeutic resistance in oral squamous cell carcinoma. *EBioMedicine,* Volume 4, pp. 138-145.

Birchmeier, C., Birchmeier, W. & Brand-Saberi, B., 1996. Epithelial-mesenchymal transitions in cancer progression. *Cells Tissues Organs,* 153(6), pp. 217-226.

Blanpain, C., Lowry, W. E., Pasolli, H. A. & E., F., 2006. Canonical Notch signaling functions as a commitment switch in the epidermal lineage. *Genes Dev,* Volume 20, pp. 3022–3035.

Braakhuis, et al., 2003. A genetic explanation of Slaughter's concept of field cancerization: evidence and clinical implications. *Cancer Research,* Volume 63, pp. 1727–1730.

Bray, 2006. Notch signalling: a simple pathway becomes complex. *Nature revies molecular cell biology,* 7(9), pp. 376-382.

Brennan, K. & Gardner, P., 2002. Notching up another pathway. *Bioessays,* 24(5), pp. 405-410.

Brou, C. et al., 2000. A novel proteolytic cleavage involved in Notch signalling: the role of the disintegrin-metalloprotease TACE. *Molecular Cell,* 5(2), pp. 207-216.

Cabrera, C. V., 1990. Lateral inhibition and cell fate during neurogenesis in Drosophila: the interaction between scute, Notch and Delta. *Development,* 109(3), pp. 733-742.

Calenic, B. et al., 2015. Oral keratinocyte stem/progenitor cells: specific markers, molecular signaling pathways and potential uses. *Periodontology 2000,* 69(1), pp. 68-82.

Califano, Riet & Westra, 1996. Genetic progression model for head and neck cancer: implications for field cancerization. *Cancer Research,* 11(54), p. 2488–2492.

Cancer Genome Atlas Network, 2015. Comprehensive genomic characterization of head and neck squamous cell carcinomas. *Nature,* 517(7536), p. 576.

Cancer Research UK, 2016. *Head and neck cancers survival statistics.* [Online] Available at: http://www.cancerresearchuk.org/health-professional/cancer-statistics/statistics-by-cancer-type/head-and-neck-cancers/survival#heading-Zero [Accessed 16 September 2017].

Cao, B. et al., 2015. Latent transforming growth factor-beta binding protein-1 in circulating plasma as a novel biomarker for early detection of hepatocellular carcinoma. *International journal of clinical and experimental pathology,* 8(12), p. 16046.

Capaccione, K. M. & Pine, S. R., 2013. The Notch signalling pathway as a mediator of tumor survival, *Carcinogenesis,* 34(7), pp. 1420-1430.

Cartier-Michaud, A. et al., 2012, Matrix-bound PAI-1 supports cell blebbing via RhoA/ROCK1 signalling. *PLoS One,* 7(2), p. e32204.

Casas, E. et al., 2011. Snail2 is an essential mediator of Twist1-induced epithelial mesenchymal transition and metastasis. *Cancer Res,* 71(2), pp. 245-254.

Casey, L. M. et al., 2006. Jag2-Notch1 signalling regulates oral epithelial differentiation and palate development. *Development dynamics,* 235(7), pp. 1830-1844.

Cerami, E. et al., 2012. The cBio Cancer Genomics Portal: An Open Platform for Exploring Multidimensional Cancer Genomics Data. *Cancer Discovery* , 2(5), pp. 401-404.

Chen, X. & Wong, S., 2014. *Cancer Theranostics.* 1st ed. s.1.: Academic Press.

Chen, Z. et al,. 2010. Cancer/testis antigens and clinical risk factors for liver metastasis of colorectal cancer: a predictive panel. *Diseases of the Colon & Rectum,* 53(1), pp. 31-38.

Chung, et al., 2004. Molecular classification of head and neck squamous cell carcinomas using patterns of gene expression. *Cancer Cell,* Volume 5, pp. 489-500.

Chu, Q. et al,. 2013. Prolonged inhibition of glioblastoma xenograft initiation and clonogenic growth following in vivo Notch blockade. *Clinical Cancer Research,* 19(12), pp. 3224-3233.

Clayton, E. et al., 2007. A single type of progenitor cell maintains normal epidermis. *Nature,* 446(7132), p. 185.

Conceição Pereira, M., Oliveira, D. T., Landman, G. & Kowalski, L. P., 2007. Histologic subtypes of oral squamous cell carcinoma: prognostic relevance. *Journal of the Canadian Dental Association,* 73(4).

Conti, M. A. et al., 2015. Conditional deletion of nonmuscle myosin II-A in mouse tongue epithelium results in squamous cell carcinoma. *Scientific reports,* Volume 5, p. 14068.

Cordle, J. et al., 2008. Localization of the delta-like-1-binding site in human Notch-1 and its modulation by calcium affinity.. *J Biol Chem,* b(283), p. 11785–11793..

Dai, M. Y. et al., 2015. Downregulation of Notch1 induces apoptosis and inhibits cell proliferation and metastasis in laryngeal squamous cell carcinoma. *Oncol Rep,* 34(6), pp. 3111-3119.

Das, D. K. et al., 2015. Automated identification of keratinization and keratin pearl area from *in situ* oral histological images. *Tissue and Cell,* 47(4), pp 349-358.

De Cecco, L. et al., 2015. Head and neck cancer subtypes with biological and clinical relevance: Meta-analysis of gene-expression data. *Oncotarget,* 6(11), p. 9627.

De Strooper, B. et al., 1999. A presenilin-1-dependent γ-secretase-like protease mediates release of Notch intracellular domain. *Nature*, 398(6727), p.518.

Denis, et al., 2004. Final results of the 94–01 French Head and Neck Oncology and Radiotherapy Group randomized trial comparing radiotherapy alone with concomitant radiochemotherapy in advanced-stage oropharynx carcinoma. *Journal of Clinical Oncology,* 22(1), pp. 69-76.

Dotto, 2008. Notch tumor suppressor function. *Oncogene,* 27(38), pp. 5115-5123.

Dotto, 2009. Crosstalk of Notch with p53 and p63 in cancer growth control. *Nature Reviews Cancer,* 9(8), pp. 587-595.

Dover, R. & Watt, F. M., 19987. Measurement of the rate of epidermal terminal differentiation: expression of involucrin by S-phase keratinocytes in culture and in psoriatic plaques. *J. Invest. Derm,* Volume 89, pp. 349-352.

Duan, L., Yao, J., Wu, X. & Fan, M., 2006. Growth suppression induced by Notch1 activation involves Wnt-beta-catenin down-regulation in human tongue carcinoma cells. *Biol Cell,* 98(8), pp. 479-490.

Duray, et al., 2011. Immune suppression in head and neck cancers: a review. *Clinical and Developmental Immunology.*

Ehebauer, M., Hayward, P. & Arias, A. M., 2006. Notch, a universal arbiter of cell fate descisions. *Science,* 314(5804), pp. 1414-1415.

Estrach, S. et al., 2006. Jagged 1 is a β-catenin target gene required for ectopic hair follicle formation in adult epidermis. *Development,* Volume 133, p. 4427–4438.

Estrach, S. et al., 2008. Role of the Notch ligand Delta1 in embryonic and adult mouse epidermis. *Journal of Investigative Dermatology,* 128(4), pp. 825-832.

Fazio, C. & Ricciardiello, L., 2016. Inflammation and Notch signaling: a crosstalk with opposite effects on tumorigenesis. *Cell death & disease,* 7(12), p. 2515.

Fitzmaurice, C. et al., 2017. Global, Regional, and National Cancer Incidence, Mortality, Years of Life Lost, Years Lived With Disability, and Disability-Adjusted Life-years for 32 Cancer Groups, 1990 to 2015: A Systematic Analysis for the Global Burden of Disease Study. *JAMA oncology,* 3(4), pp. 524-548.

Follenzi, A., Santambrogio, L. & Annoni, A., 2007. Immune responses to lentiviral vectors. *Current gene therapy.* 75(5), pp. 306-315.

Fortini, M. & Artavanis-Tsakonas, S., 1994. The suppressor of hairless protein participates in notch receptor signalling. *Cell,* 79(2), pp. 273-282.

Franken, N. A. et al., 2006. Clonogenic assay of cells in vitro.. *Nat Protoc,* 1(5), pp. 2315-2319.

Fryer, C. J., White, J. B. & Jones, K. A., 2004. Mastermind recruits CycC:CDK8 to phosphorylate the Notch ICD and coordinate acitvation with turnover. *Molecular Cell,* 16(4), pp. 509-520.

Fuchs, E., 2008. Skin stem cells: rising to the surface. *The Journal of cell biology,* 180(2 ), pp. 273-284.

Gao, J. et al., 2013. Integrative analysis of complex cancer genomics and clinical profiles using the cBioPortal. *Sci Signal,* 6(269), p. 1.

Gao, J. et al., 2017. 3D clusters of somatic mutations in cancer reveal numerous rare mutations as functional targets. *Genome Medicine,* 9(1), p. 4.

Gao, W. at al., 2012. Anti-cancer effects of curcumin on head and neck cancers. *Anti-Cancer Agents in Medicinal Chemistry (Formerly Current Medicinal Chemistry-Anti-Cancer Agents),* 12(9), pp. 1110-1116.

Ghadially, R., 2012. 25 years of epidermal stem cell research. *Journal of Investigative Dermatology,* 132(3), pp. 797-810.

Giefing, M. et al., 2008. Chromosomal gains and losses indicate oncogene and tumor suppressor gene candidates in salivary gland tumors. *Neoplasma,* 55(1), pp. 55-60.

Gillison, et al., 2000. Evidence for a causal association between human papillomavirus and a subset of head and neck cancers. *Journal of the National Cancer Institute ,* 92(9), pp. 709-720.

Gokulan & Halagowder, 2014. Expression pattern of Notch intercellular domain (NICD) and Hes-1 proteins in preneoplastic and neoplastic human oral squamous epithelium: their correlation with c-Myc, clinicopathological factors and prognosis in oral cancer. *Med Oncol,* Volume 31, p. 126.

Goldie, S. J. et al., 2012. FRMD4A upregulation in human squamous cell carcinoma promotes tumor growth and metastasis and is associated with poor prognosis. *Cancer Res,* Volume 72, p. 3424–3436.

Go, M. J., Eastman, D. S. & Artavanis-Tsakonas, S., 1998. Cell proliferation control by Notch signalling in Drosophila development. *Development,* 125(11), pp. 2031-2040.

Gordon, W. R. et al., 2007. Structural basis for autoinhibition of Notch. *Nature structural and molecular biology,* 14(4), p. 295.

Gray, G. et al., 1999. Human ligands of the Notch receptor. *The American journal of pathology,* 154(3), pp. 785-794.

Grivennikov, S. I., Greten, F. R. & Karin, M., 2010. Immunity, inflammation, and cancer. *Cell,* 104(6), pp. 883-899.

Halls, S., 2017. *Comedo carcinoma of the breast.* [Online] Available at: http://breast-cancer.ca/comed-carc/
[Accessed 25 September 2017].

Harper, L. J. et al., 2007. Stem cell patterns in cell lines derived from head and neck squamous cell carcinoma. *Journal of Oral Pathology & Medicine,* 36(10), pp. 594-603.

Hartmann, et al., 2002. The disintegrin/metalloprotease ADAM 10 is essential for Notch signalling but not for α-secretase activity in fibroblasts. *Human molecular genetics ,* 11(21), pp. 2615-2624.

Hassan, K. A. et al., 2013. Notch pathway activity identifies cells with cancer stem cell-like properties and corelates with worse survival in lung adenocarcinoma. *Clinical Cancer Research.* 19(8), pp. 1972-1980.

Hayes, T. F. et al., 2016. Integrative genomic and functional analysis of human oral squamous cell carcinoma cell lines reveals synergistic effects of FAT1 and CASP8 inactivation.. *Cancer Lett,* 383(1), pp. 106-114.

Hayward, P. et al., 2005. Notch modulates Wnt signalling by associating with Armadillo/β-catenin and regulating its transcriptional activity. *Development,* 132(8), pp. 1819-1830.

Hermsen, et al., 2001. New chromosomal regions with high-level amplifications in squamous cell carcinomas of the larynx and pharynx, identified by comparative genomic hybridization. *The Journal of pathology,* 194(2), pp. 177-182.

Hijioka, Setoguchi & Miyawaki, 2010. Upregulation of Notch pathway molecules in oral squamous cell carcinoma. *International Journal of Oncology,* 36(4), pp. 817-822.

Hirsch, T. et al., 2017. Regression of the entire human epidermis using transgenic stem cells. *Nature,* 551(7680), p. 327.

Holderfield, M. T. & Hughes, C. C., 2008. Crosstalk between vascular endothelial growth factor, notch, and transforming growth factor-β in vascular morphogenesis. *Circulation Research,* 102(6), pp. 637-652.

Hou, X., Tashima, Y. & Stanley, P., 2012. Galactose Differentially Modulates Lunatic and Manic Fringe Effects on Delta1-induced NOTCH Signaling. *J Biol Chem,* 287(1), pp. 474-483.

Hsiao, Y. J. et al., 2016. SPANXA suppresses EMT by inhibiting c-JUN/SNAI2 signaling in lung adenocarcinoma. *Oncotarget,* 7(28), p. 44417.

Hsu, Y. C., 2015. The Theory and Practice of Lineage Tracing. *Stem Cells,* 33(11), pp. 3197-3204.

Hu, B. et al., 2012. Multifocal epithelial tumors and field cancerization from loss of mesenchymal CSL signaling. *Cell,* 149(6), p. 120.

Huret, J. L. et al., 2012. Atlas of genetics and cytogenetics in oncology and haematology in 2013. *Nucleic acids research.* 41(D1), pp. D920-D924.

Islaslab.org, 2014. *Cancer Biology: Tumor Suppressor Functions and Mutations of NOTCH1 in HNSCC.* [Online]
Available at: http://islaslab.blogspot.co.uk/2014/05/tumor-suppressor-functions-and.html
[Accessed 1 August 2014].

Ito, M. et al., 2005. Stem cells in the hair follicle bulge contribute to wound repair but not to homeostasis of the epidermis. *Nat Med,* 11 pp. 1351-1354.

Jaffe, E. A., Nachman, R. L., Becker, C. G. & Minick, C. R., 1973. Culture of human endothelial cells derived from umbilical veins. Identification by morphologic and immunologic criteria. *Journal of Clinical Investigation,* 52(11), p. 2745.

Jaimes, N. et al., 2012. Pearls of keratinizing tumors. *Archives of dermatology,* 148(8), pp. 976-976.

Jaiswal, Jaiswal, Kumar & Sharma, 2013. Field cancerization: concept and clinical implications in head and neck squamous cell carcinoma.. *Journal of Experimental Therapeutics and Oncology,* 10(3), pp. 209-214.

Janes, S. M. & Watt, F. M., 2006. New roles for integrins in squamous-cell carcinoma. *Nature Reviews Cancer,* 6(3), pp. 175-183.

Jarriault, 1995. Signalling downstream of activated mammalian Notch. *Nature,* pp. 355-358.

Javorhazy, A. et al., 2016. Lack of TMEM27 expression is associated with postoperative progression of clinically localized conventional renal cell carcinoma. *Journal of cancer research and clinical oncology,* 142(9), pp. 1947-1953.

Jemal, A. et al., 2007. Cancer Statistics, 2007. *CA Cancer J Clin,* 57(1), pp. 43-66.

Jensen, K. B. et al., 2009. Lrig1 expression defines a distinct multipotent stem cell population in mammalian epidermis. *Cell Stem Cell,* 4, pp. 427-439.

Jiang, W. et al., 2015. Downregulation of VGLL4 in the progression of esophageal squamous cell carcinoma. *Tumor Biology,* 36(2), pp. 1289-1297.

Jiao, J. & Li, S., 2012. Effect of Notch1 on cell cycle, apoptosis and migration of laryngeal squamous cell carninoma cell line Hep-2. *Zhonghua Zhong Liu Za Zhi,* 34(2), pp. 104-109.

Jing, P. et al., 2016. MicroR-140-5p suppresses tumor cell migration and invasion by targeting ADAM10-mediated Notch1 signaling pathway in hypopharyngeal squamous cell carcinoma. *Exp Mol Pathol,* 100(1), pp. 132-138.

Jin, et al., 2006. Cytogenetic abnormalities in 106 oral squamous cell carcinomas. *Cancer genetics and cytogenetics,* 164(1), pp. 44-53.

Johnson, S. E. & Barrick, D., 2012. Dissecting and circumventing the requirement for RAM in CSL-dependent Notch signalling. *PLoS one,* 7(8), p. e39093.

Jones, P. H., Simons, B. D. & Watt, F. M., 2007. Sic transit gloria: farewell to the epidermal transit amplifying cell?. *Cell stem cell,* 1(4), pp. 371-381.

Joo, Y. H., Jung, C. K., Kim, M. S. & Sun, D. I., 2009. Relationship between vascular endothelial growth factor and Notch1 expression and lymphatic metastasis in tongue cancer. *Otolaryngology—Head and Neck Surgery,* 140(4), pp. 512-518.

Kadam, S. & Emerson, B. M., 2003. Transcriptional specificity of human SWI/SFN BRG1 and BRM chromatin remodelling complexes. *Molecular cell,* 11(2), pp. 377-389.

Kagawa, S. et al., 2015. Cellular senescence checkpoint function determines differential Notch1-dependent oncogenic and tumor-suppressor activities. *Oncogene,* 34(18), pp. 2347-2359.

Kakuda, S. & Haltiwanger, R. S., 2017. Deciphering the fringe-mediated Notch code: Identification of activating and inhibiting sites allowing discrimination between ligands. *Developmental cell,* 40(2), pp. 193-201.

Kandachar. V. & Roegress, F., 2012. Endocytosis and control of Notch signalling. *Current Opinions in Cell Biology,* 24(4), pp. 534-540.

Kanojia, D. & Vaidya, M. M., 2006. 4-nitroquinoline-1-oxide induced experimental oral carcinogenesis. *Oral oncology,* 42(7), pp. 655-667.

Keats, J. J. et al., 2012. Clonal competition with alternating dominance in multiple myeloma. *Blood,* 120(5), pp. 1067-1076.

Khalesi, S., 2016. Review of Head and Neck Squamous Cell Carcinoma Risk Factors with More Focus on Oral Cancer. *Journal of Detistry and Oral Disorders,* 2(6), p. 1032.

Kitagawa, M. et al., 2001. A human protein with sequence similarity to Drosophila Mastermind coordinates the nuclear form of Notch and a CSL protein to build a transcriptional activator complex on target promoters. *Molecular and cellular biology,* 21(13), pp. 4337-4346.

Klinakis, et al., 2011. A novel tumour-suppressor function for the Notch pathway in myeloid leukaemia. *Nature,* 473(7246), pp. 230-233.

Koontongkaew, 2013. The tumor microenvironment contribution to development, growth, invasion and metastasis of head and neck squamous cell carcinomas. *Journal of Cancer ,* Volume 4, p. 66–83.

Kopan & IIagan, 2009. The Canonical Notch Signaling Pathway: Unfolding the Activation Mechanism. *Cell,* 137(2), pp. 216-233.

Kouprina, N. et al., 2004. The SPANX gene family of cancer/testis-specific antigens: rapid evolution and amplification in African great apes and hominids. *Proceedings of the National Academy of Science of the United States of America,* 101(9), pp. 3077-3082.

Krämer, A., Green, J., Pollard Jr, J. & Tugendreich, S., 2013. Causal analysis approaches in ingenuity pathway analysis. *Bioinformatics,* 30(4), pp. 523-530.

Krisanaprakornkit, S. & Iamaroon, A., 2012. Epithelial-mesenchymal transition in oral squamous cell carcinoma. *ISRN Oncology,* p. 681469.

Kumar, S., Das, A. & Sen, S., 2014. Extracellular matrix density promotes EMT by weakening cell-cell adhesions. *Molecular BioSystems,* 10(4), pp. 838-850.

Kurozumi, A. et al., 2016. Tumor-suppressive microRNA-223 inhibits cancer cell migration and invasion by targeting ITGA3/ITGB1 signaling in prostate cancer. *Cancer science,* 107(1), pp. 84-94.

Kutler, D. et al., 2016. High incidence of head and neck squamous cell carcinoma in patients with Faconi anemia. *Arch Otolaryngol Head Neck Surg.* 129(1), pp. 106-112.

Kwon, et al., 2011. Notch post-translationally regulates [beta]-catenin protein in stem and progenitor cells. *Nature cell biology,* 13(10), pp. 1244-1251.

Leader, M., Collins, M., Patel, J. & Henry, K., 1987. Vimentin: an evaluation of its role as a tumour marker. *Histopathology.* 11(1), pp. 63-72

Lee, et al., 2009. Gain-of-function mutations and copy number increases of Notch2 in diffuse large B-cell lymphoma. *Cancer science ,* 100(5), pp. 920-926.

Leemans, Boudewijn, Braakhuis & Brakenhoff, 2011. Molecular biology of head and neck cancers. *Nature reviews cancer,* Volume 11, pp. 9-22.

Lee, S. H. et al., 2012. TNFα enhances cancer stem cell-like phenotype via Notch-Hes1 activation in oral squamous cell carcinoma. *Biochemical and biophysical research communications,* 424(1), pp. 58-64.

Leha, A. et al., 2016. A high content platform to characterise human induced pluripotent stem cells. *Methods.* 96, pp. 58-64.

Le, J. M., Squarize, C. H. & Castilho, R. M., 2014. Histone modifications: Targeting head and neck cancer stem cells. *World J Stem Cells,* 6(5), pp. 511-525.

Leong, K. G. et al., 2007. Jagged1-mediated Notch activation induces epithelial-to-mesenchymal transition through Slug-induced repression of E-cadherin.. *Journal of Experimental Medicine,* p. 204.

Levy, V. et al., 2007. Epidermal stem cells arise from the hair follicle after wounding. *FASEB J,* 21, pp. 1358-1366.

Liao, S. et al., 2011. Inhibitory effect of curcumin on oral carcinoma CAL-27 cells via suppression of Notch-1 and NF-κB signaling pathways. *J Cell Biochem,* 112(4), pp. 1055-1065.

Liu, Y., Cox, S. R., Morita, T. & Kourembanas, S., 1995. Hypoxia regulates vascular endothelial growth factor gene expression in endothelial cells. *Circulation research,* 77(3), pp. 638-643.

Li, W. et al., 2015. [IL-23 promotes invasion of esophageal squamous cell carcinoma cells by activating DLL4/Notch1 signaling pathway]. *Chinese journal of cellular and molecular immunology,* 31(6), pp. 812-815.

Lowell, S. et al., 2000. Stimulation of human epidermal differentiation by Delta–Notch signalling at the boundaries of stem-cell clusters. *Current Biology,* 10(9), pp. 491-500.

Lu, Z. et al., 2008. An activated Notch1 signaling pathway inhibits cell proliferation and induces apoptosis in human esophageal squamous cell carcinoma cell line EC9706. *Int J Oncol,* 32(3), pp. 643-651.

Mackenzie, I., 2008. Cancer stem cells. *Annals of oncology ,* 19(5), pp. v40-v43.

Mackenzie, I. C. & Fusenig, N. E., 1983. Regeneration of organized epithelial structure. *Journal of Investigative Dermatology,* 81(1), pp. 189-S194.

Macmillan, 2017. *Signs and Symptoms of Head and Neck Cancer.* [Online] Available at: http://www.macmillan.org.uk/information-and-support/head-and-neck-cancers/understanding-cancer/symptoms.html
[Accessed 1 June 2017].

Maine, E. A. et al., 2016. The cancer-testis antigens SPANX-A/C/D and CTAG2 promote breast cancer invasion. *Oncotarget,* 7(12), p. 14708.

Mali, S., 2013. Delivery systems for gene therapy. *Indian journal of human genetics,*19(1), p. 3.

Mammucari, et al., 2005. Integration of Notch 1 and calcineurin/NFAT signaling pathways in keratinocyte growth and differentiation control. *Developmental cell ,* 8(5), pp. 665-676.

Mandasari, M. et al., 2005. Integration of Notch1 and calcineurin/NFAT signalling pathways in keratinocyte growth and differentiation control. *Developmental Cell,* 8(5), pp. 665-676.

Mandasari, M. et al., 2016. A facile one-step strategy for the generation of conditional knockout mice to explore the role of Notch1 in oroesophageal tumorigenesis. *Biochemical and biophysical research communications,* 469(3), pp. 761-767.

Marques Filho, M. F. et al., 2006. Glycosphingolipid expression in squamous cell carcinoma of the upper aerodigestive tract.. *Brazilian journal of otorhinolaryngology,* 72(1), pp. 25-30.

Martincorena, I. et al., 2015. High burden and pervasive positive selection of somatic mutations in normal human skin. *Science,* 348(6237), pp. 880-886.

McCauley, H. A. & Guasch, G., 2013. Serial orthotopic transplantation of epithelial tumors in single-cell suspension. *Stem Cell Niche: Methods and Protocols,* pp. 231-245.

Meng, Q., Ren, M., Li, Y. & Song, X., 2016. LncRNA-RMRP Acts as an Oncogene in Lung Cancer. *PLoS One,* 11(12), p. e0164845.

Meshi, T., Taoka, K. I. & Iwabuchi, M., 2000. Regulation of histone gene expression during the cell cycle. *Plant Molecular Biology,* 43(5-6), pp. 643-657.

Miele, L. & Osborne, B., 1999. Arbiter of differentiation and death: Notch signalling meets apoptosis. *Journal of Cellular Physiology,* 181(3), pp. 393-409.

Moellering, R. E. et al., 2009. Direct inhibition of the NOTCH transcription factor complex. *Nature* , 462(7270), pp. 182-188.

Naganawa, Y. et al., 2010. Decreased expression of FBXW7 is correlated with poor prognosis in patients with esophageal squamous cell carcinoma. *Experimental and therapeutic medicine,* 1(5), pp. 841-846.

Nanci, 2013. *Oral Mucosa, Ten Cate's Oral Histology: Development, Structure and Function.* 7th ed. s.l.:Mosby-Elsevier.

National Cancer Institute, 2013. *Head and Neck Cancers.* [Online] Available at: https://www.cancer.gov/types/head-and-neck/head-neck-fact-sheet [Accessed 31 May 2017].

Nees, et al., 1993. Expression of mutated p53 occurs in tumor-distant epithelia of head and neck cancer patients: a possible molecular basis for the development of multiple tumors. *Cancer Research,* 53(18), pp. 4189-4196.

Nickoloff, B. J. et al., 2002. Jagged-1 mediated activation of notch signaling induces complete maturation of human keratinocytes through NF-kappaB and PPARgamma. *Cell Death Differ,* 9(8), pp. 842-855.

Nicolas, M. et al., 2003. Notch1 functions as a tumor suppressor in mouse skin. *Nat Genet,* 33(3), pp. 416-421.

Niessen, K. et al., 2008. Slug is a direct Notch target required for initiation of cardiac cushion cellularization. *J. Cell Biol.,* Volume 182, pp. 315-325.

Nishida, N. et al., 2006. Angiogenesis in Cancer. *Vasc Health Risk Manag,* 2(3), pp. 213-219.

Oberg, C. et al., 2001. The Notch intracellular domain is ubiquitinated and negatively regulated by the mammalian Sel-10 homolog. *Journal of Biological Chemistry,* 276(38), pp. 35847-35853.

Old, L. J., 1982. Cancer immunology: the search for specificity. *National Cancer Institute monograph,* 60, pp.193-209.

Ong, C. et al., 2006. Target selectivity of vertebrate notch proteins. Collaboration between discrete domains and CSL-binding site architecture determines activation probability.. *J Biol Chem.,* 281(8), pp. 5106-5119.

Oshima, H. et al., 2001. Morphogenesis and renewal of hair follicles from adult multipotent stem cells. *Cell,* 104, pp. 233-245.

Pan, Y. et al., 2004. Gamma-secretase functions through Notch signaling to maintain skin appendages but is not required for their patterning or initial morphogenesis. *Dev Cell,* Volume 7, p. 731–743.

Papagerakis, S. et al., 2014. Oral epithelial stem cells—implications in normal development and cancer metastasis. *Experimental cell research,* 325(2), pp. 111-129.

Pavón, M. A. et al., 2015. Enhanced cell migration and apoptosis resistance may underlie the association between high SERPINE1 expression and poor outcome in head and neck carcinoma patients. *Oncotarget,* 6(30), p. 29016.

Pereira, M. C., Oliveira, D. T., Landman, G. & Kowalski, L. P., 2007. Histological subtypes of oral squamous cell carcinoma: prognostic relevance. *Canadian Dental Association,* 73(4), pp. 339-344.

Peters, M. A. et al., 2001. Genetic linkage analysis of prostate cancer families to Xq27-28. *Human Heredity,* 51(1-2), pp. 107-111.

Pickering, C. R. et al., 2013. Integrative genomic characterization of oral squamous cell carcinoma identifies frequent somatic drivers. *Cancer discovery,* 3(7), pp. 770-781.

Ploscariu, N. et al., 2014. Single molecule studies of force-induced S2 site exposure in the mammalian Notch negative regulatory domain. *The Journal of Physical Chemistry B,* 118(18), pp.4761.

Pogo, B. G., Allfrey, V. G. & Mirsky, A. E., 1966. RNA synthesis and histone acetylation during the course of gene activation in lymphocytes. *Proceedings of the National Academy of Sciences,* 55(4), pp. 805-812.

Poole, M. E. et al., 2001. Chemoradiation for locally advanced squamous cell carcinoma of the head and neck for organ preservation and palliation. *Arch Otolaryngol Head Neck Surg,* 127(12), pp. 1446-1450.

Posthaus, H. et al., 2002. β-Catenin is not required for proliferation and differentiation of epidermal mouse keratinocytes. *Journal of Cell Science,* 115(23), p. 458.

Potton, C. S., 1988. Epithelial stem cells in vivo. *J Cell Sci Suppl.* 10, pp. 45-62.

Poulson, D. F., 1939. Effects of Notch deficiencies. *Drosoph Inf Serv,* 12, pp. 64.

Proweller, A. et al., 2006. Impaired notch signaling promotes de novo squamous cell carcinoma formation. *Cancer research,* 66(15), pp. 7438-7444.

Puente, et al., 2011. Whole-genome sequencing identifies recurrent mutations in chronic lymphocytic leukaemia. *Nature,* 475(7354), pp. 101-105.

Radtke, F. & Raj, K., 2003. The role of Notch in tumorigenesis: oncogene or tumour suppressor?. *Nature Reviews Cancer* , Volume 3, pp. 756-767.

Ramshankar, V. & Krishnamurthy, A., 2013. Human Papilloma Virus in Head and Neck Cancers—Role and Relevance in Clinical Management. *Indian Journal of Surgical Oncology,* 4(1), pp. 59-66.

Rangarajan, A. et al., 2001. Notch signaling is a direct determinant of keratinocyte growth arrest and entry into differentiation. *EMBO J.,* 20(13), pp. 3427-3436.

Ravindran, G. & Devaraj, H., 2012. Aberrant expression of β-catenin and its association with ΔNp63, Notch-1, and clinicopathological factors in oral squamous cell carcinoma. *Clin Oral Investig,* 16(4), pp. 1275-1288.

Raya, A. et al., 2004. Notch activity acts as a sensor for extracellular calcium during vertebrate left-right determination. *Nature,* 427(6970), p. 121.

Rheinwald, J. & Beckett, M., 1981. Tumorigenic keratinocyte lines requiring anchorage and fibroblast support cultures from human squamous cell carcinomas. *Cancer Res,* Volume 41, pp. 1657-1663.

Rheinwald, J. & Green, H., 1975. Serial cultivation of strains of human epidermal keratinocytes: the formation of keratinizing colonies from single cells. *Cell,* Volume 6, pp. 331-343.

Ribatti, D., 2017. Epithelial-mesenchymal transition in morphogenesis, cancer progression and angiogenesis. *Experimental Cell Research.* 353(1), pp. 1-5.

Rodilla, V. et al., 2009. Jagged1 is the pathological link between Wnt and Notch pathways in colorectal cancer. *Proceedings of the National Academy of Sciences,* 106(15), pp. 6315-6320.

Roed-Petersen, B. & Renstrup, G., 1969. A topographical classification of the oral mucosa suitable for electronic data processing its application to 560 leukoplakias. *Acta odontologica scandinavica,* 27(6), pp. 681-695.

Roesch-Ely, M. et al., 2007. Proteomic analysis reveals successive aberrations in protein expression from healthy mucosa to invade head and neck cancer. *Oncogene,* 26(1), pp.64-64.

Rothenberg, S. M. & Ellisen, L., 2012. The molecular pathogenesis of head and neck squamous cell carcinoma. *The Journal of Clinical Investigation,* 122(6), pp. 1951-1957.

Rousseau, A. & Badoual, C., 2011. *Head and Neck: Squamous cell carcinoma: an overview.* [Online]
Available at: http://atlasgeneticsoncology.org/Tumors/HeadNeckSCCID5078.html
[Accessed 10 September 2017].

Rousseau & Badoual, 2012. Head and neck: squamous cell carcinoma: an overveiw. *Atlas of genetics and cytogenetics in oncology and haematology,* 16(2), pp. 145-155.

Routray & Mohanty, 2014. Cancer Stem Cells Accountability in Progression of Head and Neck Squamous Cell Carcinoma: The Most Recent Trends!. *Molecular biology international* .

Ruhrberg, C. et al., 1996. Envoplankin, a novel precursor of the cornified envelope that has homology to desmoplankin. *The Journa of Cell Biology,* 134(3), pp. 715-729.

Sakamoto, K. et al., 2012. Reduction of NOTCH1 expression pertains to maturation abnormalities of keratinocytes in squamous neoplasms. *Lab Invest,* 95(5), p. 699-702.

Salemi, M., et al., 2008. SPANX-B and SPANX-C (Xq27 region) gene dosage analysis in Sicilian patients with melanoma. *Melanoma Research,* 18(4), pp. 295-299.

Salemi, M. et al., 2009. A high percentage of skin melanoma cells express SPANX proteins. *The American Journal of Dermatology,* 31(2), pp. 182-186.

Salemi, M. et al., 2010. Expression of SPANX proteins in normal prostatic tissue and in prostate cancer. *European Journal of Histochemistry,* 54(3), p. e41.

Sano, D. & Myers, J. N., 2009. Xenograft models of head and neck cancers. *Head & neck oncology,* 1(1), p. 32.

Schaaij-Visser, T. B. M. et al., 2009. Differential proteomics identifies protein biomarkers that predict local relapse of head and neck squamous cell carcinoma. *Clin Cancer Research,* 15(24), pp.7666-7675.

Sequeira, I., Legue, E., Capgras, S. & Nicolas, J.-F., 2014. Microdissection and visualization of individual hair follicles for lineage tracing studies. *Methods Molecular Biology,* Volume 1195, pp. 247-258.

Shah, A. A., Jeffus, S. K. & Stelow, E. B., 2014. Squamous cell carcinoma variants of the upper aerodigestive tract: a comprehensive review with a focus on genetic alterations. *Archives of Pathology and Laboratory Medicine,* 138(6), pp. 731-744.

Shahin, L. et al., 2017. The role of immunogenic SPANX antigens in distinct cancer stem cell subsets within triple negative breast cancers. *Washington, Proceedings: AACR Annual Meeting 2017.*

Silva-Vargas, V. et al.,2005. β-catenin and Hedgehog signal strength can specify number and location of hair follicles in adult epidermis without recruitment of bulge stem cells, *Dev Cell,* 9, pp 121-131.

Skovseth, D. K., Küchler, A. M. & Haraldsen, G., 2007. The HUVEC/Matrigel Assay An In Vivo Assay of Human Angiogenesis Suitable for Drug Validation. In: M. Sioud, ed. *Methods in Molecular Biology™.* Totowa, NJ: Humana Press Inc, pp. 253-268.

Slaughter, Southwick & Smejkal, 1953. Field cancerization in oral stratified squamous epithelium;clinical implications of multicentric origin. *Cancer,* p. 963–968 .

Slominski, A. T., 2014. Intrinsic differences between oral and skin keratinocytes. *PLoS One,* 9(9), p. e101480.

Smeets, et al., 2009. Genetic classification of oral and oropharyngeal carcinomas identifies subgroups with a different prognosis. *Analytical Cellular Pathology,* 31(4), pp. 291-300.

Song, Y. et al., 2014. Identification of genomic alterations in oesophageal squamous cell cancer. *Nature*, 509 (7498), p. 91.

Sottoriva, A. et al., 2015. A Big Bang model of human colorectal tumor growth. *Nature Genetics*, 47(3), pp. 209-216.

South, A. P. et al., 2014. NOTCH1 mutations occur early during cutaneous squamous cell carcinogenesis. *Journal of Investigative Dermatology*, 134(10), pp. 2630-2638.

Squier, C. & Brogden, K., 2010. *Human oral mucosa: development, structure and function.* s.l.:John Wiley & Sons.

Stephan, D. A. et al., 2002. Physical and transcript map of the hereditary prostate cancer region Xq27. *Genomics*, 79(1), pp 41-50.

Stransky, et al., 2011. The mutational landscape of head and neck squamous cell carcinoma. *Science*, Volume 333, p. 1157–1160.

Subramaniam, D. et al., 2012. Curcumin Induces Cell Death in Esophageal Cancer Cells through Modulating Notch Signaling. *PLoS One*, 7(2), p. e30590.

Subramanian, D. et al., 2012. Curcumin induces cell death in esophageal cancer cells through modulating Notch signalling. *PLoS One*, 7(2), pp. e30590.

Subramanian, A. et al., 2005. Gene set enrichment analysis: a knowledge-based approach for interpreting genome-wide expression profiles.. *Proceedings of the National Academy of Sciences*, 102(43), pp. 15545-15550.

Su, C. H. et al., 2009. Notch1 expression in esophageal squamous cell carcinoma and its relation with microvascular angiogenesis. *Nan Fang Yi Ke Da Xue Xue Bao*, 29(11), pp. 2255-2258.

Sun, et al., 2014. Activation of the NOTCH pathway in head and neck cancer. *Cancer research* , 74(4), pp. 1091-1104.

Sun, Y. et al., 2015. Pro-inflammatory cytokine IL-1β up-regulates CXC chemokine receptor 4 via Notch and ERK signaling pathways in tongue squamous cell carcinoma. *PloS one*, 10(7), p. e0132677.

Tabor, et al., 2004. Genetically Altered Fields as Origin of Locally Recurrent Head and Neck Cancer A Retrospective Study. *Clinical Cancer Research* , 10(11), pp. 3607-3613.

Tabor, M. et al., 2001. Persistence of genetically altered fields in head and neck cancer patients: biological and clinical applications. *Clinical Cancer Research,* 7(6), pp. 1523-1532.

The Jackson Laboratory, 2017. *FREQUENTLY ASKED NSG™ QUESTIONS.* [Online]
Available at: https://www.jax.org/jax-mice-and-services/find-and-order-jax-mice/nsg-portfolio/frequently-asked-nsg-questions#Basic facts about NSG mice
[Accessed 20 September 2017].

Thelu, J., Rossio, P. & Favier, B., 2002. Notch signalling is linked to epidermal cell differentiation level in basal cell carcinoma, psoriasis and wound healing. *BMC Dermatol,* 2 pp. 7.

Thermo Fisher Scientific, 2003. *Keratinocyte-SFM 1x: Speciality and Serum Free Media* [Online]
Available at: https://www.thermofisher.com/order/catalog/product/17005042
[Accessed 25 March 2018]

Troy, J. D. et al., 2013. Expression of EGFR, VEGF, and NOTCH1 Suggest Differences in Tumor Angiogenesis in HPV-Positive and HPV-Negative Head and Neck Squamous Cell Carcinoma. *Head Neck Pathol,* 7(4), pp. 344-345.

UCSD School of Medicine, 2018. *MedPics.* [Online]
Available at:
http://medpics.ucsd.edu/index.cfm?curpage=image&course=path&mode=browse&lesson=16&img=396
[Accessed 05 April 2018].

Union for International Cancer Control, 2014. *Head and Neck Cancer,* s1: Review of Cancer Medicines on the WHO List of Essential Medicines.

Upadhyay, P. N. S. K. E. et al., 2016. Notch pathway activation is essential for maintenance of stem-like cells in early tongue cancer. *Oncotarget*, 7(31), p. 50437.

Vardabasso, C. et al., 2014. Histone variants: emerging players in cancer biology. *Cell Mol Life Sci*, 71(3), pp. 379-404.

Vishak, S., Rangarajan, B. & Kekatpure, V. D., 2015. Neoadjuvant chemotherapy in oral cancers: Selecting the right patients. *Indian journal of medical and paediatric oncology: official journal of Indian Society of Medical & Paediatric Oncology*, 36(3), p. 148.

Vogelstein, B. et al., 2013. Cancer Genome Landscapes. *Science*, 339(6127), pp. 1546-1558.

Vooijs, M. et al., 2007. Mapping the consequence of Notch1 proteolysis in vivo with NIP-CRE. *Development*, Volume 134, p. 535–544.

Wang, C. et al., 2017. IL-17 induced NOTCH1 activation in oligodendrocyte progenitor cells enhances proliferation and inflammatory gene expression. *Nat Commun*, Volume 8.

Wang, N. J. et al., 2011. Loss-of-function mutations in Notch receptors in cutaneous and lung squamous cell carcinoma.. *Proceedings of the National Academy of Sciences*, 108(43), pp. 17761-17766.

Wang, et al., 2011. Loss-of-function mutations in Notch receptors in cutaneous and lung squamous cell carcinoma. *Proceedings of the National Academy of Sciences* , 108(43), pp. 17761-17766.

Wang, W. M. et al., 2015. Epidermal Growth Factor Receptor Inhibition Reduces Angiogenesis via Hypoxia-Inducible Factor-1α and Notch1 in Head Neck Squamous Cell Carcinoma. *PLoS One*, 10(2), p. e0119723..

Watt, F. M., Estrach, S. & Ambler, C., 2008. Epidermal Notch signalling: differentiation, cancer and adhesion. *Current Opinion in Cell Biology*, 20(2), pp. 171-179.

Watt, F. M. & Jensen, K. B., 2009. Epidermal stem cell diversity and quiescence. *EMBO molecular medicine.* 1(5), pp. 260-267.

Weber, K., Bartsch, U., Stocking, C. & Fehse, B., 2008. A multicolor panel of novel lentiviral "gene ontology" (LeGO) vectors for functional gene analysis.. *Mol Ther.*, 16(4), pp. 698-706.

Welkoborsky, H. J., Bernauer, H. & Riazimand, H., 2000. Patterns of chromosomal aberrations in metastasizing and non-metastasizing squamous cell carcinomas of the oropharynx and hypopharynx. *Ann Otol Rhinol Laryngol*, 109, pp. 401-410.

Weng, A. & Aster, J., 2004. Multiple niches for Notch in cancer: context is everything. *Curr Opin Genet Dev,* 14(1), pp. 48-54.

Weng, et al., 2004. Activating mutations of NOTCH1 in human T cell acute lymphoblastic leukemia. *Science ,* 306(5694), pp. 269-271.

Wen, Y. & Grandis, J., 2015. Emerging drugs for head and neck cancer. *Expert opinion on emerging drugs,* 20(2), pp. 313-329.

Westbrook, V. A. et al., 2000. Spermatid-specific expression of the novel X-linked gene product SPAN-X localized to the nucleus of human spermatozoa. *Biology of Reproduction.* 63(2), pp. 469-481.

Westbrook, V. A. et al., 2004. Genomic organization, incidence, and localization of the SPAN-X family of cancer-testis antigens in melanoma tumors and cell lines. *Clinical cancer research,* 10(1), pp. 101-112.

Wharton, K. A., Johansen, K. M., Xu, T. & Artavanis-Tsakonas, S., 1985. Nucleotide sequence from the neurogenic locus notch implies a gene product that shares homology with proteins containing EGF-like repeats. *Cell,* 43(3), pp. 567-581.

Wilson, G. D. et al., 2016. Cancer stem cell signalling during repopulation in head and neck cancer. *Stem Cells Int,* p. 1894782.

World Health Organisation, 2014. *Locally Advanced Squamous Carcinoma of the Head and Neck.* [Online]
Available at:

http://www.who.int/selection_medicines/committees/expert/20/applications/HeadNeck.pdf
[Accessed 2 June 2017].

Wu, L. et al., 2015. A novel IL-17 signaling pathway controlling keratinocyte proliferation and tumorigenesis via the TRAF4–ERK5 axis. *Journal of Experimental Medicine,* 212(10), pp. 1571-1587.

Xia, J. et al., 2011. Expressions of CXCR7/ligands may be involved in oral carcinogenesi. *Journal of molecular histology,* 42(2), p. 175.

Xu, Y. et al., 2012. Effect of estrogen sulfation by SULT1E1 and PAPSS on the development of estrogen-dependent cancers. *Cancer Science,* 103(6), pp. 1000-1009.

Yang, P., Huo, Z., Liao, H. & Zhou, Q., 2015. Cancer/testis antigens trigger epithelial-mesenchymal transition and genesis of cancer stem-like cells. *Current pharmaceutical design,* 21(10), pp. 1292-1300.

Yao, Duan & Fan, 2007. Gamma-secretase inhibitors exerts antitumor activity via down regulation of Notch and Nuclear factor kappa B in human tongue carcinoma cells. *Oral Dis,* Volume 13, pp. 555-563.

Yap, L. F. et al., 2005. The opposing roles of NOTCH signalling in head and neck cancer: a mini review. *Oral Disease,* 21(7), pp. 850-857.

Yaspan, B. L. et al., 2008. A halotype at chromosome Xq27 confers susceptibility to prostate cancer. *Human Genetics,* 123(4), pp. 379-386.

Yavropoulou, M. P. & Yovos, J. G., 2014. The role of NOTCH signalling in bone development and disease. *Hormones,* 13(1), pp. 24-37.

Yilmaz-Ozcan, S. et al., 2014. Epigenetic mechanisms underlying the dynamic expression of cancer-testis genes, PAGE2, -2B and SPANX-B during mesenchymal-to-epithelial transition. *PLoS One,* 9(9), p. e107905.

Yoshida, et al., 2013. The pathological significance of Notch1 in oral squamous cell carcinoma. *Laboratory Investigation ,* 93(10), pp. 1068-1081.

Yu, B. et al., 2012. Notch1 signaling pathway participates in cancer invasion by regulating MMPs in lingual squamous cell carcinoma. *Oncol Rep,* 27(2), pp. 547-552.

Yu, X. M. et al., 2016. Notch1 signaling regulates the aggressiveness of differentiated thyroid cancer and inhibits SERPINE1 expression. *Clinical Cancer Research,* 22(14), pp. 3582-3592.

Zamunér, F. T. et al., 2015. A comprehensive expression analysis of cancer testis antigens in head and neck squamous cell carcinoma revels MAGEA3/6 as a marker for recurrence. *Molecular cancer therapeutics*, 14(3), pp. 828-834.

Zendman, A. J. et al., 2003. The human SPANX multigene family: genomic organization, alignment and expression in male germ cells and tumour cell lines. *Gene,* 309(2), pp.125-133.

Zeng, Li & Chepeha, 2005. Crosstalk between tumor and endothelial cells promotes tumor angiogenesis by MAPK activation og Notch signalling. *Cancer Cell,* Volume 8, pp. 37-45.

Zhang, H. et al., 2017. The pseudogene-derived long noncoding RNA SFTA1P is down-regulated and suppresses cell migration and invasion in lung adenocarcinoma. *Tumor Biology,* 39(2), p. 1010428317691418.

Zhang, T. H. et al., 2011. Activation of Notch signaling in human tongue carcinoma. *J Oral Pathol Med*, 40(1), pp. 37-45.

Zhao, S., Huang, J. & Ye, J., 2015. A fresh look at zebrafish from the perspective of cancer research. *J Exp Clin Cancer Res,* 34(1), p. 80.

Zhao, Z. L. et al., 2016. NOTCH1 inhibition enhances the efficacy of conventional chemotherapeutic agents by targeting head neck cancer stem cell. *Scientific reports,* p. 6.

Zhu, Y. et al., 2015. Establishment and characterization of patient-derived tumor xenograft using gastroscopic biopsies in gastric cancer. *Scientific reports,* p. 5.